MACQUARIE UNIVERSITY

THE AUSTRALIAN SCHOOL OF ADVANCED MEDICINE

Experimental studies into the pathophysiology of syringomyelia

A thesis submitted to fulfil the requirements for the degree of Doctor of Philosophy at the School of Advanced Medicine, Faculty of Human Sciences, Macquarie University.

Sarah J Hemley, B. Biotechnology (Honours).

June 30, 2011

Table of Contents

Table of figures

Tables

Abbreviations

AMPA	2-amino-3-(5-methyl-3-oxo-1,2- oxazol-4-yl)propanoic acid
AQP	aquaporin
BBB	blood-brain barrier
BSCB	blood-spinal cord barrier
Bv	blood vessel
C	control
CC	central canal
CO_2	carbon dioxide
CSF	cerebrospinal fluid
CT	computer assisted tomography
DAB	3-3' diaminobenzidine
dH_2O	distilled water
DNA	deoxyribonucleic acid
DPX	Gurr's Depex mountant
DTT	dithiothreitol
EAE	experimental autoimmune encephalomyelitis
EBA	endothelial barrier antigen
ECF	extracellular fluid
ECL	enhanced chemiluminescence
EGTA	ethylene glycol tetraacetic acid
EPO	erythropoietin
GABA	γ-Aminobutyric acid
Gd	gadopentate dimeglumine
GFAP	glial fibrillary acidic protein
HEPES	4-(2-hydroxyethyl)-1-piperazineethanesulfonic acid
H_2O	water
HRP	horseradish peroxidase
Ig	immunoglobulin
JACoP	just another colocalisation plugin
Kir	potassium inwardly-rectifying channel
NHS	normal horse serum
NMDA	N-Methyl-D-aspartic *acid*
MR	magnetic resonance
MW	molecular weight
O_2	oxygen
OCT	optimal cutting temperature
PBS	phosphate-buffered saline
PMSF	phenylmethylsulfonyl fluoride
PVS	perivascular space
RECA-1	rat endothelial cell antigen
Rpm	revolutions per minute
S	syrinx
SAS	subarachnoid space
SD	standard deviation
SEM	standard error
Sh	sham-injected
SPSS	statistical package for the social sciences
TBS	tris-buffered saline
TMB	3,3',5,5'-tetramethylbenzidine
VE	vascular endothelial
VEGF	vascular endothelial growth factor

Summary

Syringomyelia, a condition in which an enlarging cyst forms within the spinal cord, can result in motor weakness and pain. The pathogenesis of syringomyelia is poorly understood and treatment outcomes are not always satisfactory. It is unlikely that more effective therapies will be developed without a greater understanding of the mechanisms underlying spinal cord cyst formation. It is generally thought that syringomyelia is simply caused by an increase in the flow of cerebrospinal fluid (CSF) into the spinal cord. However, the pathogenesis is likely to be complex and multifactorial. It was proposed that: 1) a possible contribution to fluid flow is from vessels adjacent to the cyst, through a deficiency in the blood-spinal cord barrier (BSCB); 2) an increase in the expression of the water channel protein aquaporin-4 (AQP4) could increase the movement of water into the cyst; and 3) fluid outflow contributes to the pathology. Well established animal models of posttraumatic and Chiari-associated syringomyelia were used to study BSCB integrity, AQP4 expression and fluid outflow pathways. Integrity of the BSCB was assessed using immunoreactivity to endothelial barrier antigen and by extravasation of intravascular horseradish peroxidase (HRP). Western blotting and immunofluorescence was used to examine AQP4 and glial fibrillary acidic protein (GFAP) expression. Outflow of fluid was investigated by the direct microinjection of tracer into cysts under ultrasound guidance. These studies demonstrated a prolonged disruption of the BSCB directly surrounding the cyst. This disruption may be allowing a greater volume of fluid to pass from the blood stream into the spinal cord, causing the cyst to enlarge. There was a change in the levels of AQP4, suggesting that there is an imbalance in the water movement in the spinal cord. This imbalance may be contributing to fluid accumulation in syringomyelia. The study of fluid outflow found that fluid diffuses out of cysts into the surrounding extracellular space and perivascular spaces. This is the first study to demonstrate a route for fluid flow out of the cyst and will add to our understanding of fluid movement in syringomyelia.

Statement of originality

I hereby declare that the work presented in this thesis has not been submitted for a higher degree to any other university or institution. To the best of my knowledge this submission contains no material previously published or written by another person, and is my own work unless stated otherwise. Any contribution made to the research by others is explicitly acknowledged.

This work was carried out with ethical approval from the Animal Care and Ethics Committee of Maquarie University (ARA 2010/21), the University of New South Wales (ARA 09/28B, 07/29B, 06/39B) and the institute of Medical & Veterinary Science (Central Northern Adelaide Health Service) (ARA 48/07, 79/06).

Sarah J Hemley 30 June 2011

Acknowledgements

I would like to dedicate this thesis to my partner Andy without whom my PhD experience would not have been so enjoyable. A number of other people also deserve a special mention for helping me get to this point; my friends (you know who you are), my family, my supervisor Marcus Stoodley who provided many opportunities for me to further my knowledge, research and career, Nigel Jones who was an integral part of the sheep study in Adelaide, Peter Petocz for not only assisting with the statistical analysis but also provided plenty of reading material for the long train trips to Macquarie University. Everyone at the Australian School of Advanced Medicine and the Prince of Wales Medical Research Institute for their technical assistance, and creating such a fun and friendly work environment. I would especially like to thank everyone in the Neurosurgery laboratory, particularly those working on the Syrinx project. It would be remiss of me to forget my Sprague-Dawley rats and Merino sheep, without whom this research could not have been conducted.

I would like to acknowledge and thank a number of institutions: The National Health and Medical Research Council who provided my postgraduate scholarship, research funding and financial support to attend conferences; The Column of Hope Chiari and Syringomyelia Research Foundation have generously provided research funding for most of the studies detailed in this thesis; the Brain Foundation that have granted funding which has supplemented this work.

Chapter 1

Introduction

Syringomyelia is a serious disease characterised by the formation of fluid-filled cysts or cavities (syrinxes) within the spinal cord (Figure 1). Syringomyelia occurs in association with a number of congenital and acquired pathologies and may result in considerable pain, motor weakness and even paralysis or death. The underlying pathogenesis of syringomyelia is not completely understood, and outcomes from surgical treatments are often unsatisfactory (Klekamp et al., 1997, Batzdorf et al., 1998, Klekamp et al., 2002, Koyanagi et al., 2005, Attenello et al., 2008). Further research into the mechanisms involved in syrinx formation and enlargement is needed before new or improved treatments can be developed.

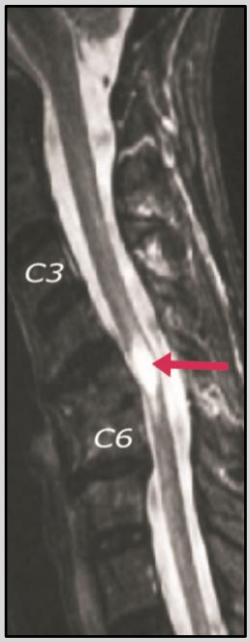

Figure 1: Posttraumatic syringomyelia. T-2 – weighted sagittal image demonstrating a syrinx (*arrow*).

History

In 1546 Charles Estienne first described spinal cord cavitations in human cadavers (Estienne, 1546). However, the term *syringomyelia* was not applied to the disease until 1827, upon the suggestion of Charles Ollivier d'Angers, after the Greek word *syrinx* meaning pipe or tube and *myelos* meaning marrow (Ollivier D'Angers, 1827). The first record of a patient displaying clinical symptoms associated with syringomyelia was in 1804. Portal described a patient with lower limb numbness that developed into progressive paralysis. At autopsy a syrinx was identified (cited in (Klekamp, 2002)). In 1867 Bastian described the first posttraumatic syrinx, and in 1915 Holmes published a report on gunshot injuries of the spinal cord describing posttraumatic cavitations (cited in (Klekamp, 2002)). Barnett and Jousse were the first to diagnose posttraumatic syringomyelia clinically. In a series of papers published in the 1960's and 70's, they identified that syringomyelia was a progressive disease that may result in a paraplegic patient losing upper limb function. They also recognised that the cavity occurred in close proximity to the initial injury, as identified by regions of arachnoiditis (Silver, 2001).

Syringomyelia has been identified in association with other pathologies, including meningitis and spinal cord tumours (Klekamp, 2002). In 1883 Cleland described the first case of syringomyelia associated with a cranio-spinal abnormality, now referred to as a Chiari malformation, in acknowledgment of an Austrian pathologist, Hans Chiari. In 1891 Chiari published a report describing three different abnormalities involving the downward displacement of the cerebellum and brainstem, extending into the spinal canal. Chiari later found that a number of patients with these malformations also had syringomyelia (Chiari, 1987). The first surgical procedure to alleviate the clinical symptoms of syringomyelia was performed in 1892 by Abbe and Coley. They performed a myelotomy (a small incision in the spinal cord) to drain the syrinx fluid. However, the patient's clinical symptoms were unchanged (Abbe and Coley, 1892).

One of the greatest impediments to treating syringomyelia at this time was due to the difficulty in diagnosing the disease, as confirmation could only be made at surgery or autopsy. In the 1920's the first breakthrough in neuroimaging was made using myelography, followed later by computer assisted tomography (CT) using contrast agents. However, it wasn't until the implementation of magnetic resonance (MR) imaging in the 1980's that the diagnosis could be made reliably in a non-invasive manner (Kokmen et al., 1985, Gillespie et al., 1986, Masaryk et al., 1986). In the 35 years after Abbe and Coley performed the first surgical procedure to drain a syrinx only 12 similar operations were reported (Aschoff and Kunze, 1993).

Terminology

Pathological cavitations within the spinal cord may be differentiated on the basis of their anatomical location within the cord. In the literature, the term *hydromyelia* is sometimes used to describe a dilatation of the central canal, while *syringomyelia* is then used to describe only those cysts that are completely separate from the central canal (Yasui et al., 1999, Johnston and Teo, 2000, Brodbelt and Stoodley, 2003a). The terms *syringohydromyelia* and *hydrosyringomyelia* may be used to describe syringes that involve both the central canal and spinal parenchyma (Milhorat et al., 1992), while *syringobulbia* or *hydrobulbia* (Johnston and Teo, 2000) have been used to indicate cavities occurring in the brainstem. However, it is often difficult to differentiate syringes using these classifications and these terms are not used consistently (Milhorat et al., 1992). As such, in this text, *syringomyelia* will be used to describe all abnormal, spinal cord cysts, apart from small non-enlarging posttraumatic cysts. The various types of syrinxes will be distinguished by the associated pathology, and referred to using terms such as *posttraumatic* or *Chiari-associated syringomyelia*.

Epidemiology

Since the widespread implementation of MR imaging, the prevalence of syringomyelia is reported to be 8.2 – 8.4 cases per 100,000 people (Aimard et al., 1993, Heiss et al., 1999, Brickell et al., 2006). This equates to approximately 25,000 people in the US and 1,800 people in Australia (Heiss et al., 1999, Brodbelt and Stoodley, 2003a, Brickell et al., 2006). Syringomyelia is most commonly associated with Chiari I malformations, accounting for close to half of all cases, while spinal cord injury is associated with approximately 10% (Williams, 1993, Moriwaka et al., 1995, Brickell et al., 2006). The average age of onset of symptoms occurs at around 28 years (Moriwaka et al., 1995, Brickell et al., 2006).

Prior to modern imaging, posttraumatic syringomyelia was reported in 3.2% of the paraplegic and tetraplegic population (Rossier et al., 1985, Schurch et al., 1996). With the assistance of MR imaging, diagnosis is now made earlier and more cases are reported. Depending on the population studied and the definition of syringomyelia, the recorded number of spinal cord injury patients with syringomyelia varies from 4.45% to 40% (Squier and Lehr, 1994, Moriwaka et al., 1995, el Masry and Biyani, 1996, Schurch et al., 1996, Abel et al., 1999, Carroll and Brackenridge, 2005). This difference most likely reflects the fact that syringomyelia may develop 1 month to more than 30 years after the initial trauma (Sigman and Gillich, 1981, Schurch et al., 1996). As such, the length of time a patient is followed in the study significantly affects the final figures. It has been estimated that as of 2010, there were 9,000 cases of diagnosed posttraumatic syringomyelia in the US, with an additional 400 cases expected to be diagnosed each year (Sigman and Gillich, 1981). There is some evidence that posttraumatic syringomyelia is more prevalent following complete spinal cord injury than incomplete injury (Rossier et al., 1985, Schurch et al., 1996, Vannemreddy et al., 2002).

Although rare, cases of familial syringomyelia of autosomal dominant or recessive inheritance have been reported (Barrett et al., 1981, Bernstein et al., 1981, Cummings et al., 1981, Naftchi et al., 1981, Sahgal et al., 1981, Zakeri et al., 1995, Koc et al., 2007). The incidence of familial syringomyelia is reported to be approximately 2% (Singer et al., 1981, Zakeri et al., 1995, Koc et al., 2007). These cases generally occur in association with a Chiari type I malformation, a condition which is thought to have an underlying genetic component, and disorders in which heretibility has been established, such as myotonic dystrophy (cited in (Zakeri et al., 1995)), neurofibromatosis and von Hippel-Lindau disease (Bernstein et al., 1981). An association between excessive strain and heavy labour has been proposed as a predisoposing factor for syringomyelia (Lawrence et al., 1981, Zakeri et al., 1995).

Conditions associated with syringomyelia

Syringomyelia is a disorder associated with numerous congenital and acquired conditions (Table 1), that result in an obstruction of CSF flow either at the foramen magnum or in the subarachnoid space (Klekamp, 2002). A study of over 1,000 patients with syringomyelia in Japan found that the majority of cases were related to Chiari malformations (51.2%), or with trauma (11%) (Moriwaka et al., 1995). Other pathologies associated with syrinx formation include spinal cord tumour (intra- or extra- medullary), non-traumatic spinal arachnoiditis, and dysraphism (Milhorat et al., 1995a, Moriwaka et al., 1995, Klekamp et al., 1997, Brickell et al., 2006).

Table 1: Conditions associated with syringomyelia [from (Milhorat et al., 1995a)]

Communicating canalicular syrinxes	Non-communicating canalicular syrinxes
Communicating hydrocephalus	Chiari I malformation
Chiari II malformation	Cervical spinal stenosis
Intraventricular or subarachnoid haemorrhage	Spinal arachnoiditis
Meningitis	Basilar impression
Normal pressure hydrocephalus	Terminal ventricle cyst
Dandy-Walker cyst	Occipital encephalocele (eg. Dandy-Walker, Chiari II malformation, & spina bifida)
Non-communicating extracanalicular syrinxes	
Trauma	**Spontaneous intramedullary haemorrhage**
Ischaemic infarction (thrombosis or embolism)	Transverse myelitis
Postmeningitic infarction	Radiation necrosis
Tumours	

Chiari-associated syringomyelia

Chiari malformations consist of a group of disorders characterised by an abnormality at the craniocervical junction. Syringomyelia is most commonly seen with a Chiari Type I malformation, an abnormality involving “crowding” of the foramen magnum and the downward displacement of the cerebellar tonsils into the spinal canal (Figure 2. *(Left)*). A study of over 300 symptomatic Chiari I patients found that 65% had a syrinx (Milhorat et al., 1999). Chiari type II involves the herniation of both the cerebellar tonsils, and the brainstem into the foramen magnum. A Chiari type II malformation is almost always observed in association with myelomeningocele and hydrocephalus (Strayer, 2001). Type III is a rare form of Chiari malformation. This type is characterised by upper cervical or occipital

encephalocele. Chiari IV involves cerebellar hypoplasia (Caldarelli et al., 2002). Syringomyelia was found to be more prevalent in patients with a herniation of 9 to 14 mm compared to those Chiari patients with a smaller or larger herniation (Stovner and Rinck, 1992).

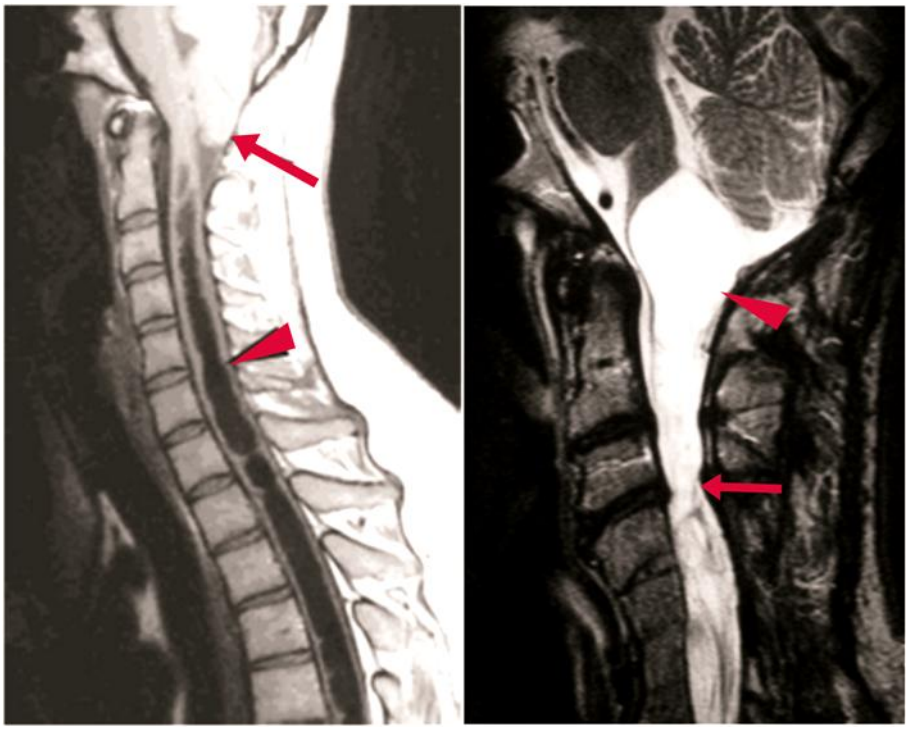

Figure 2: T-2 – weighted sagittal images demonstrating a syrinx (*arrow heads*) and the underlying pathology (*arrow*). (*Left*) Chiari-associated syringomyelia. (*Right*) Posttraumatic syringomyelia.

Spinal cord injury

Posttraumatic syringomyelia is the development of a syrinx following spinal trauma (Figure 2. *(Right)*). A syrinx causes delayed neurological deficits in spinal cord injured patients (Terre et al., 2000). While the development of a posttraumatic syrinx can occur weeks or decades after the initial injury, the average occurrence is estimated to be 9 years postinjury (Sigman and Gillich, 1981). There is evidence that earlier onset is more likely the older the patient (Vannemreddy et al., 2002). Approximately 80% of spinal cord injury patients are male (Carroll and Brackenridge, 2005). As such, posttraumatic syringomyelia is a disorder that affects many more males than females. Conditions such as Charcot joint and progressive late spinal deformity have also been linked to posttraumatic syringomyelia (Sigman and Gillich, 1981). A common consequence of spinal cord injury is the inflammation or scarring of the arachnoid layer at the site of trauma. It has been widely reported that a syrinx develops at the level of arachnoiditis (Mantulo et al., 1979, Matthews et al., 1979b, Caplan et al., 1990, Fehlings and Bernstein, 1992, Klekamp et al., 1997).

Classification and pathology

Until recently, there was no widely accepted classification system for syringomyelia. Some authors referred to an enlarged central canal as 'hydromyelia,' reserving the term 'syringomyelia' for those cases where the cyst was outside the central canal. Milhorat classified syringomyelia into three distinct groups (Figure 3) (Milhorat, 2000, Brodbelt and Stoodley, 2003a) based on studies of both MR imaging and post mortem pathological findings from 175 patients. He classified syrinxes as: *communicating*, in cases where the central canal enlargement and fourth ventricle are anatomically continuous; *noncommunicating*, if the central canal enlargement is not in communication with the fourth ventricle; and *extracanalicular* when the syrinx develops in the spinal parenchyma, separate from the central canal (Milhorat et al., 1995a, Milhorat, 2000). Other spinal cavities that do not clearly fall into these groups include *neoplastic* and *atrophic* lesions. Neoplastic cysts arise around a tumour mass, largely due to the increased permeability of blood vessels within the tumour (Milhorat, 2000, Lonser et al., 2005, Szpak et al., 2008). Atrophic cavitations occur where there is a loss of spinal cord tissue or myelomalacia (Milhorat, 2000, Seki and Fehlings, 2008, Weier et al., 2008).

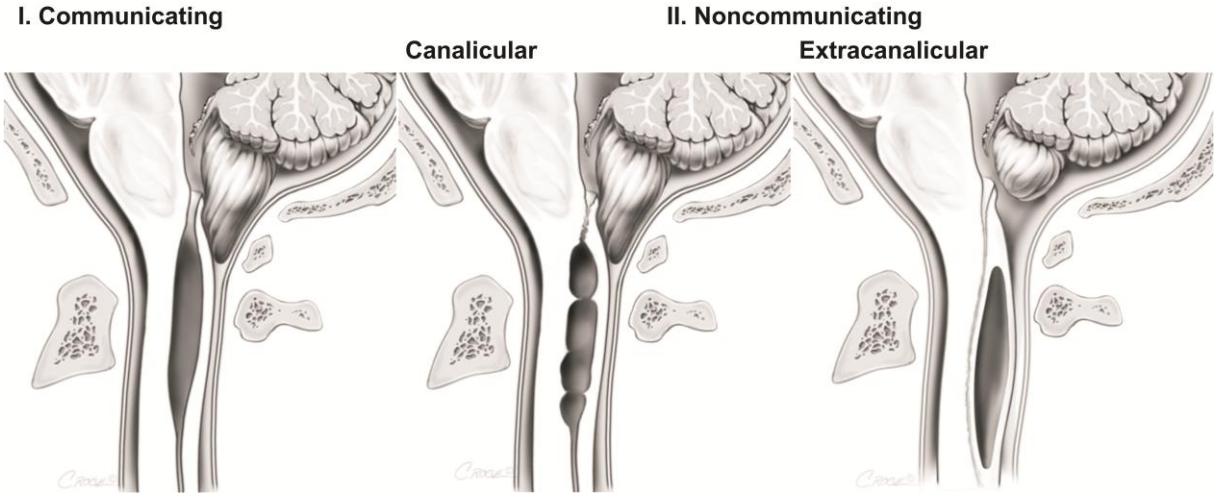

Figure 3: Pathological classification of syringomyelia. Left: communicating central canal. Centre: non-communicating central canal type in association with Chiari malformation. Right: extracanalicular type (posttraumatic) [from (Brodbelt and Stoodley, 2003a), with permission of Elsevier] (Milhorat et al., 1995a, Brodbelt and Stoodley, 2003a).

Communicating syringomyelia is most commonly associated with hydrocephalus, Chiari II malformations and encephalocele. In patients with a communicating syrinx there is typically enlargement of all cerebral ventricles in addition to the central canal dilation (Milhorat, 2000, Milhorat et al., 2003, Hagihara and Sakata, 2007).

Noncommunicating syrinxes occurring within the central canal appear as distinct cavities between central canal stenosis rostral and caudal to the enlargement. These cavities are

generally more complex than the simple dilations observed with communicating syrinxes and histologically they are characterised by intracanalicular adhesions (Milhorat et al., 1995a, Milhorat, 2000). Noncommunicating canalicular syringomyelia occurs in association with pathologies that cause a disturbance in CSF flow at or below the foramen magnum. Chiari I malformations are often associated with noncommunicating central canal dilations. Other lesions include Dandy-Walker malformations and posterior fossa tumours. 'Acquired' Chiari malformation from lumbar CSF shunting or CSF leak can also be associated with syringomyelia (Johnston et al., 1998, Milhorat, 2000, Padmanabhan et al., 2005).

Extracanalicular syringomyelia occurs following conditions that result in damage to the spinal parenchyma including trauma, ischemia or haemorrhage. These cavities typically develop in the watershed area of the cord and are lined with glial cells (Asano et al., 1996, Milhorat, 2000, Brodbelt and Stoodley, 2003a).

Clinical features

Syringomyelia is generally a slowly progressing condition with symptoms often presenting many years after the development of a syrinx. Progression is often intermittent with long periods of stability with no worsening of symptoms for a decade or more (Levy et al., 1983). Syringomyelia associated with Chiari I is symptomatic in around 80% of cases (Attenello et al., 2008), while following spinal cord injury only 1 to 9% of patients are reported to have symptomatic cysts (Wang et al., 1996, Perrouin-Verbe et al., 1998, Abel et al., 1999, Brodbelt and Stoodley, 2003a). In general, the clinical features are a direct reflection of the intrinsic damage to the spinal cord, correlating to the level, side and specific location of the cavity (Figure 4) (Milhorat et al., 1995b). Canalicular syringomyelia involving enlargement of the central canal without cord dissection may result in compression of the surrounding neural components and distension of the long tracts. This characteristically produces non-specific deficits such as spastic paraparesis. However, if the syrinx ruptures into the cord substance, deficits such as sensory loss and muscular atrophy that occur in the presence of a posttraumatic syrinx are often observed. This may cause irreparable damage to the affected spinal tracts (Milhorat et al., 1995a, Milhorat et al., 1995b, Bogdanov and Mendelevich, 2002).

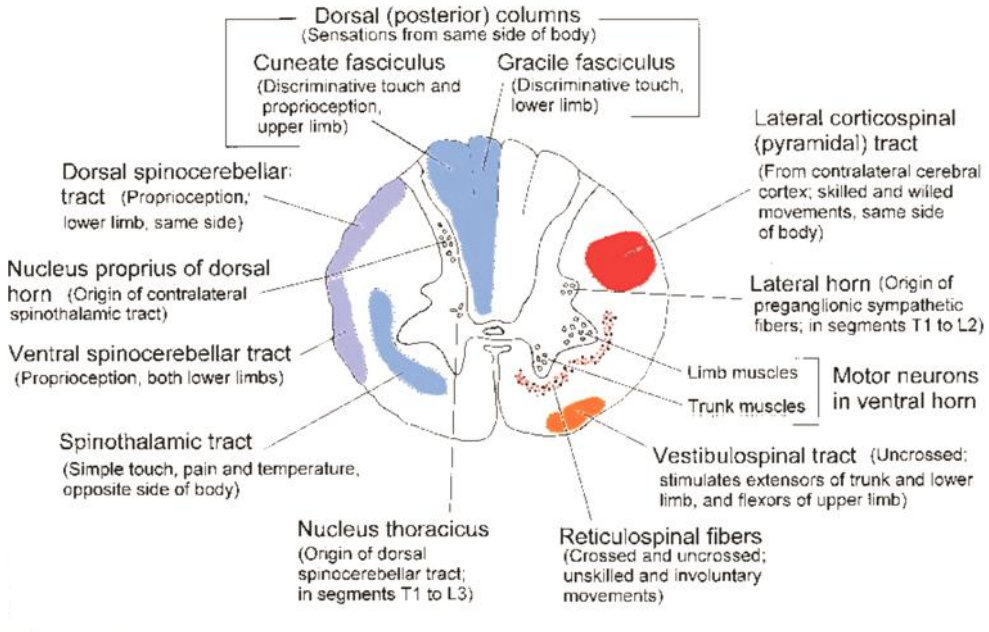

Figure 4: Cell columns and tracts of the human spinal cord from http://instruct.uwo.ca/anatomy.

Dissociated sensory loss is the classic presentation of syringomyelia, characterised as the loss of pain and temperature sensation while light touch and proprioception is maintained (Schurch et al., 1996, Ducreux et al., 2006). However, this occurs in patients with central lesions; other patients may present with a combination of motor and sensory symptoms (Schlesinger et al., 1981). Symptoms and signs may include pain (radicular pain, dysesthesia), motor weakness, oculomotor dysfunction, gait disturbance, bladder dysfunction and muscle wasting (Levy et al., 1983, Fukushima et al., 1994, Bindal et al., 1995, Milhorat et al., 1996b, Steinbok, 2004, Koyanagi et al., 2005, Aghakhani et al., 2009).

Muscle wasting and absent reflexes in the lower limbs are indicative of the expansion of a syrinx into the lumbar cord or conus medullaris (Tashiro et al., 1987). There is evidence that the acute stages of symptom progression correspond to large syrinxes and increased cord diameter, while in the chronic stages when symptoms are stable a small syrinx is usually identified (Tashiro et al., 1987). Worsening of symptoms, in particular motor deficits, is closely related to the expansion of the syrinx, and conversely, improvements following surgical intervention correspond to the collapse of the cavity (Schurch et al., 1996).

In posttraumatic cases, pain generally occurs at or above the site of injury and reflects damage to the spinothalamic tract (Schurch et al., 1996, Ducreux et al., 2006). Dysesthetic pain, often described as a dull ache or burning, pins and needles, or the sensation of the skin being stretched, is the presenting symptom in around 40% of patients (Levy et al., 1983, Van den

Bergh et al., 1990, Milhorat et al., 1996b). Pain is often exacerbated by coughing or straining (Schurch et al., 1996). Patients with syringomyelia associated with Chiari malformation may also experience pain caused by the Chiari malformation itself placing pressure or tension on the cervical nerve roots. This causes sub-occipital and lower central neck pain (Logue and Edwards, 1981, Schurch et al., 1996).

Treatment

Since the first myelotomy was performed in 1892 (Abbe and Coley, 1892), a number of techniques have been employed to treat syringomyelia. These procedures are generally performed with the aim to either drain the syrinx cavity or re-establish normal CSF pathways. Percutaneous aspiration and decompression of the syrinx in the past was thought to be a simple procedure with few complications that would in some cases stabilise or improve symptoms (Schlesinger et al., 1981). Terminal ventriculostomy (opening the central canal at the caudal end to the subarachnoid space) has also been carried out with some success on patients with communicating syringomyelia (Gardner et al., 1977, Singounas and Karvounis, 1979, Profeta and Maggi, 1980, Hashiguchi et al., 2008).

More recently, posterior fossa decompression and shunting procedures have become the most common surgical techniques. Shunting procedures drain the syrinx fluid into the subarachnoid space (syringostomy, syringosubarachnoid shunt) or to an extraspinal site (syringopleural shunt, syringoperitoneal shunt). Foramen magnum decompression and syringosubarachnoid shunting are the most common surgical procedures for syringomyelia associated with a Chiari malformation. It has been proposed by Gardner and Fahy that when a syrinx occurs in association with a hindbrain abnormality, a posterior fossa decompression is the preferable surgical procedure (Williams and Fahy, 1983). The size of the syrinx and whether the symptoms were related to the syrinx rather than compression caused by the Chiari malformation are usually the determining factors (Iwasaki et al., 2000a, Hida and Iwasaki, 2001). Large syrinxes (those occupying at least 70% of the spinal cord diameter) are more likely to be treated with a syringosubarachnoid shunt (Hida and Iwasaki, 2001). Iwasaki et al report that 93% of patients with a Chiari malformation and syringomyelia treated with a syringosubarachnoid shunt experience relief of pain (Iwasaki et al., 2000a). The results from a number of case series indicate that craniovertebral decompression is the most effective treatment for syringomyelia associated with a Chiari malformation, with insertion of a syringosubarachnoid shunt preferable as a secondary treatment (Logue and Edwards, 1981). Recently, the combination of posterior fossa decompression and syringosubarachnoid shunt

insertion has had some success with neurological improvement in around 89% of patients (Ergun et al., 2000).

The surgical procedures implemented for posterior fossa decompression also remain controversial. There is some evidence that posterior fossa decompression with duraplasty reduces cavity size in Chiari-associated syringomyelia more reliably than decompression alone (Munshi et al., 2000, Heiss et al., 2010). Some surgeons prefer bone removal without opening the dura when treating children (Genitori et al., 2000). Plugging of the central canal at the level of the obex, although rarely used today, was developed by Gardner in the belief that CSF flowed into syrinx cavities from the fourth ventricle. In this procedure the arachnoid is incised and a piece of muscle is used to block the opening of the central canal (Gardner and Angel, 1958b). This procedure is no longer performed by surgeons due to the high number of complications and lack of improvement (Logue and Edwards, 1981). However, there have been a small number of studies that reported a better outcome following posterior fossa decompression with plugging, rather than decompression alone, with an improvement in ~80% of patients (Hoffman et al., 1987).

The optimal treatment for syringomyelia not associated with Chiari malformation is even less clear. One of the main objectives in treating syringomyelia caused by blockages in the subarachnoid space is to restore CSF flow. This generally involves a laminectomy, resecting the scar tissue and duraplasty (Lam et al., 2008). In some cases due to the location or extent of the adhesion, resection is not possible. In these instances a shunt may be placed in the subarachnoid space rostral to the CSF blockage to divert CSF flow to the peritoneal or pleural cavities. Using this technique a positive clinical response was reported in 86% of patients. However, 43% experienced complications (Lam et al., 2008). An alternative surgical approach involves direct shunting and drainage of the syrinx cavity. While there is evidence to suggest that this procedure has some clinical benefits (Tator and Briceno, 1988, Hida et al., 1994, Hess and Foo, 2001, Carroll and Brackenridge, 2005), with one study reporting improvement in 31% of patients (Carroll and Brackenridge, 2005), rates of complications and recurrence are high. Klekamp et al reported that direct shunting procedures resulted in a recurrence rate of 97% in patients with syringomyelia associated with arachnoid scarring, with clinical symptoms reappearing within 2 years (Klekamp et al., 1997). Reports from multiple studies indicate that direct shunting of cavities has a high rate of failure and associated complications, occurring in 50 – 97% of patients (Sgouros and Williams, 1995, Klekamp et al., 1997, Batzdorf et al., 1998, Batzdorf, 2005). Complications arising from this

procedure include the catheter becoming blocked when the syrinx collapses, tethering of the shunt to the spinal cord itself, infections, and shunt displacement (Lam et al., 2008).

The stage of disease progression at which surgery should be considered is also problematic. There is considerable evidence that early diagnosis and treatment will lead to a more positive outcome. Reports indicate that a number of symptoms such as pain, sensory loss, and weakness will improve or stabilise following surgery. However, headache, spasticity, and bowel and bladder dysfunction are less likely to be reversed (Barbaro et al., 1984, Alzate et al., 2001). Contrary to these results, other studies have shown that conservative treatment with rehabilitation resulted in an improved neurological outcome compared to surgery in 10 patients with a posttraumatic syrinx (Ronen et al., 1999).

Radiotherapy has previously been applied to treat syringomyelia, but with little success (McIlroy and Richardson, 1965, Schlesinger et al., 1981). More recently, transplantation of human foetal or embryonic spinal cord grafts into a syrinx has been attempted. The grafts have been shown to be safe and feasible in small pilot studies, however, it is yet to be seen if the donor tissue survived and whether clinical improvements are achieved (Falci et al., 1997, Thompson et al., 2001, Wirth et al., 2001). At this stage, obliteration of a syrinx has only been demonstrated in one patient (Falci et al., 1997). Whether or not this technique will lead to long-term improvements in patients and become more widely implemented remains to be seen.

Conclusion

On the basis of the available data on surgical outcomes, there appears to be good clinical outcomes in the short term, however, long-term results are poor. The outcomes reported in these clinical studies demonstrate that current surgical treatments are not based on a complete understanding of the pathophysiology. It is not clear why restoring normal CSF flow in the subarachnoid space often results in syrinx decompression. There is also no clear evidence to suggest that one surgical technique is consistently superior to others. A better understanding of the aetiology is needed to develop improved treatments.

Theories of pathogenesis

Although the term syringomyelia was introduced in 1827 and the condition has been studied extensively since, there is still no universally accepted explanation for its development. Numerous hypotheses have been proposed. These theories have attempted to explain both the initial cyst formation and the subsequent enlargement of a syrinx. There are differences in

opinion in not only the mechanism of syrinx formation but also the source of fluid, and the pathway by which fluid flows into the syrinx. The following section will provide an overview of these theories, making the distinction between hydrodynamic and non-hydrodynamic theories, and those that propose that a syrinx contains extracellular fluid.

Non-hydrodynamic theories

Canalicular syringomyelia

Developmental malformation

The association between syringomyelia and congenital conditions such as spina bifida has given rise to a developmental theory (cited in (Klekamp, 2002)). Chiari believed that in most cases the cavity was due to a developmental defect in the central canal or a simple widening (Newton, 1969). Syringomyelia was also considered by some to be indicative of a spinal cord that had stopped developing (Ollivier D'Angers, 1827). It was thought that both hydrocephalus and syringomyelia were the result of a normal physiological state in the embryonic stage, remaining after birth, and represent a lesser abnormality that would manifest as myelocoele in a more severe state (Gardner and Angel, 1958b). Others thought that brainstem abnormalities lead to hydrocephalus and in turn a dilated central canal which eventually ruptured into the parenchyma (Cleland, 1883). Later, the association of syringomyelia with conditions that are clearly acquired, such as arachnoiditis following meningitis was recognised, discrediting the congenital theory (cited in (Levine, 2004)).

Traumatic birth

A correlation has been found between traumatic birth and patients with a Chiari malformation and syringomyelia. It has been put forward that a combination of high pressure applied to the foetal head during a difficult labour and the use of forceps may impair venous flow. These additional forces may further displace the cerebellar tonsils, and may cause the central canal to rupture, or cause haemorrhage that obstructs CSF flow (Newman et al., 1981). A case report of monozygotic twins, one with a Chiari malformation and syringomyelia and the other with only minor compression of the cerebellar tonsils, found that the twin with syringomyelia had a difficult birth, with breech delivery while the unaffected sibling had a normal delivery. This supports the theory that traumatic birth may be one cause of syringomyelia (Iwasaki et al., 2000b).

Genetic abnormalities

Although rare, a small number of cases of familial syringomyelia associated with hindbrain abnormalities have been reported, suggesting that there may be a genetic component in the pathogenesis of syringomyelia (Zakeri et al., 1995, Atkinson et al., 1998, Mavinkurve et al., 2005, Koc et al., 2007). A genetic study of Cavalier King Charles spaniels, a dog breed with a high incidence of Chiari malformations, found there to be a high heritability of syringomyelia (Lewis et al., 2010). However, the number of reported cases in humans remains too small to draw any firm conclusions. There is also not complete concordance of syringomyelia in identical twins and triplets. A number of studies on monozygotic twins and triplets have reported that only one sibling has syringomyelia (Stovner et al., 1992, Cavender and Schmidt, 1995). These studies suggest that it may be the Chiari malformation that is heritable and not syringomyelia per se (Mavinkurve et al., 2005).

Inflammation

Postinflammatory syringomyelia is associated with infections such as meningitis, tuberculosis, subarachnoid haemorrhage or chemically induced inflammation from foreign sources, such as the previously used oil-based radiographic contrast media (Tabor and Batzdorf, 1996, Daif et al., 1997, Klekamp et al., 1997). Milhorat et al demonstrated that central canal occlusion could be induced through the inoculation of reovirus type I in hamsters. The reovirus produced inflammation of ependymal cells, causing ependymal rosettes and microtubules to form, occluding the central canal, which in turn caused dilation of the central canal, and eventually a syrinx. This suggests that at least in canalicular syringomyelia, inflammatory processes are able to cause canal stenosis, and may play a role in syringomyelia (Milhorat and Kotzen, 1994). However, there is no evidence for viral infection as a cause in patients with syringomyelia. More recently, Lee et al created noncommunicating canalicular syringomyelia in chimeric rats by injecting kaolin into the spinal parenchyma. In this model the authors demonstrated a widespread activation of macrophages and microglia (Lee et al., 2005).

Immunological

Blagodatsky and colleagues found that a number of patients with syringomyelia related to hindbrain abnormalities had increased levels of IgG, IgM or IgA in the syrinx fluid. The authors suggested that immunological mechanisms may play a role in syrinx formation (Blagodatsky et al., 1993). There has been little support for this theory in recent years, and there is no clear evidence to suggest that syringomyelia has an immunological basis.

Extracanalicular syringomyelia

Neoplastic

There have been numerous reports of syringomyelia occurring in association with tumours (Lohle et al., 1994, Shimizu et al., 2004, Shenoy and Raja, 2005, Lonser et al., 2006, Rodriguez-Cano et al., 2007, Ashawesh et al., 2008). Nagahiro et al propose that syringomyelia occurring in association with a tumour occurs in two stages. Firstly, a cavity forms in the grey matter around the tumour. Secondly, the cavity extends in both the rostral and caudal direction, leading to the development of a syrinx. He suggests that the clinical symptoms and progression to syringomyelia may be due to CSF inflow exceeding the drainage of CSF. The tumour may effectively act as a subarachnoid block, altering the normal flow of CSF (Nagahiro et al., 1986). The initiation of a cavity around the tumour has alternatively been attributed to increased vascular leakage of tumour vessels (Lonser et al., 2005). A comparison of syrinx fluid and serum protein levels in patients with an associated tumour has shown levels to be similar, suggesting that extravasation of plasma and other molecules from the blood vessels in the tumour mass into the surrounding tissue cause the initial oedema (Gardner et al., 1963, Lohle et al., 1994, Lonser et al., 2005).

Ischemia

Caplan and colleagues considered vascular changes to be one of the important mechanisms in syrinx formation. The authors suggest that glial scarring in the spinal cord parenchyma occurring with inflammatory disorders destroys the spinal vasculature, and leads to ischemia. Small cysts form in these areas, which eventually merge to form a syrinx (Caplan et al., 1990). Williams agreed that the glial fibres lining a syrinx may cause damage to the surrounding vasculature and impact on the blood supply to the affected region (Williams, 1980b). Spinal cord injury also damages blood vessels and causes ischemic necrosis (Balentine, 1978). Studies have found that spinal cord blood flow significantly increases at the level of a syrinx following decompression (Milhorat et al., 1996a, Young et al., 2000). A study by Young and colleagues measured intraoperative spinal cord blood flow in patients with syringomyelia pre- and post-syrinx shunting. The results demonstrated that spinal cord blood flow increased after syrinx drainage (Young et al., 2000). A study of ischemia and spinal cord injury in dogs found that cavitations occurred in the spinal cord parenchyma after cutting the spinal root and associated blood vessels (Woodard and Freeman, 1956). These studies suggested that ischemia plays a role in syrinx formation.

Feigin et al disputed the idea that ischemia was the primary cause of syrinx formation. They propose that while ischemia might contribute to tissue necrosis in some instances, it is unlikely to be the primary mechanism because neurons are generally preserved within the spinal cord tissue adjacent to the syrinx cavity. Since neurons are susceptible to hypoxia, they are unlikely to survive in an area of ischemic injury (Feigin et al., 1971, Hall et al., 1975). A study comparing an animal model of ischemic insult with a model of kaolin induced syringomyelia, found that histologically the two conditions were very different (Hall et al., 1975). Currently, it is generally accepted that while ischemia might be one factor that contributes to spinal cord damage, it does not play a major role in the progression of an enlarging syrinx (Feigin et al., 1971, Klekamp, 2002, Levine, 2004).

Inflammation

Ravaglia et al suggested that syringomyelia might be caused by inflammation. Inflammatory processes may cause swelling of the spinal cord, thereby narrowing the subarachnoid space. Alternatively, inflammatory processes may cause a breakdown in the BSCB. An increase in BSCB permeability would result in the accumulation of protein-rich inflammatory products, and subsequently drive fluid into the cord across an osmotic gradient. The authors use the concurrence between inflammation and spinal cavities as evidence for causality between the two (Ravaglia et al., 2007). It has been well established that inflammation often leads to scarring of the subarachnoid space which alters the normal flow of CSF and may drive CSF into the cord (Batzdorf, 2005).

Arachnoiditis

There is a well-established association between arachnoiditis and syringomyelia. Arachnoiditis may be caused by infection, subarachnoid haemorrhage or tumour (Caplan et al., 1990, Fehlings and Bernstein, 1992, Milhorat et al., 1995a, Daif et al., 1997, Kakar et al., 1997, Klekamp et al., 1997, Brodbelt and Stoodley, 2003b, Kubota et al., 2008). A number of case studies have demonstrated that resecting arachnoid adhesions, thereby reconstructing the normal CSF pathways, results in decompression of a syrinx (Sgouros and Williams, 1996, Klekamp et al., 1997, Ohata et al., 2001). This suggests that arachnoiditis plays a major role in syrinx formation. A study using computer modelling of a spinal cord with arachnoiditis, found that in certain circumstances, cord tethering produced by arachnoiditis causes tensile radial stress and low pressure at the level of arachnoid adhesions. The authors postulate that the tensile radial stress may contribute to the cavity formation, and the low pressure in the cord may give rise to the inflow of extracellular fluid into the cavity. This would in turn lead to enlargement of the syrinx (Bertram et al., 2008). Other studies have shown that

arachnoiditis causes changes in pulsatile pressure waves in the subarachnoid space, which is believed to influence the flow of CSF into the spinal cord (Klekamp et al., 2001, Chang and Nakagawa, 2004). Animal models of posttraumatic syringomyelia have also demonstrated that there is an increased rate of syrinx formation with arachnoiditis compared to traumatic injury or excitotoxic injury alone (Cho et al., 1994, Yang et al., 2001). However, these studies found that arachnoiditis by itself did not produce a syrinx. This suggests that arachnoiditis, by disrupting CSF flow, contributes to the enlargement of existing oedema or cysts and is not a major factor in the initial cyst formation (Cho et al., 1994, Yang et al., 2001).

Chang et al used an electrical circuit model of CSF dynamics to investigate the effect of adhesive arachnoiditis on spinal cord pressure. They reported that there was a decrease in pressure in the subarachnoid space below the adhesive arachnoiditis. The pulsatile pressure wave within the central canal was not dampened by any blockage and so remained normal. As such, the pressure within the cord below the arachnoiditis was much higher than the pressure within the subarachnoid space. The authors suggest that this disturbance in the pressure gradient causes movement of CSF out of the central canal, leading to oedema in the extracellular space, and eventually syringomyelia (Chang and Nakagawa, 2004). The results of a study using an animal model of kaolin-induced arachnoiditis support these findings. The authors demonstrated that the pressure within the subarachnoid space was lower below the subarachnoid block than above. The pressure within the spinal cord below the arachnoiditis was higher than that in the subarachnoid space (Klekamp et al., 2001).

Hydrodynamic theories

The majority of theories on the pathogenesis of syringomyelia are based on the assumption that a syrinx simply contains CSF. These theories propose that syringomyelia is a condition caused by alterations in CSF hydrodynamics. These are generally the most cited and popular theories to date.

Canalicular syringomyelia

Water hammer

It wasn't until Gardner's re-working of the hydromyelic theory that any one hypothesis became widely referenced, and his proposal is generally referred to today as the first theory of syrinx pathogenesis. Gardner's hydrodynamic theory proposed that a hindbrain abnormality results in a blockage of the normal CSF outflow pathways from the fourth ventricle. He speculated that this causes a "water hammer" action, whereby CSF is driven directly into the

central canal, causing enlargement of the canal within the spinal cord (Gardner and Angel, 1958a). However, this theory is not consistent with the observation that in most patients the central canal is occluded between the fourth ventricle and the syrinx (Williams, 1990). It also doesn't explain syringomyelia occurring without a hindbrain abnormality.

Respiratory transmedullary

Ball and Dayan disputed Gardner's theory following a review of a series of 50 patients receiving surgical intervention for syringomyelia. The review compared results from surgery in which central canal blockage at the level of the obex was either included as part of the posterior fossa reconstruction or omitted. They found no difference between the outcomes from either surgery. This observation disputed the theory that the primary mechanism for filling the syrinx is CSF entering the central canal via the fourth ventricle. Ball and Dayan's theory, instead, concentrated on the increase in thoracic and abdominal pressures occurring in response to coughing and straining. They proposed that these pressure increases translate to increases in epidural venous pressure and spinal CSF pressure. In a normal situation the spinal CSF would move rostrally into the cranial subarachnoid space. However, in a patient with a blockage at the foramen magnum, as is the case in Chiari malformation, the CSF is not able to cross the foramen magnum. Ball and Dayan postulated that instead the CSF is directed into the spinal cord parenchyma via enlarged perivascular spaces. This fluid then pools in the extracellular space and a syrinx may be initiated. Ball and Dayan, in contrast to Gardner and Williams, believed that the central canal is only involved if a syrinx ruptures to encompass the central canal (Ball and Dayan, 1972).

Obstructed CSF drainage

Aboulker's theory postulated that a foramen magnum blockage prevents CSF from draining rostrally along the central canal into the fourth ventricle. Aboulker proposed that if the alternative pathways for CSF drainage: along the spinal subarachnoid space, dorsal root entry zone, and absorption by blood vessels, were unable to bear the extra volume of CSF, a syrinx may form (Aboulker, 1979j, a, e, i, h, g, f, c, b, m, l, k, d). Ellertsson and Greitz agreed that syringomyelia is a problem of obstructed drainage. However, they believed it to be due to inadequate drainage of fluid from the syrinx itself. They measured pressure within the subarachnoid space and the cyst in patients with syringomyelia. This study demonstrated that pressure was higher in the cyst than the subarachnoid space, although this was not significant. When intracranial pressure was raised, subarachnoid space pressure increased, followed, after an interval, by an increase in cyst pressure. Similarly, the subsequent decrease in subarachnoid pressure was not followed immediately by a decrease in pressure within the

cyst, but remained high for a time. They suggest that this is evidence of a communication between the syrinx and the subarachnoid space. They propose that this communication allows fluid to flow into the syrinx across the pressure gradient created by the delayed pressure increase. They suggest that the syrinx enlarges because the inflow of fluid into the syrinx exceeds the outflow (Ellertsson and Greitz, 1970).

Pressure dissociation

Williams developed a different hydrodynamic hypothesis. He described the phenomenon of high cranial pressure and low spinal pressure observed in patients with communicating syringomyelia, which he termed *craniospinal pressure dissociation*. He proposed that activities such as coughing and sneezing displace CSF upwards into the cranial cavity. When the pressure returns to baseline, in the normal situation, the CSF would be driven downward in the subarachnoid space. However, in patients with a Chiari malformation, the CSF is unable to flow downward into the subarachnoid space due to the obstruction at the craniocervical junction. Instead Williams proposed that the CSF is 'sucked' into the fourth ventricle and central canal, leading to enlargement of the central canal and eventually syrinx formation.

Arterial transmedullary

This theory focuses on the occlusion of the subarachnoid space at the foramen magnum rather than blockage of the fourth ventricle outlets. According to this theory, the normal compensatory flow of CSF between the cranial and spinal compartments in response to the expansion and contraction of the brain during the cardiac cycle is disrupted. In the absence of CSF movement, the cerebellar tonsils are displaced downwards during systole and caudally during diastole. They propose that the cerebellar tonsils act as a "piston", producing high-pressure waves within the cervical subarachnoid space. These pressure waves compress the spinal cord and force syrinx fluid upwards with each heartbeat. According to this theory, CSF is also pushed into the spinal cord via perivascular and interstitial spaces by these pulsatile pressure waves (Oldfield et al., 1994, Heiss et al., 1999).

Arterial pulsation perivascular space flow

Stoodley et al hypothesised that there is an arterial pulsation driven flow of CSF from the subarachnoid space to the central canal via perivascular spaces. In their study they used a CSF tracer injected into the cisterna magna to elucidate the pathway by which CSF flows into the spinal cord. They found that in the normal situation, CSF flows into the spinal cord via perivascular spaces. However, when the arterial pulsations were diminished, this flow was

absent (Stoodley et al., 1997). This theory has been elaborated on in recent years, and computational modelling has demonstrated that this flow could still occur in the presence of a mean pressure gradient. They suggest that an increase in this perivascular space flow could contribute to the enlargement of a syrinx (Bilston et al., 2003). A CSF flow study in an animal model of noncommunicating canalicular syringomyelia found that even in the presence of a syrinx, which is expected to be under high pressure, CSF still flows towards the central canal through perivascular spaces (Stoodley et al., 1999).

Elastic-jump hypothesis

The elastic-jump hypothesis was based on theoretical modelling with fluid-filled co-axial elastic tubes. The theory proposed that, as a pressure wave, caused by a cough or sneeze moves rostrally along intraspinal CSF pathways it steepens and forms an ‘elastic jump’. In the presence of a CSF blockage such as a Chiari malformation, this elastic jump causes transient high pressure in the spinal cord below the block and fluid accumulates (Carpenter et al., 2003, Elliott et al., 2009).

Extracanalicular syringomyelia

Pressure dissociation

In syringomyelia associated with arachnoiditis, as occurs following trauma, Williams suggests that small cavities may be caused initially by ischemia, and tethering of the cord to the arachnoid layer, which may cause shearing of tissue and leakage of fluid into the interstitial spaces. Following traumatic spinal cord injury, Williams agrees with Cushing’s observation that hematoma is likely to initiate cavity formation (as cited in (Williams, 1980b)).

To explain the enlargement of a posttraumatic syrinx over time, Williams speculated that pressure waves in the subarachnoid space are transmitted across the spinal parenchyma to the fluid within the syrinx. As coughing or sneezing drive CSF upwards in the subarachnoid space it is also forced upwards within the syrinx itself, followed by the subsequent downward movement. This ‘sloshing’ movement was said to lead to the weakening of the tissue adjacent to the syrinx, particularly at the rostral end of the cavity, and result in syrinx progression. Williams states that the ‘slosh’ mechanism provides an explanation for the delay between the time of injury, and syrinx formation, stating that every increase in cavity size adds to the problem. Once a critical size is reached, the syrinx enlarges at a much faster rate (Williams, 1980b).

Arterial pulsation perivascular space flow

CSF tracer studies in animal models of posttraumatic syringomyelia have been carried out with similar results to those obtained in canalicular models of syringomyelia. Brodbelt et al used an excitotoxic model of syringomyelia with arachnoiditis. They injected a tracer into the cisterna magna of rats, and found that CSF flowed from the subarachnoid space, into perivascular spaces and towards the syrinx. They also demonstrated an increase in flow at the level of arachnoiditis (Brodbelt et al., 2003c). A theory has been proposed by Bilston et al to explain how this increase in flow along perivascular spaces may occur. This hypothesis suggests that arachnoiditis causes a delay in the movement of pulse waves in the subarachnoid space, disrupting the synchronisation between CSF pulse waves and arterial pulsations. The authors state that in the normal situation, CSF is pushed into perivascular spaces when arteries are dilated. However, if the pulse wave is delayed, the CSF could be entering the perivascular spaces when the arteries are less distended, allowing an increase in fluid flow into the spinal cord (Bilston et al., 2010).

Elastic-jump hypothesis

It has been proposed that an elastic jump could also occur in the presence of arachnoiditis (Carpenter et al., 2003, Elliott et al., 2009). A more recent study re-evaluated this theory using computational modelling techniques. The authors demonstrated that while an elastic jump may occur, it could not cause changes in pressure within the cord sufficient to influence fluid flow, and as such, could not cause fluid to accumulate (Elliott et al., 2009).

Extracellular fluid

Since fluid cannot flow against a pressure gradient, and the pressure inside the syrinx and spinal cord have been shown to sometimes exceed subarachnoid space pressure (Hall et al., 1980, Klekamp et al., 2001), it is thought that CSF cannot be the only source of fluid. As such, there is increasing support for the theory that syrinx enlargement is due, at least in part, to extracellular fluid (Klekamp, 2002, Levine, 2004, Greitz, 2006).

Canalicular syringomyelia

Accumulation of extracellular fluid

Koyanagi and Houkin propose that syringomyelia associated with a Chiari I malformation is the result of an impairment in the absorption of extracellular fluid (Koyanagi and Houkin, 2010). A clinical study has demonstrated gadolinium enhancement around a syrinx cavity in a patient with a Chiari malformation. This implies that the BSCB is disrupted at least in some

patients (Ravaglia et al., 2007), and suggests that a syrinx may contain extracellular fluid from the vasculature.

CSF pressure dissociation

It has been proposed that in syringomyelia associated with lesions at the foramen magnum, the focal subarachnoid blockage can place mechanical stress on the spinal cord. This occurs due to the changes in CSF pressure above and below the block, which in turn, corresponds to changes in venous pressure. Levine states that this change results in the collapse of vessels rostral to the block, and dilation of vessels caudal to the block, placing stress on the spinal parenchyma. Continual stress causes tissue destruction, and damage to capillaries and venules may allow plasma filtrate to pass across the BSCB and into the cord (Levine, 2004).

Intramedullary pulse pressure theory

In agreement with a number of other theories, the 'intramedullary pulse pressure theory,' proposed by Greitz and colleagues states that a syrinx consists of extracellular fluid, and is the result of cord tethering. The theory proposes that the cerebellar tonsils may cause cord tethering when there is a Chiari malformation present. This mechanism proposed that an increase in pulse pressure within the spinal cord itself, relative to subarachnoid space pressure causes the spinal cord to distend near the site of tethering. This distension causes mechanical damage to surrounding tissue, and results in the accumulation of extracellular fluid within the tissue, initiating syrinx formation (Josephson et al., 2001, Greitz, 2006).

Extracanalicular syringomyelia

Accumulation of extracellular fluid

It is well established that there is a breakdown in the BSCB following traumatic spinal cord injury (Mautes et al., 2000). This leads to the development of vasogenic oedema (Goodman et al., 1974, Beggs and Waggener, 1975, Griffiths, 1975, Martinez et al., 1981, Lemke and Faden, 1990, Sharma and Olsson, 1990) and haematoma, which often spreads into the watershed area in the grey matter (Josephson et al., 2001, Ravaglia et al., 2007). Klekamp proposes that extracellular fluid accumulation could contribute to both canalicular and extracanalicular syrinx formation. He suggests that a syrinx is formed due to an accumulation of extracellular fluid in the spinal cord that is unable to be removed due to either: a blockage of CSF pathways; or, extracellular fluid flow exceeding interstitial space volume. Klekamp states that this could be due to blockage of perivascular spaces, cord tethering, or changes in arterial or venous blood flow in the spinal cord or obstruction of CSF flow (Klekamp, 2002).

Intramedullary pulse pressure theory

This theory has also been applied to extracanalicular syringomyelia, whereby arachnoiditis, bone fractures or tumours in the subarachnoid space effectively tether the spinal cord (Josephson et al., 2001, Greitz, 2006a). Prior to this theory, Williams had proposed that when arachnoiditis is present, one cause of cyst formation is tethering of the cord, resulting in mechanical damage to tissue through tearing and shear stress disrupting cells and blood vessels (Williams, 1980b).

Conclusion

Despite the many theories that have been put forward to explain the mechanisms underlying syringomyelia, none of them, as yet, seems to encompass all aspects of the condition. Some can only be applied to one type of syringomyelia, and others have very little clinical or experimental evidence to support them. Since treatments for the condition are based on these proposed theories, and given that outcomes from treatments are often not effective, it is important to work towards a better understanding of syringomyelia.

Recently, more emphasis has been placed on the contribution of extracellular fluid to syrinx formation and enlargement. One possible source of extracellular fluid is from the vasculature. This points to the need for further investigation into the structure and function of the BSCB in syringomyelia, including components such as astrocytes that play an important role in the maintenance of the barrier.

Animal models

Given the infeasibility of testing most of these theories in human patients, it would be valuable to have a clinically relevant animal model. A number of animal models have been used to test proposed theories of syrinx pathogenesis, and to gain further insight into the cellular and morphological basis of syringomyelia. The following section will review animal models that have been developed to date.

Spontaneous

There have been a few reported cases of syringomyelia occurring spontaneously in animals. A report in the 1930s pointed to spinal cavitation and gliosis in rabbits interbred for many generations (cited in (McGrath, 1965, Madsen et al., 1994)). Later, Kuwamura et al reported a murine model of congenital hydrocephalus. In these animals, the spinal canal was enlarged, with oedema in the extracellular space surrounding the central canal. Tracer studies indicated that CSF flowed across the ependymal lining into the spinal parenchyma. The authors

demonstrated that plugging of the central canal at the level of the obex in these animals resulted in decompression of the central canal, supporting Gardner's hydrodynamic theory (Kuwamura et al., 1978). There have been infrequent reports of syringomyelia occurring in horses (Hamir, 1995), cats (Tani et al., 2001, Kitagawa et al., 2007), and in a number of small-dog breeds (McGrath, 1965, Cauzinille and Kornegay, 1992, Itoh et al., 1996, Jung et al., 2006, Park et al., 2009).

Currently, the most commonly reported cases of spontaneous syringomyelia occur in cavalier King Charles spaniels (Rusbridge et al., 2000, Rusbridge et al., 2005, Chandler et al., 2008, Stalin et al., 2008). Due to the selective breeding of cavalier King Charles spaniels, in accordance with recommendations by breeder's associations, and a lack of genetic variance between breeding pairs, a characteristic feature of this breed is a small occipital bone. The result of this is a diminished caudal fossa, which is unable to accommodate the cerebellum and brainstem. This produces a Chiari-like malformation, similar to the Chiari type I malformation occurring in humans (Rusbridge et al., 2000, Rusbridge and Knowler, 2004). It is estimated that 95% of cavalier King Charles spaniels have a Chiari-like malformation and over half of these develop syringomyelia (Rusbridge and Knowler, 2003). The studies conducted so far suggest that the cavalier King Charles spaniel is a valuable model of Chiari-associated syringomyelia that could provide clues to the pathogenesis of the human condition. Clinically they have some neurological features in common. Clinical signs are generally associated with pain, and repeated scratching of the neck or shoulder area, which may be indicative of pain or dysesthesia (Rusbridge et al., 2000). Wittaker et al compared CSF composition between animals with a Chiari malformation and those with a Chiari malformation and syringomyelia. The authors reported that dogs with syringomyelia had a higher nucleated cell count, higher protein concentration, and higher number of neutrophils than those without syringomyelia (Whittaker et al.). A correlation has also been found between increased crowding in the caudal cranial fossa and syringomyelia in dogs with Chiari malformations (Driver et al., 2010). Rusbridge et al are setting up a worldwide DNA database to look at the heritability of Chiari malformations and syringomyelia in this breed in the hope of identifying the genes that may be involved. It is likely that information gathered in these animals can be extrapolated to the human condition (Rusbridge et al., 2005).

Communicating syringomyelia

The most commonly used model of experimentally induced syringomyelia was developed by McLaurin et al in 1954, and involved the intracisternal injection of kaolin. Kaolin is a hydrous aluminium silicate clay, that following administration into the cisterna magna, produces an

inflammatory response, dense arachnoiditis, and obstructs the CSF flow pathway from the fourth ventricle to the subarachnoid space (Rivlin and Tator, 1978b). The ventricles enlarge and result in raised intracranial pressure. Although CSF production continues at the same rate, it has been observed that within 3 weeks the pressure within the ventricles stabilises, indicating that an alternative outflow pathway or reabsorption process must be involved. The spinal cord is thought to act as a compensatory mechanism. In support of this, the development of hydrocephalus has been shown to give rise to dilatation of the spinal canal (Eisenberg et al., 1974, Faulhauer and Donauer, 1985). Faulhauer and Donauer studied intracranial pressure using this model in cats. They demonstrated that intracranial pressure in hydrocephalic animals decreased as the central canal dilated, supporting this mechanism of syrinx formation (Faulhauer and Donauer, 1985).

McLaurin et al suggested that the dense arachnoiditis compressed the blood vessels on the surface of the cord, producing spinal cysts by ischaemia. This was in agreement with the ischemic theory of syrinx formation ((Mc et al., 1954) cited in (Madsen et al., 1994)). Other researchers carried out experiments using models of ischemic spinal cord injury however, and found no evidence that an enlarging syrinx was produced (Wilson et al., 1969, Madsen et al., 1994, von Euler et al., 2002). Later studies, involving this model, also disputed the ischemic contribution by demonstrating that an ischemic injury produces lesions dissimilar to those produced with the hydrocephalus model (Hall et al., 1975). The kaolin model of hydrocephalus and noncommunicating syringomyelia developed by McLaurin et al has been used by numerous research groups since, and has been applied to different animal models. Differences between the human condition and these models have been noted that may limit the relevance of the kaolin model of hydrocephalus. Intracranial pressures are different in humans and these experimental animals. In humans, pressures have been reported to be equal in the head and spine at rest. CSF volume is much greater in humans, widespread arachnoiditis is not characteristic of the human condition, and tonsillar herniation is usually part of the pathology (Williams, 1980a). However, the kaolin model has been demonstrated to have some features that are consistent with the human condition. Extravasation of CSF from the canalicular syrinx to the spinal parenchyma occurs in both the animal model and the human condition. Histologically, similar changes have also been reported in the central grey matter surrounding the cavity (Eisenberg et al., 1974, Hall et al., 1976).

While this model may not perfectly represent the human condition, it has been very useful in adding to our knowledge on syringomyelia (Williams and Bentley, 1980). Chakrabortty et al used this model to investigate the ultrastructural changes around the syrinx in rabbits. They

reported stretching and flattening of ependymal cells, rupturing of the ependymal lining, demyelination, increased numbers of glial cells, oedema, and dilated perivascular spaces at the level of the syrinx (Chakrabortty et al., 1997). Yamada et al found blood flow to be impaired in the cervical cord adjacent to the cavity in dogs (Yamada et al., 1996, Chuma et al., 1997). Voelz et al used the intracisternal kaolin model in rats to examine the pathways by which CSF moves out of the spinal canal when there is an obstruction at the foramen magnum. The authors infused ferritin into the cisterna magna of animals with induced hydrocephalus and demonstrated that CSF moves from canalicular syrinxes, across the ruptured ependymal lining, into the subarachnoid space, spinal nerves, and is taken up by epidural lymphatic vessels (Voelz et al., 2007). In support of Gardner's theory, experiments in which researchers blocked the central canal, preventing communication between the fourth ventricle and the syrinx, resulted in decompression of the cavity (Becker et al., 1972).

In contradiction to Gardner's theory a number of studies have found that the central canal is not patent in all animals following the injection of kaolin into the cisterna magna, although all of these had a dilated central canal (Chakrabortty et al., 1997). Other studies demonstrated that animals with hydocephalus did not develop syringomyelia (Hall et al., 1976, James et al., 1978, Williams and Bentley, 1980). This suggests that hydrocephalus may not always be enough to initiate syrinx formation (Madsen et al., 1994). Similar models, aimed at obstructing the fourth ventricle have also been created. Milhorat et al used an inflatable balloon inserted at the craniocervical junction to induce hydrocephalus in rhesus monkeys (Milhorat et al., 1970). Yamazaki et al implanted tissue from a mammary tumour into the posterior fossa of rats, causing compression of the cerebellum. Central canal dilatation was observed from C-5 to T-8. Histologically, similar changes were observed in these animals as in the kaolin model, such as flattening and stretching of the ependymal cells and interstitial oedema (Milhorat et al., 1970, Yamazaki et al., 1995). However, the intracisternal kaolin model is still the most commonly used and widely accepted model of communicating syringomyelia.

Noncommunicating canalicular syringomyelia

Milhorat and colleagues developed a model of noncommunicating canalicular syringomyelia. The authors injected kaolin into the dorsal columns and central grey matter of the cervical spinal cord of Sprague-Dawley rats. The procedure caused transient weakness in the hindlimbs in 4 of 30 animals immediately after surgery. A number of animals developed a degree of neurological impairment 14 to 42 days later, but this was not sufficient to cause a significant deficit. Histology demonstrated kaolin and leukocytes in the spinal parenchyma at

the injection site, which had travelled to the central canal and had moved towards the fourth ventricle after 24 hours. The kaolin caused ependymal cells to proliferate within the central canal, forming adhesions, which obstructed the central canal at one or more levels rostral to the injection site. In all animals, a dilated central canal, forming an ependyma-lined syrinx, had developed at 48 hours. Stretching of axons, cell loss, and the development of myelin droplets were observed, consistent with previous studies of hydrocephalus (Milhorat et al., 1993). This model has since been used in other laboratory investigations (Rivlin and Tator, 1978a, Stoodley et al., 1999, Stoodley et al., 2000, Lee et al., 2005). Stoodley et al conducted a CSF flow study using this model. The authors demonstrated that at all time points investigated, CSF flows towards the central canal through perivascular spaces, even in the presence of a large canalicular syrinx, which is presumably under high pressure. This supports the arterial pulsation perivascular flow theory (Stoodley et al., 2000). It could be argued that this model does not completely represent the clinical condition, since there is no abnormality at the craniocervical junction. However, the model does produce many of the morphological changes observed in humans (Milhorat et al., 1993). This is currently the only animal model that produces a noncommunicating canalicular syrinx without hydrocephalus. It produces a canalicular syrinx reliably, without evidence of significant pain or neurological impairments. As such, it can be used to study the condition for an extended period.

Noncommunicating extracanalicular syringomyelia

Early experimental models of spinal cord injury involved a laminectomy, followed by contusion of the spinal cord. Trauma to the spinal cord was induced by spinal cord transection (Schubert, 1973, Ikeda and Nakagawa, 1998, McKay et al., 2007), weight-drop (Freeman and Wright, 1953, Noble and Wrathall, 1985), compression clip (Rivlin and Tator, 1978a, Cohen et al., 1985, Wallace et al., 1987, Fehlings et al., 1989), or by photochemical thrombosis (Prado et al., 1987). A number of these studies noted that cavities were present in the spinal cords of some animals following traumatic injury (Freeman and Wright, 1953, Prado et al., 1987, Wallace et al., 1987). The formation of cavitations in these models pointed to the importance of injury in the formation of a syrinx. However, not all animals developed these cavities, or cavities were reabsorbed over time (Freeman and Wright, 1953). This suggested that trauma alone may not be sufficient to produce syringomyelia, and a more reliable animal model of extracanalicular syringomyelia was needed.

Cho et al used a weight drop injury to produce mild and severe contusive spinal injury at T-7 to T-8, followed by a subarachnoid injection of either 100 or 200 mg kaolin in female Japanese White rabbits. In the weight drop method, a rod of a specified weight is dropped

from a standard height onto the exposed spinal cord. The impact could then be calculated in g/cm of force. Kaolin injected into the subarachnoid space would induce an inflammatory reaction, and dense arachnoiditis would develop, as described in the hydrocephalus model of syringomyelia (Mc et al., 1954). The authors reported that in the 100 mg kaolin group, 41.7% of animals developed a syrinx, while 55.5% of animals in the 200 mg kaolin group developed a syrinx in the first few weeks, and 100% had developed a syrinx at 4 – 9 weeks. The cavities described using this model were generally circular, separate from the central canal, and occurred at or near the site of kaolin injection. Histologically, haematoma, subarachnoid haemorrhage, necrosis, and tissue damage were observed. Other animals received a spinal cord injury only or subarachnoid injection of kaolin only. Of the spinal cord injury animals only 12.5% of animals developed a syrinx, while no cavity was present in animals in the kaolin-only group. These results suggest that arachnoiditis as the primary mechanism underlying syrinx formation is unlikely. However, it does point to the importance of arachnoiditis in the enlargement of an existing cyst. It also demonstrates the importance of a subarachnoid obstruction when creating a reliable and reproducible model of posttraumatic syringomyelia (Cho et al., 1994). More recently, Turgut et al used this same procedure. However, significant neurological deficits were reported, with 60% of animals receiving a mild injury, developing hindlimb paralysis, while all of those receiving the severe injury developed paraplegia. Over 70% of all these animals died within 6 weeks. MR imaging detected slight enlargement of the ventricles and central canal, but was unable to identify spinal cavities. At autopsy, microcysts could be seen around the central canal, which was lined by flattened and stretched ependymal cells. The ependymal lining had ruptured in some animals. This model only represents the initial stages of posttraumatic syringomyelia, and no enlarging syrinx was observed in any animals. The involvement of the ventricular system and the central canal is not characteristic of posttraumatic syringomyelia, except when a syrinx in the spinal parenchyma expands to encompass the central canal (Turgut et al., 2005).

Compression clip has been used by many researchers to produce a traumatic spinal cord injury of varying severity (Fehlings et al., 1989). This method involves the compression of the spinal cord between an adapted aneurysm clip for a specified time. Seki et al employed this method in combination with subarachnoid kaolin, to induce posttraumatic syringomyelia in Wistar rats. These animals developed hindlimb paralysis, which partially recovered over the subsequent 6 weeks. The von Frey hair test demonstrated that the animals receiving the compression and injection of kaolin displayed a significantly lower threshold for mechanical pressure. Animals had not developed a posttraumatic syrinx after 1 or 2 weeks following

injury. However, all animals had developed a posttraumatic cyst at 6 weeks. Glial scarring, macrophages, fibroblasts and collagen were evident around the cavity. The authors demonstrated apoptotic cell death in neurons, macrophages, and oligodendrocytes (Seki and Fehlings, 2008). While this model reflected many of the characteristics of posttraumatic syringomyelia, it may not necessarily model the type of injury observed in spinal cord injury patients. Trauma is more likely to be a mixture of contusive and continuous compression injury (Rowed et al., 1978). The model put forward by the authors did not produce a posttraumatic syrinx in the first 2 weeks after the initial injury. This is consistent with the delay between injury and syrinx development observed in humans. However, in an animal model this is not always feasible. The severe neurological impairment (pain, paralysis), while accurately modelling symptoms experienced by some patients, is not ideal in animal models (Seki and Fehlings, 2008). An animal model that can produce posttraumatic syrinxes reliably, soon after surgery with less pain and discomfort for animals would be preferable.

An alternative model of posttraumatic syringomyelia was developed using an intraparenchymal injection of the AMPA-metabotropic receptor agonist quisqualic acid in the rat spinal cord. This was found to produce spinal cavitations in 23 of 25 animals, caused cell death, proliferation of astrocytes, and induced inflammatory cells (Yezierski et al., 1993). This model was based on previous studies that demonstrated that following traumatic spinal cord injury, there is an increase in excitotoxic amino acids, in particular glutamate at the site of injury. These excitotoxic amino acids at high levels cause cell death (Headley and Grillner, 1990, Panter et al., 1990, Liu et al., 1991, Marsala et al., 1994, Yang et al., 2001). Similar results are observed in animals injected with quisqualic acid as those receiving a traumatic injury (Basso et al., 1996, Yezierski et al., 1998). Studies have since combined the intraparenchymal quisqualic acid injection with a subarachnoid injection of kaolin. This has been demonstrated to produce cavities that extend over a greater number of spinal levels, and are larger than those produced from quisqualic acid alone (Stoodley et al., 2000, Yang et al., 2001, Brodbelt et al., 2003a). These cavities are reported to be histologically comparable to traumatic spinal cord injury models (Yang et al., 2001). This model has been demonstrated to be reliable, producing syrinxes in ~80% of animals without causing significant neurological deficits (Stoodley et al., 2000, Yang et al., 2001, Brodbelt et al., 2003a). A criticism of this model is that it may not represent the contusive and compressive trauma observed in humans following spinal cord injury (Seki and Fehlings, 2008).

Experimental studies, combining a traumatic or excitotoxic injury with a subarachnoid space obstruction suggest that the initial injury and excitotoxic cell death may cause the initial cyst

formation, and the subsequent enlargement of the cysts and progression to syringomyelia is likely to be caused by the arachnoiditis (Cho et al., 1994, Yang et al., 2001, Seki and Fehlings, 2008). This supports the theories that consider a CSF obstruction in the subarachnoid space to be a significant component of syrinx enlargement. Whether this is due to the arachnoiditis tethering the spinal cord and causing mechanical damage to the cord as it distends (Josephson et al., 2001, Greitz, 2006), by blocking the fluid outflow pathways (Klekamp, 2002), or uncoupling the CSF pulse waves and arterial pulsations (Bilston et al., 2010), is yet to be elucidated.

Conclusion

All of the animal models that have been created so far have shortcomings, and caution needs to be exercised when applying results from animal studies to humans. Human spinal cord injury, hydrocephalus and Chiari I malformations are complex conditions that are difficult to mimic in an experimental setting. However, the many features present in the animal models that are comparable with the human condition demonstrate their usefulness. These approaches may provide useful information as to what is initiating cyst formation and the driving forces behind syrinx enlargement.

Spinal cord anatomy

Gross anatomy

The gross anatomy of the central nervous system is well described. This section will only cover those aspects directly related to the movement of fluid within the spinal cord, and structural components that may be relevant to the studies conducted in this thesis.

Cellular organisation

A cross section of the spinal cord reveals that it is organised into an inner grey matter, and surrounding white matter. The grey matter is arranged in a butterfly shape containing neurons and neuroglia, while the outer white matter consists primarily of myelinated axon fibre bundles and spinal tracts that run longitudinally through the spinal cord. Rexed was the first to describe the cytoarchitecture of the spinal cord following a histological study in cats. Rexed identified 10 laminae or cell layers in the grey matter including a region encompassing the central canal in the cat spinal cord (Figure 5) (Hu et al., 2007). This delineation has since been applied to the human spinal cord. The differences in the cell layers have been attributed to differences in function. For example, the cells in lamina I contribute to the regulation of pain signals, and generally project to higher central nervous system centres (Jean-Xavier et al., 2006, Lopez-Vales et al., 2007). Laminae VIII, IX, and some of VII make up the ventral horn

and contain the motor neurons, laminae I-VI make up the lateral horns and contain sensory neurons, and lamina VII makes up the intermediate zone and contains interneurons (Spilker et al., 2001, Nomura et al., 2002).

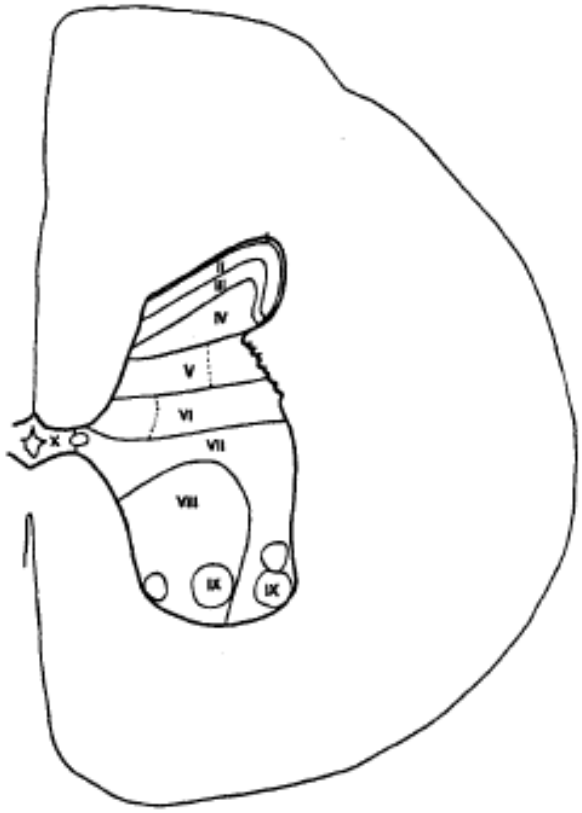

Figure 5: Schematic drawing of the lamination of the spinal cord grey matter [from (Rexed, 1952), with permission of John Wiley and Sons].

The other principal cellular component of the spinal cord is glia. Glial cells provide the structural framework and metabolic support for neurons. The two main types of glia are microglia and macroglia. Microglia remove cell debris and waste products. They are mobilised in response to infection and other pathological changes (Li et al., 2000, Kalderon et al., 2001). Macroglia are divided into four subtypes: astrocytes, oligodendrocytes, Schwann cells and ependymal cells. Schwann cells form the myelin sheath around peripheral axons, while oligodendrocytes form the myelin sheath around central axons. These myelin sheaths are critical for rapid impulse transmission.

Astrocytes were originally thought to simply provide structural and metabolic support for neurons. However, the complexity of this role, and other functions, was not well understood. Research has since demonstrated that they are a major component of the BSCB (Celichowski et al., 2006), they re-absorb neurotransmitters, and regulate nutrient and ion concentration. In doing so, astrocytes regulate neuronal activity (Brechtel et al., 2006), and they play a role in injury response, forming scar tissue at the site of injury. Changes in calcium concentration in

astrocytic endfeet have been found to modulate vascular tone in the vessels they are in contact with (Nedergaard et al., 2003). Cell culture studies demonstrate that neurons grown in the presence of astrocytes develop around seven times more synapses than those cultured without astrocytes (Brock et al., 2006, Ding et al., 2006). Astrocytes may also regulate neurogenesis, inducing the generation of neurons from stem cells (Kamada et al., 2005, Randall et al., 2005).

Ependymal cells are cuboidal or columnar in shape and line the ventricles in the brain and the central canal in the spinal cord. In early life the fluid-facing surface of ependymal cells is coated with cilia. In adulthood, cilia may remain on ependymal cells lining the ventricles in the brain, while in the spinal cord, ependymal cells are only sparsely lined with microvilli. They regulate the concentration of ions in the CSF, and the movement of CSF into the brain and spinal parenchyma. The large ciliated cuboidal ependymal cells surround the capillaries in the choroid plexus and are in contact with the CSF within the ventricles. These cells are connected by tight junctions and secrete CSF into the ventricles via active and passive mechanisms (Liu et al., 2000, Kalderon et al., 2001). Specialised types of ependymal cells called tanycytes are found in the floor of the third ventricle and cervical spinal canal (Barshes et al., 2005). Tanycytes differ from other ependymal cells in that they are elongated and have numerous microvilli and few cilia. They are characterised by long radially projecting processes. In the spinal cord these processes connect the ependyma lining the central canal to the glia limitans or to blood vessels (Rafols and Goshgarian, 1985). Although the function of tanycytes is not completely understood, it is thought that they are involved in the transport of molecules from the CSF to the blood (Gould et al., 1990, Bruni, 1998).

A number of pathological conditions are associated with glial dysfunction, demonstrating the importance of these cells. Multiple sclerosis is caused by the failure of oligodendrocytes to remyelinate axons (Hamers et al., 2001). Parkinson's disease, Huntington's disease, and amyotrophic lateral sclerosis are all caused by glial impairment (Durozard et al., 2000, Aamodt, 2007, Moller, 2010, Halliday and Stevens, 2011). An association between the number of astrocytes and brain complexity also points to the significance of glial cells. Studies demonstrate that leeches have 1 astrocyte to every 25 – 30 neurons, rodents have 1 astrocyte to every 3 neurons, while humans have 1 to every 1.4 neurons (Nedergaard et al., 2003).

Spinal meninges

The spinal cord and the spinal nerve rootlets are enclosed within the meninges. The meninges are specialised membranes that protect the spinal cord, provide stability and absorb force applied to the spinal column. The meninges are comprised of three layers: the outer dura mater, the arachnoid mater, and pia mater. The dura mater is a dense fibrous sheath surrounding the spinal cord. The dura provides tensile strength, is flexible and elastic, allowing movement during flexion and extension of the spine (McKay and McLachlan, 2004). In the spine the dura is surrounded by adipose tissue, which allows dural expansion in response to increases in blood flow and CSF volume (Martins et al., 1972, Reina et al., 2009).

The arachnoid outer layer is comprised of tightly packed cells, many tight junctions and no extracellular collagen. The arachnoid mater is believed to form a barrier between CSF in the subarachnoid space, and circulating blood in the dura. In humans, the dura and arachnoid layer are so closely situated that it is thought that there is no true subdural space (Reina et al., 2002). Other layers of the arachnoid consist of cells that form desmosomes and gap junctions. It was thought that the subarachnoid space was spanned by trabeculae that connect the arachnoid and pia mater (Weller, 2005). However, there is a disparity in the literature as to the numbers and extent of trabeculae (Parkinson, 1991). The pia mater separates the brain and spinal cord from the subarachnoid space, and also separates perivascular spaces and subpial vessels from the subarachnoid space (Tsai et al., 2004, Yeoh et al., 2004). A study of human spinal cords using scanning electron microscopy described a partially fenestrated intermediate layer between the arachnoid and pia mater, a finding that differs from the cerebral meninges and observations from animal studies. Laterally, trabeculae are present, consistent with observations in cat and dog spinal cords (Talmadge et al., 2002). In contrast to this, an anatomical study of human cadavers reported that trabeculae were absent in the anterior subarachnoid space, few trabeculae were present posteriorly in the upper cervical spinal canal, while an increasing number of trabeculae were present in the lower cervical and lumbar spinal canal (Parkinson, 1991). The trabeculae are in contact with nerves and blood vessels on the surface of the cord and the pia mater (Norreel et al., 2003).

It was believed that a leptomeningeal (arachnoid and pia) sheath surrounds nerves and blood vessels as they enter the brain and spinal parenchyma. As such, it was believed that the perivascular space or “Virchow-Robin space” as it is sometimes called, lies between this sheath and the blood vessel. Based on this, a communication between perivascular spaces and the subarachnoid space was assumed (Hashimoto et al., 2004, Koda et al., 2004). This view has since been disputed, as scanning electron microscopy studies have shown that

perivascular spaces communicate with the subpial space, but are separated from the subarachnoid space (Tsai et al., 2004). However, in microscopic studies of human specimens of leptomeningitis, inflammatory cells were observed in the subarachnoid space, subpial space, and perivascular spaces, suggesting that there is migration of molecules and cells between layers (Tsai et al., 2004). The injection of tracers such as horseradish peroxidase into the subarachnoid space of animals has demonstrated that tracer flows into perivascular spaces. This supports the initial theory that the pia mater is permeable to some substances (Cheng et al., 2003). The leptomeningeal sheath around veins lacks the outer layer observed around arteries. Anatomical studies suggest that perivascular spaces around veins are continuous with the subpial space (Moshonkina et al., 2002).

Fluid filled cavities within the central nervous system

The central nervous system of vertebrates is unique in that it contains a ventricular system. This system consists of chambers and narrow channels containing CSF. Each cerebral hemisphere contains a lateral ventricle, and the third ventricle is located in the diencephalon. The fourth ventricle is located between the brainstem and the cerebellum. The interventricular foramina of Monro connect the lateral ventricles with the third ventricle. The aqueduct of Sylvius connects the third and fourth ventricles. The fourth ventricle descends into the central canal which extends the length of the spinal cord. CSF is believed to circulate through the ventricular system, from the lateral ventricles to the third and fourth and then into the cisterna magna and subarachnoid space, around the cauda equina, and eventually returns and re-enters the blood circulation through arachnoid granulations (Trudrung et al., 2000, Kalderon et al., 2001). It has been suggested that a small amount of CSF also enters the central canal from the fourth ventricle (Dalal et al., 1999).

Fluid interfaces

Fluid interfaces form a protective barrier between the parenchyma and blood or CSF. Exchanges between CSF and central nervous system tissue occur either across the ependymal layer at the ventricles (brain) or central canal (spinal cord), or across the glia limitans, which creates the interface between central nervous system tissue and pia mater. Ependymal cells allow free paracellular diffusion between the central nervous system and CSF. The pia mater does not restrict movement of fluid between the subarachnoid space and subpial space. However, the glia limitans, which is comprised of a complex cellular network of glial origin, regulates fluid movement (Baldridge et al., 2002, Palmer, 2010). The blood-brain/spinal cord barrier (BBB/BSCB) acts as a barrier between the vasculature and the spinal cord microenvironment. The BSCB is comprised primarily of endothelial cells that line capillaries

in the spinal cord. These endothelial cells are connected by tight junctions, and are surrounded by a dense basement membrane. The basal membrane is in close contact with surrounding astrocytic endfeet (Suzuki et al., 1985, Sinescu et al., 2010).

Vasculature

Blood flow and neural function in the spinal cord are closely related. The vasculature plays an important role in the exchange of nutrients and gases, and regulates temperature by increasing blood flow to prevent localised temperature elevation (Koizumi et al., 1954). Blood vessels also act as a 'sink' to remove neurotransmitters. Angiogenesis is an essential part of the development and differentiation of the spinal cord, a number of angiogenic factors induce growth and differentiation of nerve cells and the vascular network (Zagzag, 1995).

Capillary networks

Capillaries in the spinal cord are clearly delineated based on anatomical location within the anterior, lateral and posterior columns of the spinal cord. The central grey matter is highly vascularised, which is found to correspond to areas containing synapses rich in mitochondria rather than nerve cell bodies. This suggests a correlation between tissue energy exchange and level of vascularisation (Scharrer, 1945, Nomura et al., 2002).

Arterial network

Anterior, posterolateral, and dorsal arterial networks supply the spinal cord (Figure 6). The anterior spinal artery extends from the most rostral part of the cervical cord to the filum terminale, and is located at the ventral median fissure. There are two dorsal spinal arteries found immediately ventral to the dorsal root entry zone, which generally extend along the cervical, thoracic and lumbar cords. The dorsal spinal arteries may form a continuous channel or branch into two or more parallel vessels. The lateral spinal arteries are located between the dorsal and ventral spinal roots. The median dorsal spinal artery is located in close proximity to the dorsal septum, and usually extends along all spinal cord segments. In addition to these longitudinal arteries, transverse arterial networks are also present on the surface of the spinal cord (Anderson et al., 2009, Sinescu et al., 2010).

The two vertebral arteries extend rostrally and converge to form the basilar artery. The anterior spinal artery branches off the vertebral arteries caudal to the basilar artery. Radicular arteries extend into the spinal canal through the intervertebral foramina, the entry point for spinal nerve roots and the spinal root ganglion. These radicular arteries diverge into the anterior and dorsal radicular arteries that run parallel to the corresponding spinal roots (dorsal

and ventral spinal roots respectively). Other larger radicular arteries join the anterior spinal artery. The number of anterior and dorsal radicular arteries that merge with the anterior and dorsal arteries is widely variable, although there are generally greater numbers in the cervical and lumbar enlargements and far fewer in the thoracic cord (Anderson et al., 2009, Sinescu et al., 2010).

At intermediate places along the anterior spinal artery are branches known as the ventromedian arteries. These arteries extend along the ventromedian fissure, generally in parallel along either side of the cord, entering the spinal cord between the grey commissure and ventral horn. The ventromedian arteries divide into many smaller vessels that supply the anterior and ventral part of the lateral white matter columns and the central grey matter. Penetrating branches from the pial arterial system that intersect the arteries running longitudinally along the spinal cord supply the remainder of the spinal cord (Anderson et al., 2009, Sinescu et al., 2010).

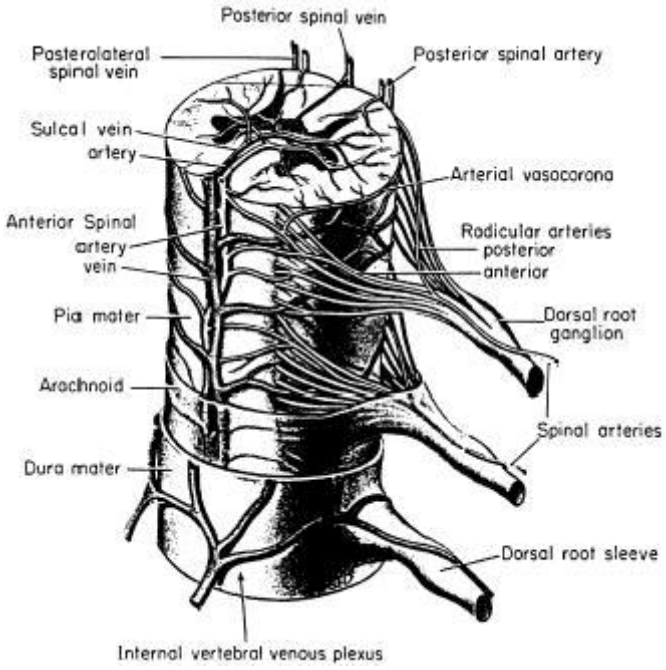

Figure 6: Arterial supply and venous drainage of the spinal cord [from (Lin et al., 2003), with permission of Demos Medical Publishing].

Venous drainage

The distribution of the venous network is similar to that of the arterial network (Figure 7). An anterior spinal vein runs parallel to the anterior spinal artery along the length of the spinal cord. However, the vein decreases in diameter in the thoracic cord. The dorsal spinal vein runs next to, or just ventral to the dorsal spinal artery. The dorsal and anterior veins are interconnected by numerous small diameter veins that encircle the spinal cord, although larger veins are sometimes present, and are more likely to be found at the cervical and lumbar

enlargements. Penetrating spinal veins drain into vessels on the surface of the cord such as the anterior and dorsomedian veins (Nomura et al., 2002).

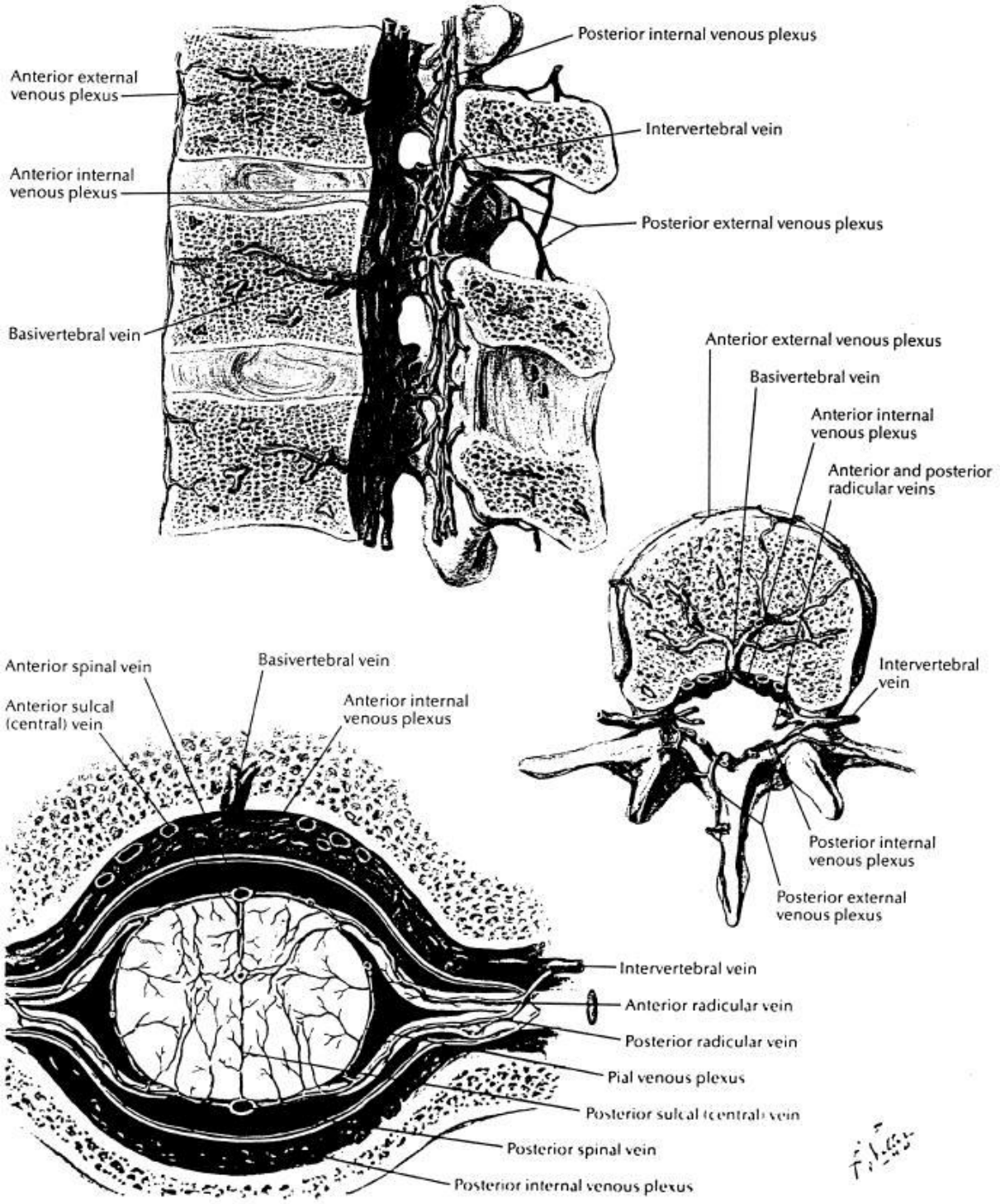

Figure 7: Veins of the spinal cord and the vertebral venous plexus [from (Lin et al., 2003), with permission of Demos Medical Publishing].

Lymphatic drainage

Lymphatic vessels have not been identified within the central nervous system. However, there is evidence that lymphatic drainage contributes to removal of toxins, interstitial fluid and CSF from the central nervous system. Laboratory investigations in animals have demonstrated that

CSF tracer molecules injected into the ventricles or subarachnoid space have been cleared from the spinal cord and are found in the lymphatic system in the spine, neck or head (McKay et al., 2007, Seif et al., 2007, Zhao et al., 2007, Reynolds et al., 2008). Bulk flow of fluid from the spinal cord interstitial spaces and subarachnoid space to the lymphatic system is estimated to contribute to one third (McKay et al., 2007) to one half (Boulton et al., 1997, Button et al., 2008, Negredo et al., 2008) of that removed by the venous system. It is thought that this provides an alternative pathway in areas where the BBB/BSCB prevents the removal of large molecules.

Fluid in the central nervous system

Cerebrospinal fluid

Cerebrospinal fluid is a clear liquid that cushions the brain and spinal cord from physical damage and transports chemicals, nutrients, waste products and other solutes between different compartments (Kalderon et al., 2001). It covers all surfaces of the central nervous system. It was thought that CSF was produced solely in the choroid plexus. However, Milhorat et al demonstrated that CSF production did not change following the removal of the choroid plexus, suggesting that it is not the only source of production (Tripovic et al.). As such, it is now thought that CSF is produced in the ventricular system, choroid plexus, ependyma, or parenchyma (Bamford et al.). It is estimated that the choroid plexus produces 80% or more of CSF (Lin et al., Kusunoki et al., 1978). Clinical studies suggest that CSF is produced at a rate of 20 mL/hour or 500 mL/day (Dashtdar and Valojerdi, 2008, Lin et al., 2008, Yang et al., 2008). The total volume of CSF is ~150 mL, suggesting CSF is replenished three times daily (Bamford et al.).

In humans, the ionic composition of CSF is similar to blood plasma. However, blood plasma is higher in protein, and there are differences in the concentration of ions, amino acids, and lipids. The concentration of Na^+ and K^+ are lower in CSF, while Cl^- is higher. CSF is more acidic, has lower levels of glucose, and contains a number of proteins not identified in plasma samples; predominately glycoproteins that play a role in central nervous system structure and function (Carr et al., 1998, Krenz and Weaver, 1998).

CSF absorption

In humans and other mammals, the primary site of CSF absorption into the vasculature is at the arachnoid villi. Arachnoid villi are herniations of the arachnoid mater that penetrate the dura and invaginate the walls of venous structures. They allow unidirectional flow of CSF into venous blood. The arachnoid villi are in contact with both CSF and blood, and take-up

CSF and deposit it into the blood stream through pores in the endothelial cell layer (Ikeda and Nakagawa, 1998). Absorption via the arachnoid villi has been demonstrated to occur predominately at the superior sagittal sinus (Talmadge et al., 1999). There is now evidence that bulk flow of CSF into the venous system occurs through the choroid plexus itself and directly into intrathecal veins (Bamford et al., Talmadge et al., 1999). There is also evidence that CSF drains into the lymphatic system. Large CSF tracer molecules have been found in lymphatics of the head, neck and spine. Tracer accumulated in dural sacs surrounding the nerve roots at the lumbosacral and cervical levels (Yates et al., 2008). Experimental studies have demonstrated that lymphatic drainage may account for up to 30% resorption in the cat and rabbit (Courtice and Simmonds, 1951, Krenz and Weaver, 1998, McKay et al., 2007).

Extracellular fluid

The extracellular space is estimated to take up 15% of total brain volume (Takeoka et al.). There is believed to be a free exchange of fluid between the extracellular space and CSF, similarities in interstitial or extracellular fluid and CSF composition suggest that CSF may be produced in the parenchyma (Mrowczynski et al., Takeoka et al.). Extracellular fluid in the central nervous system consists of CSF, and of interstitial fluid in the grey and white matter (Caldwell and Ridge, 1983). Interstitial fluid stems from the blood plasma (Krikorian et al., 1982), and water produced by brain metabolism has also been suggested as a possible source, as H_2O is generated when CO_2 is oxidised (Carter et al., 1981).

Blood-spinal cord barrier

Overview

In 1885 Paul Ehrlich made the observation that dyes injected into the vasculature of animals did not stain brain tissue. This led to the discovery that a biological barrier exists between the blood and brain tissue. The BBB/BSCB is comprised of specialised endothelial cells that line capillaries in the brain and spinal cord (Figure 8). This barrier exists in the central nervous system of all vertebrates (Abbott, 2005), and acts as a protective mechanism against variations in metabolite composition in the blood. Endothelial cells of these blood-tissue barriers are characterised by: tight junctions, composed of a number of proteins including zonula occludins, claudins, occludin, and cingulin; adherent junctions (cadherins, catenin, actinin and vinculin); and junctional adhesion molecules (Persidsky et al., 2006). Endothelial cells of the microvasculature in the brain and spinal cord are surrounded by a dense basement membrane, they have a higher mitochondrial content than non-central nervous system capillaries (Oldendorf et al., 1977) and no fenestrations (Abbott, 2005). In close association

with these endothelial cells and components of the BBB/BSCB are pericytes, neurons and astrocytic foot processes (Matthews et al., 1979a). The role of these components is not completely understood, but it is likely that they play a role in regulation and maintenance of the BBB/BSCB (Wolburg et al., 2009).

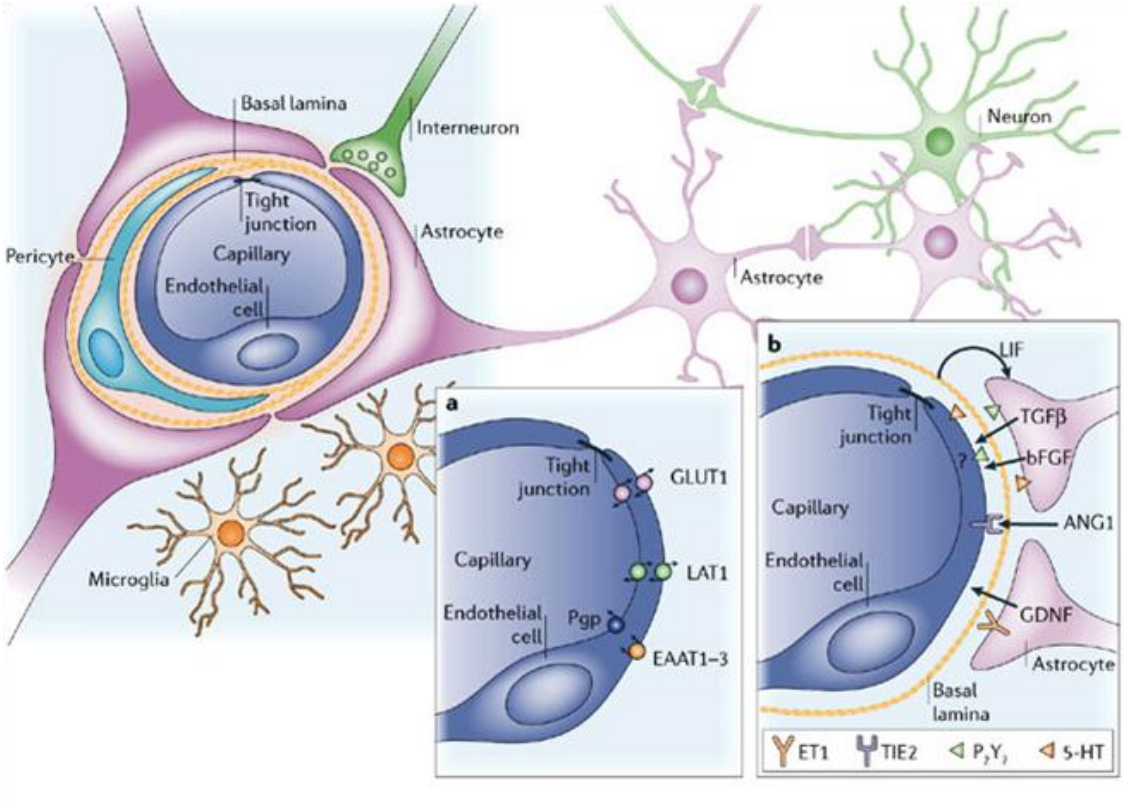

Figure 8: Cellular constituents of the blood-brain/spinal cord barrier [from (Abbott et al., 2006), with permission of Nature Publishing Group].

The structural integrity of the tight junction complex determines the permeability of water-soluble molecules across the barrier. This complex is regulated by phosphorylation, Ca^{2+} signalling and G-proteins (Palant et al., 1983, Sakakibara et al., 1997, Hopkins et al., 2000). Movement of molecules across the BBB/BSCB is restricted not only by a physical barrier (tight junctions), but a metabolic barrier comprising transport systems and enzymes including alkaline phosphatase (Persidsky et al., 2006). These enzymes metabolise nutrients, toxins and other neuro-active solutes from the blood and contribute to the polarisation between the luminal and abluminal membrane surface (Wolburg et al., 2009). Astrocytic foot processes are thought to contribute to the metabolic barrier function through secretory mechanisms. Astrocytic endfeet express high levels of the water channel protein aquaporin-4 (AQP4) and the potassium channel Kir4.1, important regulators of ion and water volume (Gelderd and Peppler, 1979, Matthews et al., 1979a).

There are a number of differences between the BBB and the BSCB. Capillaries in the spinal cord contain glycogen deposits (Suzuki et al., 1985). The function of these deposits is not well understood, although it has been suggested that they may act as a reservoir for energy storage (Matthews et al., 1979a). There is evidence that the BSCB is more permeable than the BBB (Weber and Stelzner, 1977). Laboratory investigations have demonstrated that spinal endothelial cells express lower levels of particular tight junction proteins, adherens junction proteins and transporter molecules, such as zonula occludin-1, occludin, VE-cadherin and β-catenin (Macdonald and Pearson, 1979, Matthews et al., 1979a). These differences may be relevant to spinal cord pathologies and disorders unique to the spinal cord, such as syringomyelia.

Methods for studying blood-spinal cord barrier dysfunction

Dynamic contrast-enhanced MR imaging is a non-invasive technique that can be applied to evaluate BSCB permeability. This technique involves contrast enhancement with gadopentate dimeglumine (Gd). Since Gd is a large molecule, when it is administered intravenously it cannot cross the BSCB unless the barrier is disrupted. This technique produces T-1 – weighted MR images that reveal areas where Gd has diffused into the parenchyma (Haggendal and Dahlstrom, 1973, Magnusson, 1973, Schubert, 1973, Vaptzarova et al., 1973, Reid et al., 1976, Matthews et al., 1979a). This technique is well established in humans, however it is not sensitive enough to detect enhancement in small animal models.

Vascular tracers, including radiolabeled molecules such as [^{14}C]-alpha-aminoisobutyric acid (Goridis et al., 1972), and low molecular weight molecules such as Evans blue albumin and protein luciferase have been employed to investigate the spatial and temporal integrity of the BSCB following spinal cord injury (Carlsson et al., 1973). Horseradish peroxidase (HRP) has also been widely used (Muller and O'Rahilly, 1986a, Noble and Wrathall, 1989, Beggs et al., 2010). HRP is a plant enzyme with a molecular weight of 40 kDa that reacts with the oxidisable substrate of 3-3’ diaminobenzidine (DAB). This reaction produces an insoluble brown reaction product that can be visualised by light microscopy (Muller and O'Rahilly, 1986b).

More recently, studies have focused on immunohistochemical, immunofluorescent and fluorescent live imaging analysis to examine the molecular components of the BSCB. These studies have enabled the structural changes of the BSCB to be evaluated under different conditions. These techniques have helped to elucidate the role of tight junction proteins (zonula occludins-1, Claudin-5), astrocytes, pericytes and endothelial cells in the maintenance

of the BBB and BSCB (Freeman, 1952, Rice and Plaa, 1968, Muller et al., 1986, O'Rahilly et al., 1986a, Mozer et al., 2010). Endothelial barrier antigen (EBA), a protein selectively expressed in rat endothelial cells that possess blood-tissue barrier properties, is also employed to identify BBB and BSCB dysfunction (Perdiki et al., 1998, Nishigaya et al., 2000, Katsu et al., 2010)

Endothelial barrier antigen

EBA is a protein triplet of 30, 25 and 23.5 kDa expressed at the luminal surface of endothelial cells in microvessels possessing blood-tissue barrier properties. EBA can be detected with a mouse monoclonal antibody (Sternberger and Sternberger, 1987), which has been shown to label microvessels in the brain, spinal cord, optic nerve, retina, peripheral nerves, and testicular vessels (Shimoda et al., 1954b, Gillilan, 1958, Perdiki et al., 1998, Ghabriel et al., 2002). In organs where a blood-tissue barrier is absent, such as the liver and kidney, no antigen is expressed (Sternberger and Sternberger, 1987).

The function of EBA remains largely unknown. However, by injecting anti-EBA antibody into rat vasculature, Ghabriel et al demonstrated that anti-EBA localised to endothelial cells in the brain, effectively interfering with EBA. The immunological targeting of EBA in vivo resulted in the opening of the BBB (Ghabriel et al., 2000). This added support to the view that EBA plays an important role in maintaining barrier integrity. EBA is used increasingly as a tool for detecting barrier disruption in the brain and spinal cord, having been used in rat models of experimental allergic encephalomyelitis (EAE) (Sternberger et al., 1989), stab wound injury (Rosenstein et al., 1992) and spinal cord compression (Perdiki et al., 1998). Studies show that in mature rat brains following stab wound injury, directly injured and adjacent microvessels lack EBA expression for up to two weeks following injury. Expression is then restored by three to four weeks (Rosenstein et al., 1992). EBA expression has also been studied in a model of cerebral infarction, with similar results. EBA expression was reduced at the lesion after one day, and while new vessels had formed by day seven, EBA expression was weak or absent for up to 28 days (Nishigaya et al., 2000).

The expression of EBA has been studied in rat spinal cord with and without compression injuries. These findings indicate that EBA is present in almost all microvessels in both grey and white matter in a normal spinal cord, while expression is dramatically reduced following traumatic injury (Perdiki et al., 1998). Experiments using the compression model of spinal cord injury have demonstrated a relationship between loss of EBA and oedema formation, with subsequent re-establishment of expression correlating with clearance of oedema

(Farooque et al., 1994, Perdiki et al., 1998, Ghabriel et al., 2000). These results suggest that EBA may prove useful in the study of syringomyelia.

Implications in disease

Impairment of the BBB or BSCB can contribute to numerous central nervous system pathologies including Alzheimer's disease, tumours, radiation-induced myelopathy, multiple sclerosis, neuropathic pain, amyotrophic lateral sclerosis and spinal cord injury. It is likely a compromised BBB or BSCB may be implicated in many other disorders or occurs in parallel with other diseases, exacerbating the clinical presentation.

Spinal cord injury

Spinal cord injury causes primary damage, occurring immediately, and secondary damage during the acute phase and often progressing over days to weeks and even years (Goridis et al., 1972, O'Rahilly, 1986, Noble and Wrathall, 1989). The initial injury results in the primary mechanical damage to cells, axons and vasculature. Further changes to the vasculature such as haemorrhage and vasodilation are also common (Rawe et al., 1977, Norenberg, 1994, Tator and Koyanagi, 1997). This damage to microvessels triggers the complex series of events that characterises the secondary damage to the cord. In the acute stage, oedema, haemorrhage, inflammation and disruption of the BSCB occur (Mautes et al., 2000). Disrupted blood vessels, cells and axons release toxic chemicals (Mautes et al., 2000, McDonald and Sadowsky, 2002, Thuret et al., 2006). In an animal model of cord transection it was found that barrier disruption was not restricted to the site of injury, suggesting that the vascular response is widespread, leading to subsequent oedema (Noble and Wrathall, 1987). Secondary injury can result in the expansion of damage to areas that were previously unaffected (Goridis et al., 1972, Noble and Wrathall, 1989).

Studies using vascular tracers such as Evans blue, bovine serum albumin, hydrazide and HRP have shown a strong correlation between the degree of spinal cord injury and the degree of altered BSCB permeability (Beggs and Waggener, 1975, Noble and Wrathall, 1989, Maikos and Shreiber, 2007). These changes in vascular permeability have also been found to correspond with structural changes in endothelial cell junctions following spinal compression injury in guinea pig (Jaeger and Blight, 1997). A cascade of events at the molecular and cellular level causes long-term disruption of the BSCB. There is continued infiltration of inflammatory cells, oxidative stress and free radicals, which contribute to BSCB breakdown (Matthews et al., 1979a, O'Rahilly et al., 1986b). There is evidence that astrocytes that are chronically activated also cause long-term BSCB disruption (Nesic et al., 2005).

Significance of BSCB dysfunction in syringomyelia

Experiments using a compression model of spinal cord injury have demonstrated a relationship between loss of EBA and oedema formation, with subsequent re-establishment of EBA expression correlating with clearance of oedema (Farooque et al., 1994, Perdiki et al., 1998, Ghabriel et al., 2000). Such results suggest that damage to the BSCB may indeed play a role in either the development of cord oedema and small initial cysts or the enlargement of small cysts over time to form syrinxes. Failure of the BSCB to repair after spinal cord injury may be pivotal in the subsequent development of posttraumatic syringomyelia.

Although Chiari-associated syringomyelia is not associated with an initial traumatic insult, BSCB dysfunction may still play a role in the development or progression of the condition. There is a well-established association between BSCB dysfunction and conditions such as multiple sclerosis and neuromyelitis optica that occur without traumatic injury. A Chiari-associated syrinx frequently ruptures into the surrounding spinal parenchyma (Milhorat et al., 1995a). This rupture may cause mechanical damage to the spinal tissue, and BSCB breakdown. This may contribute to the enlargement of an existing syrinx.

Aquaporins

Agre and MacKinnon were awarded the 2003 Nobel Prize in Chemistry for their discovery of aquaporins (AQPs) (Fazio et al., 1983a). Since then, AQPs have gained increasing attention for their role in a number of physiological processes. There is also increasing evidence to suggest that AQPs are implicated in numerous pathologies. The following section will review the literature on AQPs, with an emphasis on those found in the central nervous system.

History

Membranes are crucial cell structures, controlling the transfer of solutes into and out of the cell in response to the extracellular environment. Water makes up most of the cell content and is able to diffuse through the lipid bilayer unhindered albeit at a finite rate. The observation that some cells, such as mammalian erythrocytes, display a much higher permeability to water, led to the hypothesis that transport mechanisms facilitated by water-specific proteins may exist (Sidel and Solomon, 1957). Decades later, the first AQP, AQP1 was discovered in red blood cells (Preston et al., 1992). Since then, 13 AQPs have been identified in various human tissues (Ma et al., 1993, Echevarria et al., 1994, Hasegawa et al., 1994, Ishibashi et al., 1994, Jung et al., 1994, Ma et al., 1994, Preston et al., 1994, Raina et al., 1995, Ishibashi et al., 1997a, Ishibashi et al., 1997b, Kuriyama et al., 1997, Ishibashi et al., 1998a, Ishibashi et al., 1998b, Koyama et al., 1998) (Table 2).

Table 2: Aquaporins (AQPs) (Nukada and Koizumi, 1954, Shimoda et al., 1954a, Baldassarre and Fazio, 1983, Verkman, 2005)

AQP	Permeability	Tissue expressed
AQP0	Water	Eye lens fibre cells
AQP1	Water	Kidney tubules, endothelia, erythrocytes, choroid plexus, ciliary epithelium, intestinal lacteals, corneal endothelium
AQP2	Water	Kidney collecting duct
AQP3	Water, glycerol	Kidney collecting duct, epidermis, airway epithelium, conjunctiva, large airways, urinary bladder
AQP4	Water	Astroglia in brain and spinal cord, kidney collecting duct, glandular epithelia, airways, skeletal muscle, stomach, retina
AQP5	Water	Glandular epithelia, corneal epithelium, alveolar epithelium, gastrointestinal tract
AQP6	Water, chloride?	Kidney collecting duct intercalated cells
AQP7	Water, glycerol	Adipose tissue, testis, kidney proximal tubule
AQP8	Water, urea	Liver, pancreas, intestine, salivary gland, testis, heart
AQP9	Water, glycerol, small solutes	Liver, white blood cells, testis, brain
AQP10	Water, glycerol	Small intestine
AQP11	Water?	Purkinje cell dendrites, hippocampal neurons, cerebral cortical neurons, kidney, liver, testes
AQP12	?	Pancreatic acinar cells

Structure and function

AQPs are a family of small water channel proteins found in the cell membranes of bacteria, plants, invertebrates and vertebrates. AQPs mediate the bi-directional transport of water across the cell membrane in response to osmotic gradients (Agre et al., 2002). A sub-group of AQPs, termed the aquaglyceroporins, able to facilitate movement of water as well as glycerol and other neutral solutes. AQPs are typically ~30 kDa in size and consist of six membrane spanning α-helices surrounding two loops, containing the highly conserved asparagine-proline-alanine motif that form the permeable water pore (Jung et al., 1994). These monomeric AQPs form tetramers within the cell membrane (Agre et al., 2002, Verkman, 2005).

The AQPs regulate a wide range of physiological functions, including glycerol concentration in fat metabolism, concentration of urine in the kidneys, and water homeostasis in the brain. AQPs have been studied extensively, and using transgenic mice, various pathological conditions such as loss of vision (McDonald et al., 1995), kidney dysfunction (Zagzag et al., 1995), and brain oedema (Thrane et al., 2011) have been attributed to alterations in AQP expression. Currently three AQPs have been characterised in the spinal cord: AQP1, AQP9 and AQP4. Of these AQP4 is the most abundant.

Aquaporin-1

AQP1 regulates water movement in numerous organs and plays a role in the production of urine, aqueous humour in the eye (Zhang et al., 2002) and CSF. In the brain, AQP1 is expressed in the apical membrane of the choroid plexus epithelium at the CSF interface. In the spinal cord it is located in ependymal cells, and in sensory fibres of the dorsal horn (Oshio et al., 2005, Shields et al., 2007). Studies using AQP1 knockout mice found that osmotically driven transport of water across the choroid plexus epithelium was significantly reduced in mice lacking AQP1 compared to wild-type controls. This finding raises the possibility that AQP1 deletion may be beneficial after brain trauma (Oshio et al., 2005). Investigations into AQP1 expression in contused human brain tissue demonstrated that AQP1 was highly expressed in astrocyte endfeet within the oedematous tissue and to a lesser extent around cerebral microvessels (Suzuki et al., 2006). In humans, AQP1 expression has also been found to be much higher in tissue from patients with cystic hemangioblastoma compared to those with the solid form, suggesting a possible role for AQP1 in cyst formation (Chen et al., 2006). AQP1 is highly expressed in tumour microvessels, and AQP1 knockout mice exhibit a decrease in tumour growth compared to wild-type after implantation of tumour cells (Saadoun et al., 2005a). Alterations in AQP1 expression have been noted in association with a number of other conditions including hydrocephalus (Paul et al., 2010), Alzheimer's disease (Perez et al., 2007), Creutzfeldt-Jacob disease (Rodriguez et al., 2006) and diabetes (Iandiev et al., 2007).

Aquaporin-9

AQP9 is an aquaglyceroporin, permeable to water as well as glycerol, urea and other neutral solutes (Tsukaguchi et al., 1996, Tsukaguchi et al., 1998) and is strongly expressed in rat liver, testes, lung, spleen, retina, brain and spinal cord (Elkjaer et al., 2000, Badaut, 2010). In the rat brain, AQP9 is expressed on the plasma membrane of glial cells (tanycytes and astrocytes), endothelial cells of subpial blood vessels and catecholaminergic neurons (Elkjaer et al., 2000, Badaut et al., 2001, Badaut et al., 2004, Oshio et al., 2004). AQP9 has also been

described in mitochondria of astrocytes and dopaminergic neurons (Amiry-Moghaddam et al., 2005). The role of AQP9 in the brain is not known, however, it has been postulated that it may regulate cell volume in tanycytes and contribute to CSF production or reabsorption across the ependymal lining (Elkjaer et al., 2000). Studies in mice have demonstrated an increase in AQP9 labelling around the lesion following experimental cerebral ischemia (Badaut et al., 2001). Over-expression of AQP9 was found in diabetic rats, followed by a decrease following administration of insulin (Badaut et al., 2008). While under hypoxic conditions, cultured astrocytes expressed lower levels of AQP9 (Badaut and Regli, 2004). AQP9 has been implicated in water homeostasis in the brain, and is also thought to facilitate transport of lactate and glycerol to astrocytes (Badaut and Regli, 2004).

Aquaporin-4

AQP4 is unlike other AQPs found in mammalian tissues in that it lacks certain cysteine residues that confer mercurial sensitivity (Shi and Verkman, 1996); mercurials have no effect on its water permeability (Hasegawa et al., 1994). In brain and spinal cord, AQP4 is expressed in astroglia, most abundantly in membranes at the brain-blood or brain-CSF interfaces, including astrocytic endfeet surrounding capillaries, glia limitans and ependyma (Nielsen et al., 1997) (Figure 9). Studies using knockout mice have implicated AQP4 in astroglial cell migration, neural signal transduction and brain water homeostasis (Verkman et al., 2006).

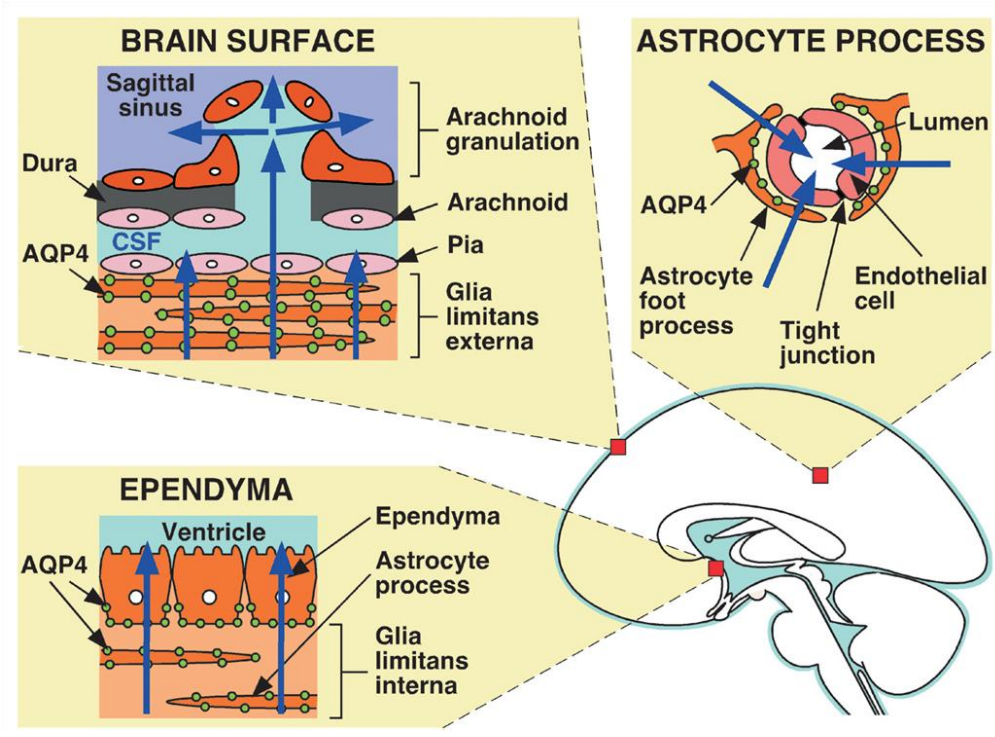

Figure 9: Schematic demonstrating location of AQP4 at the fluid interfaces in the brain [from (Papadopoulos and Verkman, 2007), with permission of Springer].

Astroglial cell migration

There is experimental evidence demonstrating the upregulation of AQP4 in reactive microglia and a markedly reduced rate of astrocyte migration in cells lacking AQP4 compared to AQP4-expressing cells in astroglial culture studies (Saadoun et al., 2005b). This corresponded to slower astrocyte migration and later glial scarring in a mouse model of stab wound injury (Saadoun et al., 2005b). This suggests that AQP4 does facilitate cell migration, although the mechanism by which it does this is not fully understood. Cell migration occurs primarily through the extension and retraction of membrane projections that propel the cell forward. It is thought that AQP4 contributes to these changes in cell shape and assists in the forward movement by facilitating uneven water uptake into the leading edge of the cell compared to the opposite side (Figure 10) (Saadoun et al., 2005b, Verkman, 2009).

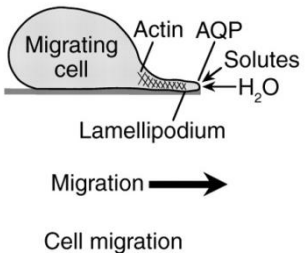

Figure 10: Proposed mechanism of AQP-facilitated cell migration, showing water entry into protruding lamellipodia in migrating cells [modified from (Verkman, 2009)].

Neural signal transduction

Astrocytes serve important functions in neurotransmitter removal and synthesis (e.g. Glutamate and GABA), as well as clearance or recycling of potassium ions and water in response to neural activity (Ransom et al., 2003). In light of the fact that AQP4 is highly expressed in astrocytes, it has been proposed that AQP4 may play a role in both ion homeostasis and neural signal transduction (Figure 11) (Manley et al., 2004). Auditory brain stem response thresholds measured in wild-type and AQP4-null mice have found that almost all animals lacking AQP4 were deaf or had a much higher threshold than wild-type mice depending on genetic background (Li and Verkman, 2001). AQP4 may maintain an osmotic equilibrium during the uptake and recycling of potassium ions in the inner ear. Hearing may be affected when an ionic imbalance occurs or when cell volume is altered (Li and Verkman, 2001). Experiments looking at the effect of AQP4 on brain excitability support this idea that AQP4 is involved in signal transduction. Studies using a chemoconvulsant to induce seizures in AQP4-null mice and wild-type controls demonstrated that six out of seven animals lacking AQP4 did not display any sign of seizure activity, while at higher doses a delay before seizure response was observed in AQP4-null mice compared to controls (Binder et al., 2004). Since

AQP4 is found to be in close contact with the potassium ion channel Kir4.1 on astrocytic endfeet, it is possible that AQP4 facilitated cell swelling in response to a hypo-osmotic environment may also influence potassium ion clearance following rapid neural activity (Lee et al., 2004, Manley et al., 2004).

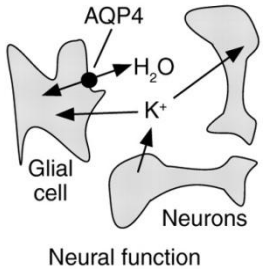

Figure 11: AQP4-dependent neuroexcitation, showing AQP4-facilitated water transport in glial cells, which communicate with neurons through changes in extracellular space volume and K+ concentration [modified from (Verkman, 2009)].

Central nervous system water homeostasis

The distribution of AQP4 predominantly at sites of fluid transport suggests a role for AQP4 in the transmembrane movement of water within the central nervous system. This role has since been established using animal models of diseases involving abnormal accumulation of fluid within the brain and spinal cord (Manley et al., 2000, Vajda et al., 2002, Bloch et al., 2005, Papadopoulos and Verkman, 2005).

Aquaporin-4 and oedema

Brain oedema

In healthy adult brain tissue, water homeostasis is maintained in response to osmotic gradients and hydrostatic pressure. Water is in the ventricles (CSF), the vasculature (blood), and brain parenchyma (within cells and the extracellular space). Disturbances in brain water content can lead to cerebral oedema, which can be intracellular or extracellular. Brain swelling due to an abnormal accumulation of water can lead to raised intracranial pressure, ischemia, and herniation. Cerebral oedema is an important component of pathological conditions such as tumour, stroke, hydrocephalus and traumatic brain injury (Fishman, 1975).

Oedema can be classified into three types depending on the underlying mechanism: cytotoxic, vasogenic and hydrocephalic (Table 3) (Klatzo, 1994). Cytotoxic (intracellular) oedema in the central nervous system involves cellular swelling, primarily involving astrocytes. Cytotoxic oedema occurs when cells fail to maintain cell volume, due to impairment in sodium and potassium pump function. Vasogenic oedema is caused by disruption of the BBB, permitting fluid to pass from the vasculature into the brain parenchyma. This results in the accumulation of plasma fluid in the interstitial space (Kimelberg, 1995). Hydrocephalic oedema occurs in association with conditions such as Chiari malformations, meningitis and subarachnoid

haemorrhage. This class describes the influx of CSF into the extracellular space due to an obstruction of normal drainage pathways (Fishman, 1975). In most conditions associated with a water imbalance both vasogenic and cytotoxic oedema are involved during different stages of disease.

Clearance of oedema fluid from the central nervous system occurs via three pathways; the ependyma (into the ventricles), the glia limitans externa (into the subarachnoid space) and via capillaries (across the BBB into the bloodstream) (Papadopoulos and Verkman, 2007).

Table 3: Causes of cerebral oedema [from (Papadopoulos and Verkman, 2007)]

Cytotoxic	Vasogenic	Hydrocephalic
Vascular Early hypoxia Early ischemia **Infection** Cerebral malaria Meningitis **Metabolic** Hyponatremia Hyperammonemia Diabetic ketoacidosis Hyperbilirubinemia Uremic **Traumatic**	**Brain Tumour** Supratentorial Infratentorial **Infection** Abscess Meningitis **Traumatic** Vascular Early hypoxia Early ischemia	**Obstructive** Tumour Aqueduct stenosis Chiari malformation Dandy-Walker **Communicating** Meningitis Subarachnoid haemorrhage Intraventricular haemorrhage

Aquaporin-4 and brain oedema

The clearance of fluid, in both cytotoxic and vasogenic oedema, occurs at AQP4-rich interfaces. A number of studies have been carried out using transgenic mice lacking AQP4 to elucidate the potential role of AQP4 in cerebral oedema. Several models of cytotoxic oedema have been used to demonstrate that AQP4-null mice have a greater survival rate and improved recovery compared to wild-type controls. In a model of hyponatraemia induced by rapid infusion of water, causing brain swelling and increased intracranial pressure, a significant increase in survival was observed in AQP4-null mice (76%) compared to wild-type (8%) (Manley et al., 2000). This protection is related to the reduced swelling of astrocytic endfeet surrounding capillaries in AQP4-deficient mice (Manley et al., 2000), and is consistent with the overall decrease in osmotically driven water permeability observed in brain tissue of AQP4-null mice (Thiagarajah et al., 2005). Protection has also been demonstrated in other models of cytotoxic oedema including bacterial meningitis (Papadopoulos and Verkman,

2005) and early focal cerebral ischemia produced by middle cerebral artery occlusion (Manley et al., 2000). Studies have also been carried out on dystrophin-null mice, which have significantly reduced expression of AQP4 on astroglial endfeet at the BBB interface and at the pial surface, although overall expression levels are normal (Vajda et al., 2002). In these animals, prolonged survival was observed following acute water intoxication compared to controls (Vajda et al., 2002).

The bi-directional permeability of AQP4 led researchers to investigate whether disruption of the AQP4 gene would impair clearance of excess water following vasogenic oedema, whereby fluid inflow occurs independently of AQP4 (Papadopoulos et al., 2004). Three models of vasogenic oedema: intracerebral fluid infusion, cortical freeze injury, and implantation of brain tumour cells, were studied in AQP4-deficient mice. In all models there were significant increases in intracranial pressure. Water infusion into the brain parenchyma in the freeze injury model caused an increase in brain water content in AQP4-deficient mice compared to wild-types, while a worsened neurological outcome was observed in AQP4-null mice in the brain tumour model (Papadopoulos et al., 2004). These experimental findings suggest that the excess fluid in the interstitial space that accumulates in vasogenic oedema must be removed at the brain-fluid barriers via an AQP4-mediated transcellular route.

The role of AQP4 in hydrocephalic oedema has also been studied using a well-established kaolin model of hydrocephalus (Bloch et al., 2006). Kaolin injected into the cisterna magna of mice causes ventricular enlargement, increases intracranial pressure and increases brain water content. It was found that in AQP4-null mice, development of hydrocephalus occurred more rapidly than in wild-type mice. Computational modelling based on this data suggests that removal of excess CSF from the parenchyma occurs primarily through AQP4-dependent pathways (Bloch et al., 2006).

Aquaporin-4 and spinal cord oedema

Oedema is well characterised in the acute stages of spinal cord injury (Nolan, 1969, Tator, 1972, Beggs and Waggener, 1975, Yeo et al., 1975, Wagner and Stewart, 1981, Mahmood et al., 2008), and is thought to be due to increased fluid flow into the cord across an impaired BSCB (vasogenic oedema). The degree of oedema has been shown to correlate with the degree of motor deficit (Sharma et al., 2005), due to compression of surrounding structures, ischemia and secondary damage. A study on AQP4 expression in a rat model of spinal cord injury demonstrated a decrease in AQP4 in the acute stages of spinal cord injury followed by a marked increase in the chronically injured cord. Water content remained significantly higher

in the early and late stages of disease in injured cords compared to controls (Nesic et al., 2006). It is established that early oedema is caused by a breakdown in the BSCB, and since AQP4 has been found to improve vasogenic oedema, it was postulated that the down-regulation of AQP4 shortly after injury impaired the removal of fluid. In the chronically injured cord it was demonstrated that up-regulation of AQP4 occurred when the BSCB was intact. Water accumulation in the chronic stage may be attributed to cytotoxic oedema due to astrocyte swelling (Nesic et al., 2006). More recently, a spinal cord compression injury model in AQP4 knockout mice found that AQP4 deficiency resulted in improved neurological outcome, decreased neuronal death, less myelin vacuolation, reduced spinal cord swelling and reduced intraparenchymal pressure. In contrast to the results found by Nesic et al (Nesic et al., 2006), this study found that AQP4 expression was significantly up-regulated two days after injury in wild-type mice (Saadoun et al., 2008).

Aquaporin-4 and syringomyelia

These studies highlight the significance of AQP4 in water movement in the central nervous system, and its potential role in abnormal water accumulation in a wide range of pathological conditions. Experimental evidence suggests that AQP4 expression may contribute to increased water content following spinal trauma, and emphasizes the importance for further study into diseases such as syringomyelia that cannot be completely explained by current theories of CSF dynamics.

It is possible that in both canalicular and posttraumatic syringomyelia that AQP4 expression may be affected. AQP4 is strongly expressed in glial cells, and to a lesser extent ependymal cells surrounding the central canal. As such, it is possible that changes in AQP4 expression could either increase the movement of water into the central canal, or alternatively prevent water from moving from the central canal into the parenchyma. This may contribute to the enlargement of the central canal in Chiari-associated syringomyelia.

AQP4 expression changes have been demonstrated following spinal cord injury. In addition, a possible causal relationship between AQP4 and spinal cord swelling has been proposed (Nesic et al., 2006, Saadoun et al., 2008). These studies point to the need for further research into AQP4 and its effect on disorders associated with spinal injury such as posttraumatic syringomyelia.

Hypotheses

In light of the extensive research carried out in previous studies, a number of hypotheses on the development and progression of syringomyelia have been proposed. In this thesis three hypotheses are investigated.

Hypothesis 1

The BSCB is compromised in both posttraumatic and Chiari-associated syringomyelia. This impairment provides a pathway for fluid to flow from the vasculature into the syrinx.

Hypothesis 2

AQP4 levels are altered in syringomyelia. This change in AQP4 expression hinders the removal of excess fluid in the spinal cord, contributing to fluid accumulation in syringomyelia.

Hypothesis 3

There are specific pathways of fluid outflow in syringomyelia.

Aims

The aims of this project were:

1. Investigate the structural and functional integrity of the BSCB in animal models of posttraumatic and Chiari-associated syringomyelia.
    I. Structural integrity: to investigate EBA expression using immunofluorescence.
    II. Functional integrity: to investigate blood vessel leakage using a vascular tracer (HRP).
2. Investigate AQP4 expression in animal models of syringomyelia.
    I. To investigate AQP4 expression qualitatively in animal models of posttraumatic and Chiari-associated syringomyelia using immunofluorescence.
    II. To investigate AQP4 expression quantitatively in posttraumatic syringomyelia using western blotting.
3. Investigate the outflow pathways for syrinx fluid in a sheep model of posttraumatic syringomyelia.
    I. To investigate the movement of tracer (HRP) from an extracanalicular syrinx into the surrounding spinal parenchyma.

Chapter 2.1

The blood-spinal cord barrier in posttraumatic syringomyelia

Object. Posttraumatic syringomyelia produces a significant burden of pain and neurological deficits in patients with spinal cord injury. The mechanism of syrinx formation is unknown and treatment is often ineffective. A possible explanation for syrinx formation is fluid leakage from the microcirculation in the presence of a compromised blood-spinal cord barrier (BSCB). The aim of this study was to investigate the structural and functional integrity of the BSCB in a model of posttraumatic syringomyelia.

Methods. The excitotoxic amino acid and arachnoiditis model of syringomyelia was used in 27 Sprague-Dawley rats. Structural integrity of the BSCB was assessed using immunoreactivity to endothelial barrier antigen (EBA), and loss of functional integrity was assessed by extravasation of intravascular horseradish peroxidase (HRP). Animals were studied after 3 days, or at 1, 3, 6, or 12 weeks after surgery. There were laminectomy-only and saline injection control animals for comparison at each timepoint.

Results. Syrinxes formed in 16 of the 17 animals injected with excitotoxic amino acid. Loss of structural and functional integrity of the BSCB in syrinx animals was noted at all timepoints. Disruption of the BSCB was most dramatic in tissue adjacent to the syrinx, and in the central and dorsal grey matter. Changes in EBA expression generally corresponded with altered vascular permeability, although in the acute stages, widespread vascular permeability occurred without a corresponding decrease in EBA expression. At the later timepoints (3 – 12 weeks) EBA expression was often absent, although no vascular leakage was observed.

Conclusions. This study demonstrated a prolonged structural and functional disruption of the BSCB in this model of posttraumatic syringomyelia. Loss of functional integrity of the BSCB, with fluid entering the interstitial space of the spinal cord, may contribute to initial cyst formation after spinal cord injury and subsequent enlargement of the cyst, to produce posttraumatic syringomyelia.

Introduction

Spinal cord injury remains a significant clinical problem, with an estimated 13,000 new cases of spinal cord injury in the US each year (Lasfargues et al., 1995, Saito et al., 2008). Up to one-third of such patients develop posttraumatic syringomyelia (Perrouin-Verbe et al., 1998, Brodbelt and Stoodley, 2003a), causing pain and neurological deficits in addition to those incurred with the original injury. Current treatments for syringomyelia are often not effective, with only 50% of patients showing improvement. It is unlikely that more effective therapies will be developed without a greater understanding of posttraumatic syrinx pathophysiology.

Existing theories of syrinx pathogenesis are based predominately on abnormalities obstructing CSF flow at the foramen magnum, as in the case of Chiari malformations (Gardner and Angel, 1958a, Ball and Dayan, 1972, Williams, 1980b, Oldfield et al., 1994, Heiss et al., 1999). These theories cannot be applied to posttraumatic syrinxes where there is usually no abnormality at the craniocervical junction and the cysts are extracanalicular rather than in the central canal. It is generally assumed that fluid flows into syrinxes from CSF surrounding the cord, with various explanations as to the driving forces and pathways involved (Gardner and Angel, 1958a, Ball and Dayan, 1972). There is experimental evidence of CSF flow from the subarachnoid space into the spinal cord via perivascular spaces in posttraumatic syringomyelia, with increased flow at the level of arachnoid adhesions (Brodbelt et al., 2003b, Brodbelt et al., 2003c). However, because the pressure inside the spinal cord can exceed subarachnoid space pressure (Klekamp et al., 2001) there may be additional sources of fluid. There is increasing support for the theory that syrinx enlargement is due, at least in part, to extracellular fluid flow (Klekamp, 2002, Levine, 2004, Greitz, 2006). One possible contribution is from vessels adjacent to the cyst, through a deficiency in the BSCB.

Disruption of the BSCB has been demonstrated in experimental models of spinal cord injury. Studies using vascular tracers such as Evans blue and HRP have shown a strong correlation between the degree of spinal cord injury and the degree of altered blood-brain barrier (BBB) permeability (Beggs and Waggener, 1975). More recently, studies have focused on immunohistochemical analysis of EBA, a protein selectively expressed in rat endothelial cells that possess blood-tissue barrier properties. Microvessels that have a compromised BSCB can be localised by their lack of EBA expression (Sternberger and Sternberger, 1987).

Experiments using a compression model of spinal cord injury have demonstrated a relationship between loss of EBA and oedema formation, with subsequent re-establishment of EBA expression correlating with clearance of oedema (Farooque et al., 1994, Perdiki et al.,

1998, Ghabriel et al., 2000). Such results suggest that damage to the BSCB may indeed play a role in either the development of cord oedema and small initial cysts or the enlargement of small cysts over time to form syrinxes. Failure of the BSCB to repair after spinal cord injury may be pivotal in the subsequent development of posttraumatic syringomyelia.

The aims of this study were to determine whether structural components of the BSCB are compromised in an animal model of posttraumatic syringomyelia, and if so, whether this compromise corresponds to a functional breakdown, providing a pathway for fluid to flow from the vasculature into the syrinx.

Materials and methods

Following ethical approval from the Animal Care and Ethics Committee of the University of New South Wales and Macquarie University, 27 10-week-old male Sprague-Dawley rats weighing 349 ± 65g (mean ± SD) were divided into five experimental groups. Each experimental group consisted of one laminectomy-only control animal, one sham-injected control animal that received four 0.5 μL spinal cord intraparenchymal injections of saline containing 1% Evans blue (Sigma-Aldrich, St. Louis, MO, US) and three or more animals undergoing a syrinx induction procedure (described below). The properties of the BSCB were investigated after 3 days, or at 1, 3, 6 or 12 weeks following the initial operation (Table 4). All procedures were performed in a sterile field under general anaesthesia induced with 4% isoflurane in oxygen and maintained with 2% isoflurane through a nose cone, which was increased as required to maintain an adequate level of anaesthesia.

Table 4: Experimental groups: Surgical procedure and survival time in experimental rats

		No. of Animals at Each Survival Point				
Experimental Group	**Initial Operation**	3 days	1 wk	3 wks	6 wks	12 wks
Control	Laminectomy only	1	1	1	1	1
Sham-injected control	4 intraparenchymal injections of saline	1	1	1	1	1
Syrinx induction	4 intraparenchymal injections of quisqualic acid & subarachnoid kaolin	3	3	3	4	4

Syrinx induction

The excitotoxic and arachnoiditis model of posttraumatic syringomyelia has been described previously (Figure 12) (Yang et al., 2001, Brodbelt et al., 2003b). Animals were placed prone, and the skin shaved and prepared with povidone iodine. A midline incision was made over the cervicothoracic junction and a laminectomy was performed from C-7 to T-1. A 29-gauge needle was used to puncture the meninges. A glass-tipped, 5 μL syringe (SGE International

Pty Ltd., Austin, TX, US) held in a stereotactic micromanipulator was then used to infiltrate four 0.5 µL injections of 24 mg/mL quisqualic acid (Tocris Cookson, Bristol, UK) and 1% Evans blue. Injections were delivered into the dorsal cord parenchyma along the right dorsal nerve rootlets between the rostral C-8 and caudal T-1 levels. Use of Evans blue allowed any leakage of quisqualic acid to be identified. Five microlitres of 250 mg/mL kaolin (sigma-Aldrich, St. Louis, MO, US) were then injected into the subarachnoid space to produce arachnoiditis. Wounds were closed with a single layer silk suture. Analgesia was administered postoperatively and the animals were allowed food and water *ad libitum*. Any excessive weight loss, limb weakness, or signs of over-self grooming were recorded.

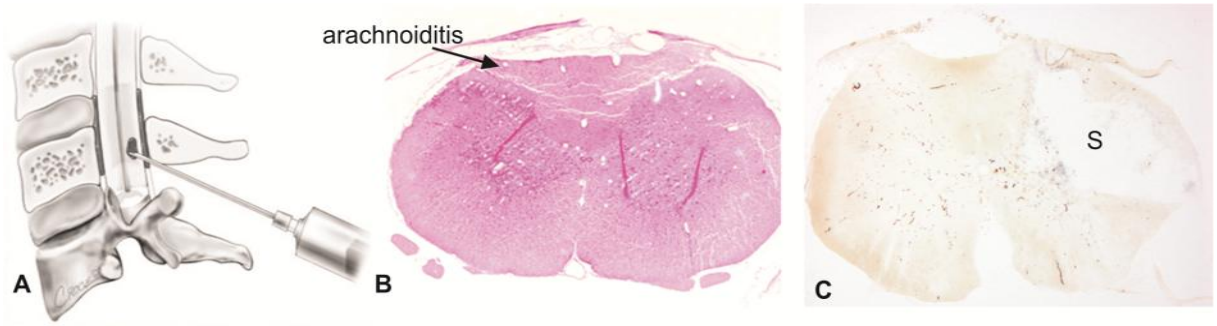

Figure 12: Extracanalicular syrinx induction procedure. A: Following a laminectomy, animals received four 0.5 µL intraspinal injections of 24 mg/mL quisqualic acid. B: Animals then received a subarachnoid injection of kaolin. This produced inflammation (arachnoiditis) around the spinal cord. C: The combination of quisqualic acid and kaolin produces an extracanalicular syrinx (S) in the spinal parenchyma.

Intravenous injection of HRP and perfusion

At 3 days, or at 1, 3, 6 or 12 weeks after syrinx induction, animals had an intraperitoneal injection of an antihistamine (1 mL of 1% promethazine solution) to prevent allergic reaction to HRP (Ma et al., 1996). The right femoral vein was exposed and cannulated with a 24-gauge catheter. After flushing the cannula with normal saline, 200 mg/kg HRP (type II, Sigma-Aldrich, St Louis, MO, US) in 0.5 mL saline was injected over a period of 2 minutes.

Ten minutes after the end of the HRP injection, the animals were rapidly perfused by intracardiac injection of 5,000 IU heparin in 1 mL of saline, followed by 500 mL of 4% paraformaldehyde (Lancaster Synthesis, Pelham, NH, US) in 0.1 M phosphate buffer (pH 7.4) under a constant pressure of 120 mm Hg.

Immunohistochemistry and detection of HRP

The spinal cord and liver were dissected out and post-fixed in 2% paraformaldehyde in 0.1 M phosphate buffer overnight. Vibratome sections (50 µm) were cut from the liver and spinal

cord and mounted on 3-amino propyl-triethoxy-silane-coated slides. Segments were removed from the spinal cord at C-2, serially from C-4 to T-4, and from L-2.

Histochemical development of HRP reaction product was conducted using 3, 3'-diaminobenzidine tetrahydrochloride (DAB) 1 mg/mL with 0.02% hydrogen peroxide for 10 minutes. The sections were rinsed in distilled water, dehydrated in graded ethanol, cleared in xylene and mounted with DPX mounting medium (Scharlau Chemie S.A.). Colour images were acquired using a Leica microscope (Leica DMR Microsystems, Wetzlar, Germany) and Zeiss digital camera (Axiocam, Zeiss, Oberkochen, Germany).

In each animal the transverse section containing the greatest syrinx area was identified from the DAB-stained sections. Images of these sections obtained at low magnification were divided into 858 grid squares, and cavity area was measured as a percentage of the cross-sectional area of the whole section (number of grid squares containing ≥ 50% lesion/total number of grid squares per section). Syrinxes were observed as cystic spaces in the spinal cord parenchyma, sometimes containing cellular debris and a loose trabecular meshwork. Syrinx length was determined by the number of segments in which cavitation was observed.

Immunofluorescence staining proceeded as follows. Spinal cord sections were rinsed with 50% ethanol/phosphate-buffered saline (PBS) for 20 minutes followed by three 10 minute washes in PBS and incubated with 15% normal horse serum (NHS) in PBS (pH 7.45) for 20 minutes. The sections were then incubated with the monoclonal antibody against rat EBA clone SMI71 (1:1,000; Sternberger Monoclonals, Berkeley, CA, US) overnight at 4°C. The following day, sections were left for 2 hours at room temperature before two 10 minute rinses with PBS and incubated with anti-mouse IgG Alexa Fluor 594 (1:800 dilution in 4% NHS/PBS Molecular Probes, Eugene, OR, US) for 2 hours. After rinsing twice for 5 minutes the sections were coverslipped with fluorescent mounting medium. Omission of the primary antibody was used for negative controls. Sections were randomly selected, and examined with a fluorescent microscope (Olympus BX51, Olympus Corp., Tokyo, Japan). Images were obtained using a digital camera (Olympus DP71, Olympus Corp.). EBA expression was graded relative to controls: normal (intense staining and distinct vascular profiles); faintly expressed or irregular staining; and no staining.

Statistical analysis

Syrinx cross-sectional area and length in different experimental groups were compared using the unpaired 2-tailed Student's *t* test. A probability value < 0.05 was considered statistically

significant. Data are presented as the mean ± SEM. Software used included Excel (Microsoft, Redmond, WA, US) and SPSS (Statistical Package for the Social Sciences, SPSS, Chicago, IL, US).

Results

The intraparenchymal injection of quisqualic acid and subarachnoid kaolin injection produced noncommunicating extracanalicular syrinxes in 16 of the 17 animals in the syrinx-induction group. In the one animal that had not developed a syrinx at 6 weeks postsurgery, glial scarring was evident, extending across two spinal segments. Syrinxes had a significantly greater maximum area (12.79 ± 3.11%) and extended over more segments longitudinally (2.94 ± 0.45) than cavities produced from injections of saline alone (area: 3.18 ± 1.50%, $p = 0.01$; segments: 1.60 ± 0.60, $p = 0.11$). No lesions were observed in the control (laminectomy-only) animals.

Barrier integrity

EBA immunostaining of controls (laminectomy-only) resulted in positive labelling of almost all microvessels in the grey and white matter at all timepoints and all spinal cord levels (Figure 13). In these sections the fluorescent signal was intense, with consistent endothelial cell staining revealing distinct vascular profiles. In all sham-injected controls, EBA expression was reduced at the surgical site, and at 3 days and 3 weeks postsurgery this reduction in EBA expression extended over two or more vertebral segments caudal to the injection site. At 3 days after surgery a cavity was present at the site of injection at C-7, C-8, and T-1, and intensity of EBA immunoreactivity was reduced. At 1 week virtually all blood vessels were stained positive for EBA, with the exception of a small region in the dorsal grey matter between C-7 and T-1 that exhibited a slight decrease in intensity. At 3 weeks, a cavity extended from C-8 to T-2, and throughout these segments few microvessels were immunopositive. Six weeks following injection with saline and Evans blue, EBA expression was reduced in the grey matter at C-8 and T-1, corresponding to an area of gliosis and residual Evans blue (as viewed under bright field). At 12 weeks, EBA staining resembled that observed 1 week after syrinx induction, with EBA immunoreactivity observed in endothelial cells of most vessels with the exception of a small region in the dorsal grey matter at the site of injection.

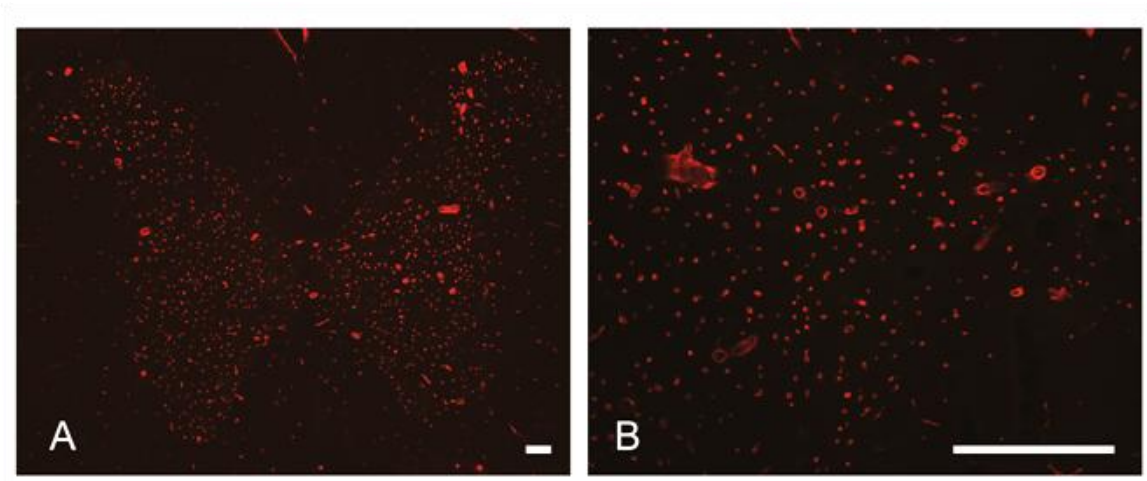

Figure 13: Photomicrographs demonstrating immunolocalisation of EBA in a control rat (laminectomy-only) spinal cord using anti-EBA antibody immunofluorescence staining. A: Essentially, all microvessels strongly express EBA. B: Higher magnification view of central grey matter in panel A. Bar = 100 µm (A), 200 µm (B).

In syrinx-induced animals, EBA immunoreactivity was reduced at the level of the syrinx at all timepoints investigated (Figure 14). At 3 days after induction almost no EBA-positive vessels could be observed in tissue adjacent to the syrinx, and although there was staining in surrounding tissue, it was markedly reduced. This decrease in staining in some cases extended to four segments caudal to the syrinx. In the 1 week survival group, the decrease in immunolabelling was limited to those segments containing a syrinx, and in some cases the spinal level caudal or rostral to the cavitation. Staining results varied within these segments, with normal staining in some sections except for a distinct region bordering the syrinx, whereas in others only the grey matter exhibited a marked reduction in EBA expression, and in some a weak intensity was observed throughout the white and grey matter. In some sections vascular profiles appeared irregular in shape.

At 3 and 6 weeks the pattern of EBA staining varied from animal to animal. In some animals a uniformly weak staining was noted in grey and white matter at the level of the syrinx, however, in both rostral and caudal spinal levels staining of vascular profiles was normal. In other animals, reduction in EBA expression was restricted to the syrinx side of the cord while blood vessels in the other side were immunoreactive (Figure 14C-E). In some animals this weakened intensity extended up to four spinal segments above and below the syrinx. In one animal in the 6 week survival group, EBA was significantly reduced in all spinal segments studied. In this animal glial scarring was observed from C-7 to T-1, but no syrinx cavity was evident.

In two animals perfused 12 weeks after surgery only a slight or moderate reduction in EBA-positive microvessels was observed below the level of the syrinx, and in general it was only in

tissue bordering the cavity that EBA expression was absent, or only faintly present. One animal at 12 weeks had developed a syrinx extending over seven segments, which at its widest had enlarged to encompass the grey matter, dorsal corticospinal tract, and dorsal funiculus. At these levels very few blood vessels were immunoreactive.

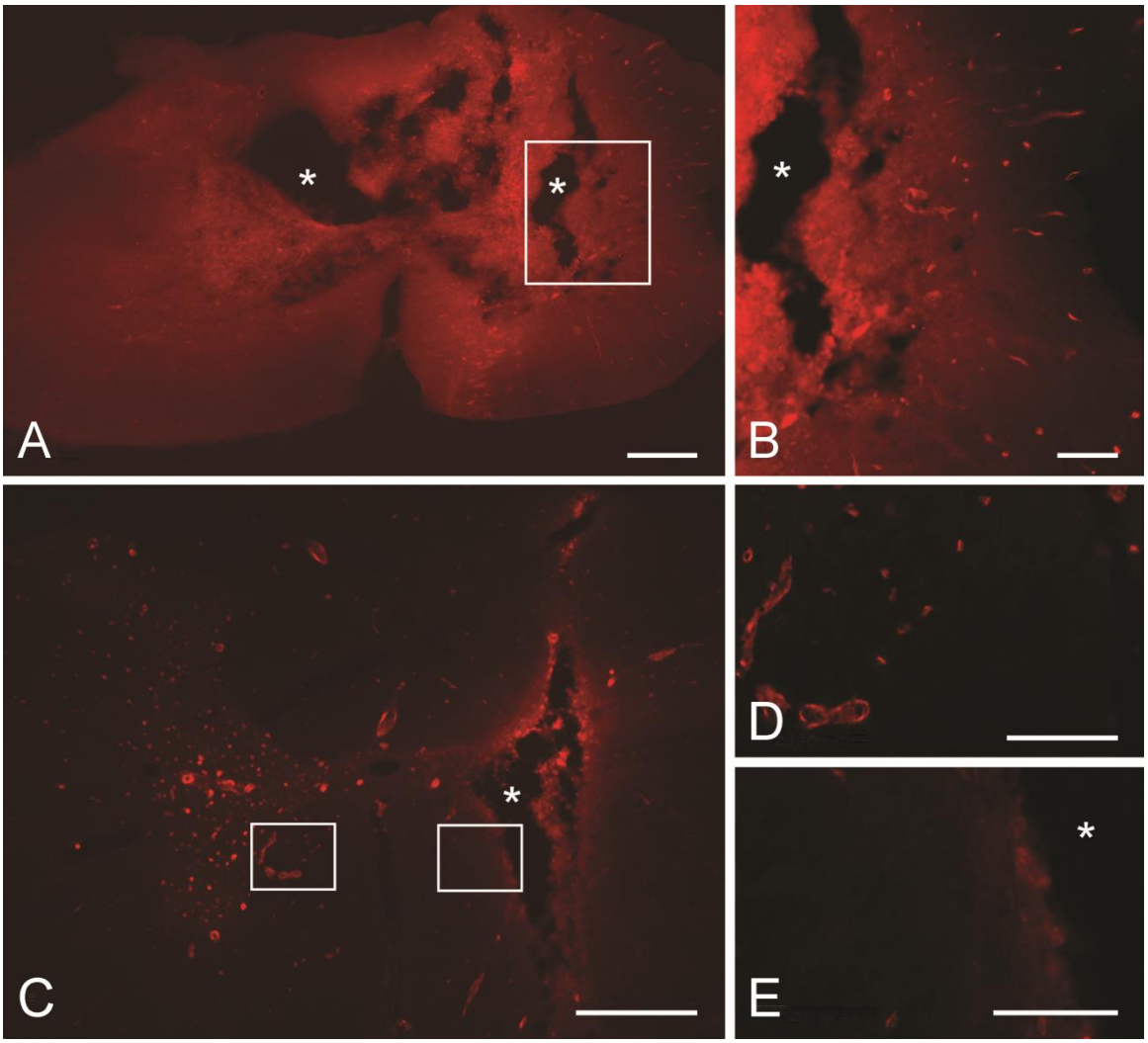

Figure 14: Photomicrographs show immunolocalisation of EBA in the spinal cord of a rat 1 week (A and B) and 6 weeks (C-E) after syrinx induction using anti-EBA antibody immunofluorescence staining. A: An extracanalicular syrinx (*) is shown predominately involving the dorsal columns and the right lateral column. The entire left side of the cord at this level has reduced immunolabelling for EBA. B: Higher power view of *inset* in panel A, demonstrating lack of EBA adjacent to the syrinx but presence closer to the surface of the cord. C: In an animal in the 6 week group, no EBA is observed in tissue bordering the syrinx (*), while distinct vascular profiles are present in a comparable location on the other side of the cord. D and E: Higher power views of *insets* shown in panel C. Bar = 300 µm (A), 50 µm (B and C), 200 µm (D), and 90 µm (E).

Barrier permeability

No HRP leakage was observed in the spinal cord at any timepoint in the laminectomy-only control groups. The organic compound DAB was observed in liver sections showing extravasation of tracer in the parenchyma, demonstrating the successful injection and circulation of HRP (Figure 15). In the sham-injected control group, HRP leakage into the cord

was observed at 3 days, and at 3 and 6 weeks after injection. No reaction product was visible at 1 or 12 weeks after surgery. At the 3 day and 3 week timepoints a cavity was present in three spinal cord levels. In these animals HRP was only present in spinal cord segments containing a cavity or visible tissue damage at the point of needle insertion. At 6 weeks, HRP leakage was extensive, with reaction product present at all spinal levels investigated.

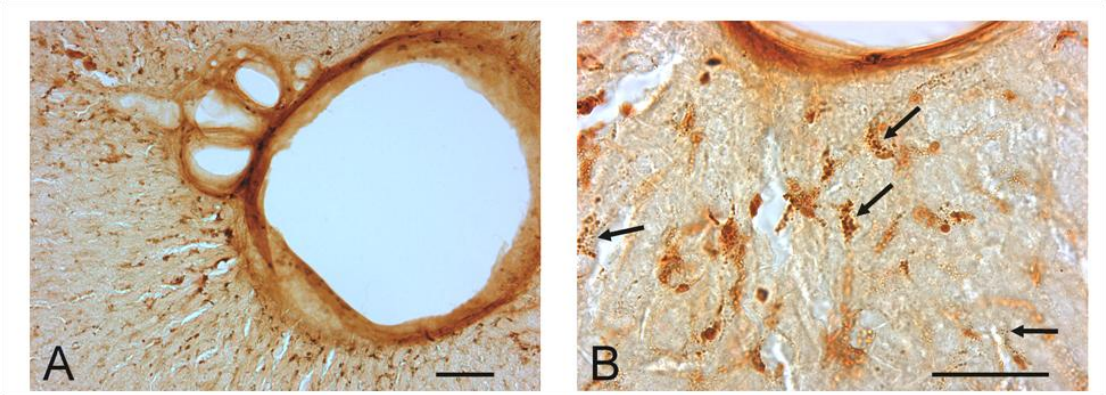

Figure 15: Colour photomicrographs showing a representative section from a liver stained for peroxidase cytochemistry using DAB. Animals were injected intravenously with HRP before perfusion with 4% paraformaldehyde. A higher magnification view of panel A (B) demonstrates HRP reaction product (*arrows*), indicating the successful administration of tracer into the circulation and normal extravasation of tracer in tissue without endothelial tight junctions. Bar = 100 µm (A), 50 µm (B).

Extravasation of HRP into the cord parenchyma could be observed in all of the syrinx-induced animals, at all timepoints investigated (Figure 16) with the exception of one 12 week and one 3 week postsurgery animal. Each of these animals demonstrated a syrinx at only one spinal cord level. The three spinal cords with HRP leakage at ≥ 10 spinal cord levels were obtained from animals killed at the earlier timepoints (3 days or 1 week after surgery). In all cases, permeability to HRP was greatest at the level of the syrinx, irrespective of whether the cavity was limited to grey matter or had enlarged into the white matter. In the majority of animals with a syrinx extending longitudinally over two or more spinal cord segments, HRP reaction product was visible in sections caudal or rostral to the cavity. In these cases HRP leakage was generally concentrated in the central grey matter, or distributed in a pattern mirroring that observed at the level of the syrinx. Leakage was also evident, although less frequently, close to the ventral median fissure, in the dorsal and ventral horns of the grey matter, and the dorsal white matter. The pattern of leakage from vessels was diffuse, and did not indicate any specific flow patterns or pathways.

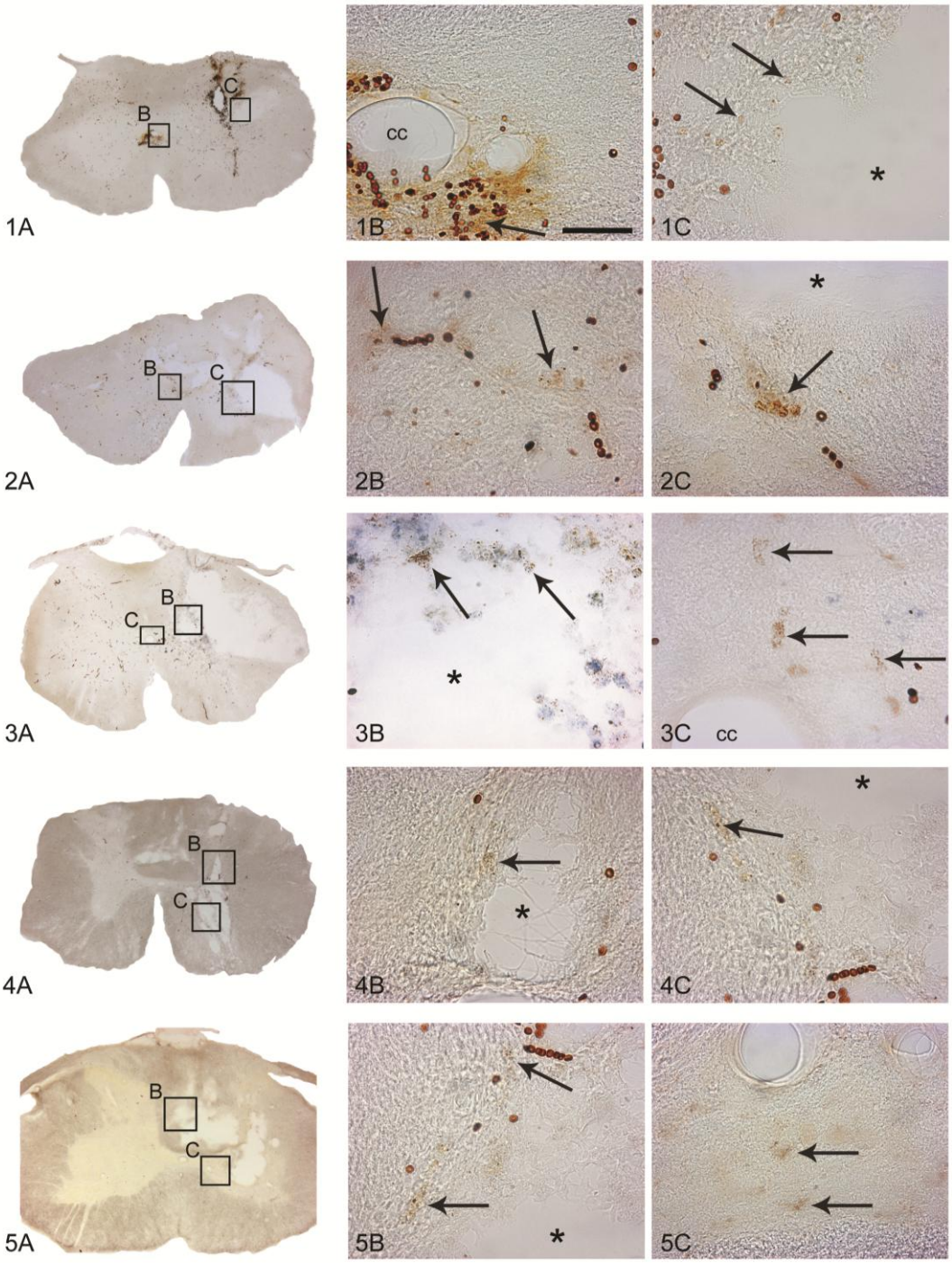

Figure 16. Photomicrographs of sections obtained from cervical spinal cords of rats at different timepoints following syrinx induction and stained with DAB. Transverse sections were obtained at 3 days (1A-C), 1 week (2A-C), 3 weeks (3A-C), 6 weeks (4A-C), and 12 weeks (5A-C) after surgery. Each animal received an intravenous injection of HRP prior to being killed, and spinal cord sections were treated for peroxidase reactivity. Higher power views of *insets* at each time point (*left column*) demonstrate areas of HRP leakage (*arrows, centre and right columns*). Staining in most animals is concentrated around the syrinx (*) and central canal (cc). Erythrocytes at the early timepoint relate to the needle tract for excitotoxic amino acid injection. Bar = 100 µm.

Discussion

Up to one-third of patients with spinal cord injury develop syringomyelia months or years after the original injury. The additional pain and neurological deficits imposed by this disorder are a significant burden on a group of patients already coping with the disability of spinal cord injury. Treatment of posttraumatic syringomyelia is usually surgical, often with unsatisfactory results. This is perhaps not surprising, considering that the cause of the disorder is still poorly understood.

Much attention has been focused on the possible mechanisms underlying the formation of syringomyelia in association with Chiari malformations. These syrinxes are usually enlargements of the spinal cord central canal, and it is assumed that an abnormality of CSF flow at the foramen magnum results in flow from the spinal subarachnoid space into the central canal, probably via perivascular spaces (Heiss et al., 1999).

In contrast, syrinxes that develop after spinal trauma are usually separate from the central canal and there is no associated craniocervical junction abnormality. Small cavities at the level of spinal cord injury are very common, yet not all these cavities enlarge to form syrinxes. There may be different mechanisms underlying the formation of initial cysts and subsequent cyst enlargement. For example, it has been proposed that the initial cavity is caused by haemorrhage or the inflammatory processes following spinal cord trauma (Williams, 1980b). In support of this theory is the observation that the likelihood of developing a syrinx is greater in cases with an intraparenchymal hematoma (Edgar and Quail, 1994).

There is general consensus that the enlargement of an initial traumatic cyst into a syrinx is related to CSF flow obstruction in the subarachnoid space. Previous animal and computer modelling studies provide evidence for CSF flow into the spinal cord and syrinx from the subarachnoid space, facilitated by the arachnoiditis that causes a focal increase in subarachnoid pressure (Klekamp et al., 2001, Brodbelt et al., 2003b, Bilston et al., 2006). One theory proposed is that pressure waves that travel through the subarachnoid space cause an increase in pressure within the syrinx, which in turn disrupts the surrounding tissue, creating a cavity into which fluid can diffuse (Gardner and McMurray, 1976, Williams, 1992). Although the movement of syrinx fluid can be observed using MR imaging (Williams, 1992), there is no evidence to support the idea that this ‘sloshing’ mechanism provides enough force to cause the necessary tissue damage required for cyst enlargement (Klekamp et al., 1997). It also does not explain the high pressures often observed in posttraumatic syrinxes.

Whereas CSF from the subarachnoid space is likely to be one source of syrinx fluid, there is also evidence suggesting that spinal cysts contain extracellular fluid that enters the interstitial space from the microcirculation. Fluid and solutes in the central nervous system extracellular space are normally very tightly controlled. Unlike in systemic vessels, endothelial cells in the brain and spinal cord are connected by tight junctions that prevent the free passage of water from plasma to the extravascular tissue. Disruption of these tight connections can lead to an increase in extracellular water in the central nervous system. A study using a thecal sac constriction model to produce spinal cord cysts found that after contrast-enhanced MR imaging, there was a slow increase in signal intensity in the cyst but not in spinal cord distal to the ligature (Josephson et al., 2001). Contrast-enhanced MR imaging in two patients with syringomyelia, one associated with an inflammatory disease of the central nervous system and the other a structural abnormality, found that signal enhancement occurred around the syrinx in each case (Ravaglia et al., 2007). These experimental and clinical findings suggest that the BSCB is impaired in the cord tissue adjacent to a cyst. It is possible that in syringomyelia associated with trauma, accumulation of extracellular fluid from a disrupted BSCB may also play a role in cyst progression (Klekamp, 2002, Levine, 2004, Greitz, 2006, Ravaglia et al., 2007).

Impairment of the BSCB could lead to an increase in extracellular fluid and provide a source for fluid flow into posttraumatic syrinxes, either alone or in combination with fluid flow from the subarachnoid space. There is strong evidence that the BSCB is disrupted following spinal cord injury. Following moderate or severe compression trauma of the rat spinal cord, there is a significant loss of BSCB integrity (assessed by EBA expression) at 4 days, which is then restored by 9 days postinjury (Perdiki et al., 1998). Other studies of BSCB integrity have reported a biphasic opening of the barrier following weight-drop injury in mice (Whetstone et al., 2003), after contusion injury in rats (Noble and Wrathall, 1989, Popovich et al., 1996), and transient opening in a mouse hemisection model of spinal cord injury (Pan et al., 2003). Re-establishment of barrier integrity in these models ranged from 14 to 21 days after injury. In our model, mechanical damage from needle insertion and fluid injection in control animals caused disruption of the BSCB that had resolved at 1 week, followed by a second-phase opening of the barrier at 3 and 6 weeks and re-establishment by 12 weeks. A contusion injury model in rats using the small molecular weight tracer [^{14}C]-α-aminoisobutyric acid found increased permeability 1 month postinjury (Popovich et al., 1996). A study involving an extensive cut in the dorsal funiculus of rat and cat spinal cords demonstrated BSCB leakage even 11 months after injury (Frisen et al., 1993). These differences in observed duration of

BSCB opening may be related to both the tracers and mechanisms implemented, and regions of spinal tissue affected by the trauma. This prolonged opening of the barrier may also be due to axonal regeneration, which takes place in the absence of an intact BSCB (Frisen et al., 1993).

Our model uses an excitotoxic injury rather than a mechanical injury. It has been demonstrated that the intraspinal injection of the excitatory amino acid quisqualic acid produces significant neuronal loss, macrophage infiltration, and astrocyte activation (Pisharodi and Nauta, 1985, Yezierski et al., 1993, Yang et al., 2001, Brodbelt et al., 2003a, Brodbelt et al., 2003c). Spinal cavities produced using this mechanism are extracanalicular and surrounded by gliosis (Yang et al., 2001). The sham-injected control animals demonstrate that the injection itself does cause minor injury to the spinal cord, as evidenced by haemorrhage in the early time points and has been shown to produce neuronal loss and inflammation (Brodbelt et al., 2003a). When used in conjunction with arachnoiditis, quisqualic acid has been shown to produce enlarging cavities that are histologically comparable to posttraumatic syrinxes in a high percentage of experimental animals (Yang et al., 2001, Brodbelt et al., 2003b, Brodbelt et al., 2003c). Although other models of posttraumatic syringomyelia have been characterised that involve spinal cord injury in combination with arachnoiditis, these have not been reliable, producing syrinxes in ~50% of animals using a model of weight-drop injury (Cho et al., 1994). More recently, a model using a clip compression injury in addition to subarachnoid kaolin injection produced cystic cavities in all animals 6 weeks after spinal cord injury (Seki and Fehlings, 2008). This model may mimic the events leading to posttraumatic syringomyelia more accurately than the excitotoxic model, and it would be useful to study them concurrently to ascertain the extent to which excitotoxity contributes to cystic cavitation and whether the findings of the previous studies regarding CSF flow (Brodbelt et al., 2003c) and the results from this study can be reproduced in this compression model. The advantage of using quisqualic injection, however, is that syrinxes are formed as early as 3 days following the initial procedure, with little neurological deficit or neuropathic pain compared with compression spinal cord injury that results in hind limb paralysis and reduced threshold for mechanical allodynia at 6 weeks (Seki and Fehlings, 2008). Because it is likely that the direct excitotoxic effect is transient (Brodbelt et al., 2003a), we believe the model provides a useful method to examine factors related to ongoing cyst development and enlargement.

In this study the size of cavitations varied among animals, even those sacrificed at the same timepoint. Variation in syrinx length has been reported using this model previously, with

syrinx length ranging from one to five segments (Brodbelt et al., 2003a, Brodbelt et al., 2003b). The difference in syrinx size observed may be due to multiple factors: the initial surgical procedure, although performed according to a stringent protocol, will never be identical; the placement of the four quisqualic acid injections varies slightly depending on vascularity on the spinal cord surface; and variations in injection depth have also been found to have a profound effect on both lesion length and extent of damage (Berens et al., 2005). Leakage of even a minute amount of quisqualic acid once injected into the parenchyma may also cause variation in cavity size.

In the present study we have demonstrated that this model disrupts the BSCB. Even in the sham-injected animals the minor mechanical injury of the normal saline injections was sufficient to cause temporary barrier disruption. In the sham-injected animals at 3 days and 3 weeks after injection, a cavity was also present, although these differed from those in the syrinx-induced animals. The cavities in the syrinx animals were often multiloculated, unlike the simple cavities observed in the sham-injected controls. Injections of saline have previously been used in models of cord oedema and syringomyelia (Williams and Weller, 1973, Naruse et al., 1997), so it was expected that in this study, some of the sham-injected animals might develop cavities. No cavities were apparent in any of the longer-term (6 or 12 week) control animals. Although the most likely explanation for the temporary cavities was the fluid injection itself, it is possible that the biphasic BSCB disruption was a contributing factor, given that no cavities were present at 1 or 12 weeks when the barrier was intact. Since only a single sham-injected animal was investigated at each timepoint it is difficult to draw any definitive conclusions.

In the syrinx-induced animals, structural components of the BSCB remained disrupted at all timepoints studied. This corresponded to functional changes in all but two experimental animals. The decrease in EBA immunostaining was more pronounced than the degree of HRP penetration. This may reflect a greater sensitivity of EBA as a marker of BSCB barrier integrity, and the use of smaller tracers and longer tracer circulation times may prove useful. Alternatively, the differences in the pattern of staining may suggest that in our model there is a delay between loss of structural integrity and barrier permeability. In a number of animals at the earlier timepoints (3 days and 1 week), changes in vascular permeability occurred in a greater number of spinal levels than changes in EBA expression. This could indicate that HRP leakage at this time is the result of mechanical damage and large amounts of excitatory amino acids due to the initial insult causing direct damage to nearby tissue (Liu et al., 1999), which also triggers secondary events including molecular changes. These results do not prove that

syrinx enlargement occurs as a result of fluid flow through an incompetent BSCB. It is possible syrinxes enlarge solely as a result of fluid flow from the subarachnoid space, and that the pressure in the syrinx damages the surrounding tissue, including the BSCB. However, it seems likely that the profound disruption of the barrier observed at the early timepoints in this study at least contributes to the initial cyst formation. Failure of recovery of the barrier around an initial cyst and continued leakage of fluid could explain subsequent cyst enlargement. A possible mechanism of posttraumatic syringomyelia formation is a cycle of fluid leaking from vessels causing cyst enlargement, pressure from an enlarging cyst causing damage to the surrounding BSCB, and this damage causing further leakage of fluid. If so, strategies aimed at minimising the BSCB breakdown at the time of original injury and repairing a damaged barrier are potential preventative and therapeutic avenues for posttraumatic syringomyelia.

Conclusion

In this model of posttraumatic syringomyelia an initial cyst forms after excitotoxic amino acid injury to the spinal cord, and then slowly enlarges. This study has demonstrated a prolonged disruption of the BSCB in this model. Loss of functional integrity of the barrier, with fluid entering the interstitial space of the spinal cord, may contribute to enlargement of the initial cyst to form posttraumatic syringomyelia. Further work is required to determine whether the findings in this model accurately represent human posttraumatic syringomyelia pathophysiology.

Chapter 2.2

The blood-spinal cord barrier in canalicular syringomyelia

Object. Chiari malformation is associated with syringomyelia in 65% of cases, and the syrinx can result in motor weakness, sensory loss and pain. The pathogenesis of syringomyelia is poorly understood and treatment is not always effective. Although it is generally thought that syringomyelia is an accumulation of CSF, there may be additional sources of fluid. The aim of this study was to investigate the structural and functional integrity of the blood-spinal cord barrier (BSCB) in a model of noncommunicating canalicular syringomyelia.

Methods. Twenty-five adult male Sprague-Dawley rats were used in this study. A model of syringomyelia was created by injecting 1.5 µL kaolin into the dorsal columns and central grey matter of the spinal cord at T-1. This model produces inflammatory occlusion of the central canal and subsequently, the formation of an ependyma-lined cavity rostral to the occlusion. Control groups consisted of laminectomy-only and saline injected animals. Structural integrity of the BSCB was assessed using immunoreactivity to endothelial barrier antigen (EBA), a marker of BSCB integrity and rat endothelial cell protein antigen-1 (RECA-1), a marker of endothelial cells. Functional integrity of the BSCB was assessed by extravasation of intravascular horseradish peroxidase (HRP) at 1, 3, 6 and 12 weeks postsurgery.

Results. At 3, 6 and 12 weeks following the intraparenchymal kaolin injection, segments of the central canal were significantly dilated compared to controls rostral to the injection site. The enlargement was most marked at 12 weeks. Extravasation of HRP was evident surrounding the central canal in 11 of 15 animals injected with kaolin, and in two of the five sham-injected animals. No disruption of the BSCB was observed in laminectomy-only controls. At 12 weeks the tracer leakage was widespread, occurring at every level observed rostral to the kaolin injection. At this timepoint there was a decrease in EBA expression in the central grey matter surrounding the central canal.

Conclusions. The results of this study demonstrate a prolonged disruption of the BSCB directly surrounding the central canal in the experimental model of Chiari-associated syringomyelia. The disruption was widespread at 12 weeks when central canal dilation was most marked. Loss of integrity of the barrier with fluid entering the interstitial space of the spinal parenchyma may contribute to enlargement of the canal and progression of syringomyelia.

Introduction

Chiari type I malformation is an abnormality at the craniocervical junction. This condition is characterised by the downward displacement of the cerebellar tonsils into the spinal canal and reduction of the CSF space at the foramen magnum. A Chiari type I malformation is the underlying condition most commonly associated with syringomyelia, and produces an isolated enlargement of the central canal. When a canalicular syrinx ruptures through into the cord substance, deficits such as sensory loss and muscular atrophy are often observed. This may cause irreparable damage to the affected spinal tracts (Milhorat et al., 1995a, Milhorat et al., 1995b, Bogdanov and Mendelevich, 2002).

Noncommunicating syrinxes occurring within the central canal appear as distinct cavities between areas of central canal stenosis both rostral and caudal to the enlargement. These cavities are generally more complex than the simple dilations observed with communicating syrinxes and histologically they are characterised by intracanalicular adhesions (Milhorat et al., 1995a, Milhorat, 2000). Until recently, it was commonly thought that fluid flows into syrinxes from CSF in the subarachnoid space, and various theories have been put forward to explain both the mechanisms involved and the route of fluid flow (Gardner and Angel, 1958a, Ball and Dayan, 1972).

There is evidence to support the view that CSF from the subarachnoid space contributes to syrinx fluid. CSF tracer studies have demonstrated that CSF moves from the subarachnoid space, through perivascular spaces and towards the central canal in animal models of noncommunicating canalicular syringomyelia (Stoodley et al., 1999). However, there is also evidence that the pressure inside the syrinx and spinal cord may exceed subarachnoid space pressure (Hall et al., 1980, Klekamp et al., 2001). Since fluid cannot flow against a pressure gradient, this suggests that there may be additional sources of fluid. Recently there has been increasing support for the theory that extracellular fluid contributes to syrinx fluid (Klekamp, 2002, Levine, 2004, Greitz, 2006).

Experiments using a compression model of spinal cord injury have demonstrated a relationship between loss of EBA and oedema formation, with subsequent re-establishment of expression correlating with clearance of oedema (Farooque et al., 1994, Perdiki et al., 1998, Ghabriel et al., 2000). These results suggest that EBA may prove useful in the study of syringomyelia, a disease likely to occur from the development of oedema, enlarging over time to form a syrinx. It is possible that the BSCB is disrupted in Chiari-associated syringomyelia as a consequence of an enlarging cyst affecting the surrounding vasculature.

The aims of this study were to determine whether the BSCB is compromised in an animal model of noncommunicating canalicular syringomyelia. Structural and functional components will be investigated to assess whether an impaired BSCB may provide a pathway for fluid to flow from the vasculature into the syrinx.

Materials and methods

Following ethical approval from the Animal Care and Ethics Committee of the University of New South Wales and Macquarie University, 25 10-week-old male Sprague-Dawley rats weighing 377 ± 132g (mean ± SD) were divided into four experimental groups (Table 5). Each experimental group consisted of one laminectomy-only control animal, one sham-injected control animal that received a 1.5 µL spinal cord intraparenchymal injection of saline containing 1% Evans blue (Sigma-Aldrich, St. Louis, Mo, US) and three or more animals undergoing a syrinx induction procedure (described below). BSCB properties were investigated 1, 3, 6 or 12 weeks following initial operation. All procedures were performed in a sterile field under general anaesthesia induced with 4% isoflurane in oxygen and maintained with 2% isoflurane through a nose cone, increased as required to maintain an adequate level of anaesthesia.

Table 5: Experimental groups: Surgical procedure and survival time in experimental rats

		No. of Animals at Each Survival Point			
Experimental Group	**Initial Operation**	1 wk	3 wks	6 wks	12 wks
Control	Laminectomy only	1	1	1	2
Sham-injected control	1 intraparenchymal injection of saline	1	1	1	2
Syrinx induction	1 intraparenchymal injection of kaolin	3	3	3	6

Syrinx induction

The model of noncommunicating experimental syringomyelia has been described previously (Milhorat et al., 1993). Animals were placed prone, and the skin shaved and prepared with povidone iodine. A midline incision was made over the cervico-thoracic junction and a T-1 laminectomy was performed. A 29-gauge needle was used to puncture the meninges. A 5 – 10 µL syringe held in a stereotactic micromanipulator was then used to inject 1.5 µL of 250 mg/mL kaolin (sigma-Aldrich, St. Louis, MO, US). Injections were into the dorsal midline of the spinal cord, with the bevel of the needle turned in a lateral direction along the longitudinal axis of the spinal cord (Figure 17). Wounds were closed with a single layer silk suture. Analgesia was administered postoperatively and the animals were allowed food and water *ad libitum*. Any excessive weight loss, limb weakness, or signs of over-self grooming were recorded.

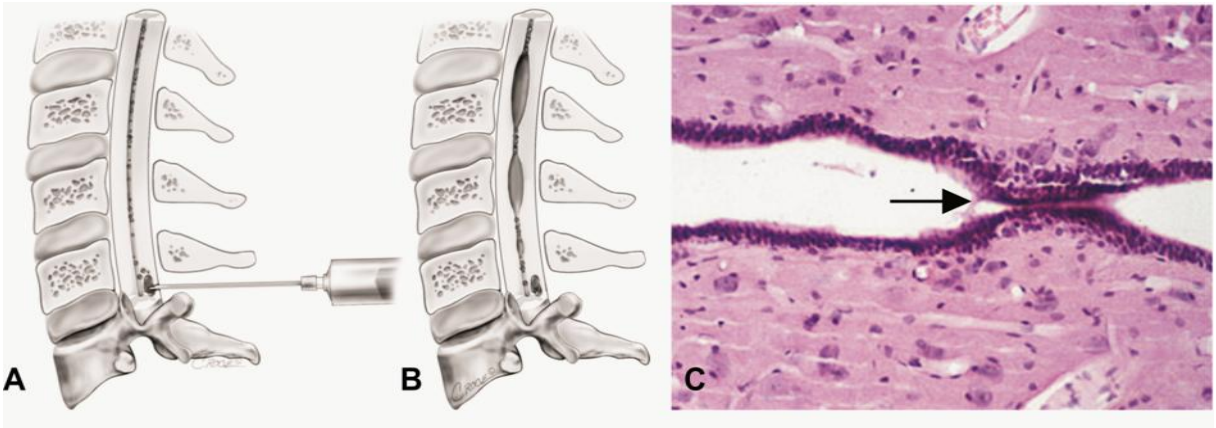

Figure 17: Canalicular syrinx induction procedure. A: Following a laminectomy, animals received an intraparenchymal injection of kaolin which migrates to the central canal. B: The kaolin induces an inflammatory reaction in the central canal resulting in occlusion. The central canal enlarges on either side of the occlusion. C: A photomicrograph of a longitudinal cervical cord section from a rat killed 1 week after kaolin injection. There is a central canal occlusion (*arrow*) and an ependyma-lined syrinx rostral and caudal to the occlusion side (hematoxylin and eosin; original magnification, ×200) [modified from (Stoodley et al., 1999)].

Intravenous injection of HRP and perfusion

At 1, 3, 6 or 12 weeks postsurgery, animals had an intraperitoneal injection of an antihistamine (1 mL of 1% promethazine solution) to prevent allergic reaction to HRP (Ma et al., 1996). The right femoral vein was exposed, the distal end ligated with 8-0 polypropylene suture and then cannulated with a 24-gauge catheter. After flushing the cannula with normal saline, 200 mg/kg HRP (type II, Sigma-Aldrich, St Louis, Mo, US) in 0.5 mL saline was injected over a period of 2 minutes. Ten minutes after the end of the HRP injection, the animals were rapidly perfused by intracardiac injection of 5,000 IU heparin in 1 mL of saline followed by 500 mL of 4% paraformaldehyde (Lancaster Synthesis) in 0.1 M phosphate buffer (pH 7.4) under a constant pressure of 120 mm Hg.

Immunohistochemistry and detection of HRP

The spinal cord and liver were dissected out and post-fixed in 4% paraformaldehyde in 0.1 M phosphate buffer overnight. Vibratome sections (50 µm) were cut from the liver and spinal cord and mounted on 3-amino propyl-triethoxy-silane-coated slides. Segments were taken from the spinal cord at C-2, and serially from C-4 to T-2. Histochemical development of HRP reaction product was carried out using 3, 3'-diaminobenzidine tetrahydrochloride (DAB) (1 mg/mL) with 0.02% hydrogen peroxide for 10 minutes. The sections were rinsed in distilled water, dehydrated in graded alcohols, cleared in xylene and mounted with DPX mounting medium (Scharlau Chemie S.A.). Colour images were acquired using a Leica DMR (Leica Microsystems, Wetzlar, Germany) and Zeiss digital camera (Axiocam, Zeiss, Oberkochen, Germany). The diameter of the central canal was measured using the interactive measurement function in AxioVision LE (Zeiss, Oberkochen, Germany). Diameter was considered the

widest transverse measurement of the lumen. Spinal sections with kaolin visible in the spinal parenchyma were not included in the analysis. It was thought that a foreign substance in the tissue may disrupt the BSCB and may interfere with the interpretation of results. Statistical analysis of spinal cord diameter was only carried out on spinal levels C-2 and C-4 to C-8. Caudal to this, the central canal was often completely occluded by kaolin, kaolin was present in the spinal parenchyma, or flattening of the central canal made it difficult to obtain accurate measurements.

Spinal cord segments from 12 week postsurgery animals were cryoprotected in 30% sucrose in phosphate buffer and embedded in OCT compound (ProSciTech, QLD, Australia). Spinal cord sections were cut transversely at 20 µm on a cryostat. Immunofluorescence staining proceeded as follows. Sections were thawed in a 37ºC oven for 10 minutes, washed twice for 10 minutes in phosphate-buffered saline (PBS). The sections were then treated with 50% ethanol/ PBS for 20 minutes followed by three 10 minute washes in PBS and incubated with 15% normal horse serum (NHS) in PBS pH 7.45 for 30 minutes. The sections were then incubated with the primary antibody overnight at 4°C. The following day, sections were left for 2 hours at room temperature before two 10 minute rinses with PBS and incubated with either anti-mouse IgG AlexaFluor 594 or anti-rabbit IgG AlexaFluor 488 (Molecular Probes, Eugene, OR, US) diluted in 4% NHS/PBS 1:400 for 2 hours. After rinsing twice for 5 minutes the sections were cover-slipped with fluorescent mounting medium (DAKO, Carpinteria, CA, US). Omission of the primary antibody was used for negative controls. Antibodies used were: EBA (SMI71, Sternberger Monoclonals, US 1:1,000), and RECA-1 (MCA970GA, AbD Serotec, UK 1:100). Fluorescent images were taken with a digital camera (Zeiss Z1, Gottingen, Germany), processed using Zeiss Axiovision software (Zeiss Z1). Colocalisation was quantified using Image-J software. Specifically, the plugin JACoP (Just Another Colocalisation Plugin) was used to quantify the Manders' coefficient for each image. The Manders' overlap coefficient produces a number between 0 and 1. A 0 value represents two non-overlapping images, while a value of 1 represents 100% colocalisation between two images (Manders et al., 1992, Bolte and Cordelieres, 2006). This analysis was carried out using three different thresholds and parameters to ensure the integrity of this technique.

Statistics

The central canal diameters and levels of HRP leakage in control and syrinx animals were compared using the unpaired 2-tailed Student's *t* test. A probability value < 0.05 was considered statistically significant. Data are presented as the mean ± SD. Software used

included Excel (Microsoft, Redmond, WA, US) and SPSS (Statistical Package for the Social Sciences, SPSS, Chicago, IL, US).

Comparison of colocalisation coefficients of RECA-1/EBA (fraction of RECA-1 overlapping EBA) were analysed using univariate analysis of variance for ratio with the following factors: spinal level (C-4, C-5, C-6, and C-7), group (control or syrinx), threshold (represents a different setting/parameter used in Image-J), animal number (nested within group), and, group and spinal level interaction. Comparisons of the main effects were assessed using Bonferroni adjusted significance. A probability value < 0.05 was considered statistically significant. Data were presented as estimated marginal means ± SEM.

Results

Barrier permeability

HRP leakage was not observed in the spinal cord at any time point in the laminectomy-only control groups. The organic compound DAB was observed in liver sections showing extravasation of tracer in the parenchyma, demonstrating the successful injection and circulation of HRP. In the sham-injected control group, HRP leakage into the cord was observed at 1 and 6 weeks after injection. No reaction product was visible at 3 or 12 weeks after surgery. At the 1 week timepoint HRP leakage was observed at three spinal levels. At the 6 week timepoint HRP was observed at two spinal levels. At this timepoint HRP extravasation was observed at C-6, corresponding to an enlarged central canal (diameter greater than 100 µm).

In the kaolin-injected group, a number of observations were made, consistent with the previously described model of noncommunicating syringomyelia (Milhorat et al., 1993). Kaolin occluded the central canal, synechial adhesions were noted, central canal enlargement was common, a ruptured ependymal lining was observed, and perivascular spaces were sometimes enlarged (Figure 18. A-C). HRP extravasation was observed in one or more syrinx animals at all timepoints (Figure 18. D).

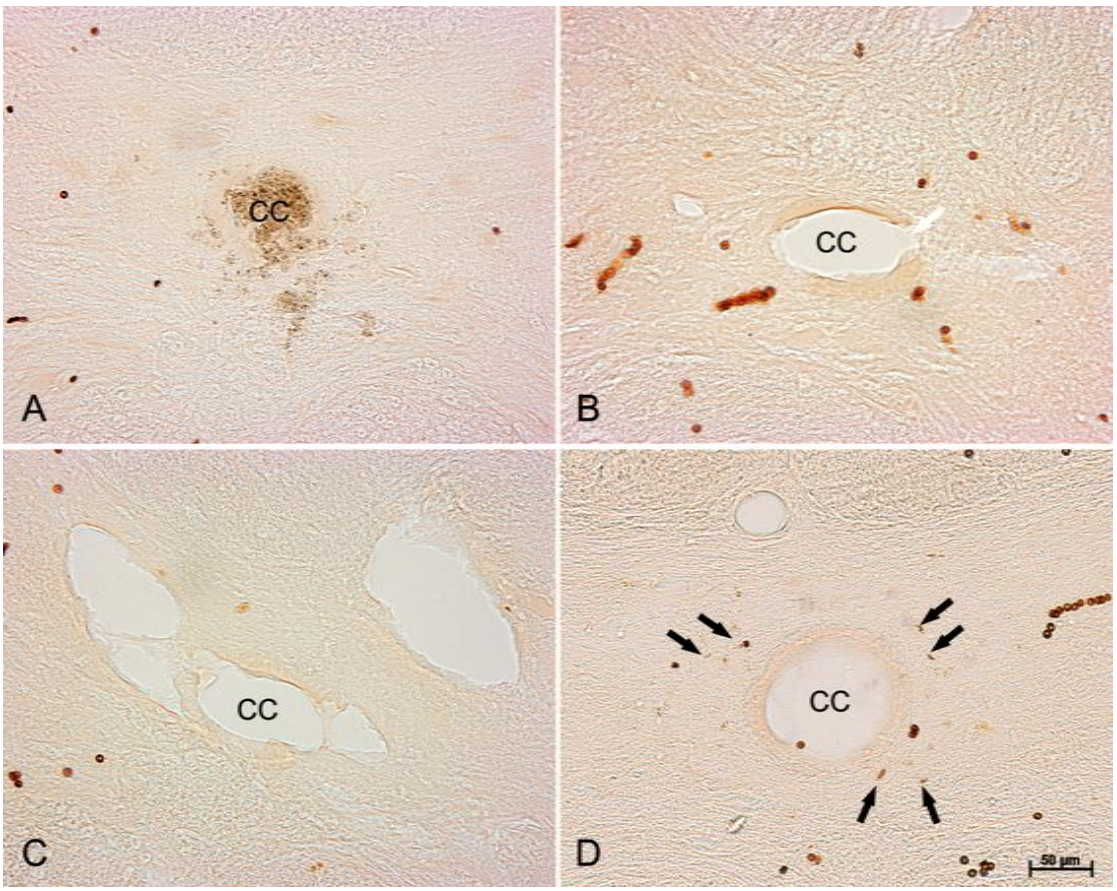

Figure 18: Representative photomicrographs of sections obtained from spinal cords of rats at different timepoints following syrinx induction and stained with DAB. Each animal received an intravenous injection of HRP prior to being killed, and spinal cord sections were treated for peroxidase reactivity. A: Transverse section obtained 6 weeks after kaolin injection demonstrating accummulation of kaolin crystals in the central canal. B: Transverse section obtained 6 weeks after kaolin injection demonstrating synechial adhesions (*white arrow*). C: Transverse section obtained 6 weeks after kaolin injection showing a grossly enlarged central canal, synechial adhesions, and disrupted ependymal lining. D: Transverse section obtained 12 weeks after kaolin injection demonstrating areas of HRP leakage (*black arrows*). Central canal (cc).

At 1 week, two animals had extensive tracer leakage at five or more spinal levels. In the other animal, HRP leakage was observed at T-1. However, at this level kaolin was present in the cord. This was not counted as a positive result. In the syrinx animals, a central canal diameter greater than 100 µm was observed in several spinal cord sections at C-4, C-5 and C-6. Central canal diameters at C-2 and C-4 were significantly smaller ($p = 0.042$ and $p = 0.0017$ respectively) in spinal sections with HRP leakage (69.22 ± 2.80, 63.37 ± 1.84 respectively) than those without HRP (80.995 ± 7.36, 93.95 ± 9.85 respectively). Significant differences were not observed at C-5 to C-7.

At 3 weeks postsurgery, HRP leakage was only observed in one animal. In this animal HRP leakage was observed at four spinal levels, C-7 to T-1 and T-3. At C-7 and C-8, no significant difference in central canal diameter was observed between sections with HRP leakage and sections with no HRP leakage ($p = 0.54$ and $p = 0.75$ respectively). No significant difference

in central canal diameter was observed between controls and kaolin animals with the exception of C-2 where central canal diameter was greater in control animals ($p = 0.016$).

At 6 weeks postsurgery, HRP leakage was observed in two animals both rostral and caudal to the kaolin injection. HRP leakage was observed at two levels in one animal and five in the other. Central canal diameters were significantly different between the spinal cords from these animals and the animal with no HRP leakage at C-2 and C-4 ($p = 0.011$, $p = 0.0277$ respectively). However, at C-2 the central canal diameters in sections from the animal with no HRP were greater, and at C-4 the diameter was smaller than in those animals in which HRP was observed. Central canal diameters were significantly higher in kaolin-injected animals than controls at C-5 and C-7 ($p = 0.033$, 0.042 respectively). In many sections the central canal diameter exceeded 100 µm.

At 12 weeks postsurgery, extravasation of HRP was observed in all three animals at 4, 6 and 10 spinal levels. A comparison of syrinx animals and controls demonstrated that central canal diameters were significantly larger in kaolin animals at C-2 ($p = 0.00096$), C-4 ($p = 0.00011$), C-5 (0.029), C-6 ($p = 0.019$) and C-8 ($p = 0.031$). There was no significant difference at C-7 ($p = 0.18$). Central canal diameter exceeded 100 µm in most sections (Figure 19.A). Central canal diameters were compared between sections in which no HRP was detected, to those with HRP leakage. At C-2, the central canal diameters were significantly greater in sections with HRP leakage ($p = 0.0033$). At C-4 there was no significant difference ($p = 0.66$) (Figure 19.B).

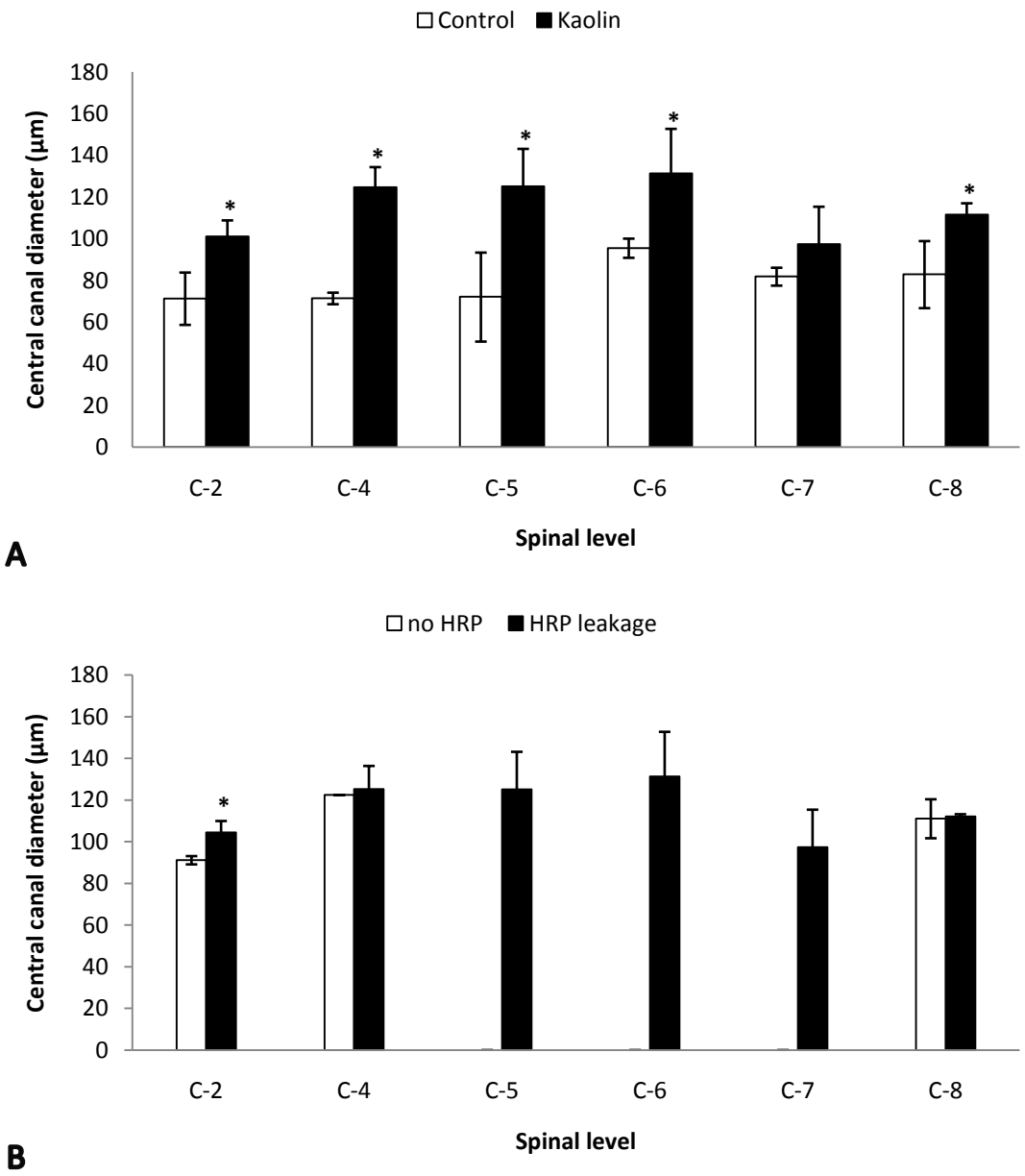

Figure 19: Central canal diameter in canalicular syringomyelia. At 12 weeks post-kaolin injection each animal received an intravenous injection of HRP prior to being killed, and spinal cord sections were treated for peroxidase reactivity. A: The central canal of animals in the canalicular syrinx (kaolin) group had a significantly greater central canal diameter than controls (laminectomy-only and sham-injected) at all spinal levels except C-7. B: HRP leakage was observed in spinal sections at all levels, although at C-2, C-4, and C-8, there were spinal sections with no HRP leakage evident. At C-2 sections with HRP leakage had a greater central canal diameter than those with no HRP leakage ($p<0.05$).

Barrier integrity

The results of the permeability study indicated that central canal enlargement was greatest at 12 weeks post-kaolin injection. As such, the following study was carried out only on animals at the 12 week timepoint.

EBA immunostaining of control sections (laminectomy-only) resulted in positive labelling of most microvessels in the grey and white matter at all spinal cord levels (Figure 20). The mean colocalisation coefficient of RECA-1/EBA in the laminectomy-only animal was 0.684 ±

0.023. In these sections the fluorescent signal was intense, with consistent endothelial cell staining revealing distinct vascular profiles. In the sham-injected control sections, the mean colocalisation coefficient of RECA-1/EBA was lower than the laminectomy-only controls (0.597 ± 0.014). This difference was significant (p = 0.0015).

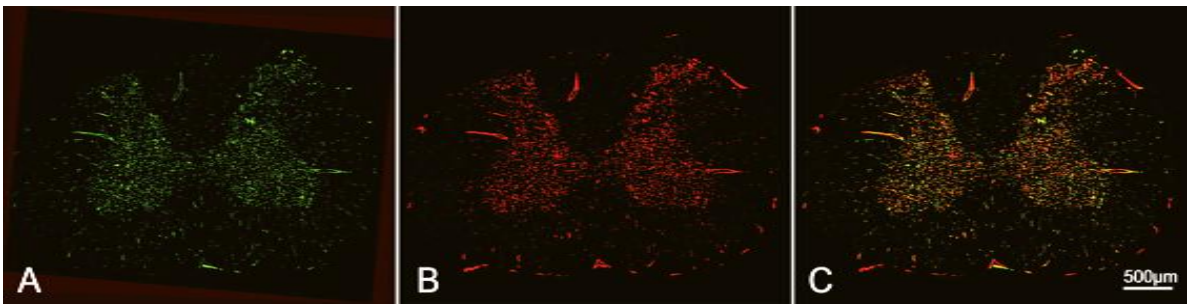

Figure 20: Representative images showing immunolocalisation of (A) RECA-1 and (B) EBA. Colocalisation is shown in (C) RECA-1 (green) and EBA (red) in spinal cord of a control (laminectomy-only) rat.

In the animals receiving an intraparenchymal injection of kaolin, EBA immunostaining still resulted in labelling of many distinct vascular profiles. Qualitatively, most sections did not appear significantly different to controls, with the exception of one animal at C-4 to C-7. In this animal, RECA-1 immunostaining demonstrated fewer, smaller blood vessels. EBA labelling did not always appear as a continuous layer around the RECA-1 positive vessels, instead, immunostaining was often interrupted (Figure 21). A comparison between the colocalisation coefficients of control (laminectomy-only) animals (0.684 ± 0.023) and syrinx animals (0.478 ± 0.008) demonstrated that RECA-1/EBA colocalisation was significantly lower in syrinx animals ($p<0.001$). Colocalisation coefficients were also significantly lower ($p<0.001$) in syrinx animals than in the sham-injected animal (0.597 ± 0.014).

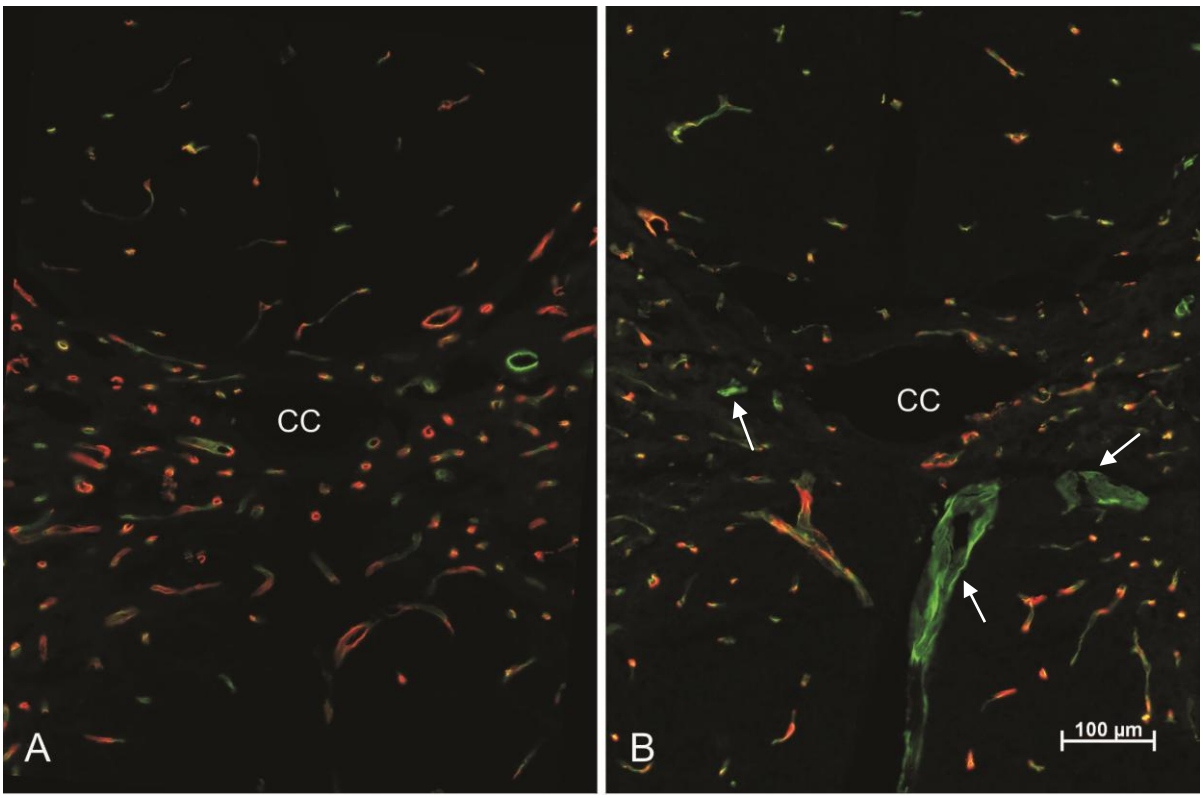

Figure 21: Photomicrographs demonstrating immunolocalisation of RECA-1 (green) and EBA (red) in spinal cord of: (A) a control (laminectomy-only) rat; and (B) a canalicular syrinx (intraparenchymal injection of kaolin) rat. A few blood vessels labelled with RECA-1 are EBA-negative (*white arrows*). Central canal (CC).

Significantly different levels of colocalisation were observed between individual animals ($p = 0.004$). There was a difference between colocalisation at different spinal levels, with the greatest concordance of EBA and RECA-1 labelling observed at C-7 (0.601 ± 0.015) and the lowest at C-4 (0.503 ± 0.012). Colocalisation was significantly higher in C-7 compared to C-4 and C-6 ($p<0.001$ for both) but not C-5. The different thresholds applied did yield different colocalisation values ($p<0.001$). However, the trends remained the same at different spinal levels (Figure 22).

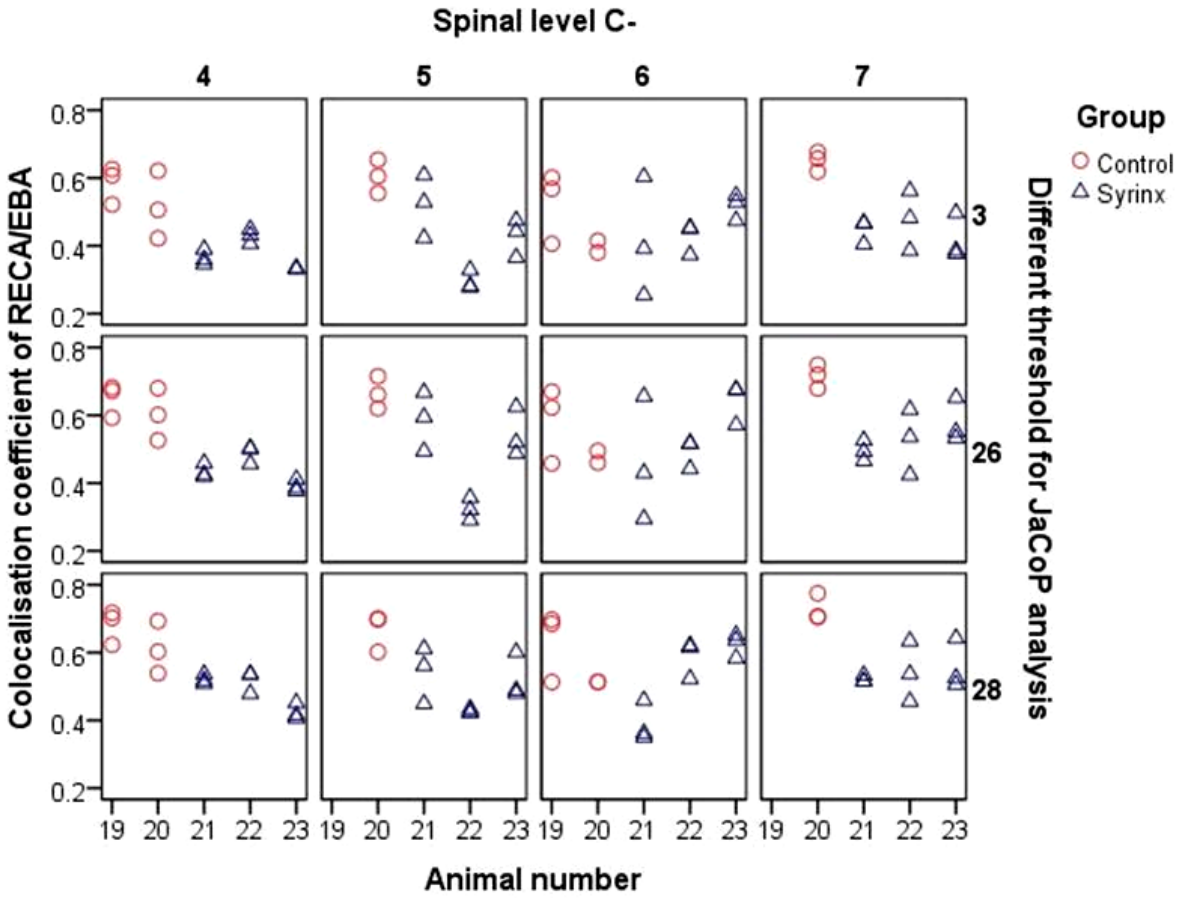

Figure 22: Colocalisation coefficient (Manders' overlap coefficient) demonstrating the fraction of RECA-1 overlapping with EBA. Comparison of colocalisation coefficients between different animals and different spinal levels are displayed. Three different thresholds and parameters were used in the Image-J, JaCoP analysis. The control group consists of a laminectomy-only (19) and sham-injected (20) rat. The syrinx group (21, 22 and 23) received an intraparenchymal injection of kaolin.

Discussion

It has generally been assumed that syrinx fluid is simply CSF from the subarachnoid space. This is likely to be a major contributing source of fluid, however, there may be other sources. There are studies that demonstrate a perivascular route for CSF flow from the subarachnoid space towards the central canal in the kaolin model of noncommunicating canalicular syringomyelia (Stoodley et al., 2000). However, recently, there has been increasing support for the theory that extracellular fluid also contributes to syrinx formation and enlargement (Klekamp, 2002, Levine, 2004, Greitz, 2006, Akiyama et al., 2008). Previous work in our laboratory has demonstrated that the BSCB is impaired adjacent to an extracanalicular syrinx in a rat model of posttraumatic syringomyelia (Hemley et al., 2009). This suggests that there is excess extracellular fluid in close proximity to the syrinx, which may contribute to increasing fluid volume within the cavity.

It is less intuitive that an impaired BSCB would play a role in syringomyelia occurring in association with a Chiari type I malformation where there is no related traumatic injury. However, many central nervous system inflammatory diseases are known to cause increased microvessel permeability (De Fazio et al., 1983a, Eisimberg et al., 1983, Correale and Villa, 2007). Recently, there have been reports of gadolinium enhancement around canalicular syrinxes in a patient with Sarcoidosis and Chiari I malformation, and a patient with Devic's disease (Ravaglia et al., 2007). This is evidence of an impaired BSCB. Due to the low sensitivity of this technique it is possible that less severe impairments in the BSCB are not detected (Fazio et al., 1983c, Grundfest-Broniatowski and Fazio, 1983), which could account for the infrequency of gadolinium enhancement in patients with syringomyelia. Given this, it is possible that the BSCB could play a role in noncommunicating canalicular syringomyelia.

Milhorat et al developed the model of noncommunicating syringomyelia described in this study (Milhorat et al., 1993). It was the first model to produce canalicular syrinxes reliably in an animal model. The intraparenchymal injection results in the drainage of kaolin molecules and inflammatory cells into the central canal. This causes ependymal cells to proliferate within the central canal, forming adhesions, which obstruct the central canal at one or more levels rostral to the injection site. The central canal expands on either side of these occlusions, producing an ependyma lined syrinx (Milhorat et al., 1993). This model has since been described in a number of studies (Stoodley et al., 1999, Stoodley et al., 2000).

The histological features of this model have been described elsewhere (Milhorat et al., 1993, Stoodley et al., 2000) and are beyond the scope of this study. However, a number of features that have been described previously were noted during the light microscopy study investigating HRP leakage. Kaolin was observed to occlude the central canal, synechial adhesions were present within the central canal in some sections, dilatation of the central canal was noted, particularly at the longest timepoint, and disruption of the ependymal cells in the central canal and subependymal oedema was observed in some cases. Stoodley et al described dilated perivascular spaces around the central canal in this model of syringomyelia, which we also observed in this study. The authors suggested that this might be the result of an inflammatory response induced by the kaolin, producing an increase in extracellular fluid. However, since the central canal continued to enlarge after 6 and 12 weeks post-kaolin injection the authors concluded this was unlikely (Stoodley et al., 1999). Similarly, in this study, central canal dilatation was most pronounced at 12 weeks.

In this study, the sham-injected controls demonstrate that the injection itself does cause either minor mechanical injury or an inflammatory response in the spinal cord, as evidenced by the HRP leakage at 1 and 6 weeks post-saline injection. In some of these sections dilatation of the central canal was noted. It is possible that the injection of a relatively innocuous substance can cause oedema. Injections of saline have previously been used in models of cord oedema and syringomyelia (Williams and Weller, 1973, Naruse et al., 1997). The injection of saline may cause an inflammatory response, and in turn the draining of these inflammatory products into the central canal, causing it to enlarge. Alternatively, the needle may cause mechanical damage to the microvasculature, and the release of plasma filtrate, protein and other molecules into the spinal parenchyma. These molecules may also drain into the central canal and induce synechiae and trabeculae. The absence of HRP leakage at 3 and 12 weeks post-injection may be indicative of a biphasic opening. However, given the small number of animals it is unlikely that this is the case, considering not all animals in the kaolin group had an impaired BSCB until 12 weeks post-kaolin injection. More animals would need to be studied to draw any definite conclusions.

Similarly, the colocalisation study investigating RECA-1 and EBA immunostaining demonstrated differences between the laminectomy-only and sham-injected control. Since the sections studied were taken from C-4 to C-8, rostral to the level of injection, this difference is unlikely to be due to direct mechanical damage to vasculature. However, the initial injection may cause secondary inflammatory responses that may result in the enlargement of the central canal. As the central canal enlarges it may place pressure on the adjacent grey matter and the surrounding vasculature.

This study demonstrated prolonged disruption of the BSCB, which was most pronounced at 12 weeks after syrinx induction. The impairment in the BSCB was not as marked or widespread as other studies involving HRP permeability following spinal cord injury (De Fazio and Kudamatsu, 1983, Gabrielli et al., 1983, Jaeger and Blight, 1997). However, this is consistent with the fact that syringomyelia is often a slowly progressing disorder. Given that animals were sacrificed 10 minutes following HRP injection, it is likely that over an extended period of time, even a small impairment, or impairment to only a few vessels, would contribute to the pathology. Previous work carried out in our laboratory in a posttraumatic model of syringomyelia reported an absence of EBA-positive labelling adjacent to the syrinx (Hemley et al., 2009). In contrast to this, in the canalicular model, there were very few vessels that appeared to be EBA-negative. However, the colocalisation study comparing RECA-1, a marker of endothelial cells and EBA immunostaining found that there was a significant

difference between EBA labelling in control versus syrinx animals. This suggests that EBA labelling, while not completely absent, is weakened or only partially expressed along microvessels. This is likely to correspond to a breakdown in the BSCB, and is consistent with the HRP leakage.

The difference in EBA labelling between spinal levels could reflect areas of central canal enlargement, or the presence of a syrinx. However, this was not always the case. Changes in EBA labelling or HRP leakage were observed surrounding central canals that were not significantly enlarged. It is possible that this reflects a BSCB breakdown preceding central canal dilatation, possibly contributing to the enlargement. The subsequent enlargement of the central canal may then in turn disrupt more microvessels in the central grey matter.

This study does not prove that an impaired BSCB contributes to the initial formation or subsequent enlargement of a syrinx in our animal model. It does, however, demonstrate that the BSCB is impaired and fluid from microvessels is able to leak into the spinal parenchyma. A study investigating the effect of recombinant VEGF165 therapy on spinal cord injury, found that injecting VEGF into the injured site exacerbated the secondary damage, and increased the lesion volume. The authors proposed that the likely mechanism for this is the increased vessel permeability induced by VEGF (Perfetti et al., 1983). It is therefore likely that increased vessel permeability in our study does correlate to an increase in syrinx volume. This suggests that therapies aimed at attenuating BSCB breakdown may be useful in the treatment of Chiari-associated syringomyelia.

Conclusion

This study has demonstrated that the BSCB is impaired in a model of noncommunicating syringomyelia, particularly in the chronic condition when central canal dilatation is greatest. A disruption in the structural integrity was demonstrated by the decrease in colocalisation of EBA and RECA-1 labelling in syrinx animals. This corresponded to a functional impairment indicated by the presence of intravascular HRP in the spinal parenchyma. This supports the theory that fluid flows from the vasculature across an impaired BSCB and into the syrinx. Since HRP leakage was evident in at least one animal at each timepoint, this suggests that BSCB disruption may contribute to the initial syrinx formation as well as the subsequent enlargement of the cavity. However, it is more likely to play a role in the enlargement of an existing syrinx, as HRP leakage was more consistent and extensive in the chronic condition. Further study is needed to confirm that BSCB impairment does lead to an increase in cavity size.

Chapter 3.1

Aquaporin-4 expression in posttraumatic syringomyelia

Object. Aquaporin-4 (AQP4) is an astroglial water channel protein that plays an important role in the transmembrane movement of water within the central nervous system. AQP4 has been implicated in numerous pathological conditions involving abnormal fluid accumulation, including spinal cord oedema following traumatic injury. AQP4 has not been studied in posttraumatic syringomyelia, a condition that cannot be completely explained by current theories of cerebrospinal fluid dynamics. The aim of this study was to examine AQP4 expression levels and distribution in an animal model of posttraumatic syringomyelia.

Methods. An excitotoxic amino acid/arachnoiditis model of posttraumatic syringomyelia was used to study AQP4 expression in 32 adult male Sprague-Dawley rats. Control groups consisted of laminectomy-only and saline injected animals. Immunofluorescence and western blotting was used to assess AQP4 and glial fibrillary acidic protein (GFAP) expression at 3 days, 1, 3, 6 or 12 weeks following syrinx induction.

Results. AQP4 was expressed in grey and white matter astrocytes, predominately at the glia limitans interna and externa, and to a lesser extent around neurons and blood vessels in both control and syrinx animals. At all timepoints a significant increase in GFAP staining in tissue surrounding syrinx cavities was observed. At the earlier timepoints the expression of AQP4 in general did not parallel this increase in GFAP, remaining similar to control levels or only slightly up-regulated. After 3 weeks, a more robust expression of AQP4 was observed around cavities.

Conclusions. The results of this study demonstrate an increase in AQP4 expression adjacent to a mature syrinx. This suggests a relationship between AQP4 and fluid accumulation in posttraumatic syringomyelia. However, whether this is a causal relationship or occurs in response to an increase in fluid needs to be established.

Introduction

Traumatic spinal cord injury is a devastating condition affecting approximately 13,000 people each year in the US (Curtis et al., 1995, Lasfargues et al., 1995, Saito et al., 2008). Of these, up to one third of people will develop a posttraumatic syrinx, which may lead to pain and an additional decline in motor and sensory function. The underlying pathogenesis of syringomyelia is not completely understood, and outcomes from surgical treatments are often unsatisfactory, with only 50% of patients showing improvement (Klekamp et al., 1997, Batzdorf et al., 1998, Klekamp et al., 2002, Koyanagi et al., 2005, Attenello et al., 2008).

Current theories of syrinx pathogenesis are based predominately on altered CSF dynamics. In the case of posttraumatic syringomyelia, it is thought that an obstruction in the subarachnoid space occurs at the time of the traumatic injury or later when arachnoid scarring develops. It is assumed that CSF flows into syrinxes from the subarachnoid space surrounding the cord, with increased flow occurring at the point of obstruction (Brodbelt et al., 2003b, Brodbelt et al., 2003c). However, since this does not entirely account for the high pressures often observed within syrinxes (Klekamp et al., 2001), there may be additional sources of fluid.

The water channel protein, AQP4 facilitates transmembrane water movement in the central nervous system. AQP4 has been implicated in a wide range of pathological conditions involving abnormal water accumulation within the brain and spinal cord (Manley et al., 2000, Vajda et al., 2002, Bloch et al., 2005, Papadopoulos and Verkman, 2005). Experimental evidence suggests that an increase in AQP4 expression may contribute to increased water content following spinal trauma. A spinal cord compression injury model in AQP4 knockout mice found that AQP4 deficiency resulted in improved neurological outcome, decreased neuronal death, less myelin vacuolation, reduced spinal cord swelling and reduced intraparenchymal pressure (Saadoun et al., 2008). A study on AQP4 expression in a rat model of spinal cord injury demonstrated a decrease in AQP4 in the acute stages of spinal cord injury followed by a marked increase in the chronically injured cord. Water content remained significantly higher in the early and late stages of disease in injured cords compared to controls (Nesic et al., 2006).

The changes in AQP4 expression following spinal cord injury and the possible causal relationship between AQP4 and spinal cord swelling demonstrated by Nesic et al and Saadoun et al (Nesic et al., 2006, Saadoun et al., 2008) point to the need for further study into AQP4 and its effect on disorders associated with spinal injury such as posttraumatic

syringomyelia. We hypothesised that AQP4 may be involved in the initial stages of syrinx formation or in the subsequent enlargement of the syrinx.

Materials and methods

Following ethical approval from the Animal Care and Ethics Committee of the University of New South Wales and Macquarie University, 32 6 – 10-week-old male Sprague-Dawley rats weighing 349 ± 65g (mean ± SD) were divided into five experimental groups for immunohistochemistry (Table 6) and another for the western blotting experiments (Table 7). Experimental groups consisted of either three normal controls (western blotting) or one laminectomy-only control (immunohistochemistry), and one sham-injected control animal that received four 0.5 µL spinal cord intraparenchymal injections of saline containing 1% Evans blue (Sigma-Aldrich, St. Louis, MO, US) and three or more animals undergoing a syrinx induction procedure (described below). In the immunohistochemistry study, AQP4 expression was investigated after 3 days, or at 1, 3, 6 or 12 weeks following the initial operation. In the western blotting experiment AQP4 expression was investigated at 12 weeks postsurgery only. All procedures were performed in a sterile field under general anaesthesia induced with 4% isoflurane in oxygen and maintained with 2% isoflurane through a nose cone, which was increased as required to maintain an adequate level of anaesthesia.

Table 6: Experimental groups for immunohistochemistry. Surgical procedure and survival time in experimental rats

		No. of Animals at Each Survival Point				
Experimental Group	**Initial Operation**	3 days	1 wk	3 wks	6 wks	12 wks
Control	Laminectomy only	1	1	1	1	1
Sham-injected control	4 intraparenchymal injections of saline	1	1	1	1	1
Syrinx induction	4 intraparenchymal injections of quisqualic acid & subarachnoid kaolin	3	3	3	3	3

Table 7: Experimental groups for Western Blotting. Surgical procedure and survival time in experimental rats

Experimental Group	**Initial Operation**	**No. of Animals at 12 wks**
Normal Control	None	3
Sham-injected control	4 intraparenchymal injections of saline	1
Syrinx induction	4 intraparenchymal injections of quisqualic acid & subarachnoid kaolin	3

Syrinx induction

The excitotoxic and arachnoiditis model of posttraumatic syringomyelia has been described previously (Yang et al., 2001, Brodbelt et al., 2003b). Animals were placed prone, and the

skin shaved and prepared with povidone iodine. A midline incision was made over the cervicothoracic junction and a laminectomy was performed from C-7 to T-1. A 29-gauge needle was used to puncture the meninges. A glass-tipped, 5 µL syringe (SGE International Pty Ltd., Austin, TX, US) held in a stereotactic micromanipulator was then used to infiltrate four 0.5 µL injections of 24 mg/mL quisqualic acid (Tocris Cookson, Bristol, UK) and 1% Evans blue. Injections were delivered into the dorsal cord parenchyma along the right dorsal nerve rootlets between the rostral C-8 and caudal T-1 levels. Use of Evans blue allowed any leakage of quisqualic acid to be identified. Five microlitres of 250 mg/mL kaolin (Sigma-Aldrich, St. Louis, MO, US) were then injected into the subarachnoid space to produce arachnoiditis. Wounds were closed with a single layer silk suture. Analgesia was administered postoperatively and the animals were allowed food and water *ad libitum*. Any excessive weight loss, limb weakness, or signs of over-self grooming were recorded.

Tissue collection, processing and immunohistochemistry

The animals were rapidly perfused by intracardiac injection of 5,000 IU heparin in 1 mL of saline, followed by 500 mL of 4% paraformaldehyde (Lancaster Synthesis, Pelham, NH, US) in 0.1 M phosphate buffer (pH 7.4) under a constant pressure of 120 mm Hg. The spinal cord was dissected out and post-fixed in 2% paraformaldehyde in 0.1 M phosphate buffer. Spinal cord segments C-7 to T-2 were paraffin-embedded, transverse tissue slices 5 – 10 µm thickness were cut and mounted on slides and left to dry overnight at 37°C. Spinal cord sections were deparaffinised, rehydrated, and antigen retrieval was performed using 0.01 M citrate buffer (pH 6.0). Sections were blocked in 15% normal horse serum (NHS) in phosphate-buffered saline (PBS) pH 7.45 for 60 minutes. The sections were then incubated with anti-AQP4 antibody (1:250; AB3594 Chemicon, Temecula, CA, US) and anti-GFAP antibody (1:800; MAB360) overnight at 4°C, followed by secondary anti-rabbit IgG Alexa Fluor 488 and anti-mouse IgG Alexa Fluor 594 (Molecular Probes, Eugene, OR, US) diluted in 4% NHS/PBS 1:400 for 2 hours. The sections were coverslipped with fluorescent mounting medium (DAKO, Carpinteria, CA). Omission of the primary antibody was used for negative controls. Fluorescent images were obtained using a digital camera (Zeiss Z1, Gottingen, Germany), processed using Zeiss Axiovision software.

Protein extraction

The animals were rapidly perfused by intracardiac injection with 180 mL of ice cold 0.1 M phosphate buffer (pH 7.4) containing 5,000 IU heparin. Spinal cord segments were dissected on ice and immediately frozen on dry ice. Samples were stored at -80°C until homogenisation. The tissue samples were sonicated four times for 10 – 15 sec in 200 µL of ice cold lysis buffer

(10 mM HEPES, 10 mM KCl, 0.1 mM EGTA, 1 mM DTT, 0.5 mM PMSF, and containing protease and phosphatase inhibitors (Calbiochem, San Diego, CA)). After vortexing for 5 seconds and centrifugation at 8,000 rpm for 8 minutes at 4°C the whole cell protein supernatant fraction was collected. Protein concentrations were determined using a Bicinchoninic acid assay (bovine serum albumin, Pierce, Rockford, IL, US).

Electrophoresis and western blotting

Samples containing 40 µg of protein and 4X NuPAGE® LDS sample buffer and 10X NuPAGE® reducing agent (Invitrogen, CA, US) were heated at 70°C for 10 minutes, and separated on a 10% NuPAGE® Novex Bis-Tris Gel. Samples were immunoblotted on to a polyvinylidene difluoride membrane using the iBlot® dry blotting system (Invitrogen, CA, US, 0.2 µm). Membranes were blocked with 4% (w/vol) non-fat dry milk in tris-buffered saline (TBS) with tween-20 for 60 minutes at room temperature and incubated with the primary antibody at 4°C overnight, washed three times in TBS containing 0.1% (w/vol) Tween-20 and then incubated with HRP-conjugated anti-mouse (1:20,000) or ant-rabbit (1:20,000) secondary antibody (Sigma-Aldrich, St. Louis, MO, US) and visualised by enhanced chemiluminescence (ECL) (RPN2232; Amersham Biosciences). The following primary antibodies were used: rabbit anti-AQP4 (Chemicon AB3594, 1:3,000); mouse anti-GFAP (Chemicon MAB360, 1:60,000); and rabbit anti-β-Actin (Sigma-Aldrich A5060, 1:3,000) as a loading control.

Signal intensity was quantified using Image-J software. Specifically, a fixed area was used to separately measure signal intensity from i) the region encompassing the ~38 kDa AQP4 band, ii) the GFAP band at ~51 kDa (Figure 23). The AQP4 quantification was expressed as a percentage of GFAP. Where possible, relative differences between samples were assessed on the same blots or using simultaneously processed gels with identical film exposure times. Spinal cord segments investigated for each animal were: C-2 to C-3, C-7 to C-8, T-1 to T-2 and T-6 to T-7.

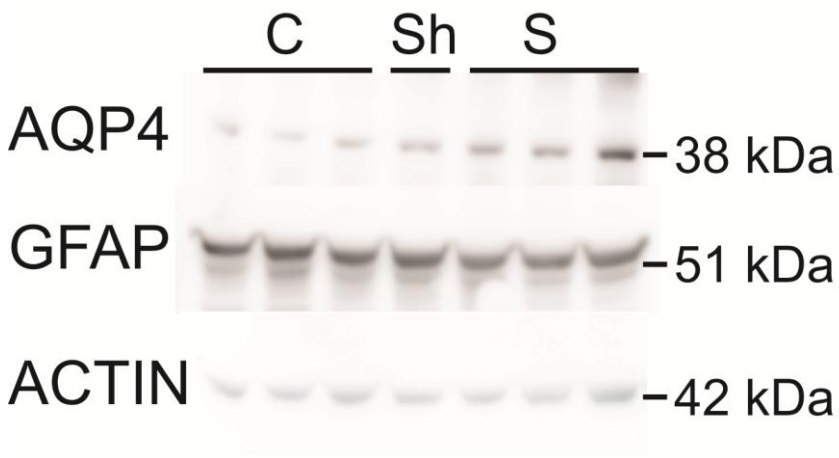

Figure 23: Representative western blot illustrating bands for AQP4, GFAP and β-Actin in control (C), a sham-injected animal (Sh) and syrinx (S) animals.

Statistics

AQP4 expression in control and syrinx animals was compared using the unpaired 2-tailed Student's *t* test. A probability value < 0.05 was considered statistically significant. Data are presented as the mean ± SD. Software used included Excel (Microsoft, Redmond, WA, US) and SPSS (Statistical Package for the Social Sciences, SPSS, Chicago, IL, US).

Results

AQP4 and GFAP expression pattern in controls

In control (laminectomy-only) animals, AQP4 was primarily expressed in grey and white matter astrocytes (Figure 24). In the grey matter, AQP4 was strongly expressed surrounding capillaries, and more diffusely throughout the grey matter, particularly surrounding neuronal bodies (Figure 24. B). Colocalisation of GFAP and AQP4 was very limited in the grey matter, however, GFAP expression was observed in glial processes adjacent to astrocytic endfeet labelled with AQP4. AQP4 was also expressed, although not as strongly, in ependymal cells lining the central canal (Figure 24. C). In the white matter AQP4 was expressed in radial astrocytes, predominately at the glia limitans externa and colocalised with GFAP positive astrocytes (Figure 24. D).

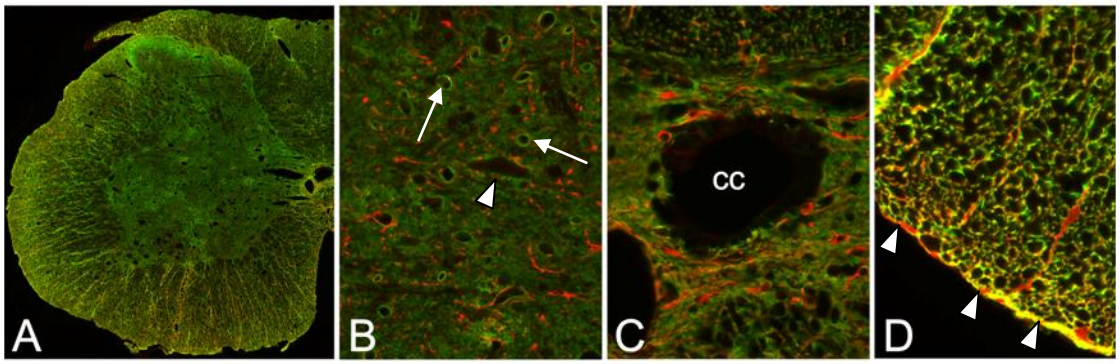

Figure 24: Immunolocalisation of AQP4 (green) and GFAP (red) in control (laminectomy-only) rat spinal cord. Colocalisation of AQP4 and GFAP shown in yellow. (B-D) High magnification (x40) images of (A). (B) AQP4 is expressed around capillaries (*arrows*) and neuronal bodies (*arrow head*) in grey matter; (C) in ependymal cells and grey matter surrounding the central canal; and (D) at the glia limitans externa (*arrow heads*). CC = central canal.

In sham-injected controls a small cavity was observed at 3 days, and at 1, 6, and 12 weeks following the intraparenchymal injection of saline and Evans blue. These cavities were restricted to the dorsal horn grey matter or dorsal white matter. At 3 weeks after induction a larger cavity was observed in the dorsal white matter, extending into dorsal grey matter. There was an increase in GFAP positive astrocytes and AQP4 expression surrounding the cavity at all time points (Figure 25).

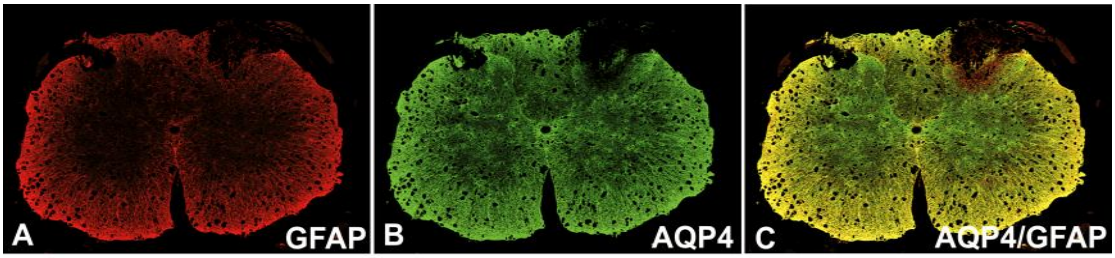

Figure 25: Representative images showing immunolocalisation of (A) GFAP (red) and (B) AQP4 (green) in spinal cord of a sham-injected control rat. Colocalisation of AQP4 and GFAP in the merged image (C) shown in yellow. A small cavity is present in the grey matter of the right dorsal horn.

AQP4 and GFAP expression pattern in posttraumatic syringomyelia

The intraspinal injection of quisqualic acid and subarachnoid kaolin injection produced a noncommunicating extracanalicular syrinx cavity in all 15 animals. At all timepoints (3 days, 1, 3, 6, and 12 weeks) investigated, there was a significant increase in GFAP positive astrocytes surrounding the syrinx cavity. AQP4 expression was also upregulated directly adjacent to the cavity at all timepoints (Figure 26). At 3 days and 1 week after syrinx induction, the increase in AQP4 was not consistently proportional to the increase in the number of GFAP positive astrocytes (Figure 27). From 3 weeks after induction however, AQP4 expression was more robust, and appeared visibly similar to GFAP levels. At 12 weeks after surgery, levels of AQP4 had increased, with expression appearing to be more robust than GFAP expression surrounding the syrinx.

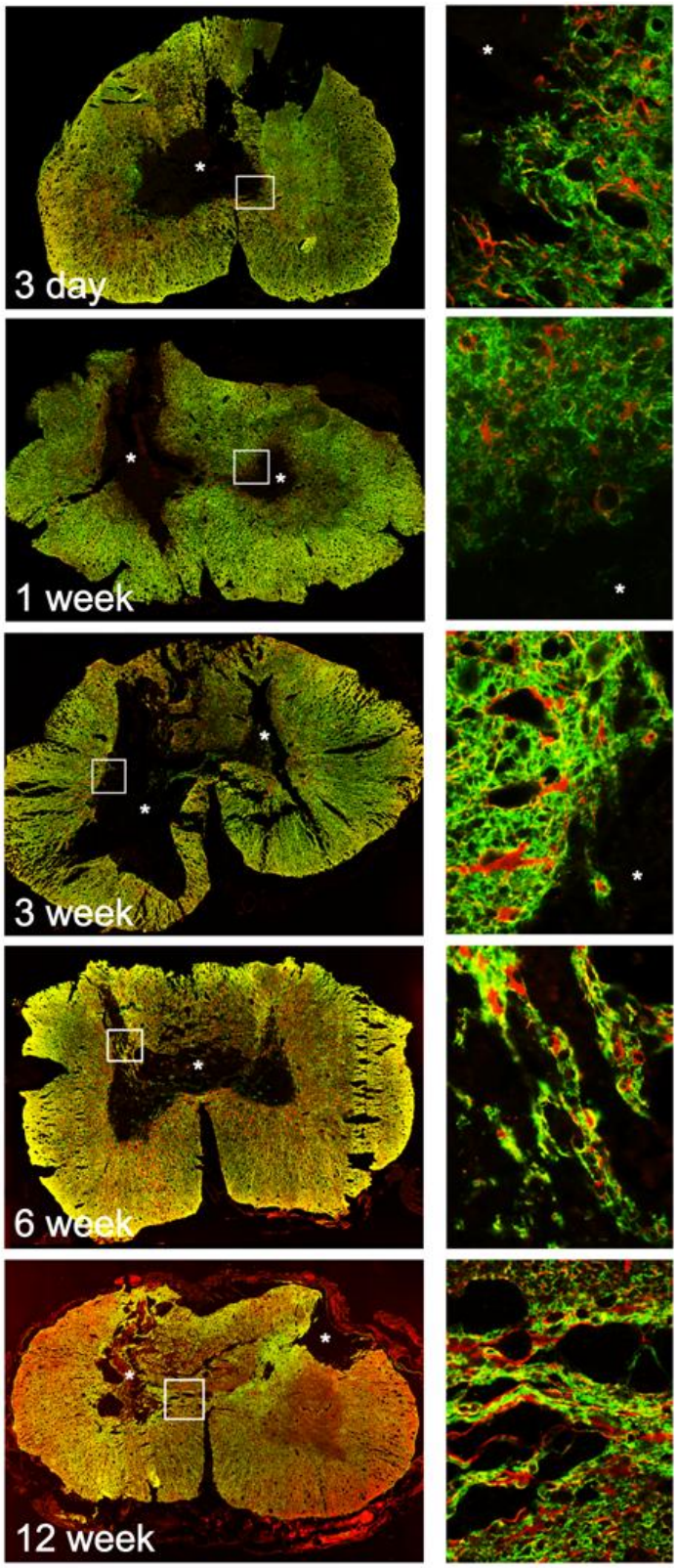

Figure 26: Immunolocalisation of AQP4 (green) and GFAP (red) in rat spinal cord at different timepoints following syrinx (*) induction. Colocalisation of AQP4 and GFAP shown in yellow. Animals received four intraparenchymal quisqualic acid injections and a subarachnoid kaolin injection. *Left* panel shows representative transverse sections of animals 3 days, 1, 3, 6, and 12 weeks after surgery. *Right* panel shows high magnification (x40) view of insets in *left* panel.

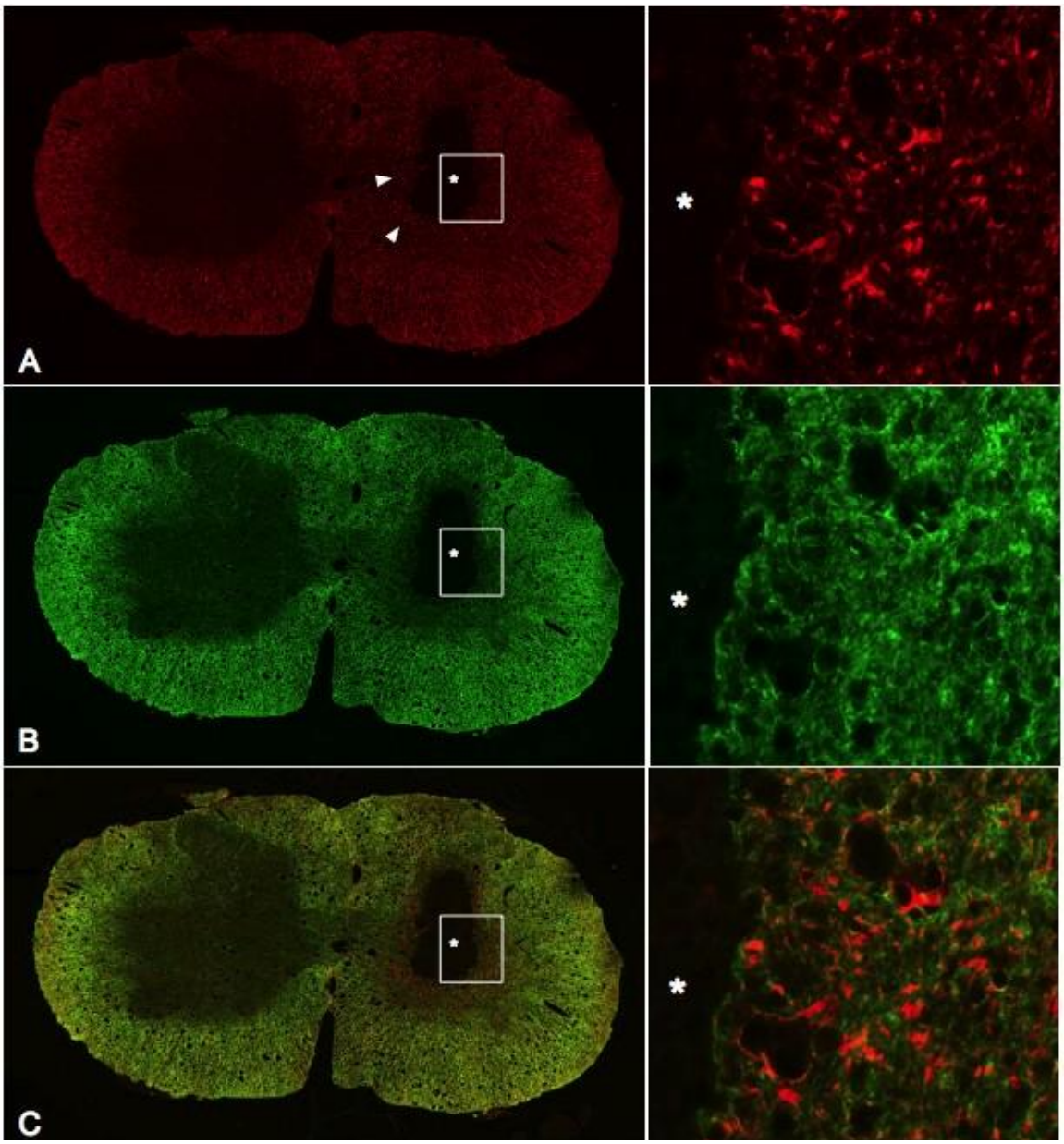

Figure 27: Representative images showing immunolocalisation of AQP4 (green) and GFAP (red) in spinal cord of a rat with a posttraumatic syrinx (*). Colocalisation of AQP4 and GFAP in the merged image (C) shown in yellow. *Left* panel shows transverse spinal sections from an animal 1 week postsurgery. *Right* panel shows high magnification (magnification x 40) view of insets in *left* panel. A: GFAP-positive astrocytes surrounding syrinx (*arrow heads*). The pattern of GFAP immunostaining suggests that astrocytes are migrating toward syrinx cavity. B: AQP4 immunostaining not as intense as GFAP shown in (A). C: GFAP positive astrocytes expressing low levels of AQP4.

Western blot analysis of AQP4 and GFAP in the chronic stages of posttraumatic syringomyelia

GFAP expression was unchanged in the sham-injected and syrinx animals in the high cervical (C-2 and C-3 pooled) and upper thoracic (T-1 and T-2 pooled) sections (Figure 28. A). GFAP expression had significantly decreased in the lower cervical region (C-7 and C-8 pooled) in syrinx animals ($p = 0.003$). There was also a decrease, although to a lesser extent in the sham-injected animal. In the lower thoracic cord (T-6 and T-7) there was a significant increase in GFAP expression ($p = 0.0003$), a change mirrored in the sham-injected animal.

Changes in AQP4 expression did not always correlate with changes in GFAP (Figure 28. B). AQP4 had significantly increased at C-2 (pooled C-2 and C-3), away from the site of syrinx induction ($p = 0.0006$). At C-7 (pooled C-7 and C-8) and T-1 (pooled T-1 and T-2), the site of syrinx induction, AQP4 expression had decreased. This was significant in the cervical region ($p = 0.01$). In the lower thoracic region (pooled T-6 and T-7) there was also a decrease in AQP4 expression although this was not significant. AQP4 expression differed in the sham-injected animal compared to controls in the cervical spinal cord. However changes were not as dramatic as the changes observed in the syrinx animals.

When AQP4 was presented as a percentage of GFAP expression there was a significant increase in AQP4 levels in syrinx animals in the upper cervical sections (C-2 and C-3 pooled) ($p = 0.006$), away from the syrinx induction site. There was a decrease in AQP4 expression in the thoracic cord both at the site of syrinx induction and caudal to the surgical site. This decrease was significant at T-6 and T-7 ($p = 0.03$). In the sham-injected animal there were differences in AQP4 expression compared to controls. However, these differences did not completely correlate with the syrinx animals, except in the lower thoracic sections. At this level AQP4 expression had decreased and was similar to the syrinx animals (Figure 28. C).

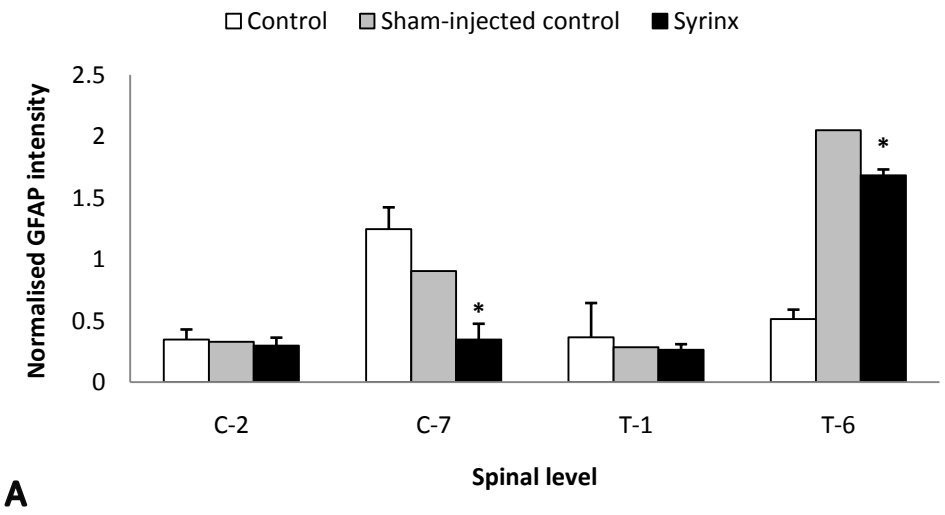

A

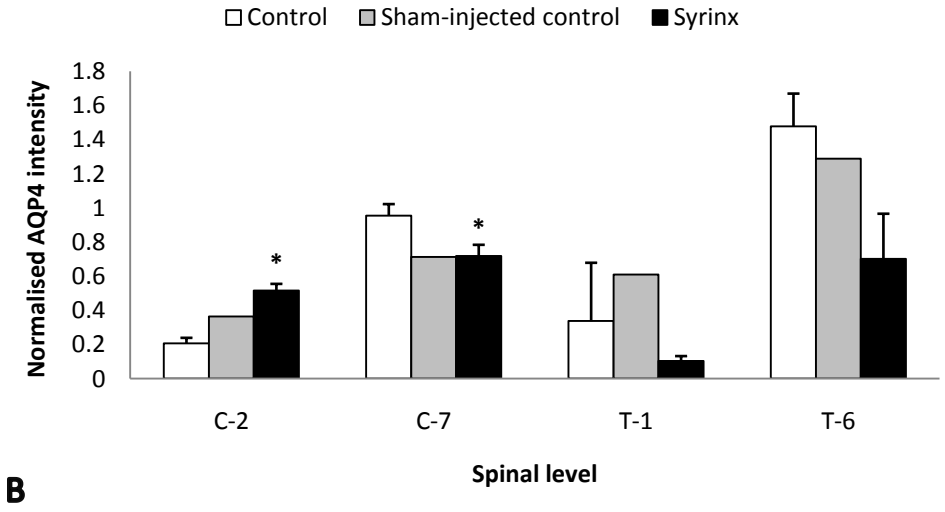

B

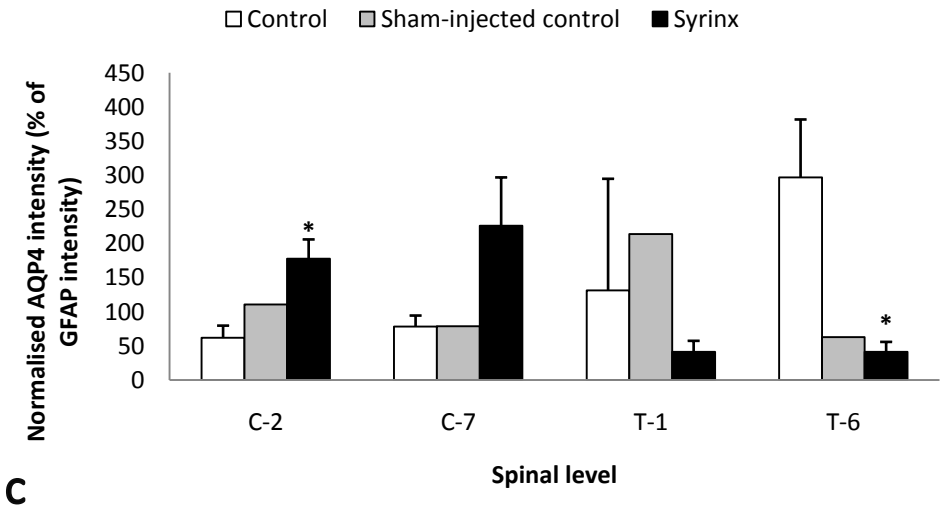

C

Figure 28: Western blot analysis of AQP4 expression at different spinal levels in control, sham-injected, and syrinx rats. Results are mean ± SD (n = 3 for control and syrinx animals, n = 1 for sham-injected, $p<0.05$). Quantitation of (A) GFAP and (B) AQP4 protein by Western blot normalised to actin. (C) Quantification of normalised AQP4 expression as a percentage (%) of GFAP expression.

Discussion

In this study we used immunohistochemistry to investigate the expression of AQP4 in spinal cords of rats with a noncommunicating extracanalicular syrinx. Previous studies have reported that AQP4 is constitutively expressed in glial cells throughout the spinal cord and in the ependymal cells lining the central canal (Nielsen et al., 1997). AQP4 labelling is particularly distinct on astrocytic foot processes in close proximity to or in contact with blood vessels (Nielsen et al., 1997). The results of our study were consistent with these reports, with AQP4 abundantly expressed at the BSCB (surrounding capillaries) and CSF interfaces (at the glia limitans interna and externa). Previous papers have suggested that AQP4 labels protoplasmic astrocytes in the grey matter which have few GFAP immunopositive processes (Oshio et al., 2004, Simard and Nedergaard, 2004, Nesic et al., 2006). GFAP is typically expressed in fibrous astrocytes (Oshio et al., 2004). This is consistent with the lack of colocalisation between AQP4 and GFAP observed in this study, predominately in the grey matter. GFAP expression was instead observed in glial processes adjacent to astrocytic endfeet densely labelled with AQP4.

This distribution of AQP4 suggests that it may play a role in regulating fluid transport between the spinal cord and bloodstream and the CSF. This is supported by studies that found a reduction in osmotic swelling in the dorsal horn of spinal cord in $AQP4^{-/-}$ mice (Solenov et al., 2002). Saadoun et al similarly found, that following spinal cord injury, $AQP4^{+/+}$ mice had increased cord swelling compared with $AQP4^{-/-}$ mice (Saadoun et al., 2008). Recent publications have reported changes in AQP4 expression in rodent brain and spinal cord in association with a number of conditions including trauma (Vajda et al., 2002, Nesic et al., 2006). The effects of changes in AQP4 expression vary, and can be beneficial or undesirable. For example, following brain injury, AQP4 has been found to facilitate water removal in vasogenic oedema, however, contributes to astrocytic swelling in cytotoxic (cellular) oedema (Manley et al., 2000, Papadopoulos et al., 2004, Papadopoulos and Verkman, 2005).

The results from this study demonstrate a change in AQP4 expression surrounding posttraumatic syrinxes. AQP4 expression increased in tissue directly adjacent to the syrinx cavity at 3 days to 12 weeks. However, at the earlier timepoints (3 days and 1 week) the increase in GFAP expression surrounding the cavity appeared to be greater than the increase in AQP4 expression. After 3 weeks, AQP4 expression more closely resembled GFAP levels, and at 12 weeks AQP4 appeared to exceed GFAP expression levels. Nesic and colleagues reported a similar result following spinal cord injury in rats (Nesic et al., 2006). In this paper they hypothesised that migrating astrocytes may not express AQP4, however, once at the site

of injury they may change their phenotype, and at that point begin expressing AQP4. A similar decrease in AQP4 levels following trauma has been observed in a model of brain injury (Zhao et al., 2005). It is established that early oedema formation following brain or spinal cord injury is caused by a breakdown in the BBB/BSCB, and since AQP4 has been found to decrease lesion size following vasogenic oedema, it was postulated that the down regulation of AQP4 shortly after injury impaired the removal of fluid. In the chronically injured cord it was demonstrated that up regulation of AQP4 occurred when the BSCB was intact. Water accumulation in the chronic stage may be attributed to cytotoxic oedema due to astrocyte swelling (Nesic et al., 2006).

The quantitative study of GFAP and AQP4 expression at 12 weeks, interestingly, found that in the syrinx animals, GFAP levels had decreased or remained similar to controls except in the lower thoracic sample. At this level, caudal to the expected location of the syrinx cavity, GFAP had significantly increased. AQP4 levels similarly decreased or remained unchanged except in the cervical cord rostral to the site of syrinx induction. In the upper cervical cord AQP4 levels had significantly increased. When AQP4 was represented as a percentage of GFAP expression, we found that there was an increase in AQP4 in the cervical cord and a decrease in AQP4 levels in the thoracic cord. This suggests that there are astrocytes that are over-expressing AQP4 in the cervical cord, and fewer astrocytes that are expressing AQP4, or expressing less AQP4 in the thoracic cord. The decrease in GFAP expression in the syrinx animals is surprising as it would be expected that astrocytes proliferate and migrate towards sites of damage. It is possible that while the overall number of astrocytes has decreased, the number of astrocytes directly surrounding the cavity has increased. This is consistent with the immunofluorescence findings. The increase in AQP4 levels in the cervical cord correlates with the increase in AQP4 directly surrounding the syrinx cavity observed with immunofluorescence. It is unclear why this was not seen in the thoracic spinal cord, particularly at T-1 where presumably there would be a syrinx cavity.

A previous study carried out in our laboratory found that in this excitotoxic model of posttraumatic syringomyelia, the BSCB is still impaired surrounding a syrinx cavity even at 12 weeks following the initial syrinx induction (Hemley et al., 2009). In this study the most significant leakage of tracer across the BSCB was observed at the earlier timepoints (3 days and 1 week). It is possible that at 3 days and 1 week, AQP4 levels were insufficient to remove fluid that was leaking from the surrounding vasculature. At the later stages, AQP4 may be contributing to astrocytic swelling around the syrinx, rather than eliminating fluid from the leaky blood vessels. Conversely, it may be that AQP4 is simply increasing in an attempt to

combat the excess fluid caused by an influx in CSF, and not contributing to the fluid accumulation. This theory is supported by a study investigating the role of AQP4 in hydrocephalic oedema. Bloch et al used a well established kaolin model of hydrocephalus in AQP4-null mice (Bloch et al., 2006). Kaolin injected into the cisterna magna of mice caused ventricular enlargement, increased intracranial pressure and increased brain water content. It was found that in AQP4-null mice, development of hydrocephalus occurred more rapidly than in wild-type mice. It was suggested that removal of excess CSF from the parenchyma occurs primarily through AQP4-dependant pathways (Bloch et al., 2006).

Syringomyelia is generally thought to be a condition caused by alterations in CSF dynamics. In the case of posttraumatic syringomyelia, arachnoiditis occurring after the initial trauma may cause a flow obstruction in the subarachnoid space. There is evidence that CSF does flow into the spinal parenchyma from the subarachnoid space via perivascular spaces. There is also an increase in the flow of CSF into the cord at the level of arachnoiditis (Brodbelt et al., 2003b, Brodbelt et al., 2003c). Given this, it is possible that AQP4 is facilitating removal of fluid from the syrinx but is unable to keep up with the influx of CSF into the spinal parenchyma. To determine whether AQP4 is removing water from the syrinx cavity in our animal model, or exacerbating the problem it would be useful to use pharmacological interventions to modulate AQP4 expression. Alternatively, adapting our model of posttraumatic syringomyelia to AQP4 knockout mice would enable a more definitive determination of the role of AQP4.

Given the changes in AQP4 expression patterns observed in this study it would be of interest to investigate other AQPs including AQP1 and AQP9 which label a different subset of astrocytes in the spinal cord (Oshio et al., 2004). It would be useful to carry out the quantitative study in animals in the acute stages of posttraumatic syringomyelia to determine whether overall AQP4 expression is changed, or if it is only a shift in the distribution of AQP4, moving to the area of increased fluid (the syrinx cavity).

Conclusion

We have demonstrated changes in AQP4 expression around posttraumatic syrinxes. Whether these changes play a detrimental or beneficial role in syrinx formation or enlargement remains to be determined.

Chapter 3.2

Aquaporin-4 expression in canalicular syringomyelia

Object. Aquaporin-4 (AQP4) has not been studied in syringomyelia associated with Chiari I malformation, a condition that cannot be completely explained by current theories of CSF dynamics. AQP4 has been implicated in numerous pathological conditions involving abnormal fluid accumulation, including spinal cord oedema. In this study it was proposed that changes in the expression of AQP4 could increase the movement of water into a syrinx. The aim of this study was to examine AQP4 expression levels and distribution in an animal model of noncommunicating canalicular syringomyelia.

Methods. A kaolin-induced model of canalicular syringomyelia was used to investigate AQP4 expression in five adult male Sprague-Dawley rats. Control groups consisted of laminectomy-only and saline-injected animals. Immunofluorescence was used to assess AQP4 and glial fibrillary acidic protein (GFAP) expression at 12 weeks following syrinx induction.

Results. AQP4 was expressed in grey and white matter astrocytes, predominately at the glia limitans interna and externa, and to a lesser extent around neurons and blood vessels in both control and syrinx animals. Expression of GFAP and APQ4 in kaolin-injected animals was varied and not significantly different to controls directly surrounding the central canal.

Conclusions. Significant changes in AQP4 expression were not observed in this model of canalicular syringomyelia. Further investigation is needed to elucidate whether subtle changes in expression levels occur in this model.

Introduction

Chiari type I malformation has been classified as a herniation of the cerebellar tonsils of more than 5 mm below the foramen magnum, and is often associated with a small posterior fossa (Ross et al., 1983). A study of over 300 symptomatic Chiari I patients found that 65% had syringomyelia (Milhorat et al., 1999), which may result in considerable pain, motor weakness and even paralysis. The pathogenesis of syringomyelia is poorly understood and treatment is not always effective. Although it is generally thought that syringomyelia is an accumulation of CSF from the subarachnoid space, there may be additional sources of fluid.

AQP4 belongs to a family of transmembrane water channel proteins with a central pore (Tarazi et al., 1983). This pore allows the movement of water molecules across a cell membrane (Brumley et al., 1983). In brain and spinal cord, AQP4 is expressed in astroglia, most abundantly in membranes at the tissue-blood or tissue-CSF interfaces, including astrocytic endfeet surrounding capillaries, glia limitans and ependyma (Nielsen et al., 1997). The distribution of AQP4 predominantly at sites of fluid transport suggests that AQP4 plays a pivotal role in the transmembrane movement of water within the central nervous system. This role has since been established using animal models of diseases involving abnormal fluid accumulation within the brain and spinal cord (Manley et al., 2000, Vajda et al., 2002, Bloch et al., 2005, Papadopoulos and Verkman, 2005).

Research has demonstrated an increase in AQP4 expression in animal models of hydrocephalus. This increase is thought to indicate that AQP4 acts as a compensatory pathway, enabling CSF absorption across the ependyma and within the parenchyma (Zotti et al., 1983). In addition, there is evidence that changes in AQP4 expression are consistent with severity and time course of hydrocephalus (Wollmer et al., 1983). There have also been reports of sporadic cases of hydrocephalus in a small percentage of $AQP4^{-/-}$ mice, a finding not observed in wild-type or AQP4 heterozygous animals (De Fazio and Ingenito, 1983). Since hydrocephalus is associated with communicating canalicular syringomyelia, it is possible that AQP4 may be of importance in the formation or enlargement of syrinxes occurring in the central canal.

It has been suggested that AQP4 may play a role in the structural integrity of ependymal cells (De Fazio and Ingenito, 1983). Feng et al noted a disorganisation of the ependymal lining surrounding the ventricles in AQP4-null mice (De Fazio and Ingenito, 1983). In support of this role, Li et al demonstrated a decrease in the expression of the gap junction protein connexin43 in ependymal cells of AQP4-null mice compared to wild-type mice. The authors

also noted detachment of ependymal cells and observed swollen astrocytes in the subependyma of animals with a disorganised or abnormal ependymal lining (Fazio et al., 1983b). Given this, we hypothesised that changes in AQP4 expression may play a role in Chiari-associated syringomyelia, which is characterised by occlusions in the central canal and dilatation both rostral and caudal to these occlusions. These events give rise to the formation of an ependyma-lined syrinx (canalicular syringomyelia) that may rupture into the surrounding spinal parenchyma. The objective of this study was to investigate the spatiotemporal changes in AQP4 expression in an animal model of noncommunicating canalicular syringomyelia.

Materials and methods

Following ethical approval from the Animal Care and Ethics Committee of the University of New South Wales and Macquarie University, five 10-week-old male Sprague-Dawley rats weighing 279 ± 40.64g (mean ± SD) were divided into either a control or syrinx group. The control group consisted of one laminectomy-only control animal, and one sham-injected control animal that received a 1.5 µL spinal cord intraparenchymal injection of saline containing 1% Evans blue (Sigma-Aldrich, St. Louis, Mo, US). The three remaining animals underwent a syrinx induction procedure (described below). AQP4 expression was investigated 12 weeks following the initial operation. All procedures were performed in a sterile field under general anaesthesia induced with 4% isoflurane in oxygen and maintained with 2% isoflurane through a nose cone, increased as required to maintain an adequate level of anaesthesia.

Syrinx induction

The model of noncommunicating canalicular syringomyelia has been described previously (Milhorat et al., 1993). Animals were placed prone, and the skin shaved and prepared with povidone iodine. A midline incision was made over the cervico-thoracic junction and a T-1 laminectomy was performed. A 29-gauge needle was used to puncture the meninges. A 5 –10 µL syringe held in a stereotactic micromanipulator was then used to inject 1.5 µL 250 mg/mL kaolin (Sigma-Aldrich, St. Louis, Mo, US). Injections were into the dorsal midline of the spinal cord, with the bevel of the needle turned in a lateral direction along the longitudinal axis of the spinal cord. Wounds were closed with a single layer silk suture. Analgesia was administered postoperatively and the animals were allowed food and water *ad libitum*. Any excessive weight loss, limb weakness, or signs of over-self grooming were recorded.

Perfusion

At 12 weeks postsurgery, animals were rapidly perfused by intracardiac injection of 5,000 IU heparin in 1 mL of saline followed by 500 mL of 4% paraformaldehyde (Lancaster Synthesis) in 0.1 M phosphate buffer (pH 7.4) under a constant pressure of 120 mm Hg.

Immunohistochemistry

Spinal cord segments from 12 week postsurgery animals were cryoprotected in 30% sucrose in phosphate buffer and embedded in OCT compound (ProSciTech, QLD, Australia). Spinal cord sections were cut transversely at 20 µm on a cryostat. Immunofluorescence staining proceeded as follows. Sections were thawed in a 37ºC oven for 10 minutes and washed twice for 10 minutes in phosphate-buffered saline (PBS). The sections were then treated with 50% ethanol/ PBS for 20 minutes followed by three 10 minutes washes in PBS and incubated with 15% normal horse serum (NHS) in PBS pH 7.45 for 30 minutes. The sections were then incubated with the primary antibody overnight at 4°C. The following day, sections were left for 2 hours at room temperature before two 10 minutes rinses with PBS and incubated with either anti-mouse IgG Alexa Fluor 594 or anti-rabbit IgG Alexa Fluor 488 (Molecular Probes, Eugene, OR, US) diluted in 4% NHS/PBS 1:400 for 2 hours. After rinsing twice for 5 minutes the sections were cover-slipped with fluorescent mounting medium (DAKO, Carpinteria, CA, US). Omission of the primary antibody was used for negative controls. Antibodies used were: AQP4 (AB3594, Chemicon, US 1:250), GFAP (MAB360, Chemicon, US 1:250). Fluorescent images were taken with a digital camera (Zeiss Z1, Gottingen, Germany), processed using Zeiss Axiovision software. All images were taken at the same exposure times for each antibody. Fluorescence signal intensity was assessed using Image-J software. Specifically, images were converted to 32-bit and threshold was adjusted to a standardised level for each captured image. The integrated density was measured for AQP4 and GFAP. The AQP4 quantification was expressed as a percentage of GFAP.

Statistics

Comparison of AQP4 and GFAP expression between control and syrinx animals and between different spinal levels was performed using univariate analysis of variance. Comparisons of the main effects were assessed using Bonferroni adjusted significance. A probability value <0.05 was considered statistically significant. Data was presented as means ± SEM. Software used included Excel (Microsoft, Redmond, WA, US) and GraphPad Prism 5 (GraphPad Software CA 92037 US).

Results

AQP4 and GFAP expression pattern in controls

In the control (laminectomy-only) animal, AQP4 was expressed in both grey and white matter, although staining was more intense and widespread in the grey matter. AQP4 was diffusely expressed throughout the grey matter, particularly surrounding the central canal and in the dorsal horns (Figure 29). AQP4 was also strongly expressed surrounding capillaries, and faintly labelled ependymal cells (Figure 29. E-F). Colocalisation of GFAP and AQP4 was very limited in the grey matter, although GFAP expression was observed in glial processes adjacent to AQP4 labelling around capillaries. In the white matter AQP4 highly colocalised with GFAP positive astrocytes, and was expressed in radial astrocytes, and was strongly expressed in glial processes at the pia mater (Figure 29. D).

In the sham-injected control animal, receiving an intraparenchymal injection of saline and Evans blue, AQP4 expression patterns were similar to the laminectomy-only control. There were some differences in the level of expression of GFAP and AQP4, but these were not significant.

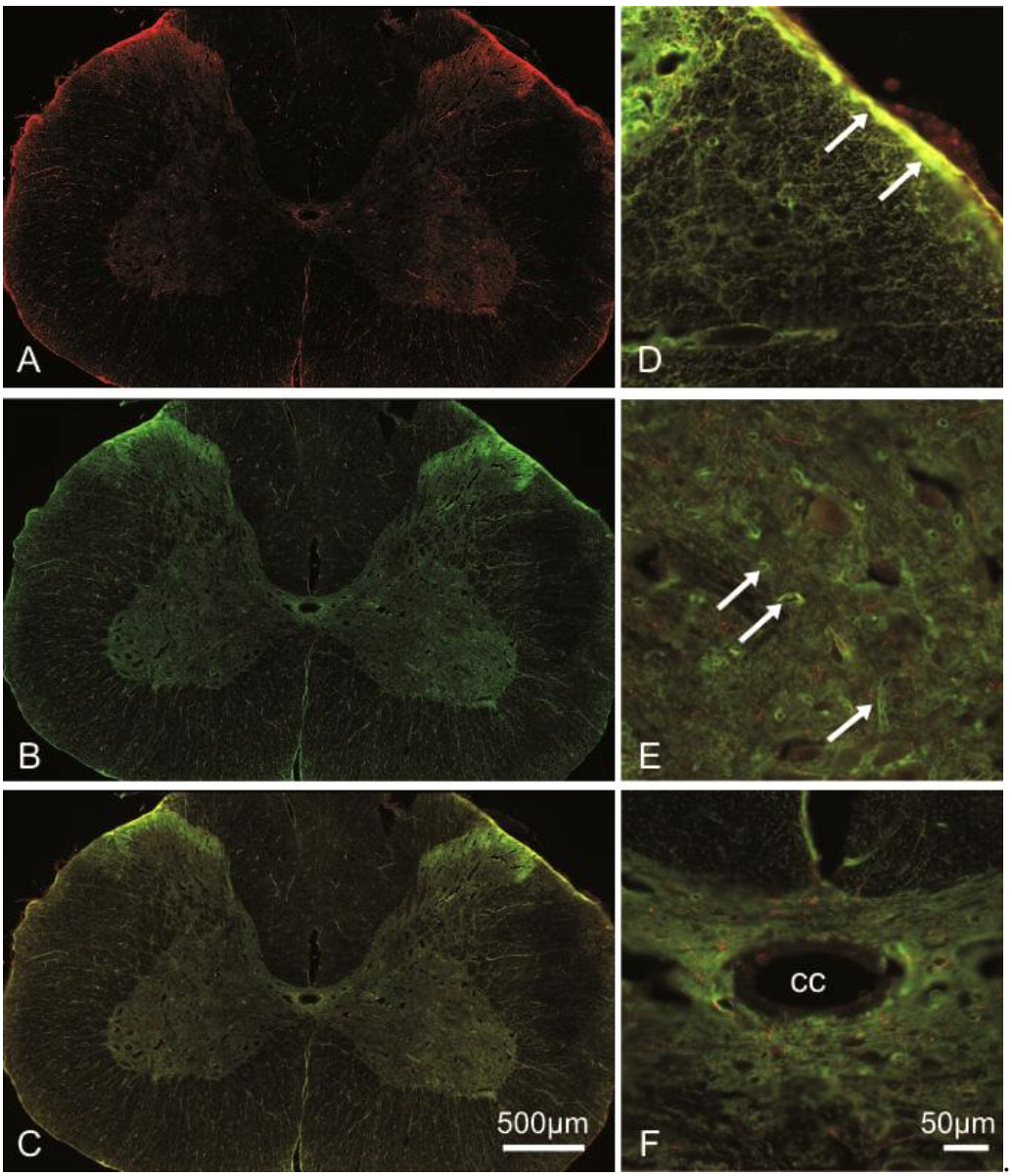

Figure 29: Immunolocalisation of (A) GFAP (red) and (B) AQP4 (green) in control (laminectomy-only) rat spinal cord. (C) Colocalisation of AQP4 and GFAP shown in yellow. (D-F) High magnification images of (C). (D) AQP4 is expressed at the glia limitans externa (*arrows*); (E) around capillaries (*arrows*) in grey matter; (F) in ependymal cells and grey matter surrounding the central canal. CC = central canal.

AQP4 and GFAP expression pattern in canalicular syringomyelia

In the spinal cords of the kaolin-injected animals, central canal enlargement was common, a ruptured ependymal lining was observed, proliferation of periependymal astrocytes was occasionally noted and perivascular spaces were sometimes enlarged (Figure 30). The pattern of immunostaining of AQP4 and GFAP in the canalicular syrinx animals was consistent with that of control animals surrounding the central canal (Figure 31).

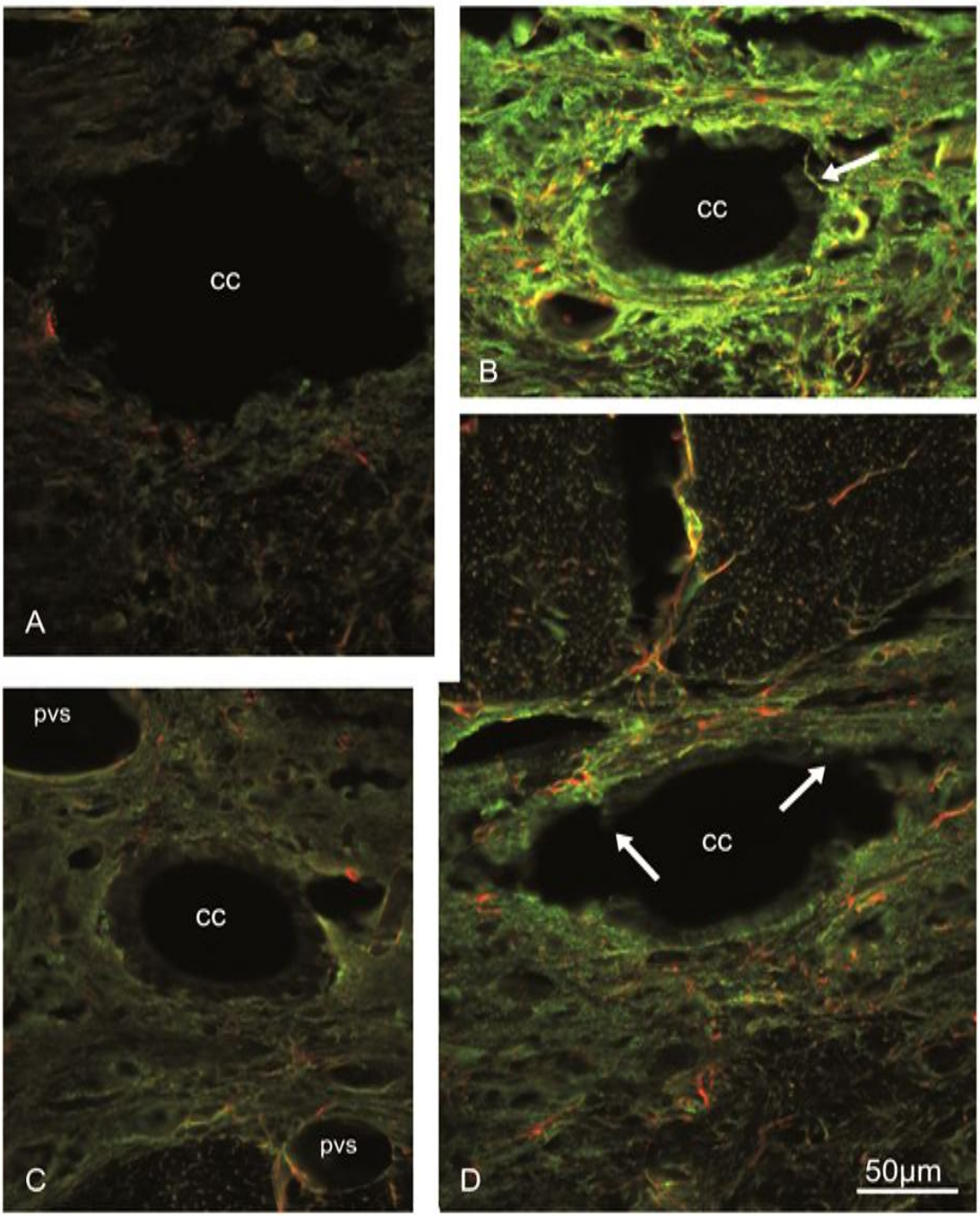

Figure 30: Immunolabelling of AQP4 (green) and GFAP (red) in rat spinal cord 12 weeks following syrinx induction. Animals received an intraparenchymal injection of kaolin. (A) shows a representative transverse section demonstrating an enlarged central canal and loss of AQP4 and GFAP labelling. (B) demonstrates an increase in AQP4 labelling surrounding the central canal and the proliferation of a periependymal astrocyte projecting into the central canal (*arrow*). (C) demonstrates dilated perivascular spaces (pvs) in the central grey matter surrounding the central canal, and a decrease in AQP4 and EBA labelling. (D) demonstrates the rupture of the ependymal layer lining the central canal. The canalicular syrinx has ruptured into the central grey matter (*arrows*). AQP4 labelling is similar to controls. (cc) = central canal

All kaolin-injected animals had AQP4-positive labelling in the central grey matter surrounding the central canal, faint staining of the ependymal lining, and intense immunostaining surrounding capillaries. Differences in the intensity of labelling and the number of labelled glial processes of GFAP and AQP4 were observed in the syrinx animals

compared to controls. However, these changes were highly varied between animals and between spinal levels. In some sections a loss of GFAP and AQP4 staining was observed around the central canal (Figure 30. C). This was observed surrounding both normal and enlarged central canals. In other sections an increase in AQP4 expression was observed compared to GFAP expression (Figure 30. B). This also occurred when the central canal was normal and dilated, or when the ependymal lining had ruptured and the syrinx had extended into the central grey matter. An increase in GFAP expression was also observed in some sections while AQP4 expression remained relatively normal or decreased.

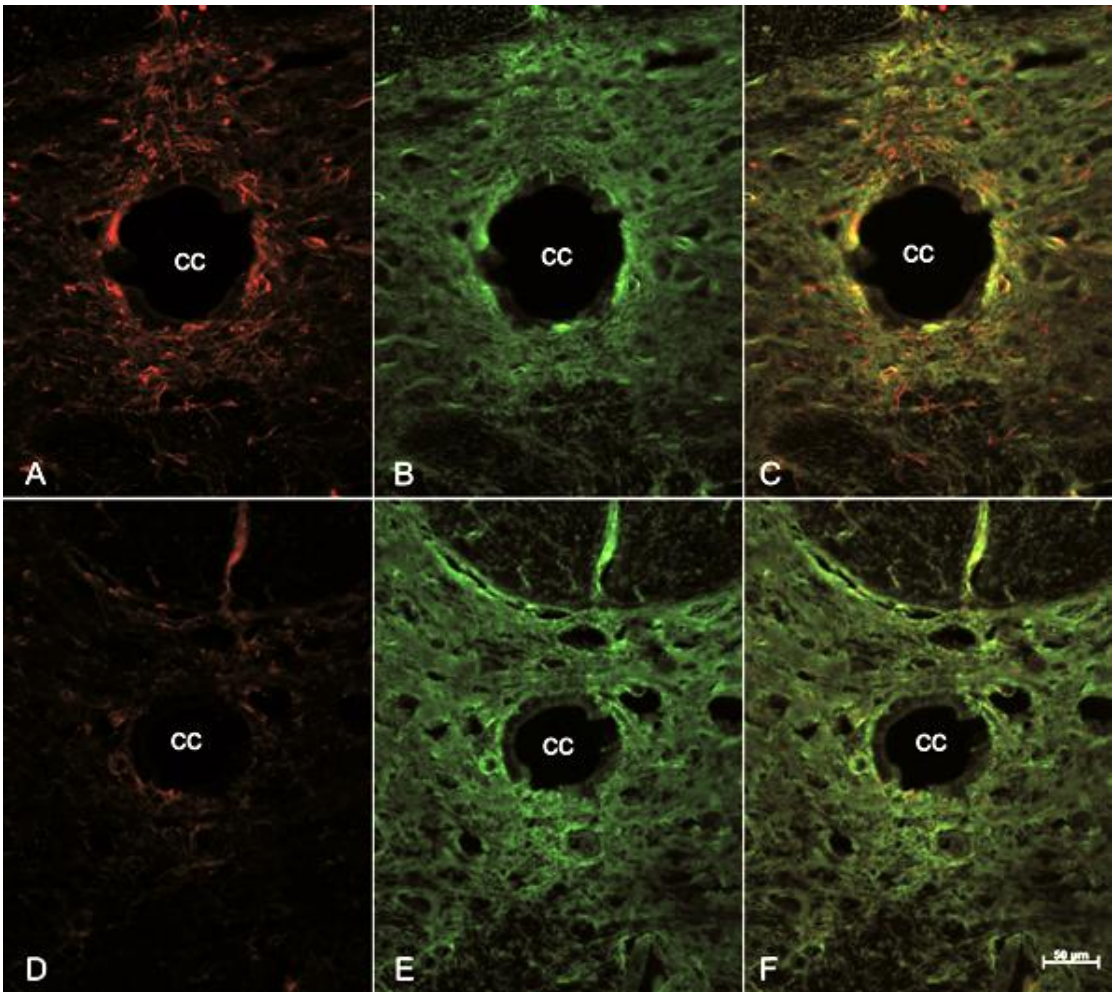

Figure 31: Immunolocalisation of (A, D) GFAP (red) and (B, E) AQP4 (green) in spinal cord of: (A-C) control (laminectomy-only); and (D-F) kaolin-injected rat. (C, F) Colocalisation of AQP4 and GFAP shown in yellow. cc = central canal.

Semi-quantitative analysis of AQP4 as a fraction of GFAP immunostaining did not demonstrate a significant difference between syrinx animals and controls (Figure 32. D). A significant difference was observed in GFAP expression between two syrinx animals (syrinx 1 & syrinx 3, $p = 0.0003$) (Figure 32. A). Significant differences were observed in AQP4 expression between the control (laminectomy-only) and 1 syrinx animal (syrinx 3, $p < 0.005$), and between different syrinx animals (syrinx 1 & syrinx 3 $p < 0.0003$, and syrinx 2 & syrinx

3, $p < 0.05$) (Figure 32. B). No significant differences were observed between individual animals when AQP4 intensity was expressed as a fraction of GFAP intensity (Figure 32. C).

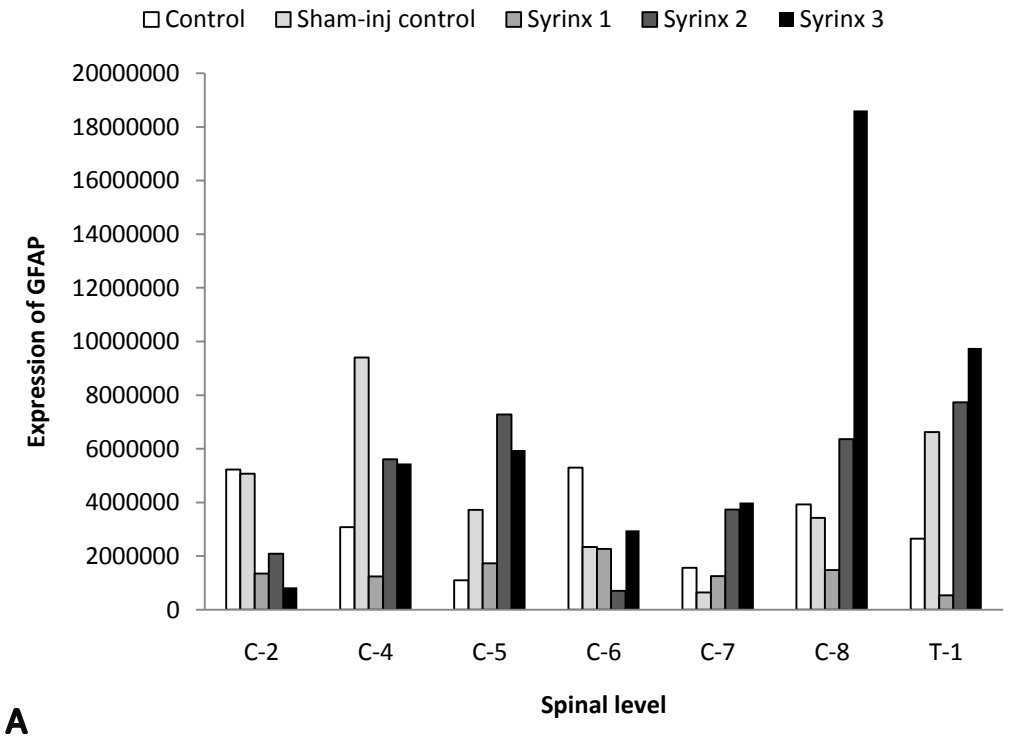

A

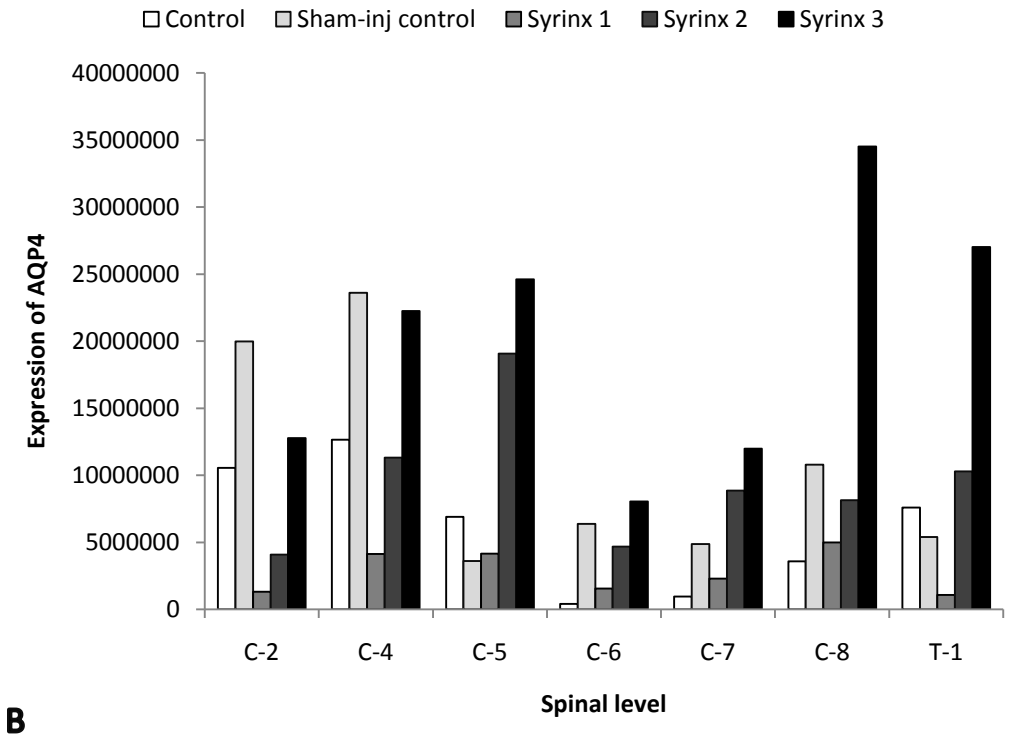

B

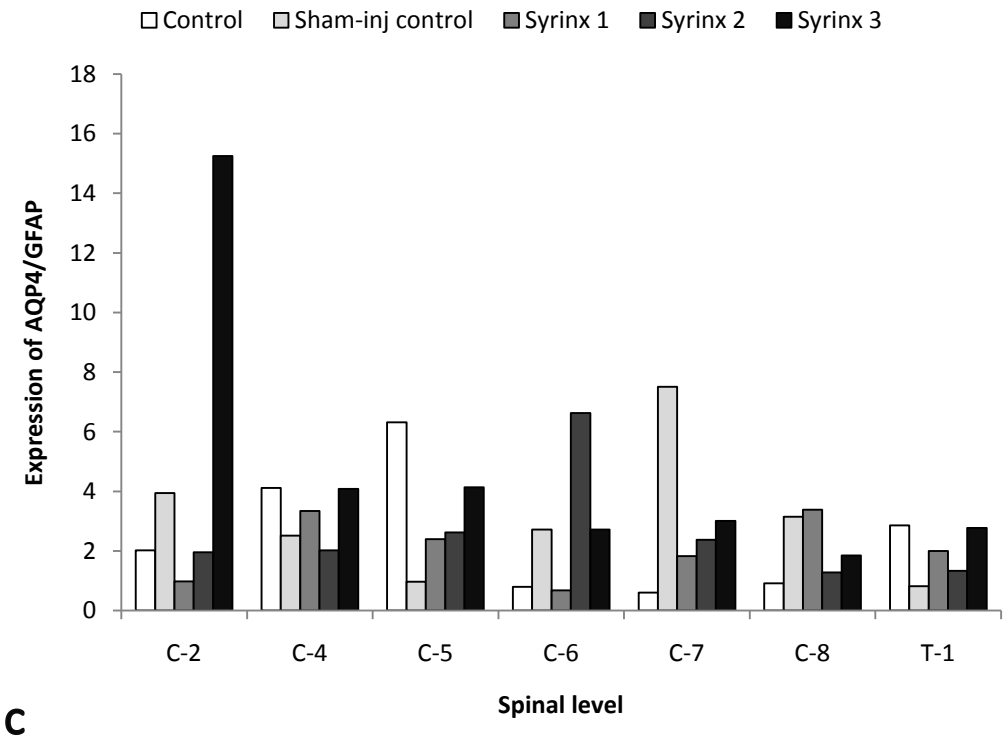

C

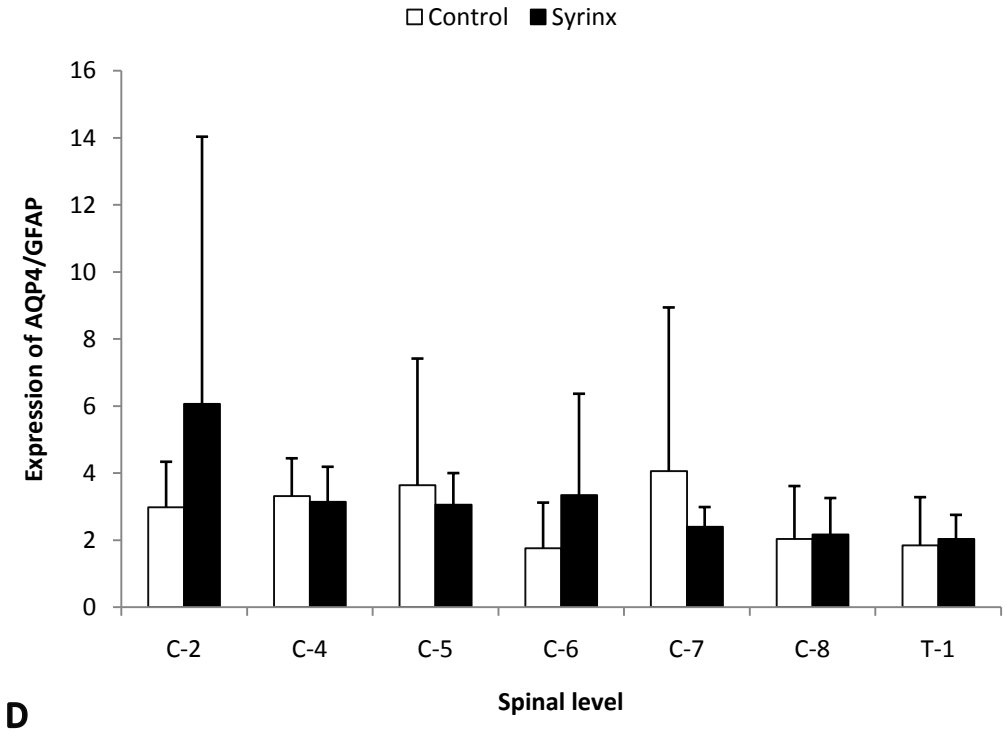

D

Figure 32: Semi-quantitative analysis of the intensity (measured as integrated density) of GFAP (A) and AQP4 (B) immunolabelling in the central grey matter of spinal cords extracted at 12 weeks from control (n=2) and syrinx animals (n=3). (C) The expression of AQP4 as a fraction of GFAP expression at different spinal levels in each animal. (D) The expression of AQP4 as a fraction of GFAP expression at different spinal levels in control vs syrinx animals.

Discussion

The results from this study are consistent with previous reports of AQP4 expression in the spinal cord (Oshio et al., 2004, Nesic et al., 2006, Misu et al., 2007). AQP4 was expressed in glial cells, and to a lesser extent ependymal cells lining the central canal. The lack of colocalisation we observed between GFAP and AQP4 in grey matter has been reported previously. Oshio et al suggested that this indicates that AQP4 labels protoplasmic astrocytes in the grey matter, while GFAP is generally expressed on fibrous astrocytes (Oshio et al., 2004). AQP4 expression was predominately observed at sites of fluid transport: at the BSCB (in astrocytic endfeet surrounding capillaries), and at CSF interfaces (the central canal and glia limitans externa). This localisation suggests a role for AQP4 in the regulation of water homeostasis in the spinal parenchyma.

This is supported by studies carried out in AQP4 knockout mice, which have an improved outcome in cytotoxic oedema. Manley et al demonstrated a decrease in cerebral oedema following water intoxication in mice lacking AQP4 compared to controls (Manley et al., 2000). A similar outcome was observed in dystrophin-null mice, which have reduced expression of AQP4 around capillaries. In these animals AQP4 deletion was also found to be beneficial following water intoxication (Vajda et al., 2002). In vasogenic oedema AQP4 deletion has been found to be detrimental, resulting in elevated intracranial pressure, and oedema in a freeze injury model (Papadopoulos et al., 2004). A study by Mao et al demonstrated that administration of sulphoraphane which enhances AQP4 expression, reduces spinal cord oedema in a murine model of spinal cord injury (Airoldi et al., 1983b).

It has been proposed that AQP4 may also play a role in CSF absorption within the parenchyma (Wollmer et al., 1983, Bloch et al., 2006). It was once thought that CSF was only absorbed through arachnoid granulations. It is now known that CSF may circulate via alternative pathways, either by absorption through the parenchyma to cerebral microvessels or via lymphatic vessels (Ingenito et al., 1983, Pisani et al., 1983). Obstruction of CSF absorption pathways or overproduction of CSF can lead to disorders such as hydrocephalus. Bloch et al reported that AQP4 knockout mice developed ventricular enlargement, and elevated intracranial pressure more rapidly compared to wild-type mice in a kaolin model of hydrocephalus (Bloch et al., 2006). Li et al reported a disorganisation of the ependymal cells lining the ventricles, a decrease in CSF production and an increase in cerebral water content in $AQP4^{-/-}$ mice compared with $AQP4^{+/+}$ mice (Fazio et al., 1983b).

These studies highlight the significance of AQP4 in water movement in the central nervous system, and its potential role in abnormal water accumulation in a wide range of pathological conditions. This emphasises the need for further study into diseases such as syringomyelia that cannot be completely explained by current theories of CSF dynamics. It is possible that in canalicular syringomyelia that AQP4 expression may be affected. As this study has demonstrated, AQP4 is strongly expressed in glial cells, and to a lesser extent ependymal cells surrounding the central canal. As such, it is possible that changes in AQP4 expression could either increase the movement of water into the central canal, or alternatively prevent water from moving from the central canal into the parenchyma. This may contribute to the enlargement of the central canal in Chiari-associated syringomyelia.

If AQP4 also plays a similar role in the structural and functional integrity of the ependymal layer lining the central canal as it does in the ventricles, a decrease in AQP4 expression could cause unregulated fluid flow into the central grey matter across a disrupted ependymal lining. Alternatively, a decrease in AQP4 could prevent the transependymal movement of CSF from the central canal into the spinal parenchyma to be absorbed at the BSCB. This could result in the enlargement of the central canal. There is evidence for rapid movement of CSF from the subarachnoid space, into perivascular spaces, and into the central canal (Airoldi et al., 1983a). It is possible that AQP4 mediates this movement across the ependyma and pia. Alterations in AQP4 expression may also affect fluid flow from the subarachnoid space.

Previous work in our laboratory has demonstrated that the BSCB is disrupted around the central canal in a kaolin model of noncommunicating canalicular syringomyelia (unpublished). Since AQP4 has been found to improve vasogenic oedema, which occurs following the opening of the BBB/BSCB (Nesic et al., 2006), an increase in AQP4 expression may be beneficial in canalicular syringomyelia. In support of this, a study investigating the effect of VEGF administration on AQP4 expression in the midbrain demonstrated that VEGF induced a BBB breakdown, and induced AQP4 expression at the BBB and glia limitans externa (Pipino et al., 1983). This suggests that AQP4 is a compensatory mechanism for increased fluid flow.

Since AQP4 expression in our model of canalicular syringomyelia was so varied it is difficult to draw any conclusions from these results. Further investigation is needed to determine the pattern of labelling. It would be useful to increase the number of animals examined and carry out a quantitative investigation in conjunction with this study to detect more subtle changes. If consistent and significant changes in AQP4 expression are not observed in Chiari-associated

syringomyelia, it is unclear why excess fluid within the central canal is not removed by AQP4 mediated pathways. A possible explanation is that the amount of fluid exceeds the capabilities of the AQP4 pathways. It is also possible that AQP4 expression levels fluctuate either in response to an increase in fluid in the central canal, an increase in fluid from the vasculature, or from the disruption of the ependymal layer lining the central canal when the syrinx ruptures. There were larger differences in AQP4 expression before normalising results to GFAP. This suggests that the number of astrocytes around the central canal also varies, and suggests that the changes in AQP4 expression for the most part reflect changes in the number of GFAP-positive cells present.

Glial scar formation is a well known phenomenon occurring in the central nervous system in response to any mechanical insult, and is known to result in an increase in GFAP synthesis (Tchirkow et al., 1983). Changes in the astrocytic population in close proximity to the syrinx in Chiari-associated syringomyelia have also been well characterised, with astrocytic proliferation and gliosis reported (Feigin et al., 1971, Klekamp, 2002, Levine, 2004). Decreases in GFAP expression have been reported in acute hyperammonemia when brain water content was high (Bucci et al., 1983), and weak GFAP expression in swollen astrocytes in human cerebral oedema has also been demonstrated (Wickremesinghe et al., 1983). This is consistent with the results of this study, and may explain the variations in GFAP expression and the subsequent changes in AQP4 expression. Given this, it is possible that at different stages of syrinx progression, both cytotoxic and vasogenic mechanisms are involved, with microglial proliferation occurring to compensate for the increased fluid due to impaired BSCB or rupture of the ependymal lining, followed by astrocytic swelling.

Conclusions

The results of this study point to the need for further investigation into the astrocytic population surrounding a canalicular syrinx and the functional role of AQP4 in syringomyelia. It may be of interest to investigate the role of AQP9, which is also expressed in the glia limitans and a different subset of astrocytes. It is thought that AQP9 may also be important in oedema formation (Badaut et al., 2001).

Chapter 4

Fluid outflow in posttraumatic syringomyelia

This was a collaborative project involving the author, Professor Marcus Stoodley and Professor Nigel Jones. Professor Stoodley and Professor Jones carried out all surgical procedures including syrinx induction and the ultrasound-guided microinjection. The author attended and assisted each surgery, carried out the processing and histological staining, analysis, and was involved in experimental planning.

Object. Syringomyelia occurs in association with a number of congenital and acquired disorders, including following spinal cord injury. It has been estimated that up to 28% of patients with a spinal cord injury will develop a posttraumatic syrinx. The mechanisms underlying the formation and enlargement of a syrinx remain largely unknown. Perivascular CSF flow has been shown to contribute to syrinx fluid in animal models of syringomyelia. However, little is known about fluid flow out of the syrinx. The aim of this study was to determine the outflow pathways in extracanalicular syringomyelia.

Methods. An excitotoxic amino acid/arachnoiditis model of posttraumatic syringomyelia was used to create extracanalicular syrinxes in ten merino wethers. At 6 – 12 weeks following syrinx induction, sheep were anaesthetised, the surgical site was re-opened, and horseradish peroxidase (HRP) was injected into the syrinx using a syringe under ultrasound guidance. Animals were then perfused with 4% paraformaldehyde, spinal cords were removed, sectioned on a vibratome, and processed for HRP.

Results. In the sheep model of extracanalicular syringomyelia, there was extravasation of HRP in a diffuse pattern around the cavity. Increased staining was observed around blood vessels and in the central grey matter adjacent to the central canal.

Conclusions. This study has provided evidence that fluid diffuses out of syrinxes into the surrounding extracellular space and perivascular spaces. The central grey matter and central canal may be major outflow conduits.

Introduction

Posttraumatic syringomyelia is the formation of a cystic cavitation within the spinal cord following trauma. Currently, it is estimated that there are 9,000 cases of diagnosed posttraumatic syringomyelia, and approximately 400 new cases reported each year in the US (Sigman and Gillich, 1981).

While posttraumatic syringomyelia occurs infrequently, with an estimated prevalence of 8.4 cases per 100,000 (Heiss et al., 1999), it can result in debilitating neurological deficits including loss of sensation, paralysis and severe pain. Current treatments for posttraumatic syringomyelia are often not effective, with high rates of complications and recurrence (Sgouros and Williams, 1995, Klekamp et al., 1997, Batzdorf et al., 1998, Batzdorf, 2005). Improved treatments are unlikely to develop without further understanding of the underlying pathogenesis.

Theories on the pathogenesis of syringomyelia have generally focused on the flow of fluid into the syrinx, and little attention has been paid to the possible routes for fluid outflow. There is experimental evidence that CSF flows from the subarachnoid space into the spinal cord via perivascular spaces in posttraumatic syringomyelia, with increased flow at the level of arachnoid adhesions (Brodbelt et al., 2003b, Brodbelt et al., 2003c). However, it is unknown whether there is also some movement out of the syrinx along these pathways. Since the progression of syringomyelia is slow, perhaps taking years to reach a clinically relevant size, it is likely that there is an outflow pathway from the syrinx into the surrounding cord. Further investigation into fluid outflow could assist in a better understanding of the filling mechanisms underlying syrinx enlargement and determine whether obstructions in fluid outflow may also contribute to the pathogenesis of this condition.

The aims of this study were to determine whether there is movement of fluid out of the syrinx, and if so, to determine the pathways for this outflow in an animal model of posttraumatic syringomyelia. In this report we describe a technique that allows the direct injection of tracer into a syrinx under ultrasound guidance.

Materials and methods

Syrinx induction

Following ethical approval from the Animal Ethics Committee of the Institute of Medical & Veterinary Science (Central Northern Adelaide Health Service), ten merino wethers weighing 45 – 58 kg were used in this study. Animals were anaesthetised, and placed in the prone

position on the operating table. Wool was then shorn and the skin marked at the incision site by identifying the first thoracic spinous process as an anatomical landmark. The skin was then prepared with povidone iodine. A midline upper thoracic incision was then made to expose the spinous processes of the second to fourth thoracic vertebrae. The latter three spinous processes were then cleared of paraspinal muscles. A T-3 laminectomy and partial T-2 and T-4 laminectomies were then performed.

Two dural incisions were made, each approximately 0.5 cm and separated by approximately 0.5 cm, at the entry point of the dorsal rootlets of T-3. A 10 µL syringe (SGE International Pty Ltd., Austin TX) fitted with a bevelled needle (0.19 mm outer diameter) was used to manually infiltrate four 5 µL quisqualic acid injections at 3 mm depth from the pial surface such that the needle orifice lay within the dorsal horn of the spinal cord with the bevel facing medially. The quisqualic acid was slowly injected over 30 seconds and the needle was left in place for a further 30 seconds after injection then slowly withdrawn to prevent leakage.

Using a Tisseal Duo 500 two-component fibrin sealant duploject two-syringe clip (Baxter Healthcare Pty Ltd. NSW), with 250 mg/mL kaolin dissolved in the thrombin component and drawn up into the double-barrelled applicator, kaolin and fibrin were slowly injected under the dura on both sides of each dural incision, for a total of 0.2 mL per sheep. The dura was closed with 6.0 prolene, fascia and muscle layers with 1.0 vicryl and subcutaneous tissue with 2.0 vicryl. The skin was closed with 2.0 silk. Analgesia and antibiotics were administered postoperatively and the animals were allowed food and water *ad libitum*. Any limb weakness, weight loss, and signs of discomfort were recorded.

HRP injection and perfusion

At 6 weeks postsurgery, animals were anaesthetised and placed in the prone position on the operating table. Wool was then shorn and a midline upper thoracic incision was then made to expose the previous surgical site (T-3 to T-4). A Sonosite MicroMaxx^{TM} Ultrasound System (Sonosite, Inc. WA, US) was used to visualise the spinal cord boundaries, central canal and identify regions of fluid accumulation. When the region of fluid accumulation (syrinx) was identified, a 10 µL syringe (SGE International Pty Ltd., Austin TX) fitted with a bevelled needle (0.19 mm outer diameter) was used to manually inject 10 µL of 3% (w/vol) HRP (Zymed Laboratories Inc., San Francisco, US) in sterile saline over 5 minutes. Ultrasound guidance was used to visualise the needle, and ensure the correct positioning of the needle point. Ten minutes following the injection of HRP the animal was rapidly perfused using a previously described protocol (Santoreneos et al., 1998). Briefly, following cannulation of the

jugular veins and carotid arteries, 10,000 IU heparin was injected, followed by 10 L of 4% paraformaldehyde (Lancaster Synthesis) in 0.1 M phosphate buffer (pH 7.4).

Immunohistochemistry and detection of HRP

The spinal cord was dissected out and post-fixed in 4% paraformaldehyde in 0.1 M phosphate buffer overnight. Vibratome sections (50 µm) were cut from the spinal cord and mounted on 3-amino propyl-triethoxy-silane-coated slides. Segments were taken from the spinal cord from T-2 to T-4. Histochemical development of HRP reaction product was carried out using 3, 3', 5, 5'-Tetramethylbenzidine (TMB), as the chromagen. Briefly, the tissue was incubated in a 0.005% TMB/0.05% sodium nitroferricyanide/0.2 M acetate buffer (pH 3.3) solution for 20 minutes before the addition of hydrogen peroxidase (0.03% final concentration) and was then incubated for 20 minutes. The sections were rinsed three times in 0.2 M acetate buffer (pH 3.3), stabilised for 15 minutes in ammonium molybdate, dehydrated in graded alcohols, cleared in xylene and mounted with DPX mounting medium (Scharlau Chemie S.A.). Colour images were acquired using a Leica DMR microscope (Leica Microsystems, Wetzlar, Germany) and Zeiss digital camera (Axiocam, Zeiss, Oberkochen, Germany).

Results

Following the syrinx induction procedure four animals developed hind-limb weakness and were unable to stand unaided. These animals were humanely euthanased according to the Animal Ethics Committee protocol, and were excluded from the remainder of the study. Histological analysis demonstrated that all six of the animals surviving to 6 weeks postsurgery developed a noncommunicating extracanalicular syrinx. Of these animals, a cavity could be identified by ultrasound in five animals. Syrinxes were generally located in the dorsal horn grey matter (Figure 33).

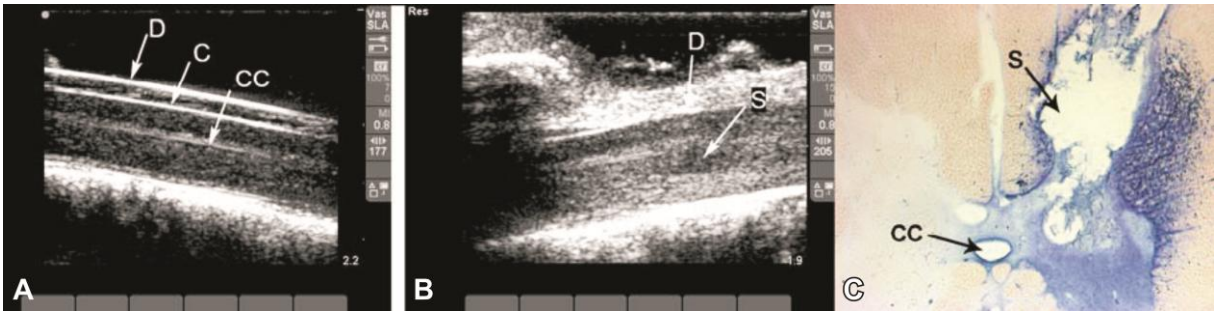

Figure 33: Ultrasound of normal sheep spinal cord (A) and a sheep with a posttraumatic syrinx (B). The images show a longitudinal representation of the spinal cord, the surrounding subarachnoid space, and dura. (C) Representative photomicrograph showing a transverse section of sheep spinal cord with an extracanalicular syrinx present in the grey matter. HRP was injected into the syrinx using ultrasound guidance and sections were stained with tetramethylbenzadine. C: spinal cord; CC: central canal; D: dura; S: syrinx.

Using ultrasound guidance we were able to identify and locate the mature cyst in vivo and accurately inject tracer into the syrinx in two animals. The injection of HRP directly into the syrinx in these animals demonstrated extravasation of HRP from the cavity. HRP reaction product was observed in a diffuse pattern in the spinal cord around the cavity. The reaction product had spread predominately in the grey matter towards the central canal. Staining was more marked around blood vessels in the grey matter and around the central canal (Figure 34).

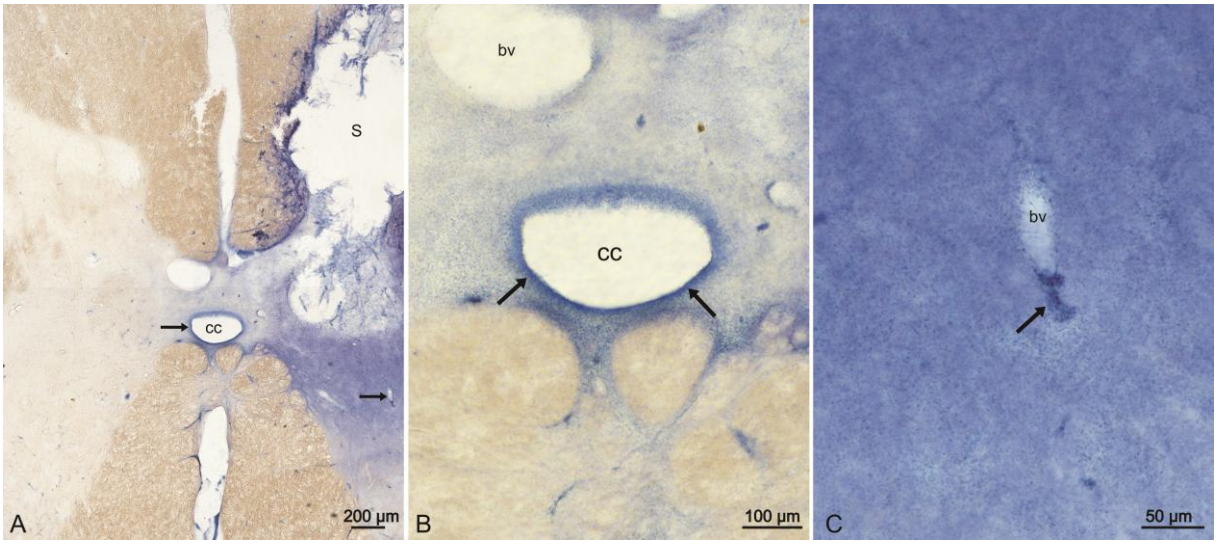

Figure 34: (A) Photomicrograph of a representative sheep spinal cord with a posttraumatic syrinx (S) present in the grey matter. At 6 weeks following syrinx induction ultrasound guidance was used to inject HRP into the syrinx. TMB was used to visualise the movement of HRP. Higher magnification images of areas in (A) indicated by *arrows* are shown in (B, C), demonstrating the diffusion of HRP from the syrinx into the grey matter, central canal (B) and around blood vessels (C). CC: central canal; S: syrinx; bv: blood vessel.

Discussion

The excitotoxic amino acid and arachnoiditis model of posttraumatic syringomyelia has been well described in rats (Stoodley et al., 2000, Yang et al., 2001, Brodbelt et al., 2003a, Brodbelt et al., 2003b, Brodbelt et al., 2003c). This study required a larger animal to enable ultrasound detection and microinjection. To the best of our knowledge this is the first report of an ovine model of posttraumatic syringomyelia. The sheep spinal cord is similar in size to a human spinal cord and we believe that this is a useful model, producing extracanalicular cavities comparable to the human condition. The procedure described in this study is technically difficult, and the success rate was relatively low. However, the technique was refined over the duration of the study, and there was a lower rate of early neurological deficits in the later animals. It is hopeful that this procedure will prove useful for studies involving the in vivo manipulation of syrinxes in the future.

It has to be considered that the microinjection of HRP may disturb the fluid within the syrinx and contribute to the outflow. However, given the small gauge of the needle, the small amount of fluid injected, and the slow rate of injection we consider this unlikely. It is also possible that outflow could be different in a non-anaesthetised animal, or in bipedal animals, in which the pulsatile pressures on the spinal cord are greater. It may be of interest to investigate fluid movement from a cavity without the presence of arachnoiditis to determine whether a blockage at the subarachnoid space may obstruct the outflow of fluid from the spinal cord.

Syrinx enlargement is caused by an imbalance between fluid inflow and outflow. Proposed mechanisms for this increased inflow are respiratory or arterial driven CSF pressure waves. An increase in pressure waves in the subarachnoid space is thought to be transmitted to the syrinx, and causes the syrinx to extend into the surrounding spinal cord tissue, stretching the tissue fibres and creating gaps where fluid pools. Williams states that this 'sloshing' mechanism provides an explanation for the delay between the time of injury, and syrinx formation, stating that every increase in cavity size adds to the problem. Once a critical size is reached, the syrinx enlarges at a much faster rate (Williams, 1980b). There is evidence for this fluid movement on phase-contrast cine MR imaging, but no evidence that the movement is sufficient to cause tissue dissection and enlargement of the syrinx (Oldfield et al., 1994). Brodbelt et al demonstrated that there is an increase in flow at the level of arachnoiditis in an excitotoxic model of syringomyelia with arachnoiditis. They injected HRP into the cisterna magna of rats, and found that CSF flowed from the subarachnoid space, into perivascular spaces and towards the syrinx (Brodbelt et al., 2003c).

More recently, Klekamp proposed that changes in outflow might also play a role in syrinx enlargement. He suggested that a syrinx is formed due to an accumulation of extracellular fluid in the spinal cord that is unable to be removed due to either: a blockage of CSF pathways; or, extracellular fluid flow exceeding interstitial space volume. Klekamp states that this could be due to blockage of perivascular spaces, cord tethering, changes in arterial or venous blood flow in the spinal cord or obstruction of CSF flow (Klekamp, 2002). It is intuitive that for a syrinx to enlarge, the amount of fluid flowing into the cavity must exceed the outflow of fluid. Whether this is due to an increase in inflow or a decrease or absence of outflow is yet to be determined.

In addition to the possible factors affecting outflow proposed by Klekamp, a number of other features might obstruct or diminish outflow, including glial scar formation, demyelination and

mechanical loading; the glial scar surrounding the syrinx may act as a barrier to the normal diffusion of fluid; axonal demyelination could reduce the removal of fluid that would normally be transported along the cord by white matter tracts; and changes in the structural properties of the spinal cord at the time of injury could also affect the outflow of fluid. The objective of this study was to investigate whether there is movement of fluid out of the syrinx, and if so, to investigate the pathways of fluid outflow. The HRP observed surrounding the syrinx in the extracanalicular model suggests that there is bi-directional flow into and out of the syrinx. This provides a possible explanation for the slow progression of disease, as the bulk of fluid flowing into the syrinx is not likely to accumulate there. The high volume of HRP reaction product evident in the spinal parenchyma surrounding the syrinx suggests that a significant amount of syrinx fluid does flow out of the syrinx. This outflow is considerable given the small amount of tracer injected and the short time between microinjection and the perfusion-fixation.

Although the outflow of tracer appeared to spread diffusely, there tended to be an increase in tracer surrounding the central canal and blood vessels. This is consistent with animal studies of CSF flow in the spinal cord. Stoodley et al demonstrated preferential flow of CSF from perivascular spaces into the central canal in rat and sheep spinal cord (Airoldi et al., 1983a, Stoodley et al., 1997). A possible contribution of syrinx enlargement is the accumulation of fluid in the extracellular space. If the inflow of fluid from the subarachnoid space or vasculature exceeds the amount of fluid that can be removed via the central canal, the outflow of fluid from the syrinx may cause oedema in the extracellular space that may eventually expand to join the syrinx cavity. This could explain the multiloculated cavities that are often observed. Alternatively, the inflow may be driven by arterial pulsations while the outflow occurs via passive diffusion. If this is the case, the inflow is likely to exceed the outflow eventually. Further investigation is needed to determine the rate of inflow versus outflow, and whether the majority of fluid can be removed across the glia limitans interna and into the central canal.

Conclusion

Although this study used a small number of animals, it has demonstrated that fluid diffuses out of syrinxes into the surrounding extracellular space and perivascular spaces. This suggests that the central grey matter and central canal may be major outflow conduits.

Chapter 5

General discussion

The following section will review the key features of the studies detailed in this thesis, including technical details, questions raised by the findings, future research directions and the possible implications for the future treatment of syringomyelia.

Experimental techniques

The excitotoxic model of posttraumatic syringomyelia used in this thesis is well established and has been described in detail (Yezierski et al., 1998, Yang et al., 2001, Brodbelt et al., 2003a, Brodbelt et al., 2003b). As mentioned previously, this model is based on the observation that there is an increase in excitotoxic amino acids, in particular glutamate following traumatic spinal cord injury. These excitotoxic amino acids at high levels cause cell death (Headley and Grillner, 1990, Panter et al., 1990, Liu et al., 1991, Marsala et al., 1994, Yang et al., 2001). Quisqualic acid is an AMPA-metabotropic receptor agonist which has been found to produce spinal cavitations in over 90% of animals, cause cell death, proliferation of astrocytes, and induce inflammatory cells (Yezierski et al., 1993). Similar results have been achieved in animals injected with quisqualic acid as in those receiving a traumatic injury (Basso et al., 1996, Yezierski et al., 1998). Using this model in combination with a subarachnoid injection of kaolin, we produced cavities in over 90% of animals. This is consistent with the previously reported ~80% of animals (Stoodley et al., 2000, Yang et al., 2001, Brodbelt et al., 2003a). These cavities are histologically comparable to those produced in traumatic spinal cord injury models (Yang et al., 2001). Until recently, this model was demonstrated to be more reliable than the published models of weight-drop or compression clip injury, can be carried out without expensive equipment, and can produce cavities without causing paralysis or other significant neurological deficits. This model has been criticised as not representing the contusive and compressive trauma observed in humans following spinal cord injury (Seki and Fehlings, 2008). Our laboratory has recently developed a traumatic injury model in combination with arachnoiditis using the Infinite Horizon Impactor (unpublished) to create the initial mechanical injury. Histological analysis and AQP4 expression are being examined in this model and results compared to those obtained using the excitotoxic model. This will help to determine the validity of the quisqualic acid model.

The noncommunicating canalicular model of syringomyelia described in this thesis is currently the only experimental model that has been developed in laboratory animals without hydrocephalus. It has been used in a number of laboratories for studies on CSF flow and macrophages in canalicular syringomyelia (Rivlin and Tator, 1978a, Stoodley et al., 1999, Stoodley et al., 2000, Lee et al., 2005). This model does not completely represent the clinical condition, since there is no Chiari malformation or other hindbrain abnormality obstructing the normal CSF pathways or compressing the cord. However, this model does produce many of the morphological changes characteristic of the human condition, including periependymal oedema, denuded ependyma, stretching of axons and cell loss (Rivlin and Tator, 1978a, Milhorat et al., 1993). It produces a canalicular syrinx consistently, without significant pain or neurological impairments. As such, it could be used to study changes over a relatively long period, up to 3 months as in these studies.

In the study of fluid outflow in the ovine model of posttraumatic syringomyelia, we developed a new technique to identify and locate an extracanalicular syrinx in vivo and directly inject tracer into the cavity. There are only a handful of papers describing ultrasound-guided microinjection (Balus et al., 1983, D'Amico et al., 1983), and none of these have been used to inject into the spinal cord or fluid-filled cysts. The technique did prove to be technically difficult, but with further optimisation is likely to be useful in the experimental manipulation of syrinxes.

Blood vessels in the spinal cord have a barrier that regulates the movement of solutes from the blood stream into the parenchyma. If this barrier is impaired, then large molecules are able to pass into the cord and result in injury to cells and tissue damage (Mautes et al., 2000). HRP has been used extensively as a vascular tracer to study BBB and BSCB permeability (Muller and O'Rahilly, 1986a, Noble and Wrathall, 1989, Beggs et al., 2010), and to study the movement of fluid in the central nervous system (De Fazio et al., 1983b, Stoodley et al., 1999, Brodbelt et al., 2003c). As such, HRP was chosen as a tracer for a number of the studies presented in this thesis. HRP also has a number of advantages over other tracers. HRP has a molecular weight of ~40 kDa, is able to flow with CSF via the regular fluid pathways, but is not so small that it simply diffuses (Brodbelt et al., 2003c). It is thought to move via bulk flow (Airoldi et al., 1983a, Havery et al., 1983, Webb et al., 1983, Brodbelt et al., 2003b). It can be detected with relative sensitivity using DAB or TMB. It is also able to be visualised following paraformaldehyde fixation (Brodbelt et al., 2003c). To build on the work with HRP, we are currently investigating in vivo imaging using fluorescent tracers.

Pathogenesis

Numerous theories have been put forward to explain the pathogenesis of syringomyelia, based on clinical observations, computer modeling and laboratory investigations. However, there is still no sufficient explanation for the condition. There has been a move away from the idea that syringomyelia is simply caused by increased CSF flowing from the subarachnoid space into the spinal cord. Instead, there is increasing support for the theory that syrinx enlargement is due, at least in part, to the accumulation of extracellular fluid (Klekamp, 2002, Levine, 2004, Greitz, 2006). It has been proposed that damage to capillaries may allow plasma filtrate to pass across the BSCB and into the cord in syringomyelia associated with abnormalities at the foramen magnum, CSF flow obstruction, spinal cord tethering, or tumour (Klekamp, 2002, Levine, 2004, Greitz, 2006). A study using a novel thecal sac constriction model, which produced spinal cord cysts, found that after contrast-enhanced MR imaging, there was a slow increase in signal intensity in the cyst but not in spinal cord caudal to the ligature (Josephson et al., 2001). Until now, there has been no experimental evidence for BSCB breakdown in posttraumatic or noncommunicating models of syringomyelia.

The results of the studies conducted in this thesis demonstrate that the BSCB is compromised in animal models of both posttraumatic (extracanalicular) and Chiari-associated (noncommunicating canalicular) syringomyelia. In posttraumatic syringomyelia this was evident at all timepoints, in both the acute and chronic condition. In the noncommunicating canalicular model, impairment in the BSCB was not consistently found at all timepoints except in the chronic condition when the central canal was greatly enlarged. This suggests that damage to the BSCB may indeed play a role in the development of a syrinx or the enlargement of cyst, contributing to the pathology. In posttraumatic syringomyelia, it is likely that the BSCB does not repair after the initial trauma and plays a role in the development of syringomyelia by providing a pathway for fluid to enter the parenchyma from the blood stream. This study does not demonstrate a causative link between increased BSCB permeability and increased cavity size. It is possible that the breakdown in the BSCB is simply a consequence of an enlarging cavity stretching the tissue and causing mechanical disruption of blood vessels. However, it seems likely that it does contribute to increased fluid flowing into the syrinx, as other studies point to the association between increased BSCB permeability and fluid accumulation (Navratil et al., 1963, Perfetti et al., 1983). It seems likely that the significant disruption of the barrier observed at the early timepoints at least contributes to the initial cyst formation.

In noncommunicating canalicular syringomyelia, increased BSCB permeability seems less likely to contribute to the initial cyst formation as HRP leakage was only observed sporadically in the acute stages after kaolin-injection (1 and 3 weeks). It wasn't until 12 weeks that there was evidence of increased BSCB permeability in all animals. Interestingly, the difference in HRP extravasation and EBA labelling between spinal levels did not always correlate with areas of central canal enlargement, or the presence of a syrinx. It is possible that this reflects a BSCB breakdown preceding central canal dilatation, possibly contributing to the enlargement. This enlargement may then result in the mechanical disruption of more microvessels in the central grey matter.

A study of contusion spinal cord injury in rats found AQP4-negative astrocytes in the acute stages, while astrocytes over-expressed AQP4 in the chronic condition. In the acute stages, AQP4-negative astrocytes were sometimes found in close proximity to AQP4-overexpressing astrocytes, which is similar to the findings in chronically injured human spinal cords. The authors suggest that this indicates that the processes involved in the conversion from AQP4-negative to AQP4-expressing occurs more rapidly in rats (Nesic et al., 2010). The study found that the increase in AQP4 expression remained high from 2 months to 11 months. The authors hypothesise that the AQP4 upregulation is permanent, and indicates cytotoxic oedema in the chronically injured spinal cord. The study observed that fluid-filled cavities occurring following spinal cord injury were surrounded by intense AQP4 staining (Nesic et al., 2010). This is consistent with what we observed in our study of posttraumatic syringomyelia. This raises the question of whether AQP4 overexpression could play a role in syrinx formation or enlargement in posttraumatic syringomyelia. Nesic et al compared cavity size following spinal cord contusion injury in rats as measured by MR imaging and the level of AQP4 expression using western blotting. The authors found no correlation between AQP4 expression and cavity size (Nesic et al., 2010). The results of our western blotting analysis demonstrated some changes in AQP4 levels between control and syrinx animals. However, a significant increase in AQP4 expression was only evident in the upper cervical spinal cord, rostral to the syrinx induction site. Since the cavity size in these animals could not be measured no conclusions about cavity size and AQP4 expression can be made. However, based on the immunofluorescence study, AQP4 expression surrounding a syrinx appeared to be more dependent on the stage of disease (acute or chronic) rather than the size of the cavity (see Figure 26).

The differential expression of AQP4 observed between animals and at different levels within the same animal in our noncommunicating canalicular model is difficult to explain. Nesic et

al observed a heterogeneous population of GFAP labelled astrocytes in chronically injured human spinal cord, with both AQP4-negative and AQP4-positive cells present. AQP4-negative astrocytes are thought to represent immature astrocytes that have been generated following injury (Nesic et al., 2010). It is possible that this accounts for the disparity in our results. Perhaps since the injury to the spinal cord happens gradually with the expansion of the central canal, even at 12 weeks the pattern of staining is more comparable to the acute stages of spinal cord injury. It is also possible that the rate of disease progression among animals was highly varied and the expression of AQP4 is a reflection of this. Although overall significant differences were not observed in AQP4 immunoreactivity between syrinx and control animals, it does appear that AQP4 expression is altered to some extent. It is likely that AQP4 still has some affect on water content either within the central canal or in the subependyma, and longer time points may be needed to observe consistent changes.

The varying results between the two models suggest that while there are commonalities between the two, there are likely to be differences in the mechanisms at play in posttraumatic and Chiari-associated syringomyelia. It is likely that increased permeability in the BSCB and changes in AQP4 expression contribute to the formation or progression of the syrinx in both cases. However, the stage at which these changes take effect and the relative contribution they make are likely to be different. While it is possible that CSF flowing from the subarachnoid space is still the primary filling mechanism, the results of this study suggest that the mechanisms are likely to be complex and multifactorial.

The outflow study presented in this thesis demonstrated that there is bi-directional flow of fluid into and out of the syrinx. For a syrinx to enlarge then, the inflow of fluid has to exceed the outflow. An explanation for this is Klekamp's theory that there is an obstruction of extracellular fluid flow towards the subarachnoid space (Klekamp et al., 2002). In our study the majority of tracer was located in the interstitial space, with intense staining surrounding the central canal and blood vessels predominately in the central grey matter. This implies that the obstruction would not be to fluid flowing in the direction of the subarachnoid space. A previous CSF tracer study suggests that fluid from the subarachnoid space tends to drain towards the central canal (Airoldi et al., 1983a), so perhaps the movement of fluid from the syrinx simply reflects the normal flow of fluid in the spinal parenchyma. In that case for the syrinx to enlarge, the inflow has to exceed outflow from the syrinx. Or, there must be an obstruction of flow at the central canal or perivascular spaces rather than the subarachnoid space as Klekamp suggests.

In our study, dilated perivascular spaces were sometimes present, particularly in the grey matter. Klekamp suggests that perivascular space dilation is indicative of an inability of fluid to empty adequately into the subarachnoid space. Although our study does not support the idea that the subarachnoid space is the major outflow conduit, this could indicate an obstruction in perivascular space flow. Klekamp also proposes that a decrease in CSF flow towards the subarachnoid space could be due to an increase in the viscosity of the extracellular fluid. This could be the result of an increase in protein content (Klekamp, 2002). This is supported, at least in part, by our findings that the BSCB is compromised in a rat model of posttraumatic syringomyelia. This would increase the protein content of the extracellular fluid and potentially reduce the rate of removal. Changes in AQP4 expression and BSCB permeability could contribute to a disparity between the inflow and removal of fluid from the spinal cord parenchyma.

Treatment Implications

A study evaluating quality of life in patients with syringomyelia reported that symptoms worsened over time in 60 – 80% of patients, only 29% were able to continue working after diagnosis, and there was no significant difference between patients who underwent surgical procedures and conservative treatment (Placak et al., 1963). The symptoms reported by the 142 patients interviewed were pain, numbness, gait ataxia, paresis, bladder disturbance and skeletal deformation, among others (Placak et al., 1963). These figures highlight the shortcomings of current treatments for syringomyelia and the need for further research into the underlying causes so that improved therapies can be developed.

The results from the studies conducted in this thesis support a role for the BSCB in the initial cyst formation, or the subsequent enlargement of a syrinx. This suggests that treatments aimed at repairing the BSCB could prove useful in preventing or slowing disease progression. A number of therapeutic agents have been developed that have the potential to attenuate the BSCB in patients with syringomyelia. These include hemin (Demyer et al., 1963), neurotrophins (Zeman, 1963c), methylprednisolone sodium succinate (Zeman, 1963a), matrix metalloproteinase inhibitors (Zeman, 1963b) and erythropoietin (EPO) (Li et al., 2004a). Perhaps the most promising of these to date is EPO. Recombinant EPO acts as a neuroprotective agent by preventing free radicals and other harmful molecules such as glutamate from forming, protects against NMDA or nitric oxide activated apoptosis (Digicaylioglu and Lipton, 2001), and by modulating angiogenesis and tissue oxygenation (Bernaudin et al., 1999). In addition to these functions there is evidence that EPO decreases BBB permeability following cerebral ischemia (Bahcekapili et al., 2007, Li et al., 2007, Chi et

al., 2008), traumatic brain injury (Grasso et al., 2007), pentylentetrazol-induced seizures (Uzum et al., 2006) and VEGF-induced opening in an in vitro model of bovine BBB (Martinez-Estrada et al., 2003). In a model of EAE, EPO (50 U/kg) administered 36 to 48 hours after the onset of EAE symptoms was found to significantly reduce BSCB permeability (Li et al., 2004b).

In this thesis evidence has been provided that suggests AQP4 may play a part in syringomyelia, particularly following traumatic spinal cord injury. Further investigation is needed to determine if changes in AQP4 expression contribute to the enlargement of the syrinx cavity. However, in the future, therapies aimed at inhibiting or enhancing AQP4 expression may improve clinical outcomes by reducing the size of the syrinx cavity without the need for surgery. Even though research into AQP4 is in its infancy, a number of laboratory studies have already put forward a number of compounds that may be clinically beneficial. Mao et al carried out a study on AQP4 expression following the administration of sulphoraphane in a murine model of spinal cord injury. Sulphoraphane, a compound found in green leafed vegetables was found to increase AQP4 levels and reduce spinal cord oedema when administered 1 hour after injury (Airoldi et al., 1983b). Acetazolamide (Annoni et al., 1983) and edaravone (Paniagua and De Fazio, 1983) inhibit AQP4 expression, and have been found to be neuroprotective in cerebral ischemia (Nesic et al., 2010). Tanimura et al demonstrated that acetazolamide reversibly inhibits water transport across AQP4 in proteoliposomes (Tanimura et al., 2009). Edaravone is a free radical scavenger found to significantly decrease AQP4 expression and reduce lesion area in a rat model of focal ischemia (Paniagua and De Fazio, 1983).

The results presented in this thesis point to the potential for non-surgical interventions in the treatment of syringomyelia. The pathogenesis of syringomyelia is likely to be complex and multifactorial, and treating either blood vessels or individual proteins in the spinal cord is unlikely to provide adequate treatment by itself. However, it is hoped that they may be used as an adjunct to current treatments.

Future investigations

The results presented in this thesis raise a number of questions and highlight the need for further investigation into certain areas of syringomyelia research. This thesis demonstrated that there is an increased permeability in the BSCB in close proximity to an extracanalicular syrinx and the central canal in noncommunicating syringomyelia. This provides evidence that fluid is able to leak from capillaries into the spinal cord parenchyma. However, no causative

link between BSCB breakdown and syrinx formation and enlargement was demonstrated. It would therefore be of interest to investigate the effect on syrinx size following attenuation of the BSCB, or following increased breakdown of the BSCB. Ghabriel et al demonstrated that administering EBA antibody to rats induced opening of the BSCB for approximately 2 hours (Fazio and Havery, 1983). Therapeutic agents such as EPO that have already been mentioned may be useful in attenuating the BSCB in our experimental models (Li et al., 2004a).

We have demonstrated that AQP4 immunoreactivity is altered in animals with experimental syringomyelia. Whether AQP4 plays a contributory role or is simply responding to changes in water content is yet to be confirmed. Again, to answer this question we would need to inhibit or enhance AQP4 expression and determine any differences in the rate of cyst formation or cavity size. Current work in our laboratory is attempting to answer this question in a model of posttraumatic syringomyelia. A research group at the University of Adelaide (South Australia) have developed an AQP4 antagonist and agonist. In collaboration with this laboratory, our research group will be determining the size of the syrinx in non-treated animals, and those receiving the AQP4 agonist and AQP4 antagonist.

Currently, AQP4 is the only AQP that has been found in human spinal cords. However, it would be of interest to investigate the expression of other AQPs in syringomyelia. It is possible that decreases in AQP4 expression may be compensated by increases in other AQPs. AQP1 has been found in sensory axons in the dorsal horns of rat spinal cord, and expression is found to change following spinal cord injury (Fazio, 1983, Oshio et al., 2004, Nesic et al., 2008). AQP9 is expressed in astrocytes and neurons in brain (Badaut, 2010). It is possible that these different AQPs work synergistically, and the expression of each may prove to be important in understanding syringomyelia.

The novel technique detailed in chapter four of this thesis could be utilised for various applications in the future. As a continuation of the outflow study it would be useful to investigate the amount of HRP remaining in the cord after longer periods of time following direct microinjection into the syrinx. This would hopefully provide insight into whether the central canal is able to facilitate the removal of the excess syrinx fluid. If not and the majority of the fluid remains within the spinal cord, extracellular fluid would accumulate, contributing to syrinx enlargement. The technique will hopefully prove useful in studies involving direct pressure recordings within the syrinx and sampling of syrinx fluid.

Conclusions

The main conclusions from this thesis are:

1. The structural and functional integrity of the BSCB is compromised in animal models of posttraumatic and noncommunicating canalicular syringomyelia.

    I. In the posttraumatic syrinx animals, structural components of the BSCB remained disrupted at all time points studied. In the canalicular model, EBA labelling, while not completely absent, was weakened or only partially expressed along microvessels.

    II. In the posttraumatic syrinx animals, the structural impairment corresponded to functional changes in all but two experimental animals. The BSCB was impaired in the model of canalicular syringomyelia, particularly in the chronic condition when central canal dilatation was greatest.

2. AQP4 expression was altered in animal models of syringomyelia.

    III. There was a significant change in AQP4 expression surrounding posttraumatic syrinxes. In the chronic condition there was a significant increase in AQP4 immunoreactivity directly adjacent to the syrinx. There were changes in AQP4 immunoreactivity in the canalicular model. However, the pattern of immunostaining was so varied that no significant trend could be identified.

    IV. Expression levels of AQP4 in posttraumatic syringomyelia were significantly different in the cervical spinal cord, decreasing at the syrinx induction site and increasing rostrally. When compared with GFAP expression, AQP4 levels had significantly increased rostrally, and significantly decreased caudally to the site of syrinx induction.

3. There is bi-directional flow of fluid into and out of the syrinx in an ovine model of posttraumatic syringomyelia.

    V. Outflow of fluid from the syrinx appeared to spread diffusely, although there was an increase in fluid surrounding the central canal and blood vessels.

References

Aamodt S (2007) Focus on glia and disease. Nature neuroscience 10:1349.

Abbe R, Coley WB (1892) Syringomyelia; operation, exploration of the cord; withdrawal of fluid. J Nerv Ment Dis 19:512-520.

Abbott NJ (2005) Dynamics of CNS barriers: evolution, differentiation, and modulation. Cell Mol Neurobiol 25:5-23.

Abbott NJ, Ronnback L, Hansson E (2006) Astrocyte-endothelial interactions at the blood-brain barrier. Nat Rev Neurosci 7:41-53.

Abel R, Gerner HJ, Smit C, Meiners T (1999) Residual deformity of the spinal canal in patients with traumatic paraplegia and secondary changes of the spinal cord. Spinal Cord 37:14-19.

Aboulker J (1979a) [Syringomyelia and intra-rachidian fluids. I. Syringomyelia: 2 conceptions]. Neurochirurgie 25 Suppl 1:9-22.

Aboulker J (1979b) [Syringomyelia and intra-rachidian fluids. II. Slowness of syringomyelia]. Neurochirurgie 25 Suppl 1:23-25.

Aboulker J (1979c) [Syringomyelia and intra-rachidian fluids. III. The ependymal canal: evolution, involution]. Neurochirurgie 25 Suppl 1:26-29.

Aboulker J (1979d) [Syringomyelia and intra-rachidian fluids. IV. Syringomyelia to the naked eye]. Neurochirurgie 25 Suppl 1:30-37.

Aboulker J (1979e) [Syringomyelia and intra-rachidian fluids. IX. The rachidian fluid: its relations with the spinal cord, its place in CSF, its movements]. Neurochirurgie 25 Suppl 1:81-97.

Aboulker J (1979f) [Syringomyelia and intra-rachidian fluids. V. Syringomyeliac cavities with low power]. Neurochirurgie 25 Suppl 1:38-54.

Aboulker J (1979g) [Syringomyelia and intra-rachidian fluids. VI. Binding of the cavity and medullary tissue with high power]. Neurochirurgie 25 Suppl 1:55-66.

Aboulker J (1979h) [Syringomyelia and intra-rachidian fluids. VII. Scoliosis]. Neurochirurgie 25 Suppl 1:67-72.

Aboulker J (1979i) [Syringomyelia and intra-rachidian fluids. VIII. Normal fluids movements and pathology out rachis]. Neurochirurgie 25 Suppl 1:73-80.

Aboulker J (1979j) [Syringomyelia and intra-rachidian fluids. X. Rachidian fluid stasis]. Neurochirurgie 25 Suppl 1:98-107.

Aboulker J (1979k) [Syringomyelia and intra-rachidian fluids. XI. Venous stasis]. Neurochirurgie 25 Suppl 1:108-110.

Aboulker J (1979l) [Syringomyelia and intra-rachidian fluids. XII. Actual surgery syringomyelia]. Neurochirurgie 25 Suppl 1:111-131.

Aboulker J (1979m) [Syringomyelia and intra-rachidian fluids. XIII. Tentative evaluation]. Neurochirurgie 25 Suppl 1:132-133.

Aghakhani N, Parker F, David P, Morar S, Lacroix C, Benoudiba F, Tadie M (2009) Long-term follow-up of Chiari-related syringomyelia in adults: analysis of 157 surgically treated cases. Neurosurgery 64:308-315; discussion 315.

Agre P, King LS, Yasui M, Guggino WB, Ottersen OP, Fujiyoshi Y, Engel A, Nielsen S (2002) Aquaporin water channels--from atomic structure to clinical medicine. J Physiol 542:3-16.

Airoldi M, Pecchio F, Albanese F, Mastromatteo V, Gariboldi A, Di Costanzo G, Fazio M (1983a) [Urinary lysozyme, beta-2-microglobulin, and alpha-glucosidase during cisplatin therapy]. Boll Soc Ital Biol Sper 59:392-398.

Airoldi M, Pecchio F, Albanese F, Mastromatteo V, Gariboldi A, Negri L, Fazio M (1983b) [Urinary enzymes during some antiblastic chemotherapy protocols]. Boll Soc Ital Biol Sper 59:399-405.

Akiyama Y, Koyanagi I, Yoshifuji K, Murakami T, Baba T, Minamida Y, Nonaka T, Houkin K (2008) Interstitial spinal-cord oedema in syringomyelia associated with Chiari type 1 malformations. J Neurol Neurosurg Psychiatry 79:1153-1158.

Alzate JC, Kothbauer KF, Jallo GI, Epstein FJ (2001) Treatment of Chiari I malformation in patients with and without syringomyelia: a consecutive series of 66 cases. Neurosurg Focus 11:E3.

Amiry-Moghaddam M, Lindland H, Zelenin S, Roberg BA, Gundersen BB, Petersen P, Rinvik E, Torgner IA, Ottersen OP (2005) Brain mitochondria contain aquaporin water channels: evidence for the expression of a short AQP9 isoform in the inner mitochondrial membrane. FASEB J 19:1459-1467.

Anderson CR, Ashwell KWS, Collewijn H, Conta A, Harvey A, Heise C, Hodgetts S, Holstege G, Kayalioglu G, Keast JR, McHanwell S, McLachlan EM, Paxinos G, Plant G, Scremin O, Sidhu A, Stelzner D, Watson C (2009) The spinal cord: A Christopher and Dana Reeve foundation text and atlas. San Diego: Academic Press.

Annoni F, Boccasanta P, Pisani F, Zennaro F, Fazio FM, Monti D, Grasso M, Micheletto G (1983) [Usefulness of the Doppler velocimetry in patients undergoing direct arterial surgery]. Arch Sci Med (Torino) 140:77-84.

Asano M, Fujiwara K, Yonenobu K, Hiroshima K (1996) Post-traumatic syringomyelia. Spine 21:1446-1453.

Aschoff A, Kunze S (1993) 100 Years syrinx-surgery--a review. Acta Neurochir (Wien) 123:157-159.

Ashawesh K, Abdulqawi R, Ahmad S (2008) Syrinx associated with an intramedullary metastasis. Intern Med 47:329-330.

Atkinson JL, Kokmen E, Miller GM (1998) Evidence of posterior fossa hypoplasia in the familial variant of adult Chiari I malformation: case report. Neurosurgery 42:401-403; discussion 404.

Attenello FJ, McGirt MJ, Gathinji M, Datoo G, Atiba A, Weingart J, Carson B, Jallo GI (2008) Outcome of Chiari-associated syringomyelia after hindbrain decompression in children: analysis of 49 consecutive cases. Neurosurgery 62:1307-1313; discussion 1313.

Badaut J (2010) Aquaglyceroporin 9 in brain pathologies. Neuroscience 168:1047-1057.

Badaut J, Brunet JF, Petit JM, Guerin CF, Magistretti PJ, Regli L (2008) Induction of brain aquaporin 9 (AQP9) in catecholaminergic neurons in diabetic rats. Brain Res 1188:17-24.

Badaut J, Hirt L, Granziera C, Bogousslavsky J, Magistretti PJ, Regli L (2001) Astrocyte-specific expression of aquaporin-9 in mouse brain is increased after transient focal cerebral ischemia. J Cereb Blood Flow Metab 21:477-482.

Badaut J, Petit JM, Brunet JF, Magistretti PJ, Charriaut-Marlangue C, Regli L (2004) Distribution of Aquaporin 9 in the adult rat brain: preferential expression in catecholaminergic neurons and in glial cells. Neuroscience 128:27-38.

Badaut J, Regli L (2004) Distribution and possible roles of aquaporin 9 in the brain. Neuroscience 129:971-981.

Bahcekapili N, Uzum G, Gokkusu C, Kuru A, Ziylan YZ (2007) The relationship between erythropoietin pretreatment with blood-brain barrier and lipid peroxidation after ischemia/reperfusion in rats. Life Sci 80:1245-1251.

Baldassarre G, Fazio B (1983) [Exploration of the tubero-hypophyseal dopaminergic system in patients with chronic parkinsonism during chronic treatment with L-DOPA]. Minerva Med 74:2867-2870.

Baldridge BR, Burgess DE, Zimmerman EE, Carroll JJ, Sprinkle AG, Speakman RO, Li SG, Brown DR, Taylor RF, Dworkin S, Randall DC (2002) Heart rate-arterial blood pressure relationship in conscious rat before vs. after spinal cord transection. Am J Physiol Regul Integr Comp Physiol 283:R748-756.

Balentine JD (1978) Pathology of experimental spinal cord trauma. I. The necrotic lesion as a function of vascular injury. Lab Invest 39:236-253.

Ball MJ, Dayan AD (1972) Pathogenesis of syringomyelia. Lancet 2:799-801.

Balus L, Fazio M, Sacerdoti G, Morrone A, Marmo W (1983) [Fibrofolliculoma, trichodiscoma and acrochordon. The Birt-Hogg-Dube syndrome]. Ann Dermatol Venereol 110:601-609.

Bamford JA, Putman CT, Mushahwar VK Muscle plasticity in rat following spinal transection and chronic intraspinal microstimulation. IEEE Trans Neural Syst Rehabil Eng 19:79-83.

Barbaro NM, Wilson CB, Gutin PH, Edwards MS (1984) Surgical treatment of syringomyelia. Favorable results with syringoperitoneal shunting. J Neurosurg 61:531-538.

Barrett CP, Guth L, Donati EJ, Krikorian JG (1981) Astroglial reaction in the gray matter lumbar segments after midthoracic transection of the adult rat spinal cord. Exp Neurol 73:365-377.

Barshes N, Demopoulos A, Engelhard HH (2005) Anatomy and physiology of the leptomeninges and CSF space. Cancer Treat Res 125:1-16.

Basso DM, Beattie MS, Bresnahan JC (1996) Graded histological and locomotor outcomes after spinal cord contusion using the NYU weight-drop device versus transection. Exp Neurol 139:244-256.

Batzdorf U (2005) Primary spinal syringomyelia. Invited submission from the joint section meeting on disorders of the spine and peripheral nerves, March 2005. J Neurosurg Spine 3:429-435.

Batzdorf U, Klekamp J, Johnson JP (1998) A critical appraisal of syrinx cavity shunting procedures. J Neurosurg 89:382-388.

Becker DP, Wilson JA, Watson GW (1972) The spinal cord central canal: response to experimental hydrocephalus and canal occlusion. J Neurosurg 36:416-424.

Beggs JL, Waggener JD (1975) Vasogenic edema in the injured spinal cord: a method of evaluating the extent of blood-brain barrier alteration to horseradish peroxidase. Exp Neurol 49:86-96.

Beggs S, Liu XJ, Kwan C, Salter MW (2010) Peripheral nerve injury and TRPV1-expressing primary afferent C-fibers cause opening of the blood-brain barrier. Molecular pain 6:74.

Berens SA, Colvin DC, Yu CG, Yezierski RP, Mareci TH (2005) Evaluation of the pathologic characteristics of excitotoxic spinal cord injury with MR imaging. AJNR Am J Neuroradiol 26:1612-1622.

Bernaudin M, Marti HH, Roussel S, Divoux D, Nouvelot A, MacKenzie ET, Petit E (1999) A potential role for erythropoietin in focal permanent cerebral ischemia in mice. J Cereb Blood Flow Metab 19:643-651.

Bernstein DR, Bechard DE, Stelzner DJ (1981) Neuritic growth maintained near the lesion site long after spinal cord transection in the newborn rat. Neurosci Lett 26:55-60.

Bertram CD, Bilston LE, Stoodley MA (2008) Tensile radial stress in the spinal cord related to arachnoiditis or tethering: a numerical model. Med Biol Eng Comput 46:701-707.

Bilston LE, Fletcher DF, Brodbelt AR, Stoodley MA (2003) Arterial pulsation-driven cerebrospinal fluid flow in the perivascular space: a computational model. Comput Methods Biomech Biomed Engin 6:235-241.

Bilston LE, Fletcher DF, Stoodley MA (2006) Focal spinal arachnoiditis increases subarachnoid space pressure: a computational study. Clinical Biomechanics 21:579-584.

Bilston LE, Stoodley MA, Fletcher DF (2010) The influence of the relative timing of arterial and subarachnoid space pulse waves on spinal perivascular cerebrospinal fluid flow as a possible factor in syrinx development. Journal of Neurosurgery 112:808-813.

Bindal AK, Dunsker SB, Tew JM, Jr. (1995) Chiari I malformation: classification and management. Neurosurgery 37:1069-1074.

Binder DK, Oshio K, Ma T, Verkman AS, Manley GT (2004) Increased seizure threshold in mice lacking aquaporin-4 water channels. Neuroreport 15:259-262.

Blagodatsky MD, Larionov SN, Manohin PA, Shanturov VA, Gladyshev Yu V (1993) Surgical treatment of "hindbrain related" syringomyelia: new data for pathogenesis. Acta Neurochir (Wien) 124:82-85.

Bloch O, Auguste KI, Manley GT, Verkman AS (2006) Accelerated progression of kaolin-induced hydrocephalus in aquaporin-4-deficient mice. J Cereb Blood Flow Metab 26:1527-1537.

Bloch O, Papadopoulos MC, Manley GT, Verkman AS (2005) Aquaporin-4 gene deletion in mice increases focal edema associated with staphylococcal brain abscess. J Neurochem 95:254-262.

Bogdanov EI, Mendelevich EG (2002) Syrinx size and duration of symptoms predict the pace of progressive myelopathy: retrospective analysis of 103 unoperated cases with craniocervical junction malformations and syringomyelia. Clin Neurol Neurosurg 104:90-97.

Bolte S, Cordelieres FP (2006) A guided tour into subcellular colocalization analysis in light microscopy. J Microsc 224:213-232.

Boulton M, Flessner M, Armstrong D, Hay J, Johnston M (1997) Lymphatic drainage of the CNS: effects of lymphatic diversion/ligation on CSF protein transport to plasma. Am J Physiol 272:R1613-1619.

Brechtel K, Tura A, Abdibzadeh M, Hirsch S, Conrad S, Schwab JM (2006) Intrinsic locomotor outcome in dorsal transection of rat spinal cord: predictive value of minimal incision depth. Spinal Cord 44:605-613.

Brickell KL, Anderson NE, Charleston AJ, Hope JK, Bok AP, Barber PA (2006) Ethnic differences in syringomyelia in New Zealand. J Neurol Neurosurg Psychiatry 77:989-991.

Brock JA, Yeoh M, McLachlan EM (2006) Enhanced neurally evoked responses and inhibition of norepinephrine reuptake in rat mesenteric arteries after spinal transection. Am J Physiol Heart Circ Physiol 290:H398-405.

Brodbelt AR, Stoodley MA (2003a) Post-traumatic syringomyelia: a review. J Clin Neurosci 10:401-408.

Brodbelt AR, Stoodley MA (2003b) Syringomyelia and the arachnoid web. Acta Neurochir (Wien) 145:707-711; discussion 711.

Brodbelt AR, Stoodley MA, Watling A, Rogan C, Tu J, Brown CJ, Burke S, Jones NR (2003a) The role of excitotoxic injury in post-traumatic syringomyelia. J Neurotrauma 20:883-893.

Brodbelt AR, Stoodley MA, Watling AM, Tu J, Burke S, Jones NR (2003b) Altered subarachnoid space compliance and fluid flow in an animal model of posttraumatic syringomyelia. Spine 28:E413-419.

Brodbelt AR, Stoodley MA, Watling AM, Tu J, Jones NR (2003c) Fluid flow in an animal model of post-traumatic syringomyelia. Eur Spine J 12:300-306.

Brumley WC, Min Z, Matusik JE, Roach JA, Barnes CJ, Sphon JA, Fazio T (1983) Identification of sulfonamide drugs in swine liver by collision-induced dissociation/mass analyzed ion kinetic energy spectrometry. Anal Chem 55:1405-1409.

Bruni JE (1998) Ependymal development, proliferation, and functions: a review. Microsc Res Tech 41:2-13.

Bucci E, di Lauro F, Martina R, De Fazio P (1983) [Odontomas and their role in the etiopathogenesis of dental impactions. Clinical aspects, therapy and statistics]. Minerva Stomatol 32:201-206.

Button DC, Kalmar JM, Gardiner K, Marqueste T, Zhong H, Roy RR, Edgerton VR, Gardiner PF (2008) Does elimination of afferent input modify the changes in rat motoneurone properties that occur following chronic spinal cord transection? J Physiol 586:529-544.

Caldarelli M, Rea G, Cincu R, Di Rocco C (2002) Chiari type III malformation. Childs Nerv Syst 18:207-210.

Caldwell JH, Ridge RM (1983) The effects of deafferentation and spinal cord transection on synapse elimination in developing rat muscles. J Physiol 339:145-159.

Caplan LR, Norohna AB, Amico LL (1990) Syringomyelia and arachnoiditis. J Neurol Neurosurg Psychiatry 53:106-113.

Carlsson A, Lindqvist M, Magnusson T, Atack C (1973) Effect of acute transection on the synthesis and turnover of 5-HT in the rat spinal cord. Naunyn Schmiedebergs Arch Pharmacol 277:1-12.

Carpenter PW, Berkouk K, Lucey AD (2003) Pressure wave propagation in fluid-filled co-axial elastic tubes. Part 2: Mechanisms for the pathogenesis of syringomyelia. J Biomech Eng 125:857-863.

Carr PA, Haftel V, Alvarez FJ, Cope TC, Fyffe RE (1998) Effect of sciatic nerve transection or TTX application on enzyme activity in rat spinal cord. Neuroreport 9:357-361.

Carroll AM, Brackenridge P (2005) Post-traumatic syringomyelia: a review of the cases presenting in a regional spinal injuries unit in the north east of England over a 5-year period. Spine 30:1206-1210.

Carter JG, Sokoll MD, Gergis SD (1981) Effect of spinal cord transection on neuromuscular function in the rat. Anesthesiology 55:542-546.

Cauzinille L, Kornegay JN (1992) Acquired syringomyelia in a dog. J Am Vet Med Assoc 201:1225-1228.

Cavender RK, Schmidt JH, 3rd (1995) Tonsillar ectopia and Chiari malformations: monozygotic triplets. Case report. J Neurosurg 82:497-500.

Celichowski J, Mrowczynski W, Krutki P, Gorska T, Majczynski H, Slawinska U (2006) Changes in contractile properties of motor units of the rat medial gastrocnemius muscle after spinal cord transection. Exp Physiol 91:887-895.

Chakrabortty S, Tamaki N, Ehara K, Takahashi A, Ide C (1997) Experimental syringomyelia: late ultrastructural changes of spinal cord tissue and magnetic resonance imaging evaluation. Surg Neurol 48:246-254.

Chandler K, Volk H, Rusbridge C, Jeffery N (2008) Syringomyelia in cavalier King Charles spaniels. The Veterinary record 162:324.

Chang HS, Nakagawa H (2004) Theoretical analysis of the pathophysiology of syringomyelia associated with adhesive arachnoiditis. J Neurol Neurosurg Psychiatry 75:754-757.

Chen Y, Tachibana O, Oda M, Xu R, Hamada J, Yamashita J, Hashimoto N, Takahashi JA (2006) Increased expression of aquaporin 1 in human hemangioblastomas and its correlation with cyst formation. J Neurooncol 80:219-225.

Cheng XP, Wang BR, Liu HL, You SW, Huang WJ, Jiao XY, Ju G (2003) Phosphorylation of extracellular signal-regulated kinases 1/2 is predominantly enhanced in the microglia of the rat spinal cord following dorsal root transection. Neuroscience 119:701-712.

Chi OZ, Hunter C, Liu X, Weiss HR (2008) Effects of erythropoietin on blood-brain barrier disruption in focal cerebral ischemia. Pharmacology 82:38-42.

Chiari H (1987) Concerning alterations in the cerebellum resulting from cerebral hydrocephalus. 1891. Pediatr Neurosci 13:3-8.

Cho KH, Iwasaki Y, Imamura H, Hida K, Abe H (1994) Experimental model of posttraumatic syringomyelia: the role of adhesive arachnoiditis in syrinx formation. J Neurosurg 80:133-139.

Chuma A, Kitahara H, Minami S, Goto S, Takaso M, Moriya H (1997) Structural scoliosis model in dogs with experimentally induced syringomyelia. Spine (Phila Pa 1976) 22:589-594; discussion 595.

Cleland J (1883) Contribution to the study of spina bifida, encephalocele, and anencephalus. J Anat Physiol 17:257-291.

Cohen WA, Young W, DeCrescito V, Horii S, Kricheff, II (1985) Posttraumatic syrinx formation: experimental study. AJNR Am J Neuroradiol 6:823-827.

Correale J, Villa A (2007) The blood-brain-barrier in multiple sclerosis: functional roles and therapeutic targeting. Autoimmunity 40:148-160.

Courtice FC, Simmonds WJ (1951) The removal of protein from the subarachnoid space. The Australian journal of experimental biology and medical science 29:255-263.

Cummings JP, Bernstein DR, Stelzner DJ (1981) Further evidence that sparing of function after spinal cord transection in the neonatal rat is not due to axonal generation or regeneration. Exp Neurol 74:615-620.

Curtis KA, Roach KE, Applegate EB, Amar T, Benbow CS, Genecco TD, Gualano J (1995) Development of the Wheelchair User's Shoulder Pain Index (WUSPI). Paraplegia 33:290-293.

D'Amico D, Favia G, Fazio A, Pigafetta P, D'Amico C, Feltrin A (1983) [Acute mucosal lesions: modern diagnostic and therapeutic approaches]. Ann Ital Chir 55:467-480.

Daif AK, al Rajeh S, Ogunniyi A, al Boukai A, al Tahan A (1997) Syringomyelia developing as an acute complication of tuberculous meningitis. Can J Neurol Sci 24:73-76.

Dalal A, Tata M, Allegre G, Gekiere F, Bons N, Albe-Fessard D (1999) Spontaneous activity of rat dorsal horn cells in spinal segments of sciatic projection following transection of sciatic nerve or of corresponding dorsal roots. Neuroscience 94:217-228.

Dashtdar H, Valojerdi MR (2008) Ultrastructure of rat seminal vesicle epithelium in the acute phase of spinal cord transection. Neurol Res 30:487-492.

De Fazio F, Beduschi G, Solera P, Luzzago A (1983a) [Graduate professional preparation in dentistry and dental prosthesis]. Minerva Stomatol 32:761-766.

De Fazio G, Kudamatsu M (1983) Inhibitory effect of Distamycin-A and a pyrazino-pyrazine derivative on tomato spotted wilt virus. Antiviral Res 3:109-113.

De Fazio P, Ingenito A (1983) [Retrograde obturation of 2 lateral canals: solution in a clinical case]. Dent Cadmos 51:15-18.

De Fazio SR, Monaco AP, Gozzo JJ (1983b) An enzyme immunoassay for urinary C-reactive protein. Diagn Immunol 1:276-283.

Demyer W, Zeman W, Palmer CD (1963) Familial Alobar Holoprosencephaly (Arhinencephaly) with Median Cleft Lip and Palate. Report of Patient with 46 Chromosomes. Neurology 13:913-918.

Digicaylioglu M, Lipton SA (2001) Erythropoietin-mediated neuroprotection involves cross-talk between Jak2 and NF-kappaB signalling cascades. Nature 412:641-647.

Ding Q, Wu Z, Guo Y, Zhao C, Jia Y, Kong F, Chen B, Wang H, Xiong S, Que H, Jing S, Liu S (2006) Proteome analysis of up-regulated proteins in the rat spinal cord induced by transection injury. Proteomics 6:505-518.

Driver CJ, Rusbridge C, Cross HR, McGonnell I, Volk HA (2010) Relationship of brain parenchyma within the caudal cranial fossa and ventricle size to syringomyelia in cavalier King Charles spaniels. The Journal of small animal practice 51:382-386.

Ducreux D, Attal N, Parker F, Bouhassira D (2006) Mechanisms of central neuropathic pain: a combined psychophysical and fMRI study in syringomyelia. Brain 129:963-976.

Durozard D, Gabrielle C, Baverel G (2000) Metabolism of rat skeletal muscle after spinal cord transection. Muscle Nerve 23:1561-1568.

Echevarria M, Windhager EE, Tate SS, Frindt G (1994) Cloning and expression of AQP3, a water channel from the medullary collecting duct of rat kidney. Proc Natl Acad Sci U S A 91:10997-11001.

Edgar R, Quail P (1994) Progressive post-traumatic cystic and non-cystic myelopathy. Br J Neurosurg 8:7-22.

Eisenberg HM, McLennan JE, Welch K, Treves S (1974) Radioisotope ventriculography in cats with kaolin-induced hydrocephalus. Radiology 110:399-402.

Eisimberg, De Fazio P, Ingenito A, Amato M (1983) [New technic for the preparation of abutment pontics in amalgam. II: Presentation of prime clinical cases]. Arch Stomatol (Napoli) 24:613-620.

el Masry WS, Biyani A (1996) Incidence, management, and outcome of post-traumatic syringomyelia. In memory of Mr Bernard Williams. J Neurol Neurosurg Psychiatry 60:141-146.

Elkjaer M, Vajda Z, Nejsum LN, Kwon T, Jensen UB, Amiry-Moghaddam M, Frokiaer J, Nielsen S (2000) Immunolocalization of AQP9 in liver, epididymis, testis, spleen, and brain. Biochem Biophys Res Commun 276:1118-1128.

Ellertsson AB, Greitz T (1970) The distending force in the production of communicating syringomyelia. Lancet 1:1234.

Elliott NS, Lockerby DA, Brodbelt AR (2009) The pathogenesis of syringomyelia: a re-evaluation of the elastic-jump hypothesis. J Biomech Eng 131:044503.

Ergun R, Akdemir G, Gezici AR, Tezel K, Beskonakli E, Ergungor F, Taskin Y (2000) Surgical management of syringomyelia-Chiari complex. Eur Spine J 9:553-557.

Estienne C (1546) La Dissection des Parties du Corps Humain Divisee en Trois Livres Paris: Simon de Collines.

Falci S, Holtz A, Akesson E, Azizi M, Ertzgaard P, Hultling C, Kjaeldgaard A, Levi R, Ringden O, Westgren M, Lammertse D, Seiger A (1997) Obliteration of a posttraumatic spinal cord cyst with solid human embryonic spinal cord grafts: first clinical attempt. J Neurotrauma 14:875-884.

Farooque M, Olsson Y, Holtz A (1994) Effect of the 21-aminosteroid U74006F and methylprednisolone on motor function recovery and oedema after spinal cord compression in rats. Acta Neurol Scand 89:36-41.

Faulhauer K, Donauer E (1985) Experimental hydrocephalus and hydrosyringomyelia in the cat. Radiological findings. Acta Neurochir (Wien) 74:72-80.

Fazio M, Canarutto P, Airoldi M, Negri L (1983a) [Cryoimmunology and tumors of the oral cavity]. Minerva Stomatol 32:783-789.

Fazio RA, Wickremesinghe PC, Arsura EL (1983b) Ketoconazole treatment of Candida esophagitis--a prospective study of 12 cases. Am J Gastroenterol 78:261-264.

Fazio T, Havery DC (1983) The determination of volatile N-nitrosamines in foods. IARC Sci Publ 175-176.

Fazio VW (1983) Regional enteritis (Crohn's disease): indications for surgery and operative strategy. Surg Clin North Am 63:27-48.

Fazio VW, Coutsoftides T, Steiger E (1983c) Factors influencing the outcome of treatment of small bowel cutaneous fistula. World J Surg 7:481-488.

Fehlings MG, Bernstein M (1992) Syringomyelia as a complication of tuberculous meningitis. Can J Neurol Sci 19:84-87.

Fehlings MG, Tator CH, Linden RD (1989) The relationships among the severity of spinal cord injury, motor and somatosensory evoked potentials and spinal cord blood flow. Electroencephalography and clinical neurophysiology 74:241-259.

Feigin I, Ogata J, Budzilovich G (1971) Syringomyelia: the role of edema in its pathogenesis. J Neuropathol Exp Neurol 30:216-232.

Fishman RA (1975) Brain edema. N Engl J Med 293:706-711.

Freeman LW (1952) Return of function after complete transection of the spinal cord of the rat, cat and dog. Ann Surg 136:193-205.

Freeman LW, Wright TW (1953) Experimental observations of concussion and contusion of the spinal cord. Ann Surg 137:433-443.

Frisen J, Fried K, Sjogren AM, Risling M (1993) Growth of ascending spinal axons in CNS scar tissue. International Journal of Developmental Neuroscience 11:461-475.

Fukushima T, Matsuda T, Tsuchimochi H, Yamamoto M, Tsugu H, Tomonaga M, Mitsudome A, Utsunomiya H, Asakawa K (1994) Symptomatic Chiari malformation and associated pathophysiology in pediatric and adult patients without myelodysplasia. Neurol Med Chir (Tokyo) 34:738-743.

Gabrielli F, Ginanneschi U, Fazio FM (1983) [Emergency situations in pathology of the left colon: validity of fibrosigmoidoscopy in differential diagnosis]. Chir Ital 35:733-741.

Gardner WJ, Angel J (1958a) The cause of syringomyelia and its surgical treatment. Cleve Clin Q 25:4-8.

Gardner WJ, Angel J (1958b) The mechanism of syringomyelia and its surgical correction. Clin Neurosurg 6:131-140.

Gardner WJ, Bell HS, Poolos PN, Dohn DF, Steinberg M (1977) Terminal ventriculostomy for syringomyelia. J Neurosurg 46:609-617.

Gardner WJ, Collis JS, Jr., Lewis LA (1963) Cystic brain tumors and the blood-brain barrier. Comparison of protein fractions in cyst fluids and sera. Arch Neurol 8:291-298.

Gardner WJ, McMurray FG (1976) ""Non-communicating'' syringomyelia: a non-existent entity. Surg Neurol 6:251-256.

Gelderd JB, Peppler RD (1979) Effect of spinal cord transection on the reproductive system in the female rat. Neuroendocrinology 29:293-299.

Genitori L, Peretta P, Nurisso C, Macinante L, Mussa F (2000) Chiari type I anomalies in children and adolescents: minimally invasive management in a series of 53 cases. Childs Nerv Syst 16:707-718.

Ghabriel MN, Lu JJ, Hermanis G, Zhu C, Setchell BP (2002) Expression of a blood-brain barrier-specific antigen in the reproductive tract of the male rat. Reproduction 123:389-397.

Ghabriel MN, Zhu C, Hermanis G, Allt G (2000) Immunological targeting of the endothelial barrier antigen (EBA) in vivo leads to opening of the blood-brain barrier. Brain Res 878:127-135.

Gillespie JE, Jenkins JP, Metcalfe RA, Ischerwood I (1986) Magnetic resonance imaging in syringomyelia. Acta Radiol Suppl 369:239-241.

Gillilan LA (1958) The arterial blood supply of the human spinal cord. J Comp Neurol 110:75-103.

Goodman JH, Bingham WG, Jr., Hunt WE (1974) Edema formation and central hemorrhagic necrosis following impact injury to primate spinal cord. Surg Forum 25:440-442.

Goridis C, Meek JL, Neff NH (1972) Monoamine oxidase activity of rat spinal cord after transection. Life Sci I 11:861-866.

Gould SJ, Howard S, Papadaki L (1990) The development of ependyma in the human fetal brain: an immunohistological and electron microscopic study. Brain Res Dev Brain Res 55:255-267.

Grasso G, Sfacteria A, Meli F, Fodale V, Buemi M, Iacopino DG (2007) Neuroprotection by erythropoietin administration after experimental traumatic brain injury. Brain Res 1182:99-105.

Greitz D (2006) Unraveling the riddle of syringomyelia. Neurosurg Rev 29:251-263; discussion 264.

Griffiths IR (1975) Vasogenic edema following acute and chronic spinal cord compression in the dog. J Neurosurg 42:155-165.

Grundfest-Broniatowski S, Fazio V (1983) Conservative treatment of bleeding stomal varices. Arch Surg 118:981-985.

Haggendal J, Dahlstrom A (1973) The time course of noradrenaline decrease in rat spinal cord following transection. Neuropharmacology 12:349-354.

Hagihara N, Sakata S (2007) Disproportionately large communicating fourth ventricle with syringomyelia: case report. Neurol Med Chir (Tokyo) 47:278-281.

Hall P, Turner M, Aichinger S, Bendick P, Campbell R (1980) Experimental syringomyelia: the relationship between intraventricular and intrasyrinx pressures. J Neurosurg 52:812-817.

Hall PV, Kalsbeck E, Wellman HN, Campbell RL, Lewis S (1976) Radiosotope evaluation of experimental hydrosyringomyelia. J Neurosurg 45:181-187.

Hall PV, Muller J, Campbell RL (1975) Experimental hydrosyringomyelia, ischemic myelopathy, and syringomyelia. J Neurosurg 43:464-470.

Halliday GM, Stevens CH (2011) Glia: initiators and progressors of pathology in Parkinson's disease. Mov Disord 26:6-17.

Hamers FP, Lankhorst AJ, van Laar TJ, Veldhuis WB, Gispen WH (2001) Automated quantitative gait analysis during overground locomotion in the rat: its application to spinal cord contusion and transection injuries. J Neurotrauma 18:187-201.

Hamir AN (1995) Syringomyelia in a stallion. The Veterinary record 137:293-294.

Hasegawa H, Ma T, Skach W, Matthay MA, Verkman AS (1994) Molecular cloning of a mercurial-insensitive water channel expressed in selected water-transporting tissues. J Biol Chem 269:5497-5500.

Hashiguchi K, Morioka T, Samura K, Yoshida F, Miyagi Y, Nagata S, Kokubo T, Yoshiura T, Sasaki T (2008) Holocord hydrosyringomyelia with terminal myelocystocele revealed by constructive interference in steady-state MR imaging. Pediatr Neurosurg 44:509-512.

Hashimoto M, Ino H, Koda M, Murakami M, Yoshinaga K, Yamazaki M, Moriya H (2004) Regulation of semaphorin 3A expression in neurons of the rat spinal cord and cerebral cortex after transection injury. Acta Neuropathol 107:250-256.

Havery DC, Hotchkiss JH, Fazio T (1983) II.4.d A rapid method for the determination of volatile N-nitrosamines in liquid and dried foods. IARC Sci Publ 219-228.

Headley PM, Grillner S (1990) Excitatory amino acids and synaptic transmission: the evidence for a physiological function. Trends Pharmacol Sci 11:205-211.

Heiss JD, Patronas N, DeVroom HL, Shawker T, Ennis R, Kammerer W, Eidsath A, Talbot T, Morris J, Eskioglu E, Oldfield EH (1999) Elucidating the pathophysiology of syringomyelia. J Neurosurg 91:553-562.

Heiss JD, Suffredini G, Smith R, DeVroom HL, Patronas NJ, Butman JA, Thomas F, Oldfield EH (2010) Pathophysiology of persistent syringomyelia after decompressive craniocervical surgery. Clinical article. J Neurosurg Spine 13:729-742.

Hemley SJ, Tu J, Stoodley MA (2009) Role of the blood-spinal cord barrier in posttraumatic syringomyelia. J Neurosurg Spine 11:696-704.

Hess MJ, Foo D (2001) Shunting for syringomyelia in patients with spinal cord injuries: self-reported, long-term effects in 8 patients. Arch Phys Med Rehabil 82:1633-1636.

Hida K, Iwasaki Y (2001) Syringosubarachnoid shunt for syringomyelia associated with Chiari I malformation. Neurosurg Focus 11:E7.

Hida K, Iwasaki Y, Imamura H, Abe H (1994) Posttraumatic syringomyelia: its characteristic magnetic resonance imaging findings and surgical management. Neurosurgery 35:886-891; discussion 891.

Hoffman HJ, Neill J, Crone KR, Hendrick EB, Humphreys RP (1987) Hydrosyringomyelia and its management in childhood. Neurosurgery 21:347-351.

Hopkins AM, Li D, Mrsny RJ, Walsh SV, Nusrat A (2000) Modulation of tight junction function by G protein-coupled events. Adv Drug Deliv Rev 41:329-340.

Hu P, Bembrick AL, Keay KA, McLachlan EM (2007) Immune cell involvement in dorsal root ganglia and spinal cord after chronic constriction or transection of the rat sciatic nerve. Brain Behav Immun 21:599-616.

Iandiev I, Pannicke T, Reichenbach A, Wiedemann P, Bringmann A (2007) Diabetes alters the localization of glial aquaporins in rat retina. Neurosci Lett 421:132-136.

Ikeda S, Nakagawa S (1998) Spinal cord transection induced c-fos protein in the rat motor cortex. Brain Res 792:164-167.

Ingenito A, Catalano C, Eisimberg M, De Fazio P (1983) [Apicoectomy with retrograde obturation in the posterior teeth]. Dent Cadmos 51:55-63.

Ishibashi K, Kuwahara M, Gu Y, Kageyama Y, Tohsaka A, Suzuki F, Marumo F, Sasaki S (1997a) Cloning and functional expression of a new water channel abundantly expressed in the testis permeable to water, glycerol, and urea. J Biol Chem 272:20782-20786.

Ishibashi K, Kuwahara M, Gu Y, Tanaka Y, Marumo F, Sasaki S (1998a) Cloning and functional expression of a new aquaporin (AQP9) abundantly expressed in the peripheral leukocytes permeable to water and urea, but not to glycerol. Biochem Biophys Res Commun 244:268-274.

Ishibashi K, Kuwahara M, Kageyama Y, Tohsaka A, Marumo F, Sasaki S (1997b) Cloning and functional expression of a second new aquaporin abundantly expressed in testis. Biochem Biophys Res Commun 237:714-718.

Ishibashi K, Sasaki S, Fushimi K, Uchida S, Kuwahara M, Saito H, Furukawa T, Nakajima K, Yamaguchi Y, Gojobori T, et al. (1994) Molecular cloning and expression of a member of the aquaporin family with permeability to glycerol and urea in addition to water expressed at the basolateral membrane of kidney collecting duct cells. Proc Natl Acad Sci U S A 91:6269-6273.

Ishibashi K, Yamauchi K, Kageyama Y, Saito-Ohara F, Ikeuchi T, Marumo F, Sasaki S (1998b) Molecular characterization of human Aquaporin-7 gene and its chromosomal mapping. Biochim Biophys Acta 1399:62-66.

Itoh T, Nishimura R, Matsunaga S, Kadosawa T, Mochizuki M, Sasaki N (1996) Syringomyelia and hydrocephalus in a dog. J Am Vet Med Assoc 209:934-936.

Iwasaki Y, Hida K, Koyanagi I, Abe H (2000a) Reevaluation of syringosubarachnoid shunt for syringomyelia with Chiari malformation. Neurosurgery 46:407-412; discussion 412-403.

Iwasaki Y, Hida K, Onishi K, Nanba R (2000b) Chiari malformation and syringomyelia in monozygotic twins: birth injury as a possible cause of syringomyelia--case report. Neurol Med Chir (Tokyo) 40:176-178.

Jaeger CB, Blight AR (1997) Spinal cord compression injury in guinea pigs: structural changes of endothelium and its perivascular cell associations after blood-brain barrier breakdown and repair. Exp Neurol 144:381-399.

James AE, Jr., Flor WJ, Novak GR, Strecker EP, Burns B (1978) Evaluation of the central canal of the spinal cord in experimentally induced hydrocephalus. J Neurosurg 48:970-974.

Jean-Xavier C, Pflieger JF, Liabeuf S, Vinay L (2006) Inhibitory postsynaptic potentials in lumbar motoneurons remain depolarizing after neonatal spinal cord transection in the rat. J Neurophysiol 96:2274-2281.

Johnston I, Jacobson E, Besser M (1998) The acquired Chiari malformation and syringomyelia following spinal CSF drainage: a study of incidence and management. Acta Neurochir (Wien) 140:417-427; discussion 427-418.

Johnston I, Teo C (2000) Disorders of CSF hydrodynamics. Childs Nerv Syst 16:776-799.

Josephson A, Greitz D, Klason T, Olson L, Spenger C (2001) A spinal thecal sac constriction model supports the theory that induced pressure gradients in the cord cause edema and cyst formation. Neurosurgery 48:636-645; discussion 645-636.

Jung DI, Park C, Kang BT, Kim JW, Kim HJ, Lim CY, Jeong SW, Park HM (2006) Acquired cervical syringomyelia secondary to a brainstem meningioma in a maltese dog. The Journal of veterinary medical science / the Japanese Society of Veterinary Science 68:1235-1238.

Jung JS, Bhat RV, Preston GM, Guggino WB, Baraban JM, Agre P (1994) Molecular characterization of an aquaporin cDNA from brain: candidate osmoreceptor and regulator of water balance. Proc Natl Acad Sci U S A 91:13052-13056.

Kakar A, Madan VS, Prakash V (1997) Syringomyelia--a complication of meningitis--case report. Spinal Cord 35:629-631.

Kalderon N, Xu S, Koutcher JA, Fuks Z (2001) Fractionated radiation facilitates repair and functional motor recovery after spinal cord transection in rat. Brain Res 904:199-207.

Kamada T, Koda M, Dezawa M, Yoshinaga K, Hashimoto M, Koshizuka S, Nishio Y, Moriya H, Yamazaki M (2005) Transplantation of bone marrow stromal cell-derived Schwann cells promotes axonal regeneration and functional recovery after complete transection of adult rat spinal cord. J Neuropathol Exp Neurol 64:37-45.

Katsu M, Niizuma K, Yoshioka H, Okami N, Sakata H, Chan PH (2010) Hemoglobin-induced oxidative stress contributes to matrix metalloproteinase activation and blood-brain barrier dysfunction in vivo. J Cereb Blood Flow Metab 30:1939-1950.

Kimelberg HK (1995) Current concepts of brain edema. Review of laboratory investigations. J Neurosurg 83:1051-1059.

Kitagawa M, Okada M, Sato T, Kanayama K, Sakai T (2007) A feline case of isolated fourth ventricle with syringomyelia suspected to be related with feline infectious peritonitis. The Journal of veterinary medical science / the Japanese Society of Veterinary Science 69:759-762.

Klatzo I (1994) Evolution of brain edema concepts. Acta Neurochir Suppl (Wien) 60:3-6.

Klekamp J (2002) The pathophysiology of syringomyelia - historical overview and current concept. Acta Neurochir (Wien) 144:649-664.

Klekamp J, Batzdorf U, Samii M, Bothe HW (1997) Treatment of syringomyelia associated with arachnoid scarring caused by arachnoiditis or trauma. J Neurosurg 86:233-240.

Klekamp J, Iaconetta G, Batzdorf U, Samii M (2002) Syringomyelia associated with foramen magnum arachnoiditis. J Neurosurg 97:317-322.

Klekamp J, Volkel K, Bartels CJ, Samii M (2001) Disturbances of cerebrospinal fluid flow attributable to arachnoid scarring cause interstitial edema of the cat spinal cord. Neurosurgery 48:174-185; discussion 185-176.

Koc K, Anik I, Anik Y, Ceylan S (2007) Familial syringomyelia in two siblings: case report. Turk Neurosurg 17:251-254.

Koda M, Hashimoto M, Murakami M, Yoshinaga K, Ikeda O, Yamazaki M, Koshizuka S, Kamada T, Moriya H, Shirasawa H, Sakao S, Ino H (2004) Adenovirus vector-mediated in vivo gene transfer of brain-derived neurotrophic factor (BDNF) promotes rubrospinal axonal regeneration and functional recovery after complete transection of the adult rat spinal cord. J Neurotrauma 21:329-337.

Koizumi K, Malcolm JL, Brooks CM (1954) Effect of temperature on facilitation and inhibition of reflex activity. Am J Physiol 179:507-512.

Kokmen E, Marsh WR, Baker HL, Jr. (1985) Magnetic resonance imaging in syringomyelia. Neurosurgery 17:267-270.

Koyama N, Ishibashi K, Kuwahara M, Inase N, Ichioka M, Sasaki S, Marumo F (1998) Cloning and functional expression of human aquaporin8 cDNA and analysis of its gene. Genomics 54:169-172.

Koyanagi I, Houkin K (2010) Pathogenesis of syringomyelia associated with Chiari type 1 malformation: review of evidences and proposal of a new hypothesis. Neurosurg Rev 33:271-284; discussion 284-275.

Koyanagi I, Iwasaki Y, Hida K, Houkin K (2005) Clinical features and pathomechanisms of syringomyelia associated with spinal arachnoiditis. Surg Neurol 63:350-355; discussion 355-356.

Krenz NR, Weaver LC (1998) Sprouting of primary afferent fibers after spinal cord transection in the rat. Neuroscience 85:443-458.

Krikorian JG, Guth L, Barrett CP, Donati EJ (1982) Enzyme histochemical changes after transection or hemisection of the spinal cord of the rat. Exp Neurol 76:623-643.

Kubota M, Shin M, Taniguchi M, Terao T, Nakauchi J, Takahashi H (2008) Syringomyelia caused by intrathecal remnants of oil-based contrast medium. J Neurosurg Spine 8:169-173.

Kuriyama H, Kawamoto S, Ishida N, Ohno I, Mita S, Matsuzawa Y, Matsubara K, Okubo K (1997) Molecular cloning and expression of a novel human aquaporin from adipose tissue with glycerol permeability. Biochem Biophys Res Commun 241:53-58.

Kusunoki T, Rowed DW, Tator CH, Lougheed WM (1978) Thromboendarterectomy for total occlusion of the internal carotid artery: a reappraisal of risks, success rate and potential benefits. Stroke 9:34-38.

Kuwamura K, McLone DG, Raimondi AJ (1978) The central (spinal) canal in congenital murine hydrocephalus: morphological and physiological aspects. Child's brain 4:216-234.

Lam S, Batzdorf U, Bergsneider M (2008) Thecal shunt placement for treatment of obstructive primary syringomyelia. J Neurosurg Spine 9:581-588.

Lasfargues JE, Custis D, Morrone F, Carswell J, Nguyen T (1995) A model for estimating spinal cord injury prevalence in the United States. Paraplegia 33:62-68.

Lawrence JM, Hamill RW, Cochard P, Raisman G, Black IB (1981) Effects of spinal cord transection on synapse numbers and biochemical maturation in rat lumbar sympathetic ganglia. Brain Res 212:83-88.

Lee GY, Jones NR, Mayrhofer G, Brown C, Cleland L (2005) Origin of macrophages in a kaolin-induced model of rat syringomyelia: a study using radiation bone marrow chimeras. Spine (Phila Pa 1976) 30:194-200.

Lee TS, Eid T, Mane S, Kim JH, Spencer DD, Ottersen OP, de Lanerolle NC (2004) Aquaporin-4 is increased in the sclerotic hippocampus in human temporal lobe epilepsy. Acta Neuropathol 108:493-502.

Lemke M, Faden AI (1990) Edema development and ion changes in rat spinal cord after impact trauma: injury dose-response studies. J Neurotrauma 7:41-54.

Levine DN (2004) The pathogenesis of syringomyelia associated with lesions at the foramen magnum: a critical review of existing theories and proposal of a new hypothesis. J Neurol Sci 220:3-21.

Levy WJ, Mason L, Hahn JF (1983) Chiari malformation presenting in adults: a surgical experience in 127 cases. Neurosurgery 12:377-390.

Lewis T, Rusbridge C, Knowler P, Blott S, Woolliams JA (2010) Heritability of syringomyelia in Cavalier King Charles spaniels. Vet J 183:345-347.

Li F, Chong ZZ, Maiese K (2004a) Erythropoietin on a tightrope: balancing neuronal and vascular protection between intrinsic and extrinsic pathways. Neurosignals 13:265-289.

Li J, Verkman AS (2001) Impaired hearing in mice lacking aquaporin-4 water channels. J Biol Chem 276:31233-31237.

Li W, Maeda Y, Yuan RR, Elkabes S, Cook S, Dowling P (2004b) Beneficial effect of erythropoietin on experimental allergic encephalomyelitis. Ann Neurol 56:767-777.

Li X, Oudega M, Dancausse HA, Levi AD (2000) The Effect of Methylprednisolone on Caspase-3 Activation after Rat Spinal Cord Transection. Restor Neurol Neurosci 17:203-209.

Li Y, Lu ZY, Ogle M, Wei L (2007) Erythropoietin prevents blood brain barrier damage induced by focal cerebral ischemia in mice. Neurochem Res 32:2132-2141.

Lin JY, Peng B, Yang ZW, Min S Number of synapses increased in the rat spinal dorsal horn after sciatic nerve transection: A stereological study. Brain Res Bull.

Lin VW, Cardenas DD, Cutter NC, Frost FS, Hammond MC, Lindblom LB, Perkash I, Waters R, Woolsey RM (eds.) (2003) Spinal Cord Medicine: Principles and Practice. New York: Demos Medical Publishing.

Lin Y, Zhu X, He Y, Wang ZY, Cao XG (2008) [Effects of transection of cervical spinal cord on lipopolysaccharide induced acute lung injury in rat]. Zhongguo Wei Zhong Bing Ji Jiu Yi Xue 20:621-624.

Liu D, Thangnipon W, McAdoo DJ (1991) Excitatory amino acids rise to toxic levels upon impact injury to the rat spinal cord. Brain Res 547:344-348.

Liu D, Xu GY, Pan E, McAdoo DJ (1999) Neurotoxicity of glutamate at the concentration released upon spinal cord injury. Neuroscience 93:1383-1389.

Liu L, Rudin M, Kozlova EN (2000) Glial cell proliferation in the spinal cord after dorsal rhizotomy or sciatic nerve transection in the adult rat. Exp Brain Res 131:64-73.

Logue V, Edwards MR (1981) Syringomyelia and its surgical treatment--an analysis of 75 patients. J Neurol Neurosurg Psychiatry 44:273-284.

Lohle PN, Wurzer HA, Hoogland PH, Seelen PJ, Go KG (1994) The pathogenesis of syringomyelia in spinal cord ependymoma. Clinical Neurology & Neurosurgery 96:323-326.

Lonser RR, Butman JA, Oldfield EH (2006) Pathogenesis of tumor-associated syringomyelia demonstrated by peritumoral contrast material leakage. Case illustration. J Neurosurg Spine 4:426.

Lonser RR, Vortmeyer AO, Butman JA, Glasker S, Finn MA, Ammerman JM, Merrill MJ, Edwards NA, Zhuang Z, Oldfield EH (2005) Edema is a precursor to central nervous system peritumoral cyst formation. Ann Neurol 58:392-399.

Lopez-Vales R, Fores J, Navarro X, Verdu E (2007) Chronic transplantation of olfactory ensheathing cells promotes partial recovery after complete spinal cord transection in the rat. Glia 55:303-311.

Ma N, Hunt NH, Madigan MC, Chan-Ling T (1996) Correlation between enhanced vascular permeability, up-regulation of cellular adhesion molecules and monocyte adhesion to the endothelium in the retina during the development of fatal murine cerebral malaria. Am J Pathol 149:1745-1762.

Ma T, Frigeri A, Hasegawa H, Verkman AS (1994) Cloning of a water channel homolog expressed in brain meningeal cells and kidney collecting duct that functions as a stilbene-sensitive glycerol transporter. J Biol Chem 269:21845-21849.

Ma T, Frigeri A, Skach W, Verkman AS (1993) Cloning of a novel rat kidney cDNA homologous to CHIP28 and WCH-CD water channels. Biochem Biophys Res Commun 197:654-659.

Macdonald JF, Pearson JA (1979) Some observations on habituation of the flexor reflex in the rat: the influence of strychnine, bicuculline, spinal transection, and decerebration. J Neurobiol 10:67-78.

Madsen PW, 3rd, Yezierski RP, Holets VR (1994) Syringomyelia: clinical observations and experimental studies. J Neurotrauma 11:241-254.

Magnusson T (1973) Effect of chronic transection on dopamine, noradrenaline and 5-hydroxytryptamine in the rat spinal cord. Naunyn Schmiedebergs Arch Pharmacol 278:13-22.

Mahmood NS, Kadavigere R, Ramesh AK, Rao VR (2008) Magnetic resonance imaging in acute cervical spinal cord injury: a correlative study on spinal cord changes and 1 month motor recovery. Spinal Cord.

Maikos JT, Shreiber DI (2007) Immediate damage to the blood-spinal cord barrier due to mechanical trauma. J Neurotrauma 24:492-507.

Manders EM, Stap J, Brakenhoff GJ, van Driel R, Aten JA (1992) Dynamics of three-dimensional replication patterns during the S-phase, analysed by double labelling of DNA and confocal microscopy. J Cell Sci 103 (Pt 3):857-862.

Manley GT, Binder DK, Papadopoulos MC, Verkman AS (2004) New insights into water transport and edema in the central nervous system from phenotype analysis of aquaporin-4 null mice. Neuroscience 129:983-991.

Manley GT, Fujimura M, Ma T, Noshita N, Filiz F, Bollen AW, Chan P, Verkman AS (2000) Aquaporin-4 deletion in mice reduces brain edema after acute water intoxication and ischemic stroke. Nat Med 6:159-163.

Mantulo PM, Makii EA, Serdiuchenko I (1979) [Segmental reflex reactions of rat spinal cord after sciatic nerve transection and thyroxine administration]. Fiziol Zh 25:492-496.

Marsala M, Sorkin LS, Yaksh TL (1994) Transient spinal ischemia in rat: characterization of spinal cord blood flow, extracellular amino acid release, and concurrent histopathological damage. J Cereb Blood Flow Metab 14:604-614.

Martinez-Estrada OM, Rodriguez-Millan E, Gonzalez-De Vicente E, Reina M, Vilaro S, Fabre M (2003) Erythropoietin protects the in vitro blood-brain barrier against VEGF-induced permeability. Eur J Neurosci 18:2538-2544.

Martinez LJ, Alderman JL, Kagan RS, Osterholm JL (1981) Spatial distribution of edema in the cat spinal cord after impact injury. Neurosurgery 8:450-453.

Martins AN, Wiley JK, Myers PW (1972) Dynamics of the cerebrospinal fluid and the spinal dura mater. J Neurol Neurosurg Psychiatry 35:468-473.

Masaryk TJ, Modic MT, Geisinger MA, Standefer J, Hardy RW, Boumphrey F, Duchesneau PM (1986) Cervical myelopathy: a comparison of magnetic resonance and myelography. J Comput Assist Tomogr 10:184-194.

Matthews MA, St Onge MF, Faciane CL (1979a) An electron microscopic analysis of abnormal ependymal cell proliferation and envelopment of sprouting axons following spinal cord transection in the rat. Acta Neuropathol 45:27-36.

Matthews MA, St Onge MF, Faciane CL, Gelderd JB (1979b) Axon sprouting into segments of rat spinal cord adjacent to the site of a previous transection. Neuropathol Appl Neurobiol 5:181-196.

Mautes AE, Weinzierl MR, Donovan F, Noble LJ (2000) Vascular events after spinal cord injury: contribution to secondary pathogenesis. Phys Ther 80:673-687.

Mavinkurve GG, Sciubba D, Amundson E, Jallo GI (2005) Familial Chiari type I malformation with syringomyelia in two siblings: case report and review of the literature. Childs Nerv Syst 21:955-959.

Mc LR, Bailey OT, Schurr PH, Ingraham FD (1954) Myelomalacia and multiple cavitations of spinal cord secondary to adhesive arachnoiditis; an experimental study. A M A 57:138-146.

McDonald JW, Sadowsky C (2002) Spinal-cord injury. Lancet 359:417-425.

McDonald WS, Zagzag D, Thorne CH (1995) Frontonasal encephalocele and associated congenital brain tumor. J Craniofac Surg 6:386-389.

McGrath JT (1965) Spinal dysraphism in the dog. With comments on syringomyelia. Pathologia veterinaria 2:Suppl:1-36.

McIlroy WJ, Richardson JC (1965) Syringomyelia: a clinical review of 75 cases. Can Med Assoc J 93:731-734.

McKay SM, Brooks DJ, Hu P, McLachlan EM (2007) Distinct types of microglial activation in white and grey matter of rat lumbosacral cord after mid-thoracic spinal transection. J Neuropathol Exp Neurol 66:698-710.

McKay SM, McLachlan EM (2004) Inflammation of rat dorsal root ganglia below a mid-thoracic spinal transection. Neuroreport 15:1783-1786.

Milhorat TH (2000) Classification of syringomyelia. Neurosurg Focus 8:E1.

Milhorat TH, Bolognese PA, Black KS, Woldenberg RF (2003) Acute syringomyelia: case report. Neurosurgery 53:1220-1221; discussion 1221-1222.

Milhorat TH, Capocelli AL, Jr., Anzil AP, Kotzen RM, Milhorat RH (1995a) Pathological basis of spinal cord cavitation in syringomyelia: analysis of 105 autopsy cases. J Neurosurg 82:802-812.

Milhorat TH, Chou MW, Trinidad EM, Kula RW, Mandell M, Wolpert C, Speer MC (1999) Chiari I malformation redefined: clinical and radiographic findings for 364 symptomatic patients. Neurosurgery 44:1005-1017.

Milhorat TH, Clark RG, Hammock MK, McGrath PP (1970) Structural, ultrastructural, and permeability changes in the ependyma and surrounding brain favoring equilibration in progressive hydrocephalus. Arch Neurol 22:397-407.

Milhorat TH, Johnson RW, Milhorat RH, Capocelli AL, Jr., Pevsner PH (1995b) Clinicopathological correlations in syringomyelia using axial magnetic resonance imaging. Neurosurgery 37:206-213.

Milhorat TH, Johnson WD, Miller JI, Bergland RM, Hollenberg-Sher J (1992) Surgical treatment of syringomyelia based on magnetic resonance imaging criteria. Neurosurgery 31:231-244; discussion 244-235.

Milhorat TH, Kotzen RM (1994) Stenosis of the central canal of the spinal cord following inoculation of suckling hamsters with reovirus type I. J Neurosurg 81:103-106.

Milhorat TH, Kotzen RM, Capocelli AL, Jr., Bolognese P, Bendo AA, Cottrell JE (1996a) Intraoperative improvement of somatosensory evoked potentials and local spinal cord blood flow in patients with syringomyelia. J Neurosurg Anesthesiol 8:208-215.

Milhorat TH, Kotzen RM, Mu HT, Capocelli AL, Jr., Milhorat RH (1996b) Dysesthetic pain in patients with syringomyelia. Neurosurgery 38:940-946; discussion 946-947.

Milhorat TH, Nobandegani F, Miller JI, Rao C (1993) Noncommunicating syringomyelia following occlusion of central canal in rats. Experimental model and histological findings. J Neurosurg 78:274-279.

Misu T, Fujihara K, Kakita A, Konno H, Nakamura M, Watanabe S, Takahashi T, Nakashima I, Takahashi H, Itoyama Y (2007) Loss of aquaporin 4 in lesions of neuromyelitis optica: distinction from multiple sclerosis. Brain 130:1224-1234.

Moller T (2010) Neuroinflammation in Huntington's disease. J Neural Transm 117:1001-1008.

Moriwaka F, Tashiro K, Tachibana S, Yada K (1995) [Epidemiology of syringomyelia in Japan--the nationwide survey]. Rinsho Shinkeigaku 35:1395-1397.

Moshonkina T, Avelev V, Gerasimenko Y, Mathur R, Bijlani RL (2002) Treadmill training accelerates restoration of locomotion after complete spinal cord transection in the rat. Indian J Physiol Pharmacol 46:499-503.

Mozer AB, Whittemore SR, Benton RL (2010) Spinal microvascular expression of PV-1 is associated with inflammation, perivascular astrocyte loss, and diminished EC glucose transport potential in acute SCI. Curr Neurovasc Res 7:238-250.

Mrowczynski W, Celichowski J, Krutki P, Gorska T, Majczynski H, Slawinska U Time-related changes of motor unit properties in the rat medial gastrocnemius muscle after spinal cord injury. I. Effects of total spinal cord transection. J Electromyogr Kinesiol 20:523-531.

Muller F, O'Rahilly R (1986a) The development of the human brain and the closure of the rostral neuropore at stage 11. Anat Embryol (Berl) 175:205-222.

Muller F, O'Rahilly R (1986b) Somitic-vertebral correlation and vertebral levels in the human embryo. Am J Anat 177:3-19.

Muller F, O'Rahilly R, Benson DR (1986) The early origin of vertebral anomalies, as illustrated by a 'butterfly vertebra'. Journal of Anatomy 149:157-169.

Munshi I, Frim D, Stine-Reyes R, Weir BK, Hekmatpanah J, Brown F (2000) Effects of posterior fossa decompression with and without duraplasty on Chiari malformation-associated hydromyelia. Neurosurgery 46:1384-1389; discussion 1389-1390.

Naftchi NE, Kirschner AK, Demeny M, Viau AT (1981) Alterations in norepinephrine, serotonin, c-AMP, and transsynaptic induction of tyrosine hydroxylase after spinal cord transection in the rat. Neurochem Res 6:1205-1216.

Nagahiro S, Matsukado Y, Kuratsu J, Saito Y, Takamura S (1986) Syringomyelia and syringobulbia associated with an ependymoma of the cauda equina involving the conus medullaris: case report. Neurosurgery 18:357-360.

Naruse H, Tanaka K, Kim A, Hakuba A (1997) A new model of spinal cord edema. Acta Neurochir Suppl 70:293-295.

Navratil J, Rathova E, Zeman B, Flach A, Dufek V (1963) [Importance of Graphic Demonstration of Pulsation of the Left Ventricle in the Esophagus (Esophagoatriogram) in the Diagnosis of Mitral Defect]. Rozhl Chir 42:759-764.

Nedergaard M, Ransom B, Goldman SA (2003) New roles for astrocytes: redefining the functional architecture of the brain. Trends Neurosci 26:523-530.

Negredo P, Rivero JL, Gonzalez B, Ramon-Cueto A, Manso R (2008) Slow- and fast-twitch rat hind limb skeletal muscle phenotypes 8 months after spinal cord transection and olfactory ensheathing glia transplantation. J Physiol 586:2593-2610.

Nesic O, Guest JD, Zivadinovic D, Narayana PA, Herrera JJ, Grill RJ, Mokkapati VU, Gelman BB, Lee J (2010) Aquaporins in spinal cord injury: the janus face of aquaporin 4. Neuroscience 168:1019-1035.

Nesic O, Lee J, Johnson KM, Ye Z, Xu GY, Unabia GC, Wood TG, McAdoo DJ, Westlund KN, Hulsebosch CE, Regino Perez-Polo J (2005) Transcriptional profiling of spinal cord injury-induced central neuropathic pain. J Neurochem 95:998-1014.

Nesic O, Lee J, Unabia GC, Johnson K, Ye Z, Vergara L, Hulsebosch CE, Perez-Polo JR (2008) Aquaporin 1 - a novel player in spinal cord injury. J Neurochem 105:628-640.

Nesic O, Lee J, Ye Z, Unabia GC, Rafati D, Hulsebosch CE, Perez-Polo JR (2006) Acute and chronic changes in aquaporin 4 expression after spinal cord injury. Neuroscience 143:779-792.

Newman PK, Terenty TR, Foster JB (1981) Some observations on the pathogenesis of syringomyelia. J Neurol Neurosurg Psychiatry 44:964-969.

Newton EJ (1969) Syringomyelia as a manifestation of defective fourth ventricular drainage. Ann R Coll Surg Engl 44:194-213.

Nielsen S, Nagelhus EA, Amiry-Moghaddam M, Bourque C, Agre P, Ottersen OP (1997) Specialized membrane domains for water transport in glial cells: high-resolution immunogold cytochemistry of aquaporin-4 in rat brain. J Neurosci 17:171-180.

Nishigaya K, Yagi S, Sato T, Kanemaru K, Nukui H (2000) Impairment and restoration of the endothelial blood-brain barrier in the rat cerebral infarction model assessed by expression of endothelial barrier antigen immunoreactivity. Acta Neuropathol 99:231-237.

Noble LJ, Wrathall JR (1985) Spinal cord contusion in the rat: morphometric analyses of alterations in the spinal cord. Exp Neurol 88:135-149.

Noble LJ, Wrathall JR (1987) The blood-spinal cord barrier after injury: pattern of vascular events proximal and distal to a transection in the rat. Brain Res 424:177-188.

Noble LJ, Wrathall JR (1989) Distribution and time course of protein extravasation in the rat spinal cord after contusive injury. Brain Res 482:57-66.

Nolan RT (1969) Traumatic oedema of the spinal cord. Br Med J 1:710.

Nomura H, Ogawa A, Tashiro A, Morimoto T, Hu JW, Iwata K (2002) Induction of Fos protein-like immunoreactivity in the trigeminal spinal nucleus caudalis and upper cervical cord following noxious and non-noxious mechanical stimulation of the whisker pad of the rat with an inferior alveolar nerve transection. Pain 95:225-238.

Norenberg MD (1994) Astrocyte responses to CNS injury. J Neuropathol Exp Neurol 53:213-220.

Norreel JC, Pflieger JF, Pearlstein E, Simeoni-Alias J, Clarac F, Vinay L (2003) Reversible disorganization of the locomotor pattern after neonatal spinal cord transection in the rat. J Neurosci 23:1924-1932.

Nukada A, Koizumi A (1954) Studies on blood count. II. A statistical analysis of the distribution type of blood corpuscles in a haemocytometer. Yokohama Med Bull 5:32-34.

O'Rahilly R (1986) The embryonic period. Teratology 34:119.

O'Rahilly R, Muller F, Bossy J (1986a) Atlas des stades du developpement des formes exterieures de l'encephale chez l'embryon humain. Arch Anat Histol Embryol 69:3-39.

O'Rahilly SP, Nugent Z, Rudenski AS, Hosker JP, Burnett MA, Darling P, Turner RC (1986b) Beta-cell dysfunction, rather than insulin insensitivity, is the primary defect in familial type 2 diabetes. Lancet 2:360-364.

Ohata K, Gotoh T, Matsusaka Y, Morino M, Tsuyuguchi N, Sheikh B, Inoue Y, Hakuba A (2001) Surgical management of syringomyelia associated with spinal adhesive arachnoiditis. J Clin Neurosci 8:40-42.

Oldendorf WH, Cornford ME, Brown WJ (1977) The large apparent work capability of the blood-brain barrier: a study of the mitochondrial content of capillary endothelial cells in brain and other tissues of the rat. Ann Neurol 1:409-417.

Oldfield EH, Muraszko K, Shawker TH, Patronas NJ (1994) Pathophysiology of syringomyelia associated with Chiari I malformation of the cerebellar tonsils. Implications for diagnosis and treatment. J Neurosurg 80:3-15.

Ollivier D'Angers CP (1827) De le Moelle Epiniere et de ses Maladies. Paris: Chez Crevot.

Oshio K, Binder DK, Yang B, Schecter S, Verkman AS, Manley GT (2004) Expression of aquaporin water channels in mouse spinal cord. Neuroscience 127:685-693.

Oshio K, Watanabe H, Song Y, Verkman AS, Manley GT (2005) Reduced cerebrospinal fluid production and intracranial pressure in mice lacking choroid plexus water channel Aquaporin-1. FASEB J 19:76-78.

Padmanabhan R, Crompton D, Burn D, Birchall D (2005) Acquired Chiari 1 malformation and syringomyelia following lumboperitoneal shunting for pseudotumour cerebri. J Neurol Neurosurg Psychiatry 76:298.

Palant CE, Duffey ME, Mookerjee BK, Ho S, Bentzel CJ (1983) Ca2+ regulation of tight-junction permeability and structure in Necturus gallbladder. Am J Physiol 245:C203-212.

Palmer AM (2010) The role of the blood-CNS barrier in CNS disorders and their treatment. Neurobiology of disease 37:3-12.

Pan W, Zhang L, Liao J, Csernus B, Kastin AJ (2003) Selective increase in TNF alpha permeation across the blood-spinal cord barrier after SCI. J Neuroimmunol 134:111-117.

Paniagua C, De Fazio A (1983) Psychodynamics of the mildly retarded and borderline intelligence adult. Psychiatr Q 55:242-252.

Panter SS, Yum SW, Faden AI (1990) Alteration in extracellular amino acids after traumatic spinal cord injury. Ann Neurol 27:96-99.

Papadopoulos MC, Manley GT, Krishna S, Verkman AS (2004) Aquaporin-4 facilitates reabsorption of excess fluid in vasogenic brain edema. FASEB J 18:1291-1293.

Papadopoulos MC, Verkman AS (2005) Aquaporin-4 gene disruption in mice reduces brain swelling and mortality in pneumococcal meningitis. J Biol Chem 280:13906-13912.

Papadopoulos MC, Verkman AS (2007) Aquaporin-4 and brain edema. Pediatr Nephrol 22:778-784.

Park C, Kang BT, Yoo JH, Park HM (2009) Syringomyelia in three small breed dogs secondary to Chiari-like malformation: clinical and diagnostic findings. Journal of veterinary science 10:365-367.

Parkinson D (1991) Human spinal arachnoid septa, trabeculae, and "rogue strands". Am J Anat 192:498-509.

Paul L, Madan M, Rammling M, Chigurupati S, Chan SL, Pattisapu JV (2010) Expression of Aquaporin 1 and 4 in congenital hydrocephalus rat model. Neurosurgery.

Perdiki M, Farooque M, Holtz A, Li GL, Olsson Y (1998) Expression of endothelial barrier antigen immunoreactivity in blood vessels following compression trauma to rat spinal cord. Temporal evolution and relation to the degree of the impact. Acta Neuropathol 96:8-12.

Perez E, Barrachina M, Rodriguez A, Torrejon-Escribano B, Boada M, Hernandez I, Sanchez M, Ferrer I (2007) Aquaporin expression in the cerebral cortex is increased at early stages of Alzheimer disease. Brain Res 1128:164-174.

Perfetti GA, Joe FL, Jr., Fazio T (1983) Reverse phase high pressure liquid chromatography and fluorescence detection of ethoxyquin in milk. J Assoc Off Anal Chem 66:1143-1147.

Perrouin-Verbe B, Lenne-Aurier K, Robert R, Auffray-Calvier E, Richard I, Mauduyt de la Greve I, Mathe JF (1998) Post-traumatic syringomyelia and post-traumatic spinal canal stenosis: a direct relationship: review of 75 patients with a spinal cord injury. Spinal Cord 36:137-143.

Persidsky Y, Ramirez SH, Haorah J, Kanmogne GD (2006) Blood-brain barrier: structural components and function under physiologic and pathologic conditions. J Neuroimmune Pharmacol 1:223-236.

Pipino G, Germiniani R, Maione G, Fazio FM (1983) [Comparative study of 2 different chemotherapeutic combinations in epidermoid carcinoma of the lung. Preliminary results]. Arch Sci Med (Torino) 140:135-138.

Pisani F, Spina E, Trunfio C, Fazio A, Oteri G, Di Perri R (1983) Intra-daily oscillations in dipropylacetic acid plasma levels with two or three daily doses of dipropylacetamide in epileptic patients. Ital J Neurol Sci 4:173-177.

Pisharodi M, Nauta HJ (1985) An animal model for neuron-specific spinal cord lesions by the microinjection of N-methylaspartate, kainic acid, and quisqualic acid. Appl Neurophysiol 48:226-233.

Placak B, Zeman B, Navratil J (1963) [Contribution to the Surgical Treatment of Anomalous Drainage of the Pulmonary Veins]. Rozhl Chir 42:794-799.

Popovich PG, Horner PJ, Mullin BB, Stokes BT (1996) A quantitative spatial analysis of the blood-spinal cord barrier. I. Permeability changes after experimental spinal contusion injury. Exp Neurol 142:258-275.

Prado R, Dietrich WD, Watson BD, Ginsberg MD, Green BA (1987) Photochemically induced graded spinal cord infarction. Behavioral, electrophysiological, and morphological correlates. J Neurosurg 67:745-753.

Preston GM, Carroll TP, Guggino WB, Agre P (1992) Appearance of water channels in Xenopus oocytes expressing red cell CHIP28 protein. Science 256:385-387.

Preston GM, Jung JS, Guggino WB, Agre P (1994) Membrane topology of aquaporin CHIP. Analysis of functional epitope-scanning mutants by vectorial proteolysis. J Biol Chem 269:1668-1673.

Profeta G, Maggi G (1980) Terminal ventriculostomy for syringomyelia. J Neurosurg Sci 24:161-168.

Rafols JA, Goshgarian HG (1985) Spinal tanycytes in the adult rat: a correlative Golgi gold-toning study. Anat Rec 211:75-86.

Raina S, Preston GM, Guggino WB, Agre P (1995) Molecular cloning and characterization of an aquaporin cDNA from salivary, lacrimal, and respiratory tissues. J Biol Chem 270:1908-1912.

Randall DC, Baldridge BR, Zimmerman EE, Carroll JJ, Speakman RO, Brown DR, Taylor RF, Patwardhan A, Burgess DE (2005) Blood pressure power within frequency range approximately 0.4 Hz in rat conforms to self-similar scaling following spinal cord transection. Am J Physiol Regul Integr Comp Physiol 288:R737-741.

Ransom B, Behar T, Nedergaard M (2003) New roles for astrocytes (stars at last). Trends Neurosci 26:520-522.

Ravaglia S, Bogdanov EI, Pichiecchio A, Bergamaschi R, Moglia A, Mikhaylov IM (2007) Pathogenetic role of myelitis for syringomyelia. Clin Neurol Neurosurg 109:541-546.

Rawe SE, Roth RH, Collins WF (1977) Norepinephrine levels in experimental spinal cord trauma. Part 2: Histopathological study of hemorrhagic necrosis. J Neurosurg 46:350-357.

Reid JL, Zivin JA, Kopin IJ (1976) The effects of spinal cord transection and intracisternal 6-hydroxydopamine on phenylethanolamine-N-methyl transferase (PNMT) activity in rat brain stem and spinal cord. J Neurochem 26:629-631.

Reina MA, De Leon Casasola O, Lopez A, De Andres JA, Mora M, Fernandez A (2002) The origin of the spinal subdural space: ultrastructure findings. Anesth Analg 94:991-995, table of contents.

Reina MA, Franco CD, Lopez A, De Andres JA, van Zundert A (2009) Clinical implications of epidural fat in the spinal canal. A scanning electron microscopic study. Acta Anaesthesiol Belg 60:7-17.

Rexed B (1952) The cytoarchitectonic organization of the spinal cord in the cat. J Comp Neurol 96:414-495.

Reynolds LF, Bren MC, Wilson BC, Gibson GD, Shoichet MS, Murphy RJ (2008) Transplantation of porous tubes following spinal cord transection improves hindlimb function in the rat. Spinal Cord 46:58-64.

Rice AJ, Plaa GL (1968) Effect of hypophysectomy and spinal cord transection on carbon tetrachloride-induced changes in the hemodynamics of the isolated perfused rat liver. Toxicol Appl Pharmacol 12:194-201.

Rivlin AS, Tator CH (1978a) Effect of duration of acute spinal cord compression in a new acute cord injury model in the rat. Surg Neurol 10:38-43.

Rivlin AS, Tator CH (1978b) Regional spinal cord blood flow in rats after severe cord trauma. J Neurosurg 49:844-853.

Rodriguez-Cano L, Bartralot R, Garcia-Patos V, Mollet J, Malagelada A, Castells A (2007) Cervico-thoracic lipoma associated with occult syringohydromyelia. Pediatr Dermatol 24:E76-78.

Rodriguez A, Perez-Gracia E, Espinosa JC, Pumarola M, Torres JM, Ferrer I (2006) Increased expression of water channel aquaporin 1 and aquaporin 4 in Creutzfeldt-Jakob disease and in bovine spongiform encephalopathy-infected bovine-PrP transgenic mice. Acta Neuropathol 112:573-585.

Ronen J, Catz A, Spasser R, Gepstein R (1999) The treatment dilemma in post-traumatic syringomyelia. Disabil Rehabil 21:455-457.

Rosenstein JM, Krum JM, Sternberger LA, Pulley MT, Sternberger NH (1992) Immunocytochemical expression of the endothelial barrier antigen (EBA) during brain angiogenesis. Brain Res Dev Brain Res 66:47-54.

Ross TM, Fazio VW, Farmer RG (1983) Long-term results of surgical treatment for Crohn's disease of the duodenum. Ann Surg 197:399-406.

Rossier AB, Foo D, Shillito J, Dyro FM (1985) Posttraumatic cervical syringomyelia. Incidence, clinical presentation, electrophysiological studies, syrinx protein and results of conservative and operative treatment. Brain 108 (Pt 2):439-461.

Rowed DW, McLean JA, Tator CH (1978) Somatosensory evoked potentials in acute spinal cord injury: prognostic value. Surg Neurol 9:203-210.

Rusbridge C, Knowler P, Rouleau GA, Minassian BA, Rothuizen J (2005) Inherited occipital hypoplasia/syringomyelia in the cavalier King Charles spaniel: experiences in setting up a worldwide DNA collection. The Journal of heredity 96:745-749.

Rusbridge C, Knowler SP (2003) Hereditary aspects of occipital bone hypoplasia and syringomyelia (Chiari type I malformation) in cavalier King Charles spaniels. The Veterinary record 153:107-112.

Rusbridge C, Knowler SP (2004) Inheritance of occipital bone hypoplasia (Chiari type I malformation) in Cavalier King Charles Spaniels. J Vet Intern Med 18:673-678.

Rusbridge C, MacSweeny JE, Davies JV, Chandler K, Fitzmaurice SN, Dennis R, Cappello R, Wheeler SJ (2000) Syringohydromyelia in Cavalier King Charles spaniels. Journal of the American Animal Hospital Association 36:34-41.

Saadoun S, Bell BA, Verkman AS, Papadopoulos MC (2008) Greatly improved neurological outcome after spinal cord compression injury in AQP4-deficient mice. Brain 131:1087-1098.

Saadoun S, Papadopoulos MC, Hara-Chikuma M, Verkman AS (2005a) Impairment of angiogenesis and cell migration by targeted aquaporin-1 gene disruption. Nature 434:786-792.

Saadoun S, Papadopoulos MC, Watanabe H, Yan D, Manley GT, Verkman AS (2005b) Involvement of aquaporin-4 in astroglial cell migration and glial scar formation. J Cell Sci 118:5691-5698.

Sahgal V, Sahgal S, Subramani V (1981) Morphological and histochemical correlation of recovery after spinal transection in rat. Paraplegia 19:1-6.

Saito F, Nakatani T, Iwase M, Maeda Y, Hirakawa A, Murao Y, Suzuki Y, Onodera R, Fukushima M, Ide C (2008) Spinal cord injury treatment with intrathecal autologous bone marrow stromal cell transplantation: the first clinical trial case report. J Trauma 64:53-59.

Sakakibara A, Furuse M, Saitou M, Ando-Akatsuka Y, Tsukita S (1997) Possible involvement of phosphorylation of occludin in tight junction formation. J Cell Biol 137:1393-1401.

Santoreneos S, Stoodley MA, Jones NR, Brown CJ (1998) A technique for in vivo vascular perfusion fixation of the sheep central nervous system. J Neurosci Methods 79:195-199.

Scharrer E (1945) Capillaries and mitochondria in neurophil. J Comp Neurol 83:237-243.

Schlesinger EB, Antunes JL, Michelsen WJ, Louis KM (1981) Hydromyelia: clinical presentation and comparison of modalities of treatment. Neurosurgery 9:356-365.

Schubert J (1973) Effect of spinal transection on the metabolism of 5-hydroxyindoles formed in vivo from 3H-tryptophan in the rat spinal cord. Acta Physiol Scand 87:557-566.

Schurch B, Wichmann W, Rossier AB (1996) Post-traumatic syringomyelia (cystic myelopathy): a prospective study of 449 patients with spinal cord injury. J Neurol Neurosurg Psychiatry 60:61-67.

Seif GI, Nomura H, Tator CH (2007) Retrograde axonal degeneration "dieback" in the corticospinal tract after transection injury of the rat spinal cord: a confocal microscopy study. J Neurotrauma 24:1513-1528.

Seki T, Fehlings MG (2008) Mechanistic insights into posttraumatic syringomyelia based on a novel in vivo animal model. Laboratory investigation. J Neurosurg Spine 8:365-375.

Sgouros S, Williams B (1995) A critical appraisal of drainage in syringomyelia. J Neurosurg 82:1-10.

Sgouros S, Williams B (1996) Management and outcome of posttraumatic syringomyelia. J Neurosurg 85:197-205.

Sharma HS, Badgaiyan RD, Alm P, Mohanty S, Wiklund L (2005) Neuroprotective effects of nitric oxide synthase inhibitors in spinal cord injury-induced pathophysiology and motor functions: an experimental study in the rat. Ann N Y Acad Sci 1053:422-434.

Sharma HS, Olsson Y (1990) Edema formation and cellular alterations following spinal cord injury in the rat and their modification with p-chlorophenylalanine. Acta Neuropathol 79:604-610.

Shenoy SN, Raja A (2005) Cystic cervical intramedullary schwannoma with syringomyelia. Neurol India 53:224-225.

Shi LB, Verkman AS (1996) Selected cysteine point mutations confer mercurial sensitivity to the mercurial-insensitive water channel MIWC/AQP-4. Biochemistry 35:538-544.

Shields SD, Mazario J, Skinner K, Basbaum AI (2007) Anatomical and functional analysis of aquaporin 1, a water channel in primary afferent neurons. Pain 131:8-20.

Shimizu T, Saito N, Aihara M, Kurihara H, Nakazato Y, Ueki K, Sasaki T (2004) Primary spinal oligoastrocytoma: a case report. Surg Neurol 61:77-81; discussion 81.

Shimoda Y, Hanazono N, Koizumi A, Murakami A, Kadowaki K (1954a) Electroencephalographic group studies on children with mental deficiency, behavior problem, congenital blindness, deafness, dumbness and other neurological and psychiatric disorders. Folia Psychiatr Neurol Jpn 8:200-201.

Shimoda Y, Hanazono N, Koizumi A, Murakami A, Kadowaki K, Tanaka T (1954b) EEG changes and age factor. II. the frequency analysis, topographical abnormality and paroxysmal discharges on the EEG of normal children in from 4 to 15 years of age. Folia Psychiatr Neurol Jpn 8:202-203.

Sidel VW, Solomon AK (1957) Entrance of water into human red cells under an osmotic pressure gradient. J Gen Physiol 41:243-257.

Sigman HH, Gillich A (1981) Role of hypothermia in the production of gastric ulcers in a rat spinal cord transection model. Dig Dis Sci 26:60-64.

Silver JR (2001) History of post-traumatic syringomyelia: post traumatic syringomyelia prior to 1920. Spinal Cord 39:176-183.

Simard M, Nedergaard M (2004) The neurobiology of glia in the context of water and ion homeostasis. Neuroscience 129:877-896.

Sinescu C, Popa F, Grigorean VT, Onose G, Sandu AM, Popescu M, Burnei G, Strambu V, Popa C (2010) Molecular basis of vascular events following spinal cord injury. J Med Life 3:254-261.

Singer HS, Coyle JT, Frangia J, Price DL (1981) Effects of spinal transection on presynaptic markers for glutamatergic neurons in the rat. Neurochem Res 6:485-496.

Singounas EG, Karvounis PC (1979) Terminal ventriculostomy in syringomyelia. Acta Neurochir (Wien) 46:293-295.

Solenov EI, Vetrivel L, Oshio K, Manley GT, Verkman AS (2002) Optical measurement of swelling and water transport in spinal cord slices from aquaporin null mice. J Neurosci Methods 113:85-90.

Spilker MH, Yannas IV, Kostyk SK, Norregaard TV, Hsu HP, Spector M (2001) The effects of tubulation on healing and scar formation after transection of the adult rat spinal cord. Restor Neurol Neurosci 18:23-38.

Squier MV, Lehr RP (1994) Post-traumatic syringomyelia. J Neurol Neurosurg Psychiatry 57:1095-1098.

Stalin CE, Rusbridge C, Granger N, Jeffery ND (2008) Radiographic morphology of the cranial portion of the cervical vertebral column in Cavalier King Charles Spaniels and its relationship to syringomyelia. Am J Vet Res 69:89-93.

Steinbok P (2004) Clinical features of Chiari I malformations. Childs Nerv Syst 20:329-331.

Sternberger NH, Sternberger LA (1987) Blood-brain barrier protein recognized by monoclonal antibody. Proc Natl Acad Sci U S A 84:8169-8173.

Sternberger NH, Sternberger LA, Kies MW, Shear CR (1989) Cell surface endothelial proteins altered in experimental allergic encephalomyelitis. J Neuroimmunol 21:241-248.

Stoodley MA, Brown SA, Brown CJ, Jones NR (1997) Arterial pulsation-dependent perivascular cerebrospinal fluid flow into the central canal in the sheep spinal cord. J Neurosurg 86:686-693.

Stoodley MA, Gutschmidt B, Jones NR (1999) Cerebrospinal fluid flow in an animal model of noncommunicating syringomyelia. Neurosurgery 44:1065-1075; discussion 1075-1066.

Stoodley MA, Jones NR, Yang L, Brown CJ (2000) Mechanisms underlying the formation and enlargement of noncommunicating syringomyelia: experimental studies. Neurosurg Focus 8:E2.

Stovner LJ, Cappelen J, Nilsen G, Sjaastad O (1992) The Chiari type I malformation in two monozygotic twins and first-degree relatives. Ann Neurol 31:220-222.

Stovner LJ, Rinck P (1992) Syringomyelia in Chiari malformation: relation to extent of cerebellar tissue herniation. Neurosurgery 31:913-917; discussion 917.

Strayer A (2001) Chiari I malformation: clinical presentation and management. J Neurosci Nurs 33:90-96, 104.

Suzuki H, Christofides ND, Anand P, Chretien M, Seidah NG, Polak JM, Bloom SR (1985) Regional distribution of a novel pituitary protein (7B2) in the rat spinal cord: effect of neonatal capsaicin treatment and thoracic cord transection. Neurosci Lett 55:151-156.

Suzuki R, Okuda M, Asai J, Nagashima G, Itokawa H, Matsunaga A, Fujimoto T, Suzuki T (2006) Astrocytes co-express aquaporin-1, -4, and vascular endothelial growth factor in brain edema tissue associated with brain contusion. Acta Neurochir Suppl 96:398-401.

Szpak GM, Lewandowska E, Schmidt-Sidor B, Pasennik E, Modzelewska J, Stepien T, Zdaniuk G, Kulczycki J, Wierzba-Bobrowicz T (2008) Giant cell ependymoma of the spinal cord and fourth ventricle coexisting with syringomyelia. Folia neuropathologica / Association of Polish Neuropathologists and Medical Research Centre, Polish Academy of Sciences 46:220-231.

Tabor EN, Batzdorf U (1996) Thoracic spinal Pantopaque cyst and associated syrinx resulting in progressive spastic paraparesis: case report. Neurosurgery 39:1040-1042.

Takeoka A, Kubasak MD, Zhong H, Kaplan J, Roy RR, Phelps PE Noradrenergic innervation of the rat spinal cord caudal to a complete spinal cord transection: effects of olfactory ensheathing glia. Exp Neurol 222:59-69.

Talmadge RJ, Roy RR, Caiozzo VJ, Edgerton VR (2002) Mechanical properties of rat soleus after long-term spinal cord transection. J Appl Physiol 93:1487-1497.

Talmadge RJ, Roy RR, Edgerton VR (1999) Persistence of hybrid fibers in rat soleus after spinal cord transection. Anat Rec 255:188-201.

Tani K, Taga A, Itamoto K, Iwanaga T, Une S, Nakaichi M, Taura Y (2001) Hydrocephalus and syringomyelia in a cat. The Journal of veterinary medical science / the Japanese Society of Veterinary Science 63:1331-1334.

Tanimura Y, Hiroaki Y, Fujiyoshi Y (2009) Acetazolamide reversibly inhibits water conduction by aquaporin-4. J Struct Biol 166:16-21.

Tarazi R, Coutsoftides T, Steiger E, Fazio VW (1983) Gastric and duodenal cutaneous fistulas. World J Surg 7:463-473.

Tashiro K, Fukazawa T, Moriwaka F, Hamada T, Isu T, Iwasaki Y, Abe H (1987) Syringomyelic syndrome: clinical features in 31 cases confirmed by CT myelography or magnetic resonance imaging. Journal of neurology 235:26-30.

Tator CH (1972) Acute spinal cord injury: a review of recent studies of treatment and pathophysiology. Canadian Medical Association journal 107:143-145 passim.

Tator CH, Briceno C (1988) Treatment of syringomyelia with a syringosubarachnoid shunt. The Canadian journal of neurological sciences 15:48-57.

Tator CH, Koyanagi I (1997) Vascular mechanisms in the pathophysiology of human spinal cord injury. J Neurosurg 86:483-492.

Tchirkow G, Lavery IC, Fazio VW (1983) Crohn's disease in the elderly. Dis Colon Rectum 26:177-181.

Terre R, Valles M, Vidal J (2000) Post-traumatic syringomyelia following complete neurological recovery. Spinal Cord 38:567-570.

Thiagarajah JR, Papadopoulos MC, Verkman AS (2005) Noninvasive early detection of brain edema in mice by near-infrared light scattering. J Neurosci Res 80:293-299.

Thompson FJ, Reier PJ, Uthman B, Mott S, Fessler RG, Behrman A, Trimble M, Anderson DK, Wirth ED, 3rd (2001) Neurophysiological assessment of the feasibility and safety of neural tissue transplantation in patients with syringomyelia. J Neurotrauma 18:931-945.

Thrane AS, Rappold PM, Fujita T, Torres A, Bekar LK, Takano T, Peng W, Wang F, Thrane VR, Enger R, Haj-Yasein NN, Skare O, Holen T, Klungland A, Ottersen OP, Nedergaard M, Nagelhus EA (2011) Critical role of aquaporin-4 (AQP4) in astrocytic Ca2+ signaling events elicited by cerebral edema. Proc Natl Acad Sci U S A 108:846-851.

Thuret S, Moon LD, Gage FH (2006) Therapeutic interventions after spinal cord injury. Nat Rev Neurosci 7:628-643.

Tripovic D, Al Abed A, Rummery NM, Johansen NJ, McLachlan EM, Brock JA Nerve-Evoked Constriction of Rat Tail Veins Is Potentiated and Venous Diameter Is Reduced after Chronic Spinal Cord Transection. J Neurotrauma.

Trudrung P, Wirth U, Mense S (2000) Changes in the number of nitric oxide-synthesizing neurones on both sides of a chronic transection of the rat spinal cord. Neurosci Lett 287:125-128.

Tsai EC, Dalton PD, Shoichet MS, Tator CH (2004) Synthetic hydrogel guidance channels facilitate regeneration of adult rat brainstem motor axons after complete spinal cord transection. J Neurotrauma 21:789-804.

Tsukaguchi H, Shayakul C, Berger UV, Mackenzie B, Devidas S, Guggino WB, van Hoek AN, Hediger MA (1998) Molecular characterization of a broad selectivity neutral solute channel. J Biol Chem 273:24737-24743.

Tsukaguchi K, Yoneda T, Yoshikawa M, Fu A, Tokuyama T, Okamoto Y, Yamamoto C, Takenaka H, Okamura H, Narita N (1996) [Interaction between nutrition and production of IL-1 beta, TNF alpha, and IL-6 by peripheral blood monocytes in patients with lung cancer]. Nihon Kyobu Shikkan Gakkai Zasshi 34:778-784.

Turgut M, Cullu E, Uysal A, Yurtseven ME, Alparslan B (2005) Chronic changes in cerebrospinal fluid pathways produced by subarachnoid kaolin injection and experimental spinal cord trauma in the rabbit: their relationship with the development of spinal deformity. An electron microscopic study and magnetic resonance imaging evaluation. Neurosurg Rev 28:289-297.

Uzum G, Sarper Diler A, Bahcekapili N, Ziya Ziylan Y (2006) Erythropoietin prevents the increase in blood-brain barrier permeability during pentylentetrazol induced seizures. Life Sci 78:2571-2576.

Vajda Z, Pedersen M, Fuchtbauer EM, Wertz K, Stodkilde-Jorgensen H, Sulyok E, Doczi T, Neely JD, Agre P, Frokiaer J, Nielsen S (2002) Delayed onset of brain edema and mislocalization of aquaporin-4 in dystrophin-null transgenic mice. Proc Natl Acad Sci U S A 99:13131-13136.

Van den Bergh R, Hoorens G, Van Calenbergh F (1990) Syringomyelia: a retrospective study. Part I: Clinical features. Acta neurologica Belgica 90:93-99.

Vannemreddy SS, Rowed DW, Bharatwal N (2002) Posttraumatic syringomyelia: predisposing factors. Br J Neurosurg 16:276-283.

Vaptzarova KI, Popov PG, Vesely J, Cihak A (1973) Depressed synthesis of DNA in regenerating rat liver after spinal cord (C7) transection. Experientia 29:1505-1506.

Verkman AS (2005) More than just water channels: unexpected cellular roles of aquaporins. J Cell Sci 118:3225-3232.

Verkman AS (2009) Aquaporins: translating bench research to human disease. J Exp Biol 212:1707-1715.

Verkman AS, Binder DK, Bloch O, Auguste K, Papadopoulos MC (2006) Three distinct roles of aquaporin-4 in brain function revealed by knockout mice. Biochim Biophys Acta 1758:1085-1093.

Voelz K, Kondziella D, von Rautenfeld DB, Brinker T, Ludemann W (2007) A ferritin tracer study of compensatory spinal CSF outflow pathways in kaolin-induced hydrocephalus. Acta Neuropathol 113:569-575.

von Euler M, Janson AM, Larsen JO, Seiger A, Forno L, Bunge MB, Sundstrom E (2002) Spontaneous axonal regeneration in rodent spinal cord after ischemic injury. J Neuropathol Exp Neurol 61:64-75.

Wagner FC, Jr., Stewart WB (1981) Effect of trauma dose on spinal cord edema. J Neurosurg 54:802-806.

Wallace MC, Tator CH, Lewis AJ (1987) Chronic regenerative changes in the spinal cord after cord compression injury in rats. Surg Neurol 27:209-219.

Wang D, Bodley R, Sett P, Gardner B, Frankel H (1996) A clinical magnetic resonance imaging study of the traumatised spinal cord more than 20 years following injury. Paraplegia 34:65-81.

Webb KS, Libbey LM, Hotchkiss JH, Scanlan RA, Fazio T, Castegnaro M (1983) V.3 Mass spectrometric analysis of N-nitroso compounds and derivatives. IARC Sci Publ 449-462, 473.

Weber ED, Stelzner DJ (1977) Behavioral effects of spinal cord transection in the developing rat. Brain Res 125:241-255.

Weier K, Naegelin Y, Thoeni A, Hirsch JG, Kappos L, Steinbrich W, Radue EW, Gass A (2008) Non-communicating syringomyelia: a feature of spinal cord involvement in multiple sclerosis. Brain 131:1776-1782.

Weller RO (2005) Microscopic morphology and histology of the human meninges. Morphologie 89:22-34.

Whetstone WD, Hsu JY, Eisenberg M, Werb Z, Noble-Haeusslein LJ (2003) Blood-spinal cord barrier after spinal cord injury: relation to revascularization and wound healing. J Neurosci Res 74:227-239.

Whittaker DE, English K, McGonnell IM, Volk HA Evaluation of cerebrospinal fluid in Cavalier King Charles Spaniel dogs diagnosed with Chiari-like malformation with or without concurrent syringomyelia. J Vet Diagn Invest 23:302-307.

Wickremesinghe PC, Dayrit PQ, Manfredi OL, Fazio RA, Fagel VL (1983) Quantitative evaluation of bile diversion surgery utilizing 99mTc HIDA scintigraphy. Gastroenterology 84:354-363.

Williams B (1980a) Experimental communicating syringomyelia in dogs after cisternal kaolin injection. Part 2. Pressure studies. J Neurol Sci 48:109-122.

Williams B (1980b) On the pathogenesis of syringomyelia: a review. J R Soc Med 73:798-806.

Williams B (1990) Syringomyelia. Neurosurg Clin N Am 1:653-685.

Williams B (1992) Pathogenesis of post-traumatic syringomyelia. Br J Neurosurg 6:517-520.

Williams B (1993) Pathogenesis of syringomyelia. Acta Neurochir (Wien) 123:159-165.

Williams B, Bentley J (1980) Experimental communicating syringomyelia in dogs after cisternal kaolin injection. Part 1. Morphology. J Neurol Sci 48:93-107.

Williams B, Fahy G (1983) A critical appraisal of "terminal ventriculostomy" for the treatment of syringomyelia. J Neurosurg 58:188-197.

Williams B, Weller RO (1973) Syringomyelia produced by intramedullary fluid injection in dogs. J Neurol Neurosurg Psychiatry 36:467-477.

Wilson CB, Bertan V, Norrell HA, Jr., Hukuda S (1969) Experimental cervical myelopathy. II. Acute ischemic myelopathy. Arch Neurol 21:571-589.

Wirth ED, 3rd, Reier PJ, Fessler RG, Thompson FJ, Uthman B, Behrman A, Beard J, Vierck CJ, Anderson DK (2001) Feasibility and safety of neural tissue transplantation in patients with syringomyelia. J Neurotrauma 18:911-929.

Wolburg H, Noell S, Mack A, Wolburg-Buchholz K, Fallier-Becker P (2009) Brain endothelial cells and the glio-vascular complex. Cell Tissue Res 335:75-96.

Wollmer P, Rhodes CG, Allan RM, Maseri A, Fazio F (1983) Regional extravascular lung density and fractional pulmonary blood volume in patients with chronic pulmonary venous hypertension. Clin Physiol 3:241-256.

Woodard JS, Freeman LW (1956) Ischemia of the spinal cord; an experimental study. J Neurosurg 13:63-72.

Yamada H, Yokota A, Haratake J, Horie A (1996) Morphological study of experimental syringomyelia with kaolin-induced hydrocephalus in a canine model. Journal of Neurosurgery 84:999-1005.

Yamazaki Y, Tachibana S, Ohta N, Yada K, Ohama E (1995) Experimental model of chronic tonsillar herniation associated with early stage syringomyelia. Acta Neuropathol 90:425-431.

Yang CC, Shih YH, Ko MH, Hsu SY, Cheng H, Fu YS (2008) Transplantation of human umbilical mesenchymal stem cells from Wharton's jelly after complete transection of the rat spinal cord. PLoS One 3:e3336.

Yang L, Jones NR, Stoodley MA, Blumbergs PC, Brown CJ (2001) Excitotoxic model of post-traumatic syringomyelia in the rat. Spine (Phila Pa 1976) 26:1842-1849.

Yasui K, Hashizume Y, Yoshida M, Kameyama T, Sobue G (1999) Age-related morphologic changes of the central canal of the human spinal cord. Acta Neuropathol 97:253-259.

Yates C, Charlesworth A, Allen SR, Reese NB, Skinner RD, Garcia-Rill E (2008) The onset of hyperreflexia in the rat following complete spinal cord transection. Spinal Cord 46:798-803.

Yeo JD, Payne W, Hinwood B, Kidman AD (1975) The experimental contusion injury of the spinal cord in sheep. Paraplegia 12:279-298.

Yeoh M, McLachlan EM, Brock JA (2004) Chronic decentralization potentiates neurovascular transmission in the isolated rat tail artery, mimicking the effects of spinal transection. J Physiol 561:583-596.

Yezierski RP, Liu S, Ruenes GL, Kajander KJ, Brewer KL (1998) Excitotoxic spinal cord injury: behavioral and morphological characteristics of a central pain model. Pain 75:141-155.

Yezierski RP, Santana M, Park SH, Madsen PW (1993) Neuronal degeneration and spinal cavitation following intraspinal injections of quisqualic acid in the rat. J Neurotrauma 10:445-456.

Young WF, Tuma R, O'Grady T (2000) Intraoperative measurement of spinal cord blood flow in syringomyelia. Clin Neurol Neurosurg 102:119-123.

Zagzag D (1995) Angiogenic growth factors in neural embryogenesis and neoplasia. Am J Pathol 146:293-309.

Zagzag D, Friedlander DR, Miller DC, Dosik J, Cangiarella J, Kostianovsky M, Cohen H, Grumet M, Greco MA (1995) Tenascin expression in astrocytomas correlates with angiogenesis. Cancer Res 55:907-914.

Zakeri A, Glasauer FE, Egnatchik JG (1995) Familial syringomyelia: case report and review of the literature. Surg Neurol 44:48-53.

Zeman FD (1963a) Toxic Effects Ascribed to Prolonged Abuse of Acetophenetidin (Phenacetin); a Review of the World Literature. J Chronic Dis 16:1085-1098.

Zeman MS (1963b) The Use of Premarin as a Topical Agent in the Treatment of Atrophic Rhinitis. (a Clinical and Histological Study.). Laryngoscope 73:1219-1233.

Zeman W (1963c) Disturbances of Nucleic Acid Metabolism Preceding Delayed Radionecrosis of Nervous Tissue. Proc Natl Acad Sci U S A 50:626-630.

Zhang D, Vetrivel L, Verkman AS (2002) Aquaporin deletion in mice reduces intraocular pressure and aqueous fluid production. J Gen Physiol 119:561-569.

Zhao J, Moore AN, Clifton GL, Dash PK (2005) Sulforaphane enhances aquaporin-4 expression and decreases cerebral edema following traumatic brain injury. J Neurosci Res 82:499-506.

Zhao J, Wecht JM, Zhang Y, Wen X, Zeman R, Bauman WA, Cardozo C (2007) iNOS expression in rat aorta is increased after spinal cord transection: a possible cause of orthostatic hypotension in man. Neurosci Lett 415:210-214.

Zotti GC, Aceto A, Santini M, Testa S, Sfarzo A, Fazio FM (1983) [Long-term survival of patients with pulmonary carcinoma]. Minerva Chir 38:561-570.

Appendix

Publications arising from this thesis

1. **Hemley SJ**, Tu J, Stoodley MA. (2009). Role of the blood spinal-cord barrier in post-traumatic syringomyelia. J neurosurg Spine, Dec;11(6):696-704.
2. **Hemley SJ**, Stoodley MA. Aquaporin-4 expression in posttraumatic syringomyelia. (In preparation).
3. **Hemley SJ**, Stoodley MA. Aquaporin-4 expression and vascular changes in Chiari-associated syringomyelia. (In preparation).
4. **Hemley SJ**, Jones NR, Stoodley MA. Fluid outflow pathways in posttraumatic syringomyelia. (In preparation).

Presentations at scientific meetings

1. **Hemley S**, Stoodley M. Aquaporin-4 expression and vascular changes in experimental syringomyelia. International Symposium for Syringomyelia. Berlin, Germany, December 2010.
2. **Hemley S**, Stoodley M. Aquaporin-4 expression and vascular changes in experimental syringomyelia. Macquarie neurosurgical research and clinical symposium, Macquarie University, New South Wales, November 2010.
3. **Hemley S**, Stoodley M. Aquaporin-4 expression in an animal model of posttraumatic syringomyelia. Presented at the 2010 Annual Scientific Meeting of the Spine Society of Australia. Christchurch, New Zealand, April 2010.
4. **Hemley SJ**, Stoodley MA. Aquaporin-4 expression and vascular changes in Chiari-associated syringomyelia. Presented at the Spinal Research Symposium VIII. Adelaide, South Australia, August 2010.
5. **Hemley SJ**, Stoodley MA. Aquaporin-4 expression in an animal model ofpost-traumatic syringomyelia. Presented at the Adelaide Centre for Spinal Research. Spinal Symposium VII, August 2009, Barossa Valley, South Australia.
   Awarded the NuVasive Prize for best presentation by a PhD Candidate.
6. **Hemley SJ**, Stoodley MA. Aquaporin-4 expression in an animal model of post-traumatic syringomyelia. Presented at the NSA Annual Scientific Meeting, September 2009, Alice Springs, Northern Territory.
7. **Hemley SJ**, Jones NR, Stoodley MA. Fluid inflow and outflow in animal models of syringomyelia. Presented at the Adelaide Centre for Spinal Research. Spinal Symposium VI, August 2008, Barossa Valley, South Australia.